COLLECTORLESS FLOTATION OF CHALCOPYRITE AND SPHALERITE ORES

by

Gerald Harvey Luttrell

Thesis submitted to the Faculty of the
Virginia Polytechnic Institute and State University
in partial fulfillment of the requirements for the degree of

MASTER OF SCIENCE

in

Mining and Minerals Engineering

APPROVED:

R. H. Yoom, Chairman

J. R. Craig

J. P. Wightman

J. R. Lucas

W. E. Foreman

December, 1982
Blacksburg, Virginia

ACKNOWLEDGMENTS

The author wishes to express his sincere appreciation to Dr. R. H. Yoon for his inspiration and guidance throughout the course of this investigation. Special thanks are given to Mark Pritzker for his invaluable suggestions and assistance, particularly with respect to his computer calculations concerning the distribution of polysulfide species, and to Dr. J. G. Dillard for his informative suggestions with regard to the various surface analysis techniques used during the course of this study. He is also grateful to the mining companies who supplied the ore samples used in this investigation.

The author acknowledges the financial support of the National Science Foundation (Grant No. CPE - 8011456), which made this work possible, and Dr. J. R. Lucas for the Mining and Minerals Resource Research Institute Fellowship.

Additional gratitude is expressed to Beth Dillinger, Diana Fay, Kansas Luttrell, Wayne Slusser and Jim Overfelt for their technical assistance, and to the graduate students of the Mining and Minerals Engineering Department for their friendship and support. Finally, the author wishes to express his deep appreciation to his parents, and especially to his wife, Kay, for their continued patience, support and understanding.

TABLE OF CONTENTS

LIST OF FIGURES

LIST OF TABLES

I. INTRODUCTION

1.1 General

Froth flotation is a physio-chemical process employed for the selective separation of finely divided solids from one another in an aqueous suspension. Most of the important raw materials for the production of nonferrous metals such as copper, lead, zinc, nickel, cobalt, molybdenum, mercury and antimony, as well as numerous nonmetallic minerals, are obtained from ores that are first subjected to flotation treatment (Leja, 1982, p. 30).

The majority of naturally occurring minerals are hydrophilic. Therefore, the success of a flotation process relies on the ability of certain surface-active compounds, called collectors, to adsorb selectively onto a desired mineral surface and render it hydrophobic. As a result of this induced hydrophobicity, the mineral adheres to air bubbles which rise to the pulp surface where they are removed. In theory, the flotation process can be applied to any system where individual components display differences in their affinity toward air and water. Activators may be added to promote collector adsorption and depressants may be necessary to inhibit the adsorption of a collector on unwanted minerals. A frothing agent is also added to the pulp to improve air dispersion by producing finer bubbles and to prevent the coalescence of separate air bubbles. At

the pulp surface, a frother promotes the formation of a stable froth which permits removal of the concentrate.

It is important to realize that flotation processes rely upon surface phenomenon. Small changes in the chemical environment may, therefore, have drastic effects on flotation response. In addition, flotation processes take place in an extremely complex environment of solid-gas, solid-liquid and liquid-gas interfaces. Thus, direct studies of these processes are difficult. Sutherland and Wark (1955) exemplified the complexity of sulfide mineral flotation by listing over thirty operating variables, of which only about twenty could be controlled by the plant metallurgist.

The first froth flotation process in the United States was installed in the Montana Basin Reduction Plant by James M. Hyde in 1911 (Gaudin, 1962, p. 11). Froth flotation has since become the most significant technological advance known to the mineral processing industry. The amount of ore treated anually by froth flotation is currently in excess of 2×10^9 tons, which makes this process one of the most impressive applications of surface chemistry technology practiced today (Leja, 1982, p. 31).

Prior to the early 1900's, gravity separation techniques were extensively employed for the mineral processing of ores. Since these methods could be used only on relatively coarse mineral particles, extremely fine or

slimed minerals could not be effectively processed. In contrast, the advent of flotation has made possible the recovery of mineral wealth from complex, low-grade ores which might have otherwise been economically worthless. Currently, some companies mine and process ores which are lower in average grade than the refuse of past operations where gravity concentration was employed. For instance, the importance of flotation to the copper industry is illustrated by the drop in the average grade of copper ores treated in the U.S. from 1.57% Cu content in 1953 to 0.40% Cu content in 1979 (Schroeder, 1979). As a result, the capacity of individual flotation plants has increased more than twenty times during this same period (Leja, 1982, p. 34). World demand for copper is projected to steadily increase at an annual rate of approximately 3.9% over the next 20 years (Mineral Facts and Problems, 1980). This fact, combined with the trend of concentrating ever lower grade ores, assures that flotation will assume an ever-increasing importance to the minerals industry.

Although most minerals occurring in nature are hydrophilic, some are naturally hydrophobic. For example, the flotation of graphite, talc, sulfur or molybdenite does not require the addition of a collector (Gaudin, Miaw and Spedden, 1957). Until recently, most sulfide minerals were considered naturally hydrophilic. As a result, sulfide flotation is generally accomplished after the addition of

thiol-type collectors. However, some sulfide minerals have been shown to float in the absence of collectors, suggesting that they may be naturally hydrophobic.

From a practical standpoint, the concentration of sulfides using a collectorless flotation process could reduce reagent costs by as much as 75 percent (Lepetic, 1974). In addition, environmental considerations make the collectorless flotation scheme attractive since sodium cyanide and other toxic reagents used in conventional treatment can potentially be eliminated or reduced. Despite numerous advances in sulfide flotation, a basic understanding of the chemical and physical principles involved in the process still lags behind industrial application. Thus, a better understanding of the collectorless flotation process and its related surface chemistry may aid in the development of a fundamental theory for sulfide flotation.

1.2 Literature Review

The question as to whether sulfide minerals are naturally hydrophobic or not has long been the subject of considerable controversy. It began with the observation that sulfide minerals were less wettable by water than associated gangue minerals. Haynes (1860) and Everson (1886) exploited this difference in wettability for upgrading sulfide minerals. This process, which became known as bulk-oil flotation, was based on the ability of sulfides to be preferentially wetted by oil in the presence of water. As a result, sulfide minerals were separated into the oil/water interface while silicious gangue remained in the water. This process was later abandoned since large amounts of oil were generally required. Another early process which relied on the differences in wettability of sulfide minerals was the skin-flotation process (Bradford, 1885). In this process, finely ground dry ore was slowly brought into contact with water. The less wettable sulfide minerals floated on the water surface while the silicious gangue minerals, which wet more easily, sank. Both of these processes, however, became obsolete when Ballot, Sulman and Picard (1905) utilized a rising stream of air bubbles as the buoyant medium for carrying-oil coated sulfide minerals to the surface of the pulp.

Early reports by Sulman (1930) and Gaudin (1932)

indicated that some sulfides such as galena and chalcopyrite were floatable without the addition of a collector. Ravitz and Porter (1933), Ravitz (1940) and Herd and Ure (1941) claimed that galena cleaned of any oxide coating would float without the addition of xanthate and that small amounts of oxygen or an oxidizing agent prevented flotation. Ravitz and Porter (1933) expanded this concept further and suggested that the function of xanthate was to chemically remove oxidized products from mineral surfaces. They believed that the mineral, once cleaned of oxidation products, would reveal its inherent floatability. However, spectroscopic evidence such as electron diffraction studies made by Hagihara (1952) and infrared studies made by Leja, Little and Poling (1962) showed that xanthates were actually present on mineral surfaces that had been treated with a collector solution. These results, combined with the fact that different xanthates produced different contact angles on the same mineral surfaces (Sutherland and Wark, 1955, p. 111) overwhelmingly disproved this theory and established that sulfide minerals are rendered hydrophobic by the adsorption of heteropolar xanthate molecules.

Contrary to the hypothesis that clean sulfides are naturally floatable, Knoll and Baker (1941) showed that clean galena did not float without a collector and did not adsorb xanthate. Wark (1938, p. 127) attempted to produce a clean galena surface by treatment with sodium sulfide. His

results showed that galena flotation was not possible unless a collector was added, and that sodium sulfide, even when added in small amounts, is an effective depressant. It was also discovered that the natural floatability of pure chalcopyrite was suppressed when small amounts of either an oxidizing agent ($KMnO_4$) or a reducing agent (Na_2S) were added (Gaudin, 1932, p. 165).

The reasons for the differences in observations by the various early investigators are not clear. An attempt was made to explain these contradictions by Taggart et al. (1934) who argued that the apparent natural floatability could be attributed to either the contamination of samples by oily substances or the use of frothers which have collecting properties. So convincing were these arguments against the concept of natural floatability of sulfides that the topic was not seriously considered again for the next two decades.

Other investigators (Plaksin, 1959; Glembotskii, Klassen and Plaksin, 1963) suggested that the natural hydrophobicity exhibited by many metal sulfides was due to the adsorption of molecular oxygen. They speculated that the oxygen adsorption promoted dehydration of sulfide minerals, thus allowing air bubbles to displace water molecules more readily from the mineral surface.

Recently, however, there has been renewed interest in the topic of collectorless flotation. Boyce et al. (1970)

have reported that galena and sphalerite are being floated without the use of a collector in the first eight cells of each rougher bank at the Tsumeb concentrator in South Africa. Also, Lepetic (1974) has shown that chalcopyrite can be successfully concentrated using only a frother after dry autogenous grinding. Chalcopyrite from primary ore deposits (thermal vein deposits) responded well to this type of treatment, whereas chalcopyrite from secondary copper sulfides did not.

A major contribution was made to the understanding of collectorless flotation when Heyes and Trahar (1977) discovered that chalcopyrite could be floated without a collector, but only under oxidizing conditions. The possibility that organic substances were responsible for the observed natural hydrophobicity was considered unreasonable in view of the extreme precautions taken to avoid possible contamination. Collectorless flotation has also been attributed to the use of frothers, such as amyl alcohol or polypropylene glycol, which may have collecting properties. Yet, Heyes and Trahar (1977) have shown that chalcopyrite could be floated in the absence of organic frothers by adding alkali salts to promote frothing.

Using electrochemical techniques, Gardner and Woods (1979) confirmed the result of Heyes and Trahar and suggested further that anodic oxidation of the chalcopyrite surface was responsible for its natural floatability. The

surface species formed during this anodic oxidation was proposed to be elemental sulfur, a well known hydrophobic entity.

The concept that electrochemical reactions may be important in conferring hydrophobicity in sulfide mineral systems was reported more than 50 years ago (Kamieski, 1931). Since that time, additional studies have provided evidence for the occurrence of electrochemical reactions in sulfide flotation systems (Salamy and Nixon, 1953; Kamienski and Pomianowski, 1954; Plaksin and Bessonov, 1957; Tolun and Kitchener, 1964; Majima and Takeda, 1968; Toperi and Tolun, 1969). However, it was not until the 1970's that electrochemical techniques were applied so that a direct correlation between floatability and potential could be made (Gardner and Woods, 1973; Chander and Fuerstenau, 1975). This was accomplished by using a bed of particles as an electrode, which could be floated after electrochemical manipulation.

The experimental results showing the floatability of chalcopyrite as a function of potential, as reported by Heyes and Trahar (1977) and Gardner and Woods (1979), are shown in Figure 1.1. Since it was shown that the flotation of chalcopyrite could be controlled electrochemically, it was concluded that the critical factor in collectorless flotation was potential and not the chemical system used to obtain that potential. Further investigation by Gardner and

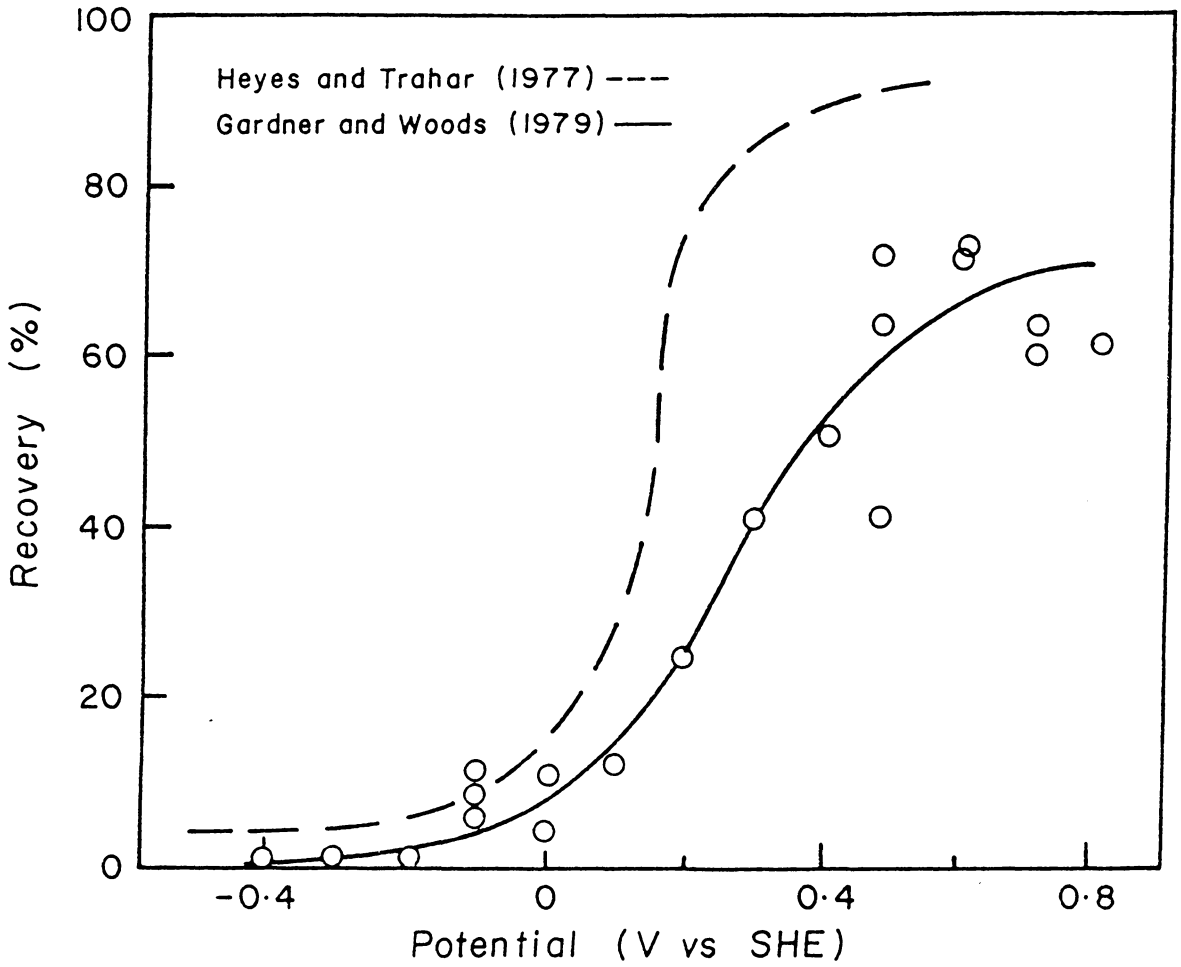

Figure 1.1 Recovery of chalcopyrite after 30 minutes of flotation as a function of conditioning potential.

Woods (1979) using linear potential sweep voltammetry was performed in an attempt to identify the processes which induced hydrophobicity to the mineral surface. The voltammogram obtained at pH 11 is shown in Figure 1.2. As shown, an anodic current flows at potentials greater than approximately -100 mV that gives rise to a peak at about +150 mV. They noted that chalcopyrite becomes naturally floatable at approximately the same potential as the beginning of the anodic current flow. Thus, it was considered that products formed by this electrochemical reaction rendered the chalcopyrite surface hydrophobic. The cathodic peak observed during the negative sweep was considered as a reduction of products formed by the anodic process. It was concluded that the onset of flotation coincided with the oxidation of chalcopyrite by the following reaction:

$$CuFeS_2 + 3H_2O \longrightarrow CuS + Fe(OH)_3 + \overset{\circ}{S} + 3H^+ + 3e \qquad [1.1]$$

In acidic solutions, on the other hand, Gardner and Woods suggested another reaction as given below:

$$CuFeS_2 \longrightarrow CuS + \overset{\circ}{S} + Fe^{2+} + 2e \qquad [1.2]$$

In both reactions chalcopyrite is being oxidized to form elemental sulfur, which the authors believed caused the

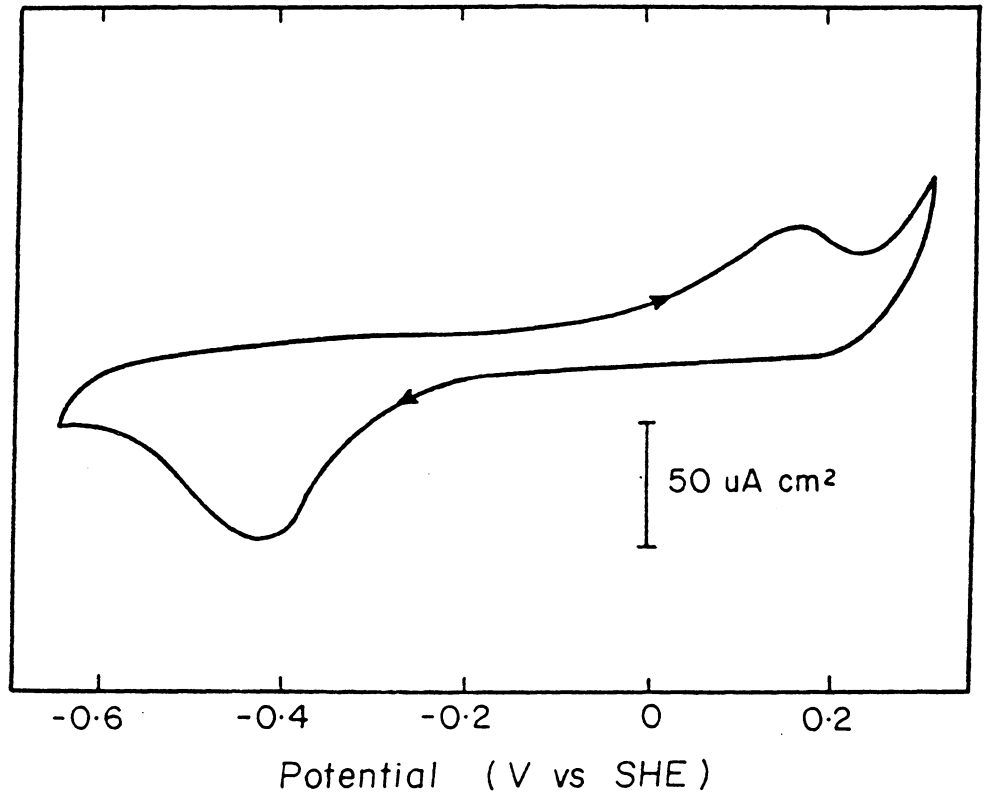

Figure 1.2 Voltammogram for chalcopyrite in pH 11 buffer solution. Linear potential sweeps at 4 mV/s starting at the rest potential (Gardner and Woods, 1979).

collectorless flotation. Gardner and Woods (1979) calculated the standard potential, E°, for the oxidation in alkaline solutions to be 0.547 volts from the free-energy data listed by Latimer (1952). Then, they calculated the half-cell potential, E_h, for the oxidation of chalcopyrite at pH 11 and 25°C using the Nernst equation as follows,

$$E_h = E^\circ + \frac{RT}{nF} \ln [\ H^+\ ] \qquad [1.3]$$

$$= 0.547 + 0.059 \log [\ H^+\ ]$$

$$= 0.547 + 0.059\ (-11)$$

$$= -0.102 \text{ volts at pH } 11$$

in which R is the gas constant, T the absolute temperature and F the Faraday constant.

The onset of flotation was observed to occur at the E_h corresponding to this value, which was considered as evidence for the oxidation mechanism represented by Equation 1.1. Thus, according to this theory, elemental sulfur formed during the oxidation of the chalcopyrite is responsible for collectorless flotation.

In contrast to the theory proposed by Gardner and Woods, Finkelstein et al. (1975) showed earlier that there was no correlation between the degree of natural floatability of sulfide minerals and the amount of elemental sulfur found on the mineral surfaces. Fuerstenau and

Sabacky (1981) reported that most sulfide minerals, including chalcopyrite and sphalerite, were naturally floatable when ground and floated in an essentially oxygen-free environment. The results of Fuerstenau and Sabacky's experiments are shown in Table 1.1. These investigators noted that a clean sulfide should be inherently hydrophobic since the sulfide ions on the surface lattice are probably incapable of forming hydrogen bonds with water as was originally suggested by Finkelstein et al. (1975).

Yoon (1981) showed that chalcopyrite and sphalerite could be floated without collectors when the ore sample was treated with sodium sulfide. This reagent was considered as a surface-cleaning agent which could remove hydrophilic surface oxidation products by the following sulfidization reaction:

$$\overset{M^{2+}\ A^{2-}}{\boxed{\text{Sulfide Mineral}}} + 2Na^{+} + S^{2-} \longrightarrow \overset{M^{2+}\ S^{2-}}{\boxed{\text{Sulfide Mineral}}} + 2Na^{+} + A^{2-} \qquad [1.4]$$

In this reaction, M^{2+} represents the cation on the sulfide mineral surface and A^{2-} represents the hydrophilic surface oxidation product, such as SO_4^{2-}, $S_2O_3^{2-}$, $S_3O_6^{2-}$, $2OH^{-}$, etc. The clean, unoxidized surface of the sulfide mineral exposed

Table 1.1 Flotation Recovery of Sulfides from Various Sources (Fuerstenau and Sabacky, 1981)

Mineral	Flotation recovery (%)
Galena	
Coeur D'Alene, Idaho	100
Bixby, Missouri	100
Pitcher, Oklahoma	100
Galena, South Dakota	100
Chalcopyrite	
Temagami, Ontario	100
Sudbury, Ontario	100
Beaver Lake District, Utah	97
Messina, Transvaal	93
Chalcocite	
Kennecott, Alaska	100
Evergreen, Colorado	88
Butte, Montana	86
Superior, Arizona	83
Pyrite	
Amba Saguas, Spain	92
Custer, South Dakota	85
Zacatecase, Mexico	83
Naica, Mexico	82
Sphalerite	
Keystone, South Dakota	56
Joplin, Missouri	47
Creede, Colorado	46
Pitcher, Oklahoma	41
Sphalerite (Cu^{2+} activated)	
Keystone, South Dakota	100
Joplin, Missouri	100
Creede, Colorado	100
Pitcher, Oklahoma	100

by the sulfidization reaction was considered to be responsible for collectorless flotation. Since sodium sulfide was a strong reducing agent, it was suggested that collectorless flotation might be possible in a reducing environment.

1.3 Objectives of the Proposed Work

The purpose of this investigation was 1) to establish the conditions necessary for the collectorless flotation of chalcopyrite and sphalerite, and 2) to investigate the possible mechanisms associated with the collectorless flotation phenomenon. To meet these objectives, batch flotation tests were conducted on six chalcopyrite ore samples and two sphalerite ore samples from the United States, Canada and Australia. During some of these tests, potential measurements were conducted using a platinum-calomel electrode pair so that flotation response could be related to the redox conditions of the ore pulp. Particular attention was given to the role of sodium sulfide in collectorless flotation. Micro-flotation experiments were performed with pure chalcopyrite samples to determine the effect of potential on the collectorless flotation of chalcopyrite.

In order to better understand the mechanisms involved, efforts were made to identify the surface species responsible for collectorless flotation. The surface analysis techniques employed include 1) x-ray photoelectron spectroscopy (XPS), 2) quantitative mass spectrometry, and 3) UV analysis of the surface species after solvent extraction. On the basis of the results of the flotation tests and the surface analyses, possible mechanisms for

collectorless flotation of chalcopyrite and sphalerite were proposed.

II. EXPERIMENTAL

2.1 Materials

2.1.1 Ore Samples

a. Copper Ores: The chalcopyrite ores used for this investigation are described in Table 2.1. Each ore was assigned an alphabetical symbol for short-hand identification. Note that the samples vary greatly in location of origin, copper grade and content of associated gangue minerals. The companies which participated were requested to send only coarse samples so that possible surface oxidation during shipment would be kept to a minimum.

Flotation feed was prepared by crushing the ore to -20 mesh and splitting it into 1000-gram lots. The samples, thus prepared, were stored in a freezer at or below -20°C in an attempt to minimize additional surface oxidation prior to grinding.

b. Sphalerite Ores: The sphalerite ores that were obtained for this study are described in Table 2.2. The sample preparation procedure for these ores was identical to that of the chalcopyrite ores with the exception that they were split and stored in 500-gram lots.

2.1.2 Pure Minerals

Pure lump samples of chalcopyrite from the Transvaal

Table 2.1 Description of the Chalcopyrite Ores Used in the Present Work

Symbol	Source	Mineralization
A	Kennecott, Ray Mines (Hayden, Arizona)	chalcopyrite (0.6% Cu) and molybdenite
B	Craigmont Mines Limited (British Columbia)	chalcopyrite (1.34% Cu) in quartz and magnetic matrix
C	Falconbridge Copper (Chibougamau, Quebec)	chalcopyrite (2.0% Cu), 30% below 25 microns disseminated in quartz, 30% other common sulfides
D	Asarco, Mission Unit (Sahuarita, Arizona)	chalcopyrite (0.6% Cu), silver and molybdenite
E	Mount Isa Limited (Australia)	chalcopyrite (3.8% Cu), 7% lead, 6% zinc and 192 gm/ton silver
F	Kennecott, Utah Mine (Salt Lake City, Utah)	chalcopyrite (0.6% Cu), silver, gold and molybdenite

Table 2.2 Description of the Sphalerite Ores Used in the Present Work

Symbol	Source	Mineralization
G	New Jersey Zinc (Jefferson City, TN)	sphalerite (2.5% Zn) and limestone
H	New Jersey Zinc (Center Valley, PA)	sphalerite (6.9% Zn), 5.2% sulfur, 2.8% iron, 13.7% calcium, 8.1% magnesium and 14.3% quartz

Deposit, South Africa were obtained from Ward's Scientific Company for special laboratory studies. Specimens were checked microscopically for purity and those pieces contaminated by quartz were discarded. The pure specimens were then crushed using an agate mortar and pestle and hand-screened to obtain a -65/+100 mesh fraction. The sample, thus prepared, was cleaned of quartz particles by passing it through a Franz Isodynamic Separator.

Two different samples of the Transvaal chalcopyrite were used in the present investigation. A freshly fractured sample was prepared by crushing hand-picked specimens in an agate mortar and screening it to obtain a -65/+100 mesh fraction. Pieces of chalcopyrite that appeared to be discolored due to superficial oxidation were removed with a pair of tweezers. For some experiments, samples were fractured under an ultra-pure nitrogen atmosphere to prevent possible oxidation during grinding. Those samples that were fractured under nitrogen were stored under a nitrogen blanket until use. The second sample used was from the same deposit but had been crushed and sized to -65/+100 mesh four years prior to this study. The sample has since been stored in a dry atmosphere without precautions to prevent surface oxidation.

High surface area samples used in mass spectrometry and UV spectrophotometry were prepared by dry-grinding samples of -100 mesh chalcopyrite for three hours in a mechanical

agate mortar. The entire grinding device was contained within a plastic glove box that was being continuously flooded with ultra-pure nitrogen gas. After grinding, the sample was transferred under a nitrogen blanket to a vacuum dessicator. The dessicator was filled with fresh silica gel and flooded with nitrogen gas prior to the evacuation by a mechanical vacuum pump. All samples were stored in this vacuum until use.

2.1.3 Chemicals

Commercial grade potassium amyl xanthate (AERO 350) and sodium diisopropyl dithiophosphate (AERO 211) from American Cyanamid were used as collectors for the batch flotation of chalcopyrite and sphalerite ores, respectively. Certified A.C.S. grade cupric sulfate ($CuSO_4 \cdot 5H_2O$) from the Fisher Scientific Company was used in some experiments as an activator for sphalerite flotation. Sodium sulfide flakes, from the Fisher Scientific Company, were used as a surface-cleaning agent for sulfide minerals in batch collectorless flotation tests. The sodium sulfide flakes consisted of 60-62% Na_2S, more than 35% water of crystallization, 1.5% sodium chloride and 2% unspecified other sodium salts. In tests where higher quality sodium sulfide was required, reagent grade sodium sulfide crystals ($Na_2S \cdot 9H_2O$) from the Fisher Scientific Company were used. As suggested by Chen and Morris (1972), sodium sulfide crystals were carefully

scraped to remove oxidized surface layers and then washed with distilled water prior to weighing and dissolution. Dowfroth 250, a polypropylene glycol ether with an average molecular weight of 250, was used as the frothing agent in all flotation experiments. For pH adjustment, lime, sodium hydroxide or hydrochloric acid were used.

In some flotation experiments, purified hydrazine hydrate ($N_2H_4 \cdot H_2O$) from the Fisher Scientific Company was used as another reducing agent for comparison with sodium sulfide. Certified A.C.S. grade potassium permanganate crystals from the Fisher Scientific Company were used as an oxidizing agent to control the pulp potential during flotation.

Denatured ethyl alcohol and certified A.C.S. grade acetone (Fisher Scientific Company) were used for extracting and dissolving elemental sulfur from the surfaces of chalcopyrite samples for spectrometric analysis. Laboratory grade sublimed sulfur was obtained from the Fisher Scientific Company for use in making standard sulfur solutions for quantitative analysis.

Compressed ultra-pure (mininum 99.999%) nitrogen was obtained from Airco Industrial Gases for experiments where exclusion of oxygen was desired. The oxygen content of the nitrogen was less than 1 ppm.

2.2 Equipment

2.2.1 Potential Measurement

The potential across a bright platinum-calomel electrode pair was monitored during some of the flotation experiments conducted on the various chalcopyrite samples. A reverse-sleeve calomel reference electrode was used in batch flotation experiments since it provided better conductivity and a faster response time in slurries and suspensions. Since space was limited in the micro-flotation cell, a miniature calomel reference electrode was used in these tests. Both electrodes were refilled weekly with saturated potassium chloride solution to prevent possible contamination of the electrolyte.

A pin platinum electrode was used in most oxidation-reduction potential measurements. However, a special disc-type platinum electrode was used in some micro-flotation experiments where good contact was desired between the platinum surface of the electrode and chalcopyrite particles. All electrodes used in the experiments were purchased from Fisher Scientific Company.

The potential measurements were accomplished using a high-impedance Altex Model 3500 digital millivoltmeter. Potentials were monitored as a function of time using a Pedersen Model 27 MR strip chart recorder.

2.2.2 Micro-Flotation

Flotation of pure mineral samples was accomplished using a Partridge and Smith type flotation cell (1971) made of Pyrex. The apparatus is shown schematically in Figure 2.1. Bubbles were generated by sparging ultra-pure nitrogen gas through a medium porosity glass frit at the bottom of the cell. Gas flow rate was monitored using a Gilmont Micrometer Capillary Flowmeter. A gentle agitation of the suspension was supplied by means of a Teflon coated magnetic stirring bar (1/2"L x 1/8"D) and a Sybron Nuova II magnetic stirrer.

2.2.3 Automated Batch Flotation Machine

A standard Denver Model D-12 laboratory flotation machine was modified in the present work to improve flotation testing. The major advantages of the automation included improved reproducibility of test results, minimized operator bias, ease of operation, and interchangeability of different sized cells. A simplified schematic of the apparatus and a three-dimensional view of the flotation cell are shown in Figures 2.2 and 2.3, respectively.

An electronic pulp level controller was developed, which was found to be more sensitive, less bulky, and easier to operate than the Mariotte bottle used by Harris and Raja (1966) or the diaphragm level sensor used by the Leed automatic flotation machine (Dell and Bunyard, 1972). Its

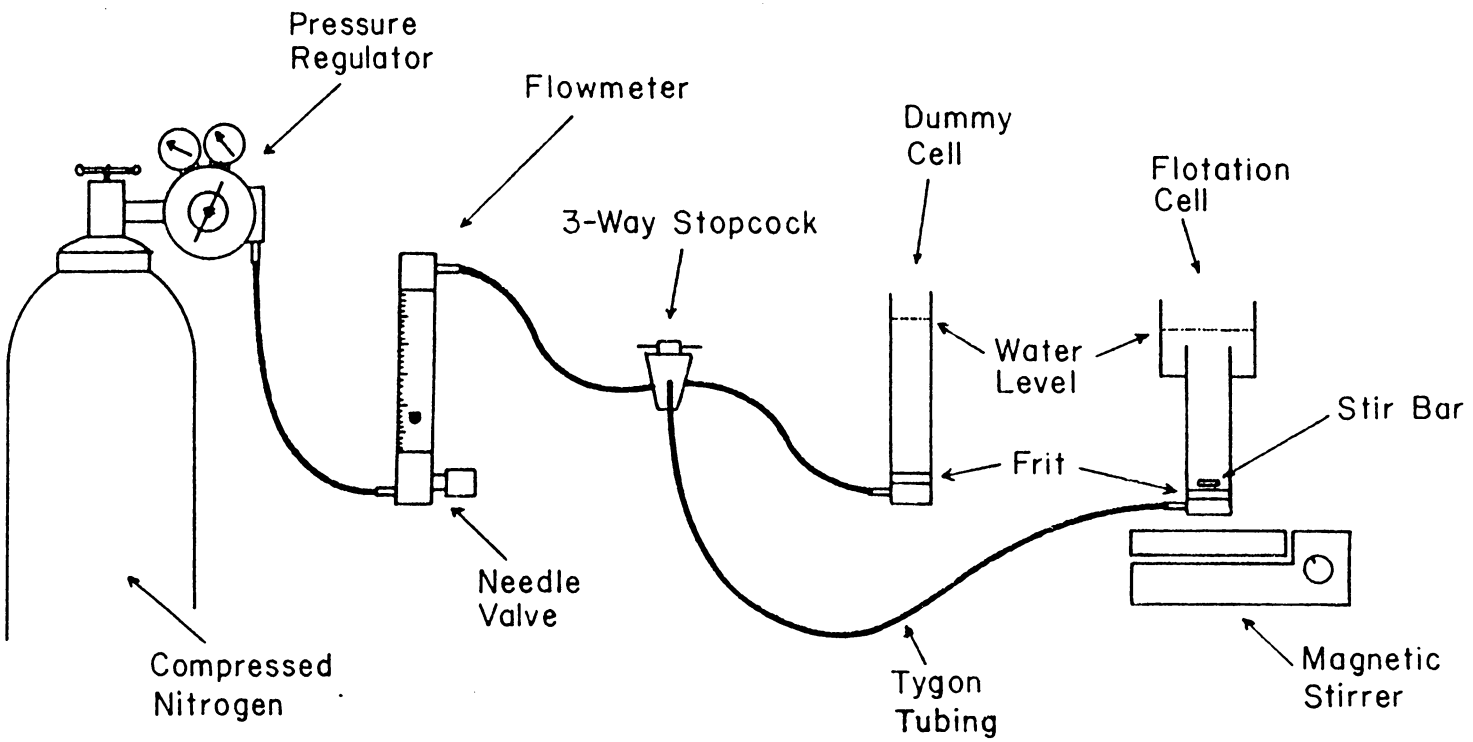

Figure 2.1 Schematic diagram of the micro-flotation apparatus.

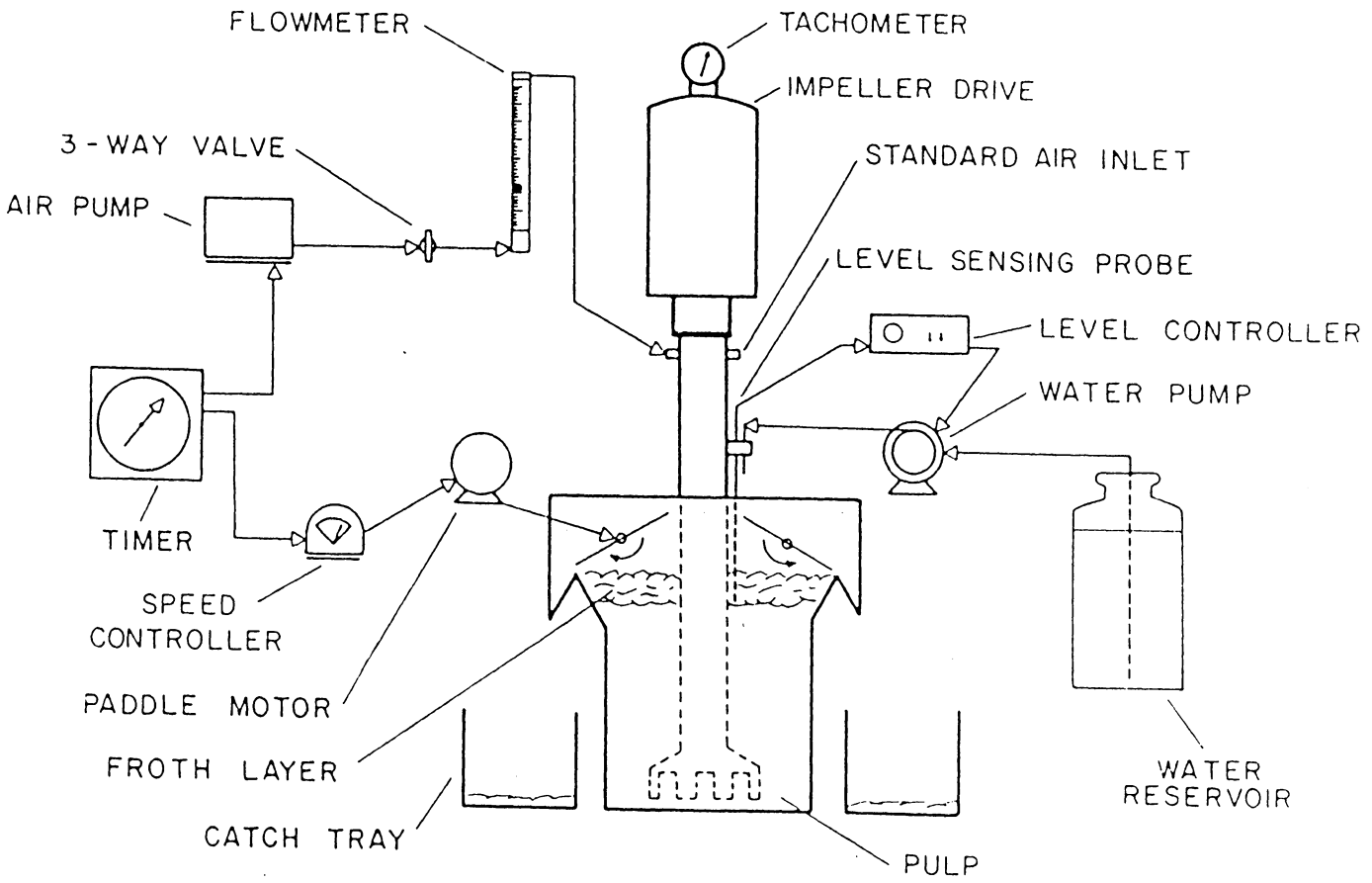

Figure 2.2 Schematic diagram of the automated batch flotation apparatus.

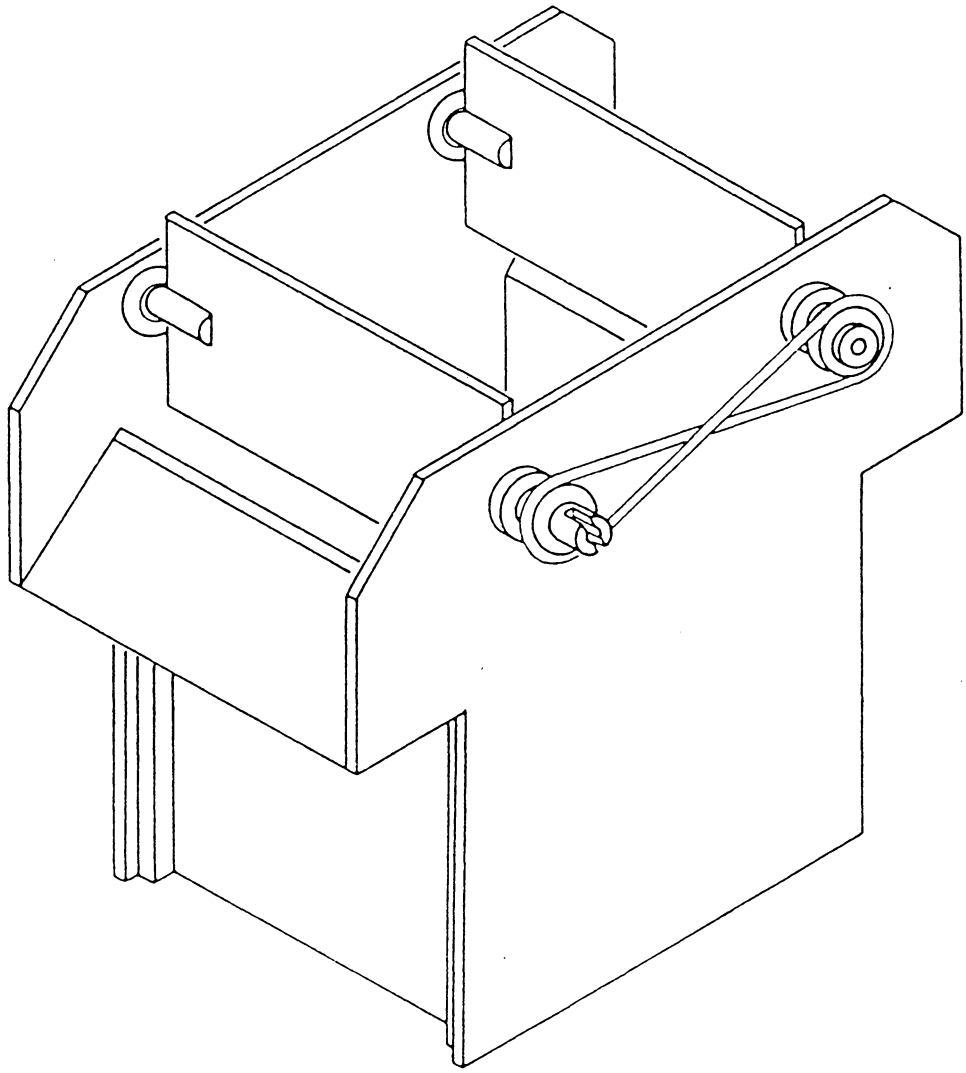

Figure 2.3 Two-paddle design of the plexi-glas flotation cell.

electronic circuit diagram is given in Figure 2.4.

A manuscript describing the flotation machine used in the present work has been published in the International Journal of Mineral Processing. A copy of the manuscript is given in Appendix I.

2.2.4 Mass Spectrometer

Quantitative determination of elemental sulfur present on the surface of chalcopyrite was made by means of a Varian MAT 112 Mass Spectrometer. The instrument was capable of scanning the mass range from 1 to 1000 amu with linear scan rates up to 100 mass units per second.

Samples to be analyzed could be entered directly as a liquid or solid. Solid samples were placed in specially designed Pyrex glass capillary tubes 1 cm in length. The capillary tube was placed at the end of a stainless steel rod for insertion into a vacuum lock. The sample inlet probe temperature could be raised or lowered to suit particular specifications. A simplified schematic diagram depicting the general layout of the mass spectrometer used in this investigation is shown in Figure 2.5.

The spectrometer was equipped with an electron multiplier tube which was used in the pulse counting mode for fast scans. The use of the electron multiplier tube allows a signal gain of approximately 10^{-7} electrons per ion. Thus, it was even possible to count a single ion arriving at

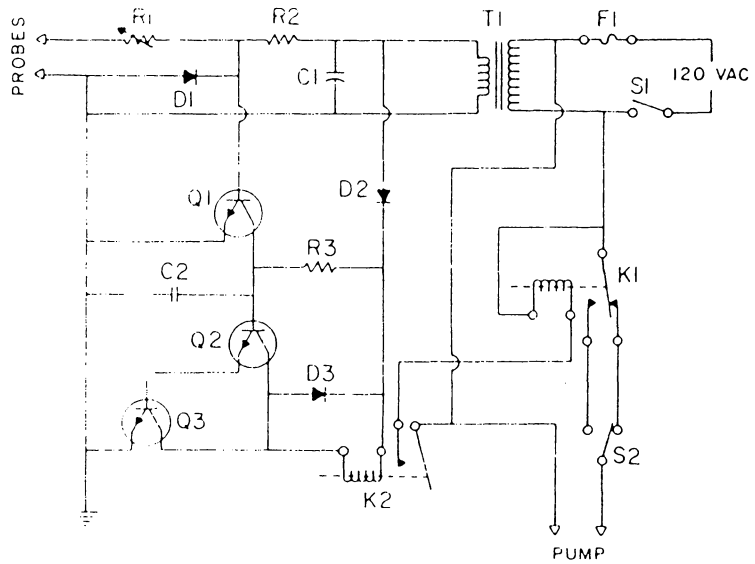

LEVEL CONTROLLER - PARTS LIST

R1 - 50,000 ohm Potentiometer
R2 - 300,000 ohm, 0.5 watt, 5% Resistor
R3 - 470,000 ohm, 0.5 watt, 5% Resistor
T1 - 120 VAC to 6.3 VAC @ 300 mA Power Transformer
F1 - 8 amp Fuse
S1 - SPST Switch
S2 - SPDT Switch
Q1,Q2,Q3 - 2N3904 NPN Transistor
K1 - 110 VAC, SPST Relay (Coil rated at 250 to 500 ohms)
D1,D2,D3 - 1N4002 Diode
C1 - 500 uF, 25 VDC, Electrolytic Capacitor
C2 - 0.5 uF, 25 VDC, Mylar Capacitor

Figure 2.4 Electrical circuit diagram of the pulp level controller.

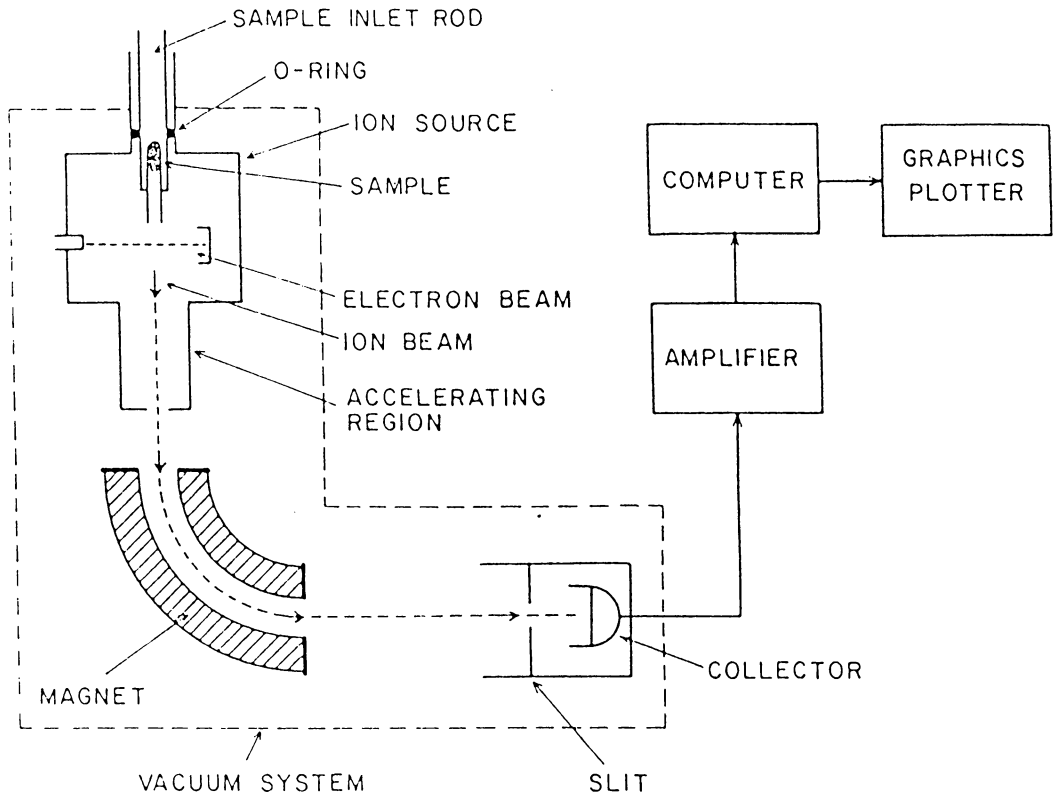

Figure 2.5 Simplified schematic diagram of the mass spectrometer.

the detector. This makes mass spectrometry useful in a number of applications where most other analytical devices do not have sufficient sensitivity. At maximum sensitivity, the instrument had the capability of detecting down to 1 x 10^{-9} grams of volatile material. Vacuum was maintained at less than 10^{-5} torr during testing.

Data from the spectrometer was collected and processed by a Digital Electronics Corporation computer which had been modified by Varian for this particular application. The data was then recalled from the computer memory and reduced to yield the desired information. The resultant mass spectra was plotted in graphical or tabular form on a Tektronix Video/Hardcopy unit.

2.2.5 X-Ray Photoelectron Spectroscopy

Surfaces of both pure minerals and flotation concentrates were analyzed by a Dupont 650 X-Ray Photoelectron Spectrometer (XPS). A magnesium anode was used for the generation of x-rays of monoenergetic $K\alpha_{1,2}$ radiation (1253.7 eV). These x-rays strike the sample and eject photoelectrons which pass through a non-dispersive high- and low-pass filter energy analyzer. A simplified system schematic for this instrument is shown in Figure 2.6. The electrons transmitted through the analyzer were detected by means of an electron multiplier.

The data from the spectrometer was in analog form

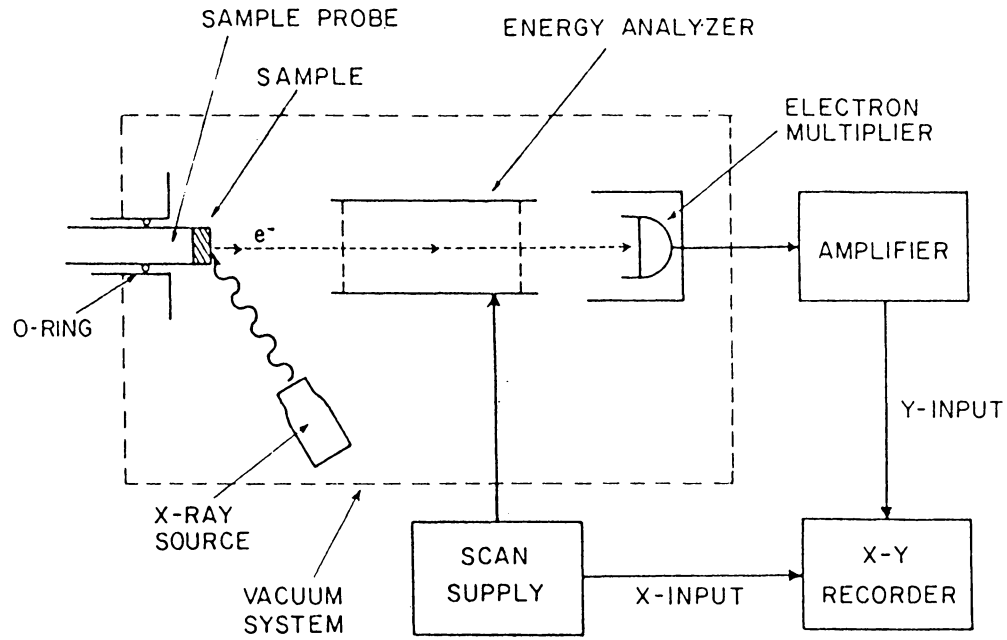

Figure 2.6 Simplified schematic diagram of the x-ray photoelectron spectrometer.

(counts/second/centimeter) and plotted on the vertical scale against electron binding energy in eV, decreasing from left to right, on the horizontal scale. The analog data was first collected on a Nicolet Series 1070 Signal Averaging Computer. This device allows digital smoothing to be performed prior to plotting on a built-in 11" x 17" X-Y plotter.

The Dupont 650 XPS was capable of scanning a binding energy ranging from 0 to 1200 eV. Scanning speed was linear at 6 rates from 0.002 to 5 eV/second.

Some of the samples were analyzed using a more advanced instrument (Perkin-Elmer Model 550 ESCA/SAM Spectrometer) which was equipped with an argon sputtering gun for depth profiling.

When desired, spectra were curve-resolved using a digitizer (Numonics Model 1224 Electronic Digitizer) interfaced with a Northstar Micro-Computer. The curve-fitting computer program developed in the present work is given in Appendix II. The program allowed simple curve fitting of up to three peaks per individual unresolved envelope and performed three basic operations. Firstly, the unresolved envelope was corrected by subtraction of a linear baseline caused by a rising background level which increased with binding energy. Secondly, after the standard binding energies and peak widths at half intensity were entered into the program, up to three best-fitting Gausian peaks were

obtained. Finally, if the fit was found to be statistically undesirable (i.e., variance was too high), then newly designated peak locations and widths could be entered.

2.2.6 UV Spectrophotometry

The concentration of elemental sulfur dissolved in ethanol was determined using a double beam Varian DMS 90 UV-VIS Spectrophotometer. This particular instrument could operate in either absorbance or percent transmittance readout modes at fixed or scanning wavelengths. Wavelength scanning capability was from 190 to 900 nm. When in the scanning wavelength mode, wavelength could be recorded as a function of absorbance by means of a Hewlett Packard 7015B X-Y Recorder. Absorbance was also given by an LED readout. When in the fixed wavelength mode, the absorbance could be recorded as a function of time. The absorbance range of the spectrophotometer was from -0.5 to +2.5. The instrument monochromater was automatically calibrated at 350 nm when the instrument was initially switched on.

2.3 Procedure

2.3.1 Potential Measurements

Pulp potentials were measured by placing a bright platinum-calomel electrode pair into the suspension and obtaining a millivolt reading from a high-impedance voltmeter. In some tests, "contact potentials" were also measured at the end of conditioning by placing a disc-type platinum electrode against the particle bed. Potentials so measured, converted to the standard hydrogen scale by assuming that the calomel reference electrode has a potential of 0.254 volts on this scale (Bates, 1964), are referred to throughout this report as "potential." In general, positive potentials are associated with oxidizing conditions and negative potentials with reducing. By no means is it implied that this potential represents the reversible Nerst potential (Heyes and Trahar, 1977; Gardner and Woods, 1979). Performance of the electrode pair was checked prior to each test by calibration in ZoBell solution (Garrels and Christ, 1965, p. 135). The ZoBell solution consists of 1/300 moles/l potassium ferrocyanide, 1/300 moles/l potassium ferricyanide and 1/10 moles/l potassium chloride which yields a measured potential of 0.430 volts at 25°C. Since platinum is susceptible to poisoning by sulfide (Natarajan and Iwasaki, 1973), the platinum electrodes were mechanically cleaned prior to each test using emery paper.

2.3.2 Micro-Flotation

Micro-flotation experiments were conducted on pure chalcopyrite (Transvaal Deposit, South Africa) and pyrite (Huanzala District, Peru) samples using a Partridge and Smith-type flotation cell described earlier. In each test, a 1.0 gram sample of -65/+100 mesh fraction was placed in the flotation cell with approximately 70 ml of doubly distilled water. After adding appropriate reagents, a gentle agitation was provided to the particle bed for approximately 5 minutes. Pulp potentials were raised or lowered by adding various amounts of 1% potassium permanganate solution or 1% sodium sulfide solution, respectively. Manual stirring of the solution with a glass rod was done to ensure complete mixing.

Potentials were monitored during the conditioning period in some of the batch flotation experiments. After conditioning, a one minute flotation time was employed by passing approximately 40 ml/minute of ultra-pure nitrogen gas through a glass frit to generate bubbles. No frothers were used in any of the micro-flotation experiments. Some micro-flotation experiments were conducted in buffer solutions of pH 4.0 (0.05 moles/l potassium biphthalate), 7.0 (0.05 moles/l potassium phosphate monobasic / sodium hydroxide) and 10.0 (0.05 moles/l potassium carbonate / potassium borate / potassium hydroxide) while controlling the potential by adding varying amounts of 1% sodium sulfide

solution.

2.3.3 Batch Flotation

In conventional flotation tests, potassium amyl xanthate (AERO 350) and sodium diisopropyl dithiophosphate (AERO 211) were used as collectors for chalcopyrite and sphalerite, respectively. In collectorless flotation tests, sodium sulfide flakes were used as a surface cleaning agent for sulfide minerals. Dowfroth 250 was used as the frother in all the batch flotation tests. Once the necessary amount of frother was determined, the same amount was used for all succeeding tests. For pH adjustment, lime, sodium hydroxide and hydrochloric acid were used. All batch flotation tests were performed using an automated laboratory flotation machine described previously.

To prepare for chalcopyrite flotation, a 1000-gram sample was wet-ground for 30 minutes at 90 revolutions per minute in a McDaniel porcelain laboratory ball mill (23 x 21 cm) using 600 ml of tap water and 10 kg of steel balls (1.0 to 2.5 cm diameter). Some tests were made after dry-grinding the ore using a 6 kg-load of porcelain balls (2.5 cm diameter) as grinding media.

The ground ore pulp was transferred to a 4-liter rougher flotation cell which was mounted on an automated laboratory flotation machine. After filling the remaining cell volume with tap water to within 1 cm of the overflow

cell lip, appropriate reagents were added to the cell and the pulp was conditioned for a desired time. When using sodium sulfide, a 15-minute conditioning time was employed for both rougher and scavenger flotation stages. For cleaner stages, the pulp was agitated for 3 minutes before flotation. A typical flowsheet for sodium sulfide flotation is shown in Figure 2.7. In some tests, potentials of the pulp were monitored during the entire 15-minute conditioning, 5 minute flotation and 10 minute trail periods using a strip chart recorder. In conventional flotation, only a 5 minute conditioning time was employed prior to the rougher and scavenger flotation. All flotation stages were allowed to proceed until exhaustion unless otherwise noted.

Two different procedures were used in the flotation of sphalerite. When using a 1000-gram sample, the procedure was the same as previously described for chalcopyrite flotation, except that copper sulfate was added 5 minutes prior to the rougher and scavenger flotation stages. However, the majority of sphalerite flotation experiments were performed without cleaning stages using 500 grams of ore and the 2-liter flotation cell. The various experimental parameters used in these flotation tests are given in Appendix III. In the experiments where 500 grams of ore were used, a constant flotation time of 5 minutes was employed.

After flotation, each flotation product was dried and

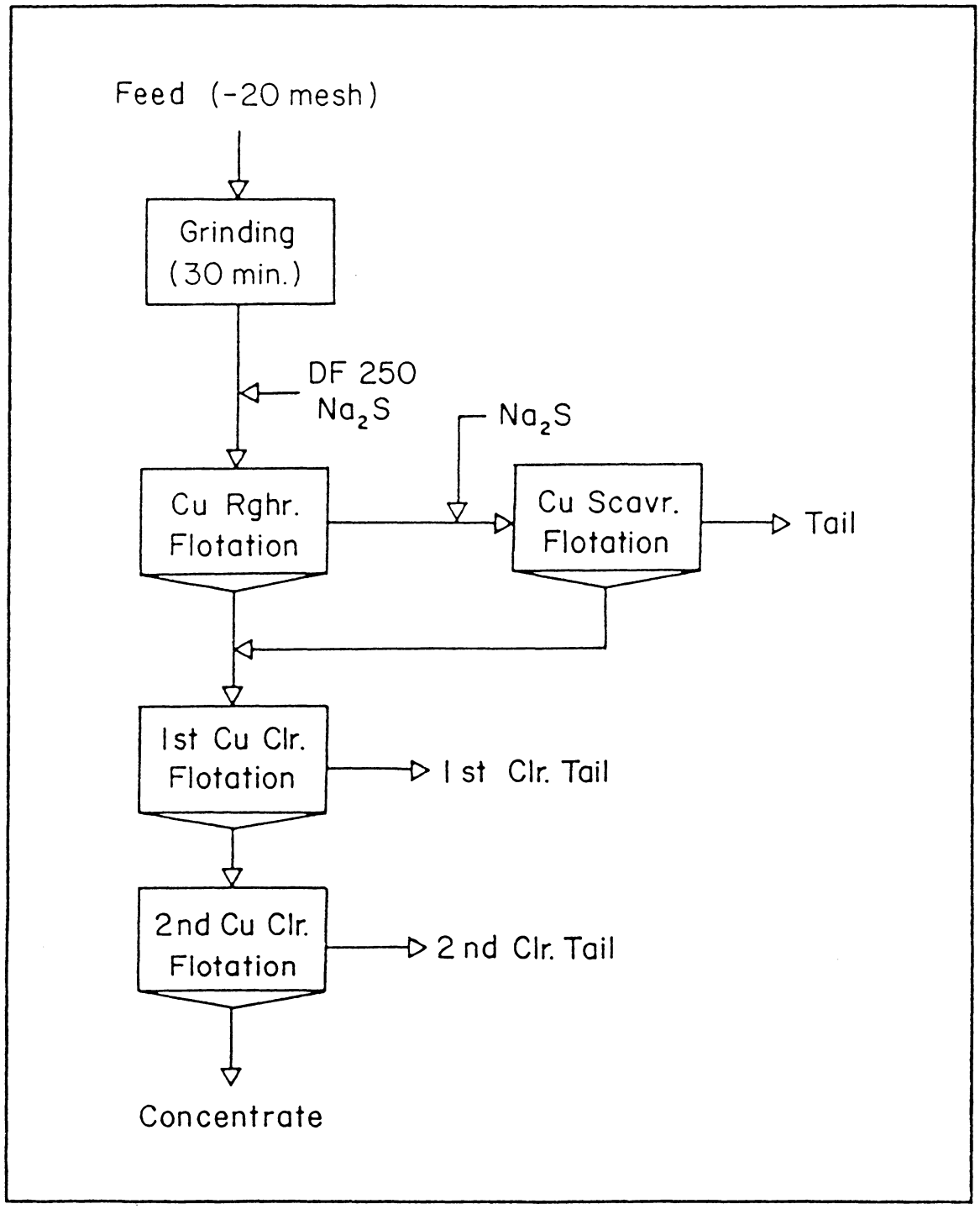

Figure 2.7 Typical laboratory flowsheet used in the batch flotation of chalcopyrite with sodium sulfide.

weighed. A fraction of each was then digested in a 1:1 mixture of hydrochloric and nitric acid, and the filtrate was analyzed for copper and/or zinc using a Spectrospan IV plasma emission spectrometer. This unit is more suitable for mineral processing applications than an atomic absorption unit because it has a greater dynamic linearity range and, therefore, requires less dilutions. A detailed assaying procedure is included in Appendix IV.

2.3.4 Mass Spectrometry

In order to determine the amount of sulfur formed on chalcopyrite conditioned at various pH values, a series of mass spectrometry experiments was performed using a finely ground chalcopyrite sample. These samples were prepared by dry grinding a sample of -100 mesh chalcopyrite under an ultra-pure nitrogen atmosphere for a period of 3 hours. Grinding was accomplished using a mechanically operated agate mortar and a pestle. Transfer of the ground sample was done only in sealed nitrogen-filled containers.

After grinding, 1-gram fractions of the chalcopyrite powder were placed in 50 ml of doubly distilled water which had been adjusted to pH values ranging from 2 to 12. Hydrochloric acid and sodium hydroxide solutions were used to adjust the pH. The samples were conditioned in the solutions of various pH values for 10 minutes. The samples were then transferred to centrifuge vials and centrifuged at

3250 rpm for 10 minutes. When completed, the supernatant solution was carefully removed and discarded. The solid remaining in the centrifuge vial was placed in a vacuum desiccator over silica gel and flushed with ultra-pure nitrogen. A vacuum was then applied by means of a mechanical pump and the samples were allowed to dry for 3 hours. A 2 mg fraction of the chalcopyrite sample, thus prepared, was carefully weighed into a sampling vial made of a glass capillary tube 1 cm in length which was sealed at one end.

Calibration standards of elemental sulfur were prepared in the following manner. Laboratory grade sulfur was dissolved in acetone to produce a standard of 2.5×10^{-6} grams sulfur/ml acetone. From this stock solution, aliquotes were taken and mixed with 1 gram samples of the finely pulverized chalcopyrite. The acetone was then evaporated under a light vacuum created by a tap water aspirator. Once the sample had dried, it was lightly mixed using a glass stirring rod to obtain a homogenous sample. From each sample, 2 mg fractions were then carefully weighed into glass capillary tubes as described previously. All the procedures, with the exception of weighing, were carried out in a plastic glovebox flooded with ultra-pure nitrogen.

The sample tubes used in these experiments were baked overnight at 300°C and then allowed to cool in a desiccator. Above 200°C most oxygen- and nitrogen-containing compounds are thermally decomposed (Willard, Merrit and Dean, 1965, p.

430). Once cleaned, handling was done only with clean tweezers. Great care was taken to prevent cross contamination between samples. The vacuum manifold of the spectrometer was also baked overnight before use so as to ensure low background levels.

It should be noted that the largest sources of errors associated with this experimental procedure were probably due to weighing and sampling errors. The dry chalcopyrite sample was exposed to air only during weighing, loading and insertion into the spectrometer. This typically required less than 5 minutes of total air exposure. Once a sample was prepared, it was taken within 6 hours for testing in the mass spectrometer.

Just prior to introducing the sample vial into the ionization chamber, scanning between mass numbers 50 to 80 was begun. Quantitative detection of elemental sulfur was based on the intensity of the S_2^+ peak at M/e = 64. This peak was chosen since it is the most intense peak in the mass spectrum of elemental sulfur (Bradt et al., 1956; Berkowitz, 1965; Ralston, Alabaster and Healy, 1981). Approximately 6 seconds were required to complete a single scan. Data from each successive scan was stored as it was obtained on a computer disc. During the scanning period, the sample inlet probe was heated to approximately 90°C to aid vaporization from the solid surface.

Scans were continued until the peak intensities of

interest approximately returned to the normal backgound levels. This generally required less than 10 minutes. Once scanning was terminated, data was plotted as relative peak intensity versus scan number for a given mass number. The area under this curve was considered as representative of the amount of a particular vaporized component, which in this investigation was sulfur.

Calibration of the mass spectrometer was accomplished using perfluorokerosene-L.

2.3.5 X-Ray Photoelectron Spectroscopy

a. General Procedure: Most of the XPS spectra were collected using a Dupont 650 Spectrometer. Vacuum was maintained below 10^{-6} torr for the generation of x-rays and clean transmission of electrons. Anode current and voltage were typically operated at 22 mA and 10 kV, respectively. Sample temperature was observed to increase only slightly during the analysis.

To obtain a spectrum, samples were first horizontally mounted on a 0.25-inch diameter cylindrical sample peg by means of double-sided adhesive tape. Caution was exercised during mounting to avoid cross contamination between samples. The sample peg was then screwed into the tip of an inlet probe and pushed up through the bottom of the device into a vacuum lock. Once the desired vacuum was reached and the sample had degassed sufficiently, the vacuum lock was

opened and the sample was introduced into the analyzer chamber. Analyzer voltages were then switched on and spectra collected. Analyzer voltages could not be switched on if the vacuum pressure was in excess of 10^{-5} torr.

To avoid interference of the copper-zinc alloy peg with copper in the sulfide samples, gold-plated sample pegs were used in place of the usual bronze pegs. Charge correction was made by assigning a binding energy of 284.6 eV to the main carbon peak and adjusting the other peaks according to the shift which the carbon 1s peak exhibited.

Collection of a set of spectra for a given sample generally required less than 45 minutes. This, of course, depended upon the number of elements under examination and the particular setting of instrument parameters (i.e., scanning speed, number of scans, etc.). Typically, only the carbon 1s, sulfur 2p, iron 2p, copper 2p and copper Auger spectra were obtained. Longer scans were performed on some samples to determine the effects of photoreduction.

b. XPS on Pure Mineral Samples: XPS was used to identify the surface species formed on chalcopyrite which had been subjected to a number of different treatments (e.g., as a function of the potential of the solution in which the samples were immersed). The results were compared with those suggested by Gardner and Woods (1979) on the basis of their electrochemical studies. Since elemental

sulfur and CuS were identified by these investigators as the oxidation products on chalcopyrite, the XPS spectra of pure samples of elemental sulfur and covellite were also obtained for comparison with those of chalcopyrite samples treated under various conditions. The elemental sulfur and covellite samples were analyzed by XPS as received without special surface treatment.

Various micro-flotation products were analyzed by XPS. After flotation, both the float and non-float products were dried separately under vacuum in a desiccator over silica gel. Each sample was then removed for the desiccator, quickly weighed in air, and returned to the vacuum. The weighing procedure generally required less than 5 minutes. Samples were maintained under vacuum until XPS analysis was done (less than 24 hours). Since sample mounting generally required less than 5 minutes, samples were exposed to air for a total of no more than 10 minutes prior to analysis.

c. XPS on Copper Ores: Surface analyses were also performed on flotation concentrates from the Ray Mines and Mount Isa chalcopyrite ores. It was thought that the surface chemistry of pure minerals might be different from that of actual ore samples. XPS analysis of concentrates from the Mount Isa ore were obtained after flotation at pH values of 6.5 and 10.0 using 3 lb/ton of sodium sulfide. Concentrates from the Ray Mines ore used for the XPS

analysis were obtained by flotation both with and without sodium sulfide. In order to determine the surface conditions of chalcopyrite prior to flotation, chalcopyrite was concentrated from each of these ores by a gravity separation technique and were analyzed by XPS.

In order to compare the surface of chalcopyrite with that of the bulk, XPS spectra was taken of a chalcopyrite concentrate before and after argon-sputtering. For this particular experiment, a Texasgulf copper-zinc ore from Canada was used. The ore contained 2.78% Cu, 0.10% Pb, 6.92% Zn, 12.80% Fe and 0.40 oz/ton Ag. A Perkin-Elmer Model 550 ESCA/SAM was used for the collection of these spectra. The flotation concentrate analyzed by XPS was obtained after four stages of cleaner flotation at pH 6.0. The ore had been wet-ground with 1.5 lb/ton of technical grade sodium sulfide.

2.3.6 UV-VIS Spectrophotometry

To supplement the surface analysis results obtained by using XPS and mass spectrometric techniques, chalcopyrite samples treated under various conditions were contacted with ethanol, and the ethanol extract was analyzed for elemental sulfur by UV spectrophotometry. This technique is not as sensitive as the others employed in the present work, but has a distinct advantage in that the chalcopyrite samples need not be dried for analysis.

The UV-analyses were conducted both with and without drying the chalcopyrite samples to see if there was any difference. After conditioning, the chalcopyrite suspension was centrifuged at 3750 rpm for 10 minutes, and the supernatant solution was removed and discarded. A fraction of the moist chalcopyrite left in the centrifuge vial was vacuum-dried over silica gel for 2 hours, and 0.25 grams of the dried sample was contacted with 50 ml of ethanol in a flask. The contact time was allowed for 30 minutes during which the suspension was continuously agitated by means of a mechanical shaker. The suspension was then centrifuged at 3750 rpm for 10 minutes. A portion of the supernatant solution was placed in a cuvette and the absorbance was measured at 275 nm with pure ethanol in the reference cuvette. Friedman and Kerker (1953) and Bass (1953) have reported that elemental sulfur dissolved in ethanol showed a characteristic peak at 275 nm.

The remainder of the chalcopyrite in the centrifuge vial was transferred into a 50-ml flask while the chalcopyrite was still moist. The sample was then contacted with 50 ml ethanol, centrifuged and the supernatant solution was analyzed at 275 nm in the same manner as with the vacuum-dried sample. After the UV spectra was taken, the exact weight of the chalcopyrite sample was determined by drying and weighing the solid remaining in the centrifuge vial. The detailed calibration procedure is given in Appendix V.

III. EXPERIMENTAL RESULTS

3.1 Micro-Flotation

3.1.1 Flotation of Chalcopyrite

a. Effect of Potential: Figure 3.1 shows the results of the micro-flotation tests conducted on pure samples of chalcopyrite as a function of potential. The mineral sample used in these experiments was freshly fractured in air just before each experiment. The potentials were controlled by adding varying amounts of a 1% sodium sulfide solution. The pH was allowed to vary freely depending on the volume of sodium sulfide solution added. In each experiment, both the pulp potential and contact potential were recorded.

When the freshly fractured sample was placed in doubly distilled water, the potential of the solution was measured to be +552 mV. At this potential, 84% of the chalcopyrite floated. As the potential was reduced by adding increasing amounts of sodium sulfide, the floatability was reduced gradually as shown in Figure 3.1. These results appear to confirm the finding of Heyes and Trahar (1977) and Gardner and Woods (1979) that collectorless flotation is possible only under oxidizing conditions.

Figure 3.1 also shows that the contact and solution potentials differ by approximately 100 mV. Nevertheless, both curves display the same trend.

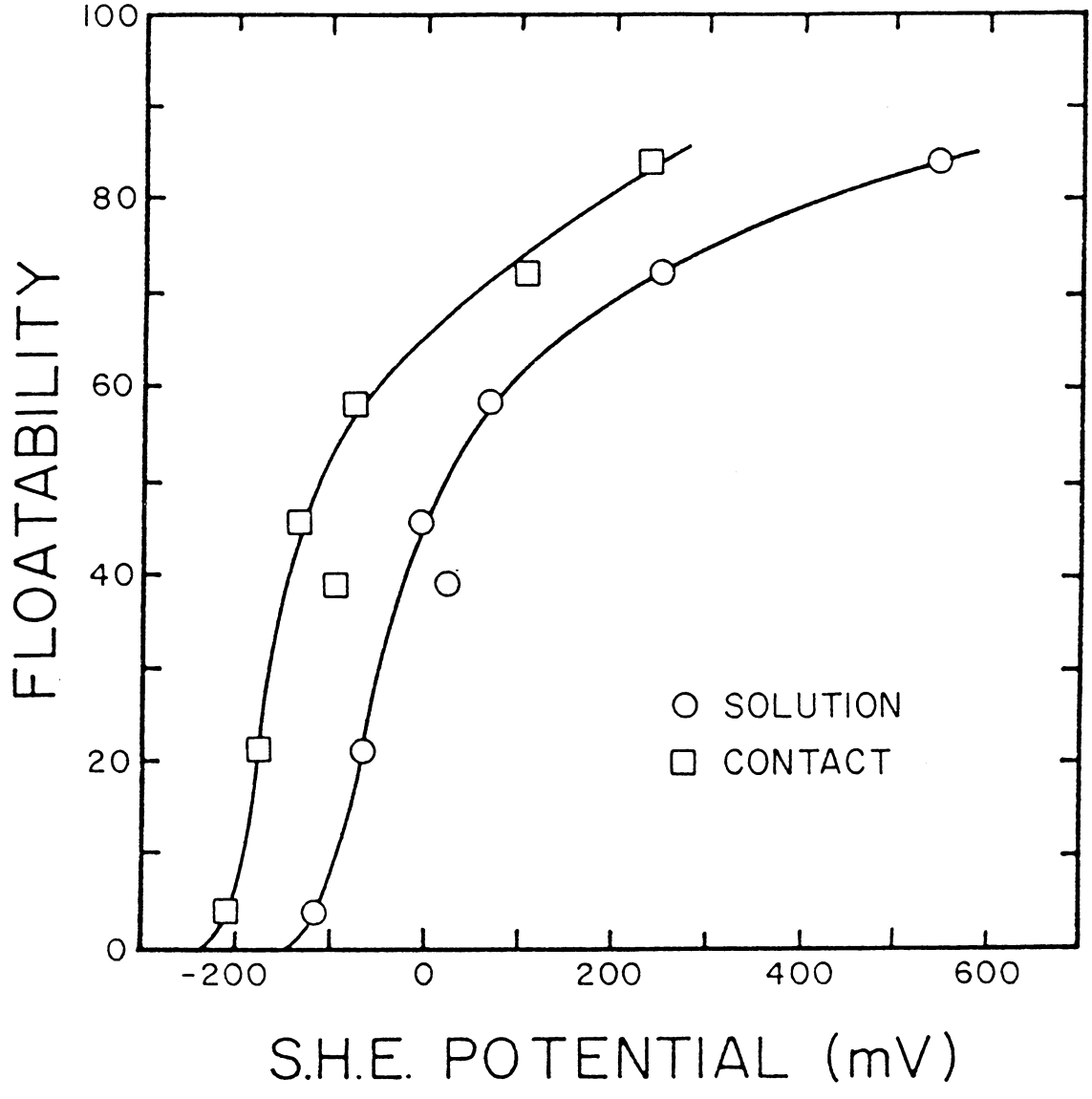

Figure 3.1 Potential versus percent floatability for pure chalcopyrite fractured in air. In each test, potentials were measured 1) by immersing a platinum pin electrode in supernatant solution and 2) by contacting a platinum disc electrode with chalcopyrite bed.

b. Effect of Surface Oxidation: Micro-flotation experiments were also conducted on samples fractured under an ultra-pure nitrogen atmosphere. As shown in Figure 3.2, almost complete flotation (99%) was obtained at a high oxidizing potential of +561 mV when no sodium sulfide was added. As the potential became more reducing, the floatability was decreased. These results again support the finding that an oxidizing condition is necessary for collectorless flotation. However, when the sample was allowed to oxidize in air for three weeks, the maximum floatability was reduced to 36.4% even at a potential as high as +569 mV, and further decreased at lower potentials as shown in Figure 3.2. These results may suggest that collectorless flotation requires not only an oxidizing environment but also that the mineral surface be relatively clean (i.e., free of hydrophilic oxidation products).

Table 3.1 shows the results of the micro-flotation tests conducted on a chalcopyrite sample (-65/+100 mesh) that had been dry-stored in excess of four years with no precautions to prevent oxidation. When the sample received no sodium sulfide treatment, flotation was not possible even at an oxidizing potential of +520 mV. Only after washing with sodium sulfide solutions did the collectorless flotation become possible under oxidizing conditions. After repeated washing in a 1% sodium sulfide solution, the sample became floatable and gave 57% recovery. The floatability

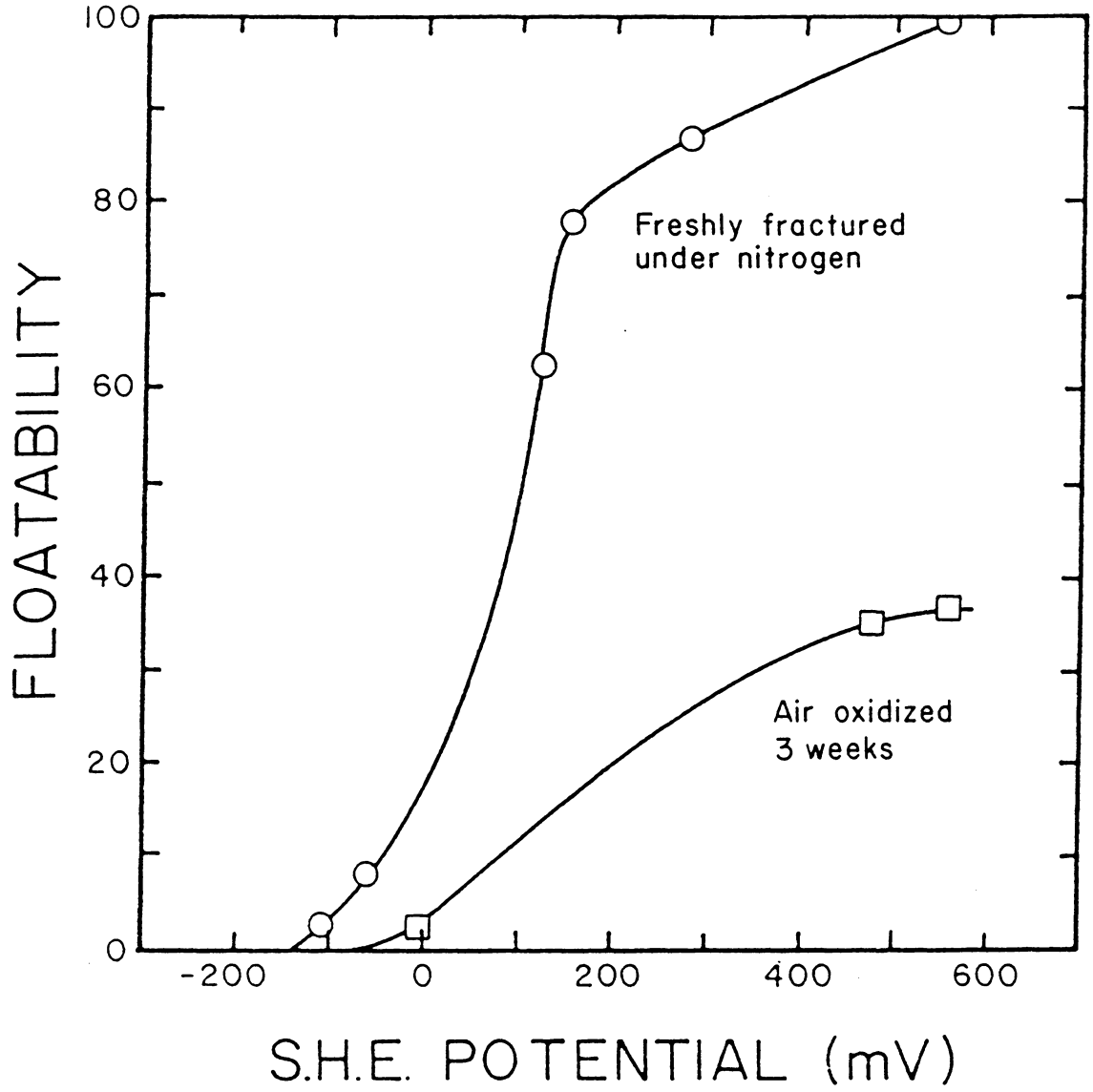

Figure 3.2 Potential versus percent floatability of pure chalcopyrite. No pH control was attempted.

Table 3.1 Results of the Micro-Flotation Tests Conducted on the Heavily Oxidized Chalcopyrite Sample Treated Under Various Conditions

Description	Potential	Floatability
No sodium sulfide treatment	+520 mV	0%
Cleaned by 1% sodium sulfide solution, followed by washing with water	+519 mV	57%
Cleaned by 1% sodium sulfide solution, followed by washing with water and drying	+517 mV	98%
Cleaned by 10% sodium sulfide solution, followed by washing with water	+504 mV	93%

was further increased to 93% by using a stronger sodium sulfide solution (10%) for cleaning the surface. Note also that the floatability of the sample cleaned in the 1% sodium sulfide solution was improved from 57% to 98% after the sample had been dried overnight in air.

These results suggest that for collectorless flotation to occur, it is necessary to have both a relatively clean sulfide surface and slightly oxidizing conditions. It is difficult, however, to understand what the drying process is doing to the surface of the chalcopyrite.

c. Effect of pH: In the micro-flotation tests described in previous paragraphs, an addition of sulfide solution reduced the potential, but it also raised the pH. Therefore, a series of micro-flotation tests were conducted in buffer solutions of pH 4.0, 7.0 and 10.0 while controlling the potential with a sodium sulfide solution. Samples used in these experiments were freshly fractured under ultra-pure nitrogen. The results, given in Figure 3.3, show that the chalcopyrite floated without a collector at potentials above approximately -100 mV at the three pH's investigated. It is important to note, however, that the floatability increases with decreasing pH, which may be attributed to the increased thermodynamic stability of elemental sulfur with decreasing pH.

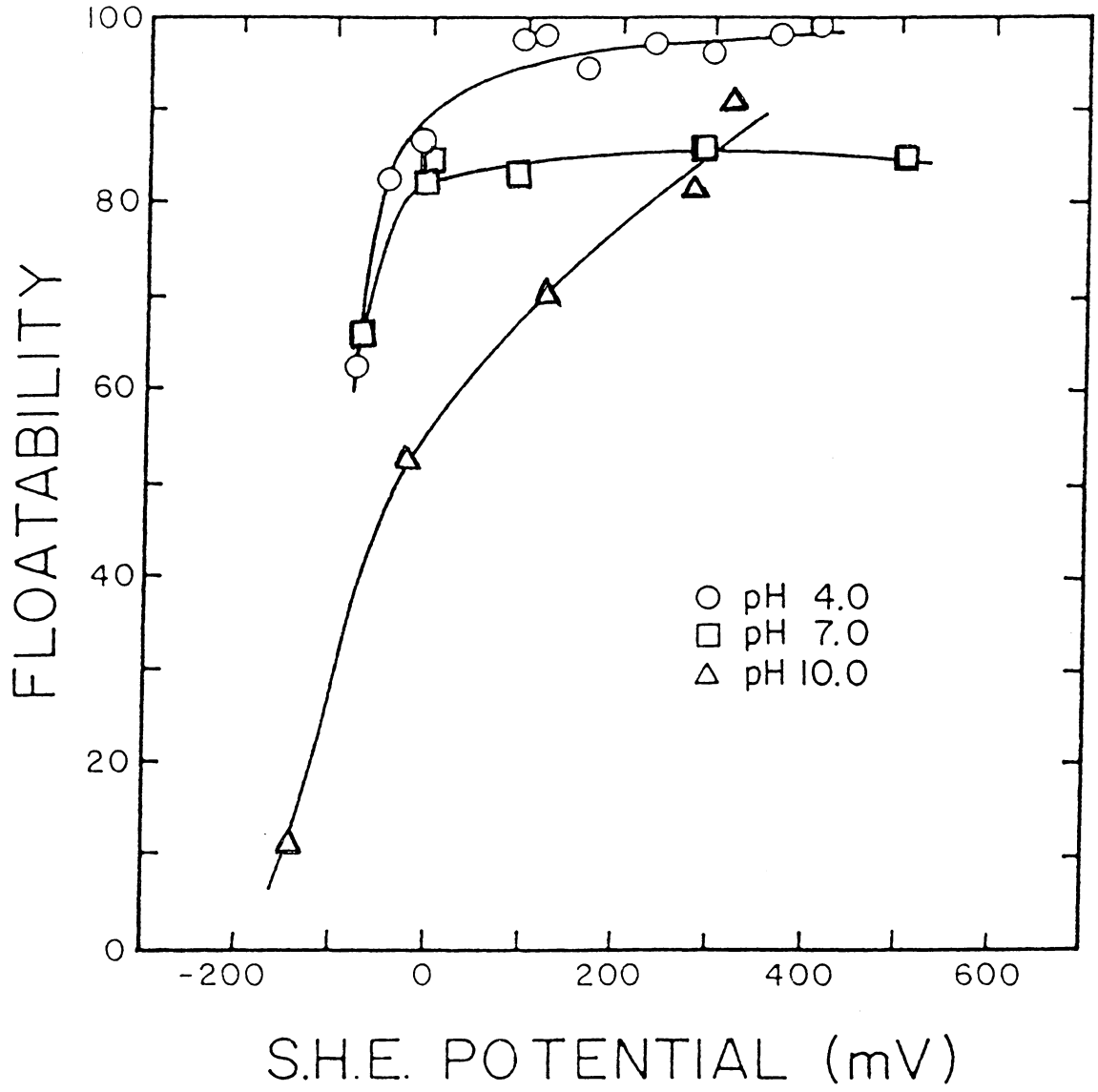

Figure 3.3 Potential versus percent floatability of chalcopyrite in buffer solutions of 4, 7 and 10 for pure chalcopyrite fractured under an ultra-pure nitrogen atmosphere.

d. Hydrazine as a Reducing Agent: In order to determine the effect that reducing agents other than sodium sulfide have on the floatability of chalcopyrite, a series of tests was conducted using hydrazine to control the potential. The results of these experiments are shown in Figure 3.4. The pH was allowed to vary freely with hydrazine addition. As shown, the flotation behavior followed the same trend as that obtained using sodium sulfide as a reducing agent (Figure 3.2).

e. Effect of Potassium Permanganate: Heyes and Trahar (1977) have reported that the collectorless flotation of chalcopyrite was improved by the addition of potassium permanganate, a strong oxidizing agent. Therefore, a group of experiments was performed in which the potentials were raised by adding various amounts of a potassium permanganate solution. Potassium permanganate was added to raise the potential above +215 mV, and sodium sulfide was added to reduce the potential below +215 mV. The results of this series of tests are shown in Figure 3.5. Contrary to Heyes and Trahar's finding, the addition of potassium permanganate adversely affected floatability. A comparison of Figure 3.2 with Figure 3.5 shows that the chalcopyrite flotation was depressed with potassium permanganate at potentials where a maximum floatability was expected. This indicates that some factors in addition to the oxidizing/reducing

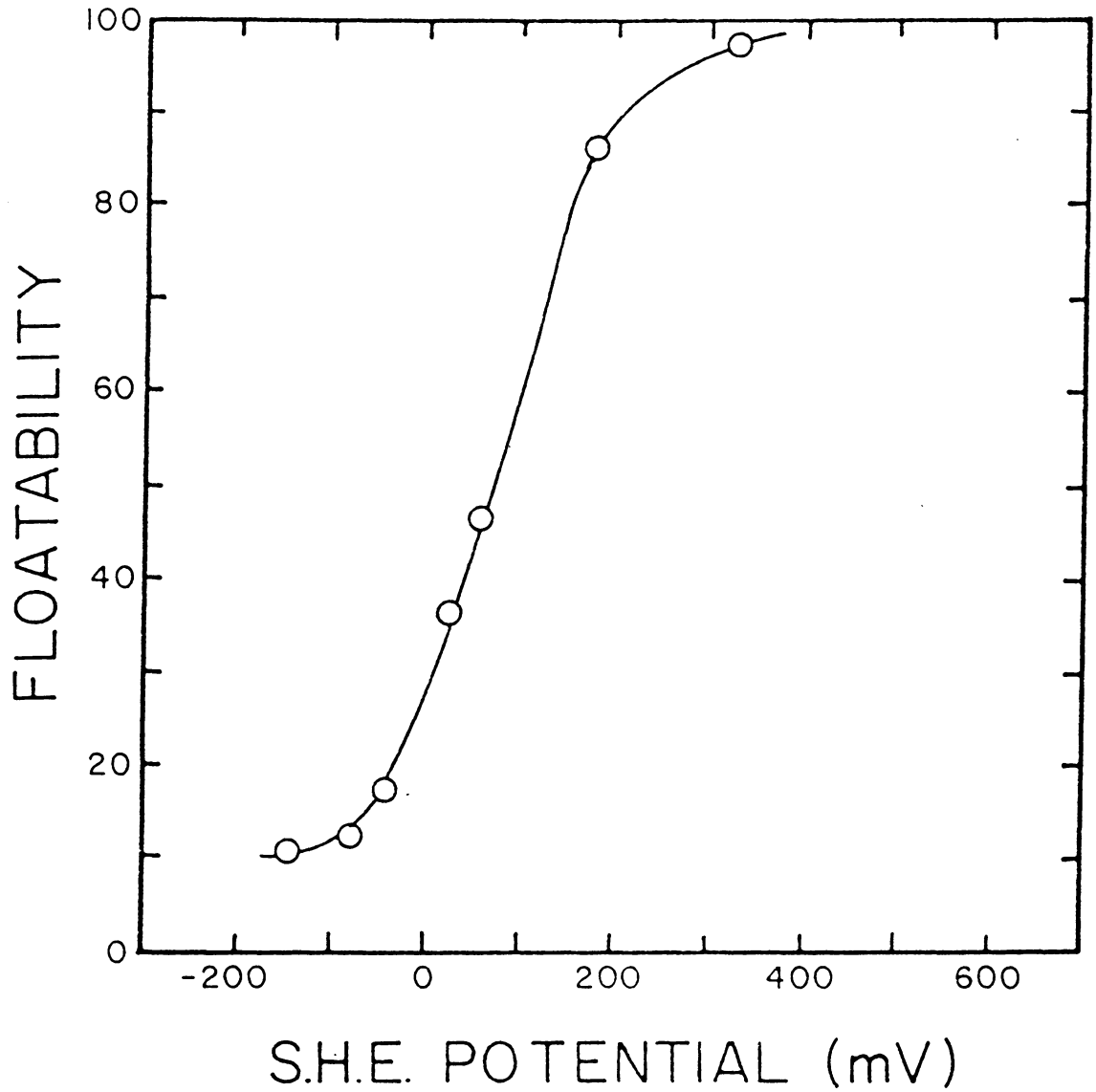

Figure 3.4 Potential versus percent floatability of pure chalcopyrite fractured under a nitrogen atmosphere. Potential was controlled by adding various amounts of hydrazine.

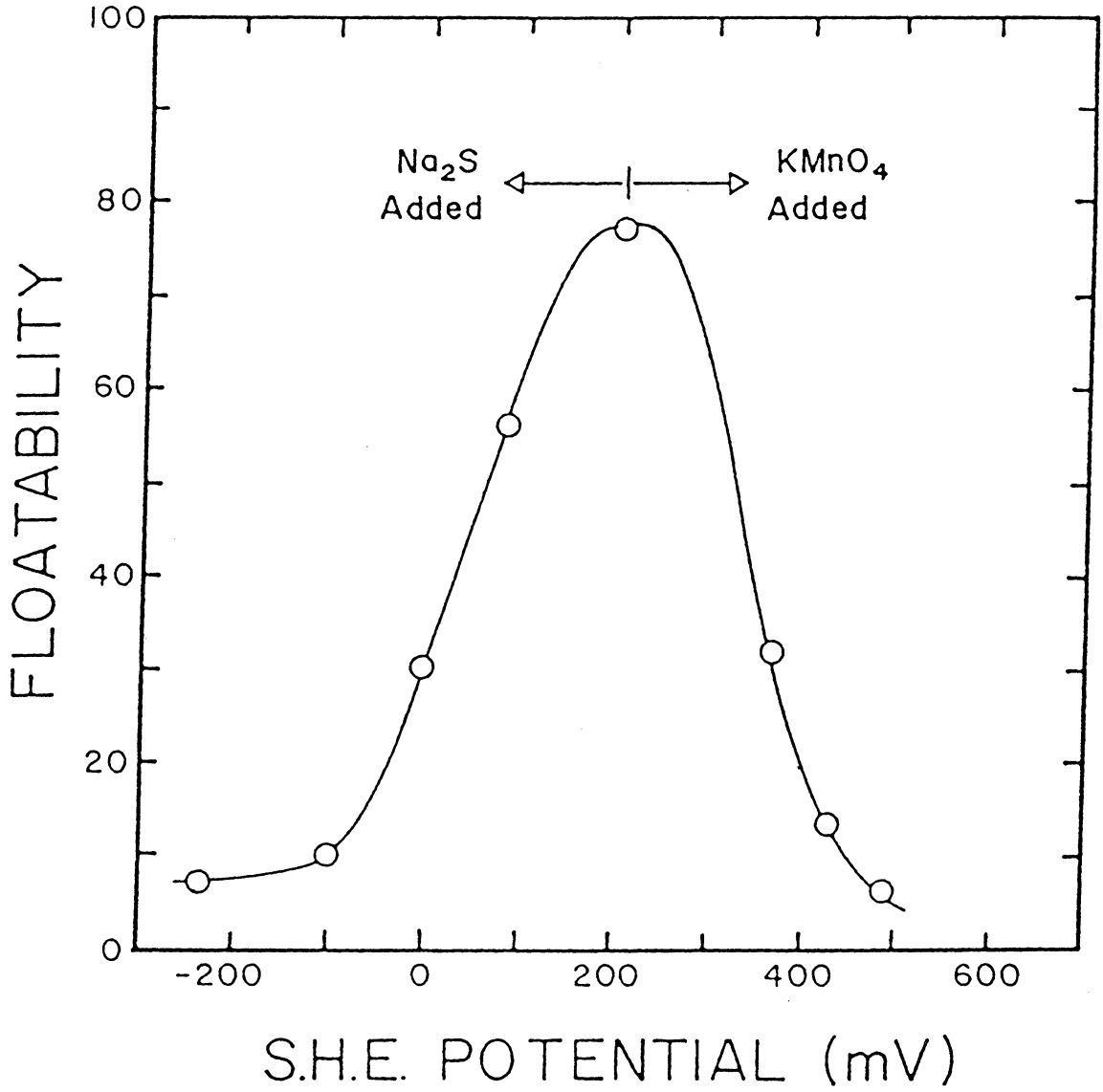

Figure 3.5 Potential versus percent floatability of pure chalcopyrite fractured in air. Potential was controlled using sodium sulfide and potassium permanganate.

conditions may determine the floatability of chalcopyrite.

3.1.2 Flotation of Pyrite

In the batch flotation tests conducted on ore samples containing both chalcopyrite and pyrite, chalcopyrite had been shown to float in preference to pyrite. In order to explain this selectivity, a series of micro-flotation experiments were performed on a pyrite sample as a function of potential. The sample was fractured and screened under an ultra-pure nitrogen atmosphere to minimize oxidation. The results are shown in Figure 3.6. For comparison, the floatability of chalcopyrite is also shown in Figure 3.6 as a dashed curve. These results show that pyrite floats at a lower critical protential than chalcopyrite. Thus, it is difficult to explain the selective flotation of chalcopyrite against pyrite on the basis of the results shown in Figure 3.6. It may be possible that the oxidation behavior of a mixture of sulfide minerals is significantly different from that of individual minerals.

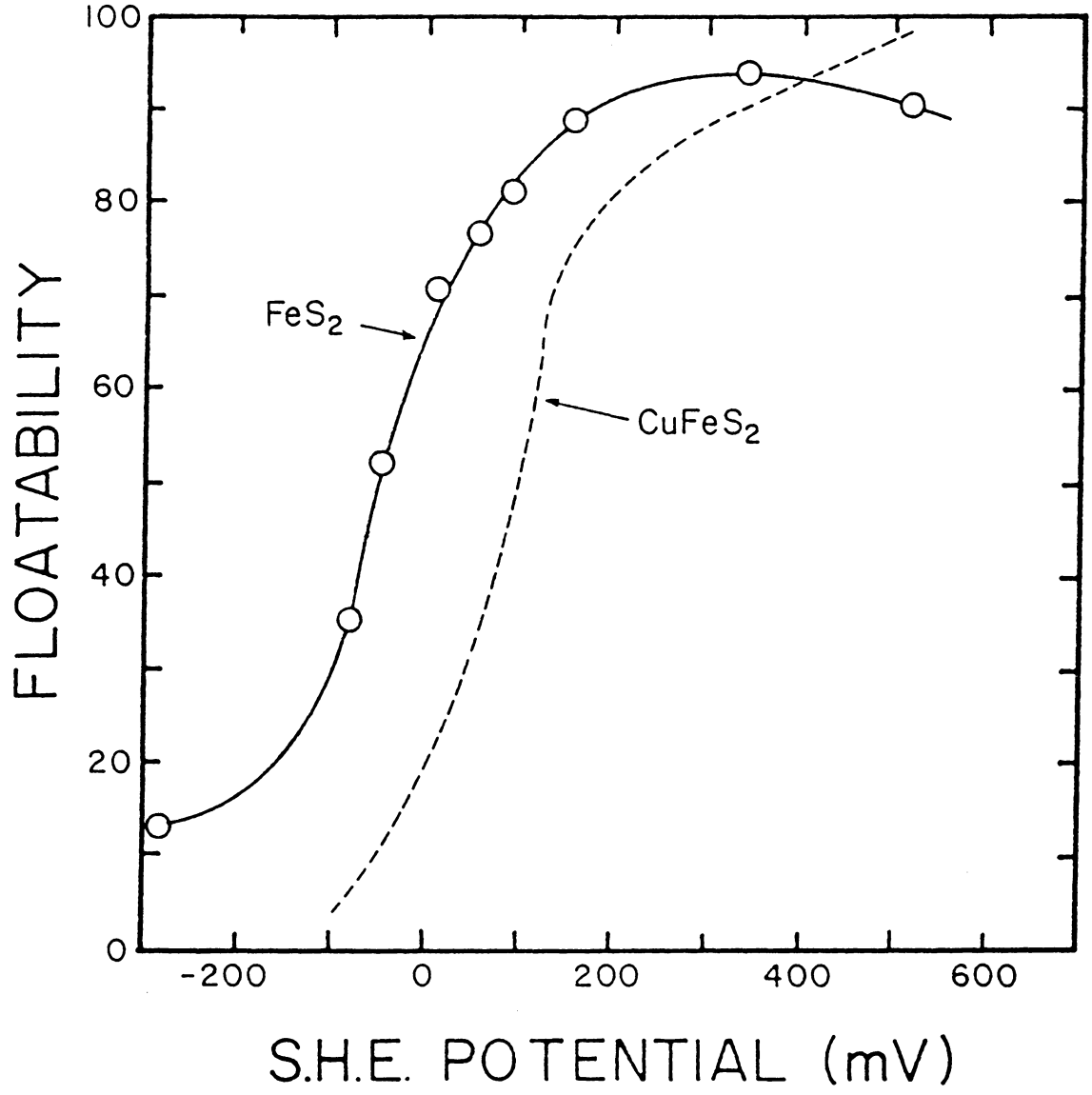

Figure 3.6 Potential versus percent floatability of pure pyrite and chalcopyrite freshly fractured under ultra-pure nitrogen.

3.2 Batch Flotation

3.2.1 Flotation of Chalcopyrite Ores

a. Effect of Sodium Sulfide: Heyes and Trahar (1977) reported that chalcopyrite in the Mount Lyell ore was floatable without a collector while chalcopyrite in the Mount Isa ore was not. On the basis of these results, they classified chalcopyrite ores into two groups: (1) those ores which require no collector or minimal amounts of collectors, and (2) those for which normal collector additions are required. However, no explanations were given for this difference in behavior.

The results of the present investigation seem to suggest the same. The chalcopyrite in the Ray Mines, Craigmont and Falconbridge ore samples floated well with frother alone (Figures 3.7, 3.8 and 3.9), while the chalcopyrite in the Mission Unit, Mount Isa and Utah Mine ores did not (Figures 3.10, 3.11 and 3.12). When the latter samples were treated with 3 lb/ton of sodium sulfide, however, chalcopyrite floated well without a collector. In fact, with the ore sample from the Utah Mine, the collectorless flotation technique yielded better results than did the conventional flotation using potassium amyl xanthate as a collector (Figure 3.12). On the other hand, an attempt to float the Mission Unit ore using 3 lb/ton of sodium sulfide was not very successful. As will be shown later, this was

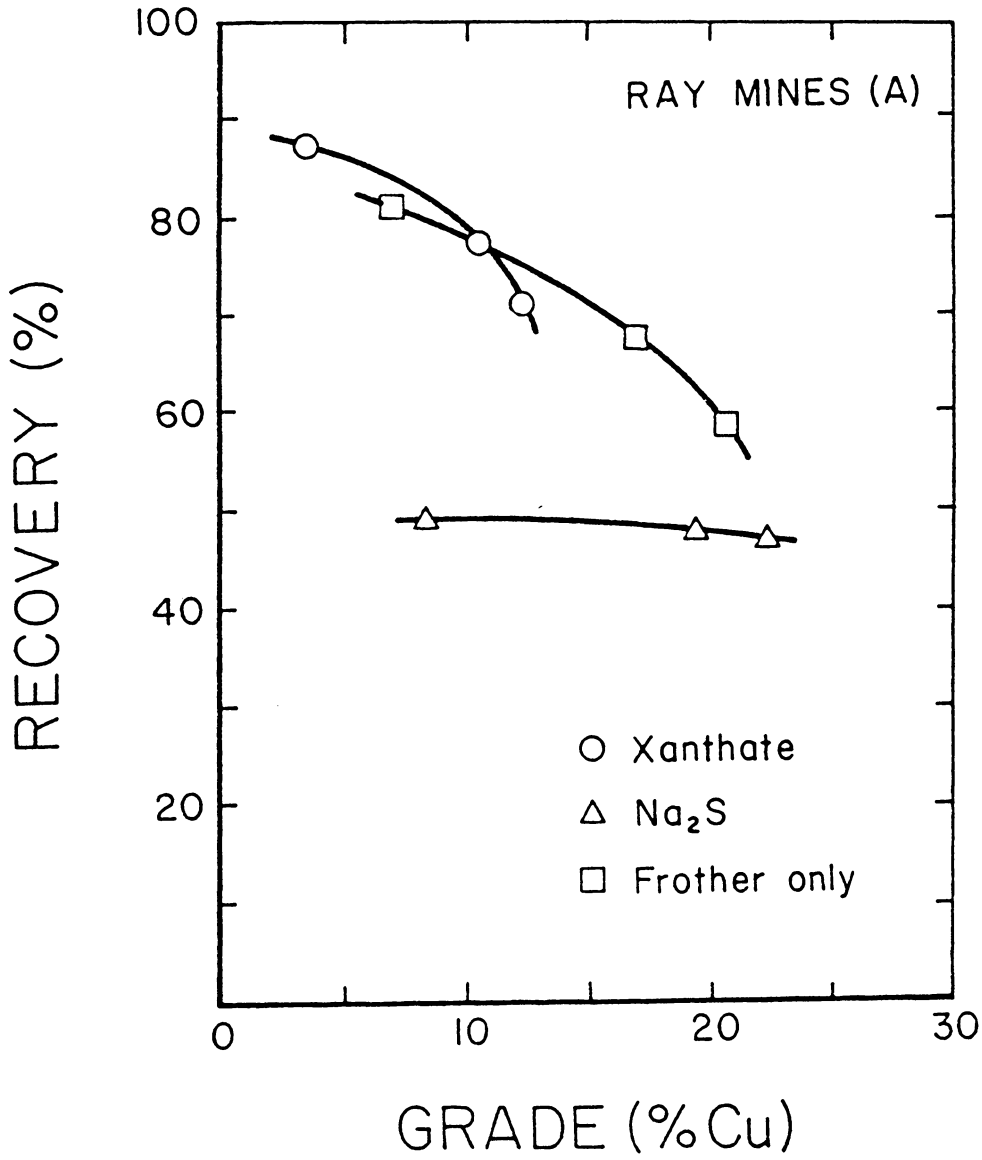

Figure 3.7 Recovery versus grade curves for the batch flotation of the Ray Mines copper ore using 1) 0.03 lb/ton AERO-350, 2) 3 lb/ton Na_2S and 3) 0.14 lb/ton DF-250.

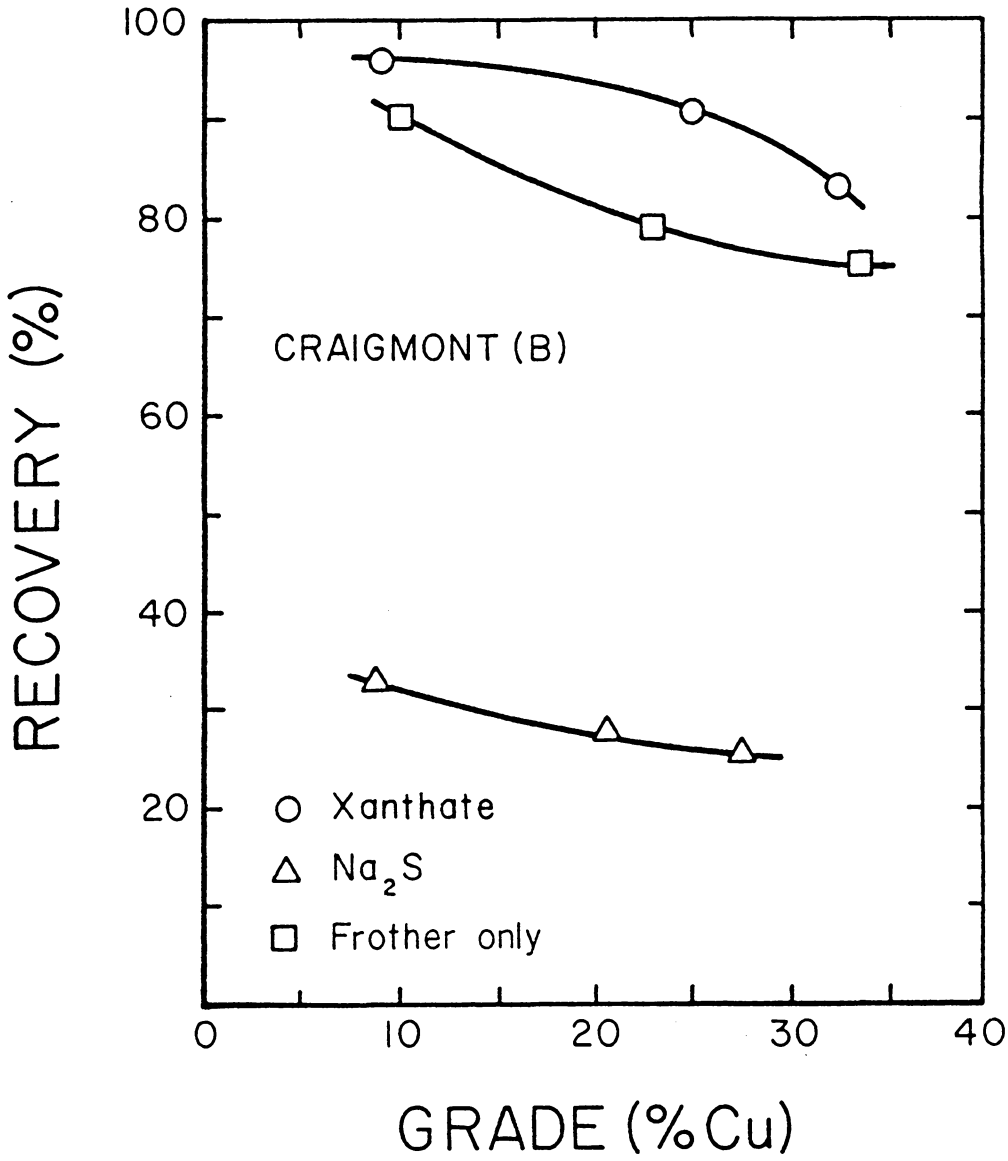

Figure 3.8 Recovery versus grade curves for the batch flotation of the Craigmont copper ore using 1) 0.12 lb/ton AERO-350, 2) 3 lb/ton Na_2S and 3) 0.26 lb/ton DF-250.

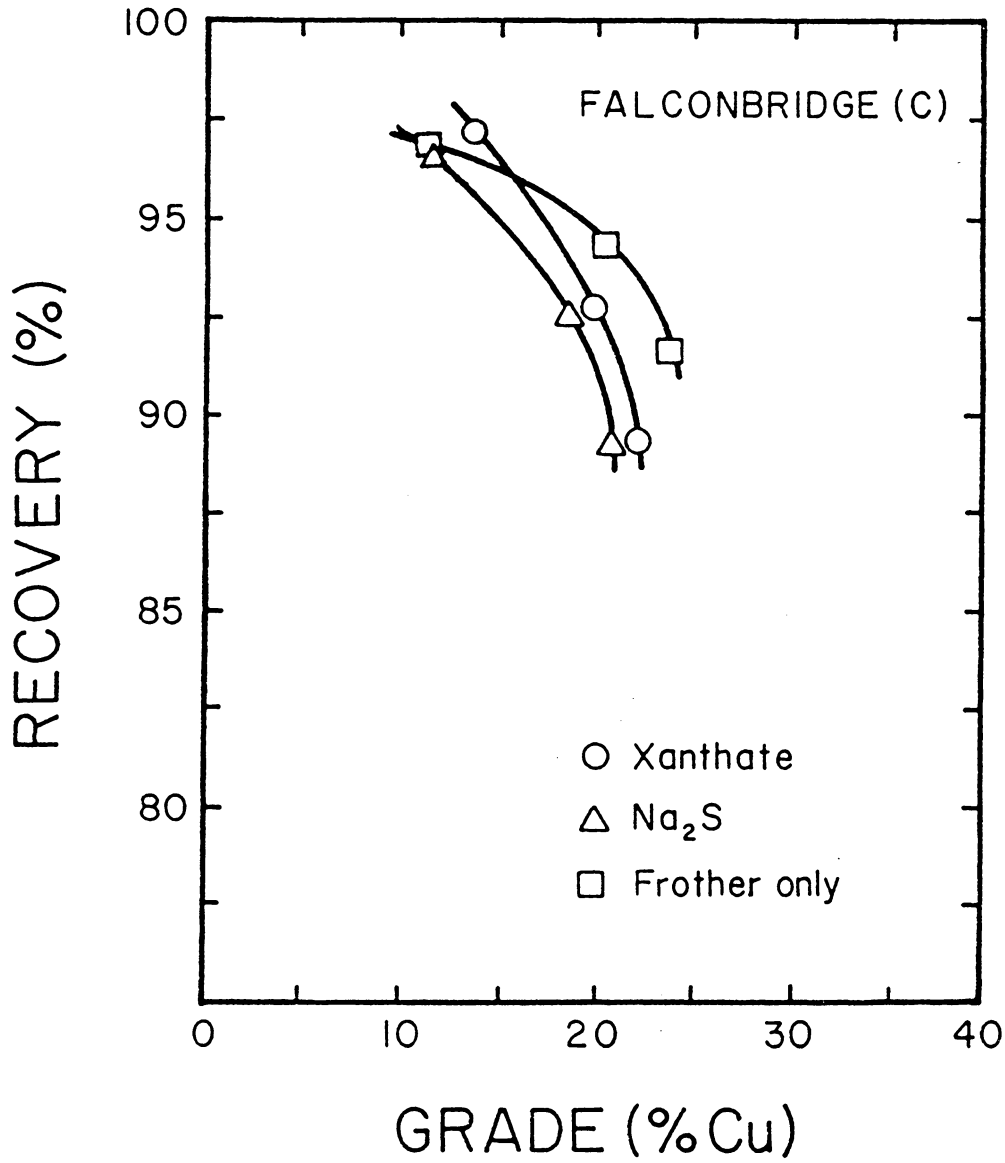

Figure 3.9 Recovery versus grade curves for the batch flotation of the Falconbridge ore using 1) 0.05 lb/ton AERO-350, 2) 3 lb/ton Na_2S and 3) 0.20 lb/ton DF-250.

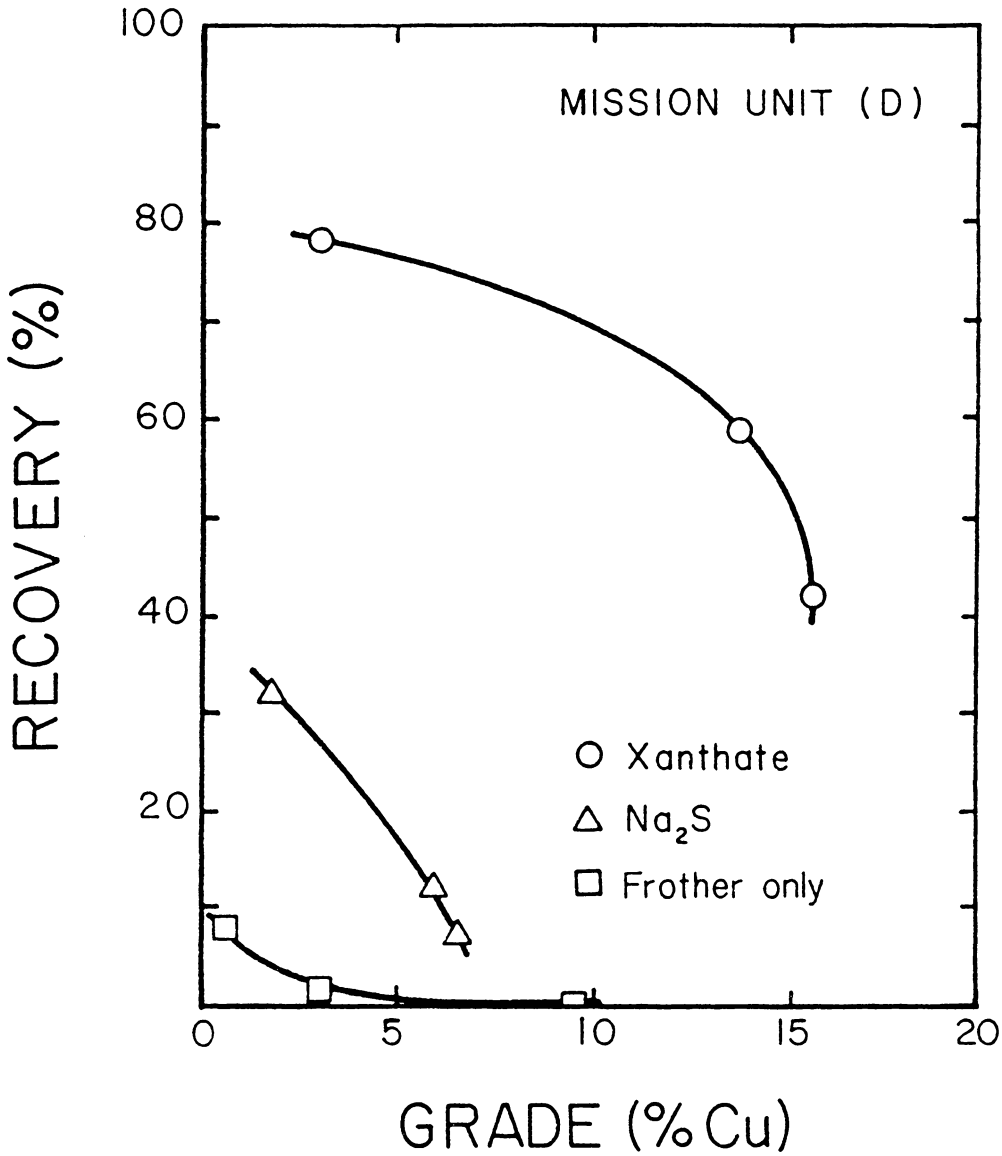

Figure 3.10 Recovery versus grade curves for the batch flotation of the Mission Unit ore using 1) 0.06 lb/ton AERO-350, 2) 3 lb/ton Na_2S and 3) 0.12 lb/ton DF-250.

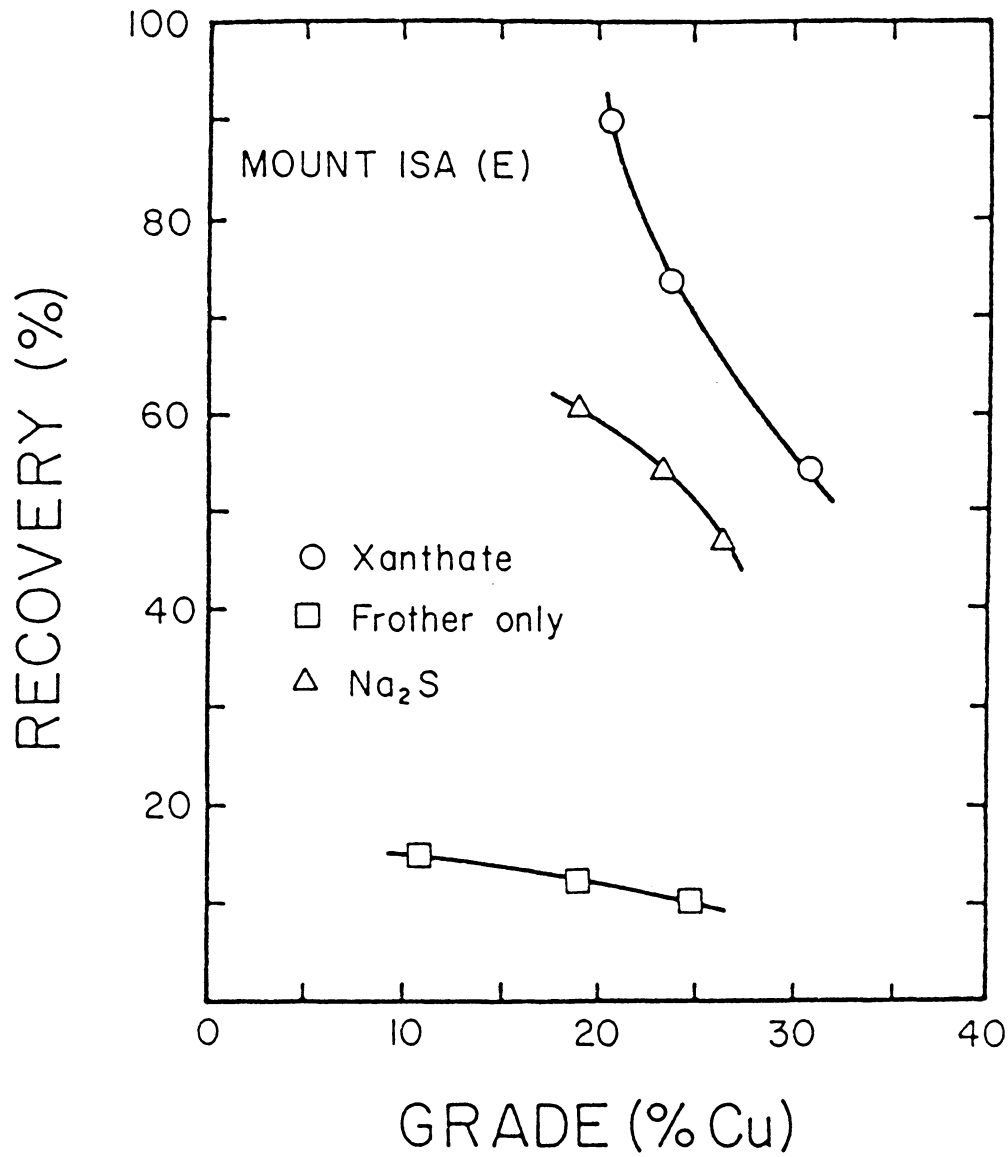

Figure 3.11 Recovery versus grade curves for the batch flotation of the Mount Isa copper ore using 1) 0.15 lb/ton AERO-350, 2) 3 lb/ton Na_2S and 3) 0.12 lb/ton DF-250.

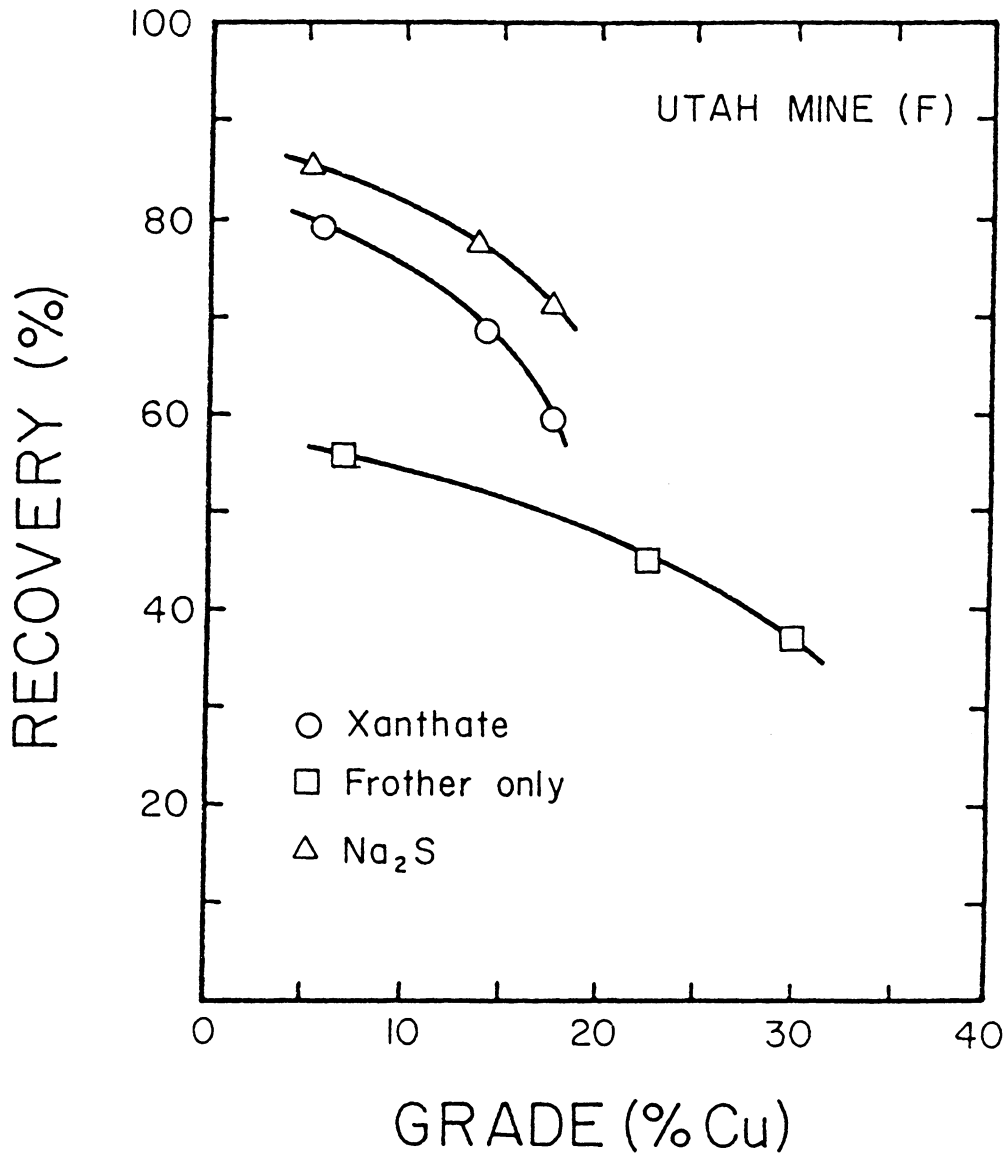

Figure 3.12 Recovery versus grade curves for the batch flotation of the Utah Mine copper ore using 1) 0.03 lb/ton AERO-350, 2) 3 lb/ton Na_2S and 3) 0.12 lb/ton DF-250.

due to excessive sodium sulfide additions.

From the results shown in Figure 3.7 to 3.12, it may thus be concluded that chalcopyrite can be floated without xanthate irrespective of the type of ore in which the mineral is present. Heyes and Trahar's suggestion that there may be two types of ores, one being floatable without a collector and the other requiring a collector for flotation, probably originated from the fact that some sulfides are n-type semi-conductors and others are p-type. However, Pridmore and Shuey (1976) showed that almost all chalcopyrite samples in nature are n-type semi-conductors. Therefore, the difference in the natural floatabilities may be explained by the possibility that heavily oxidized ore samples require a cleaning agent whereas unoxidized samples require little or no cleaning agent. This hypothesis is supported by Lepetic's (1974) result which showed that chalcopyrite from primary ore deposits responded well to collectorless flotation whereas chalcopyrite from secondary copper-sulfide deposits did not.

b. Effect of pH: It has been previously reported that collectorless flotation of chalcopyrite was best at a slightly acidic pH (Yoon, 1981). This was confirmed with the Mount Isa ore (Figure 3.13). By lowering the pH to 6.5 from its natural pH of 11.1, the rougher recovery was improved by about 20%. Note that this result was superior

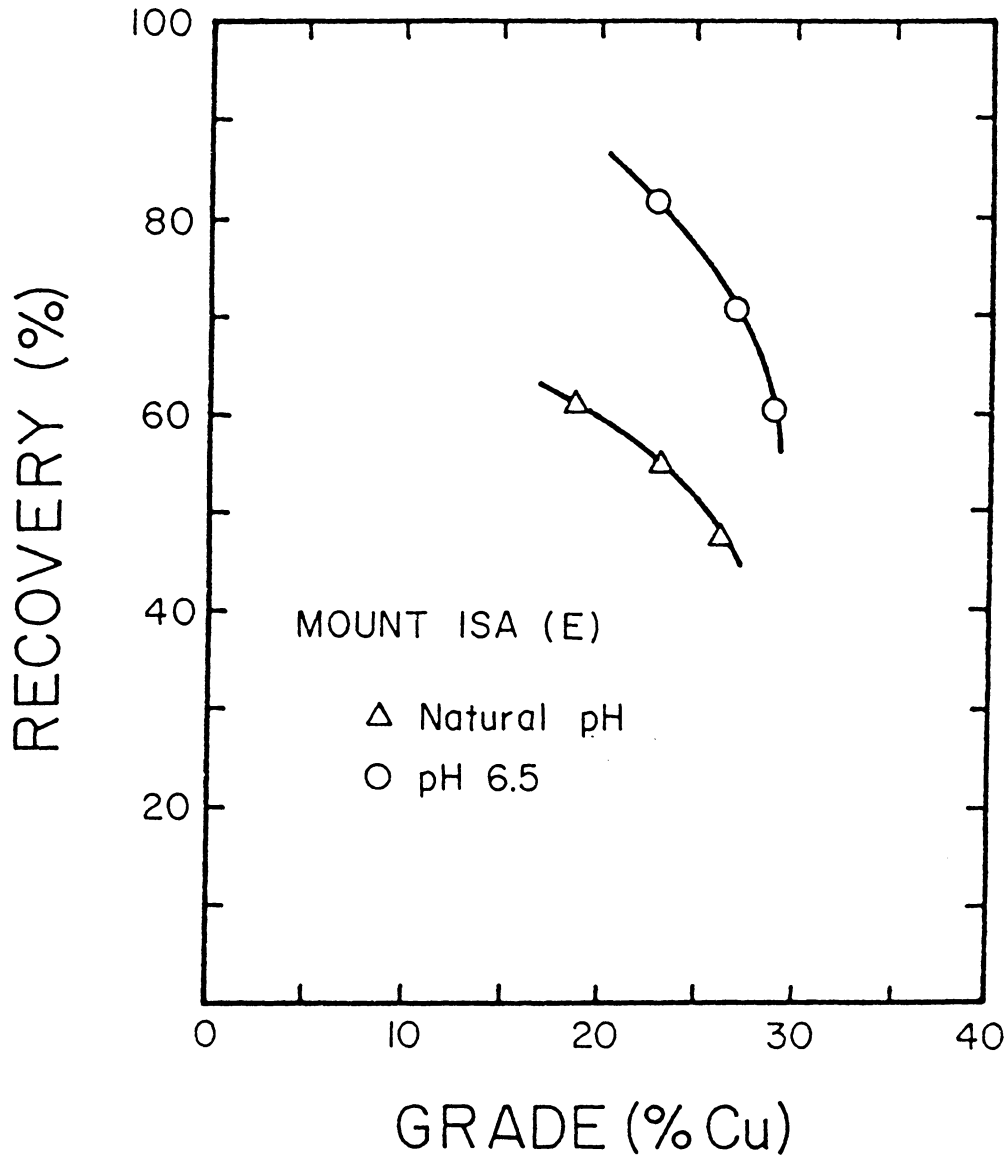

Figure 3.13 Recovery versus grade curves for the batch flotation of the Mount Isa copper ore using 3 lb/ton of sodium sulfide.

to that of the conventional flotation using xanthate as a collector (Figure 3.13).

c. Effect of Potential: Figure 3.14 shows the potential of a bright platinum-calomel electrode pair inserted into the ore pulp during conditioning, flotation and trail periods. At time zero, 3 lb/ton of sodium sulfide was added to the pulp, causing a sharp drop in the potential to -50 to -210 mV depending on the initial pulp potential. As shown in Figure 3.14, the initial potentials of the six chalcopyrite ore samples ranged from approximately +100 to +270 mV. Once sodium sulfide was added and the pulp conditioning began, the potential gradually increased toward a positive value. In all cases, the rise was very slight during the first 10 minutes. With the ores from the Utah Mines and Mount Isa, however, the potential began to rise more rapidly after about 10 minutes and reached beyond 0 mV by the time flotation was started.

In Figure 3.15, the rougher recoveries of these tests are plotted against the potentials at the end of the 15-minute conditioning time. The dashed curve in this figure represents the results of the micro-flotation tests conducted on pure chalcopyrite samples which has been shown previously in Figure 3.2. This shows clearly that the pulp potential at the time of flotation is crucial. In general, the higher the potential, the higher the recovery, irrespec-

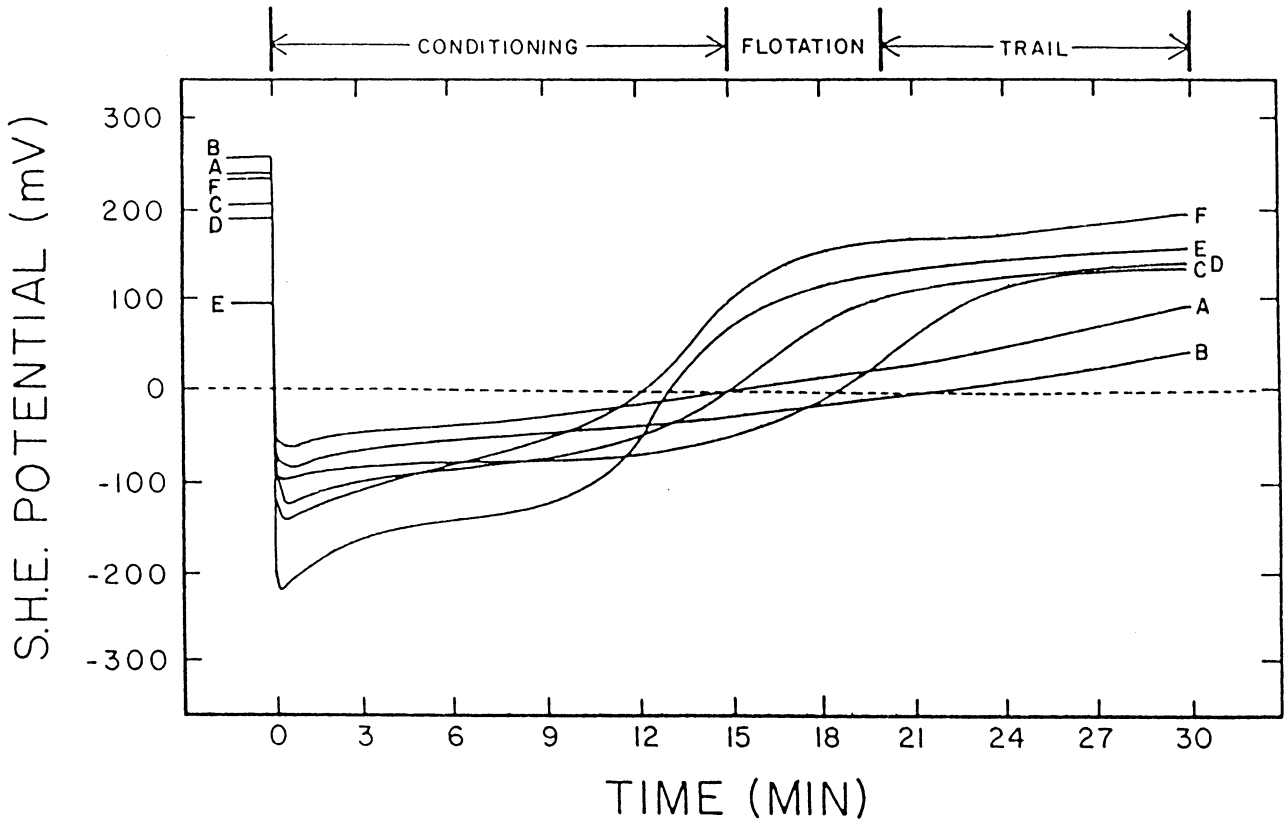

Figure 3.14 Potential of a bright platinum-calomel electrode pair immersed in the flotation pulp during the conditioning, flotation and trail periods. 3 lb/ton sodium sulfide was used for rougher flotation.

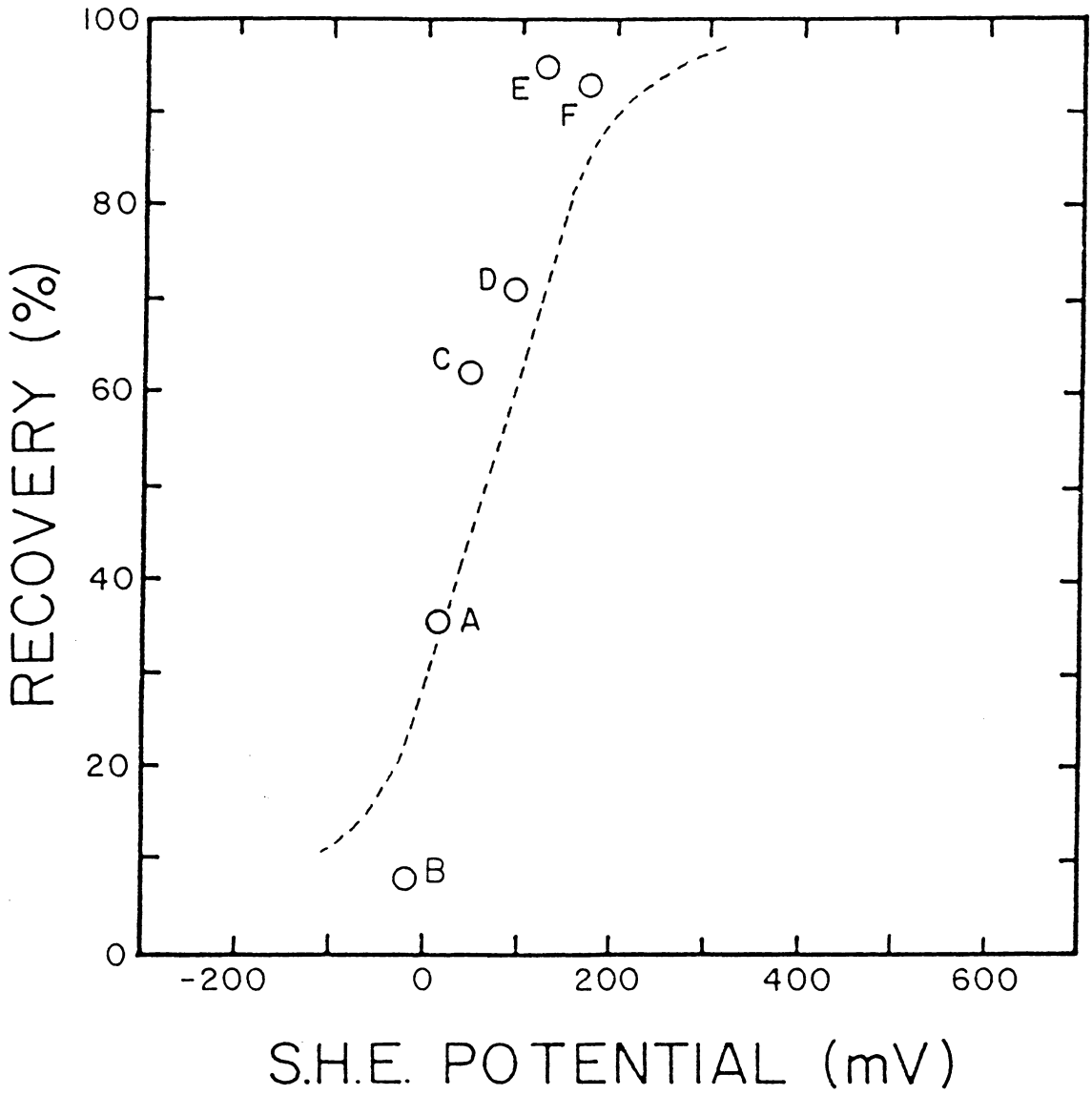

Figure 3.15 Recovery versus potential for the batch flotation of various chalcopyrite ores after conditioning 15 minutes with 3 lb/ton of sodium sulfide. Dashed curve represents the results of the micro-flotation of pure chalcopyrite with sodium sulfide.

tive of the origin or type of the ore samples.

Clearly, the potential of the pulp should be oxidizing at the time of flotation. Note, however, that all the ore samples exhibited positive potentials after grinding (see potentials at time 0, Figure 3.14). Yet, one half of the ore samples tested in the present work did not float well with a frother only. Flotation of these samples required the addition of sodium sulfide for surface cleaning.

Figure 3.14 also shows that, after the addition of sodium sulfide, some ores recover their potentials more quickly than others. In general, the ore samples that floated well with a frother only were slow in recovering their oxidizing potentials (Craigmont, Ray Mines and Falconbridge). The potentials of the pulp became positive more quickly with those ores that did not float well using a frother alone (Utah Mine, Mission Unit and Mount Isa). This may be explained by the possibility that S^{2-} ions in solution are more quickly consumed in displacing the hydrophilic surface oxidation products which may be present on these ores. The results obtained with the Craigmont ore may further illustrate this point. This ore sample did not respond well to collectorless flotation when 3 lb/ton of sodium sulfide was used (Figures 3.8 and 3.16). However, after allowing the ore (-20 mesh) to oxidize in air for 3 months, the flotation recovery was improved drastically, as shown in Figure 3.16. This improved flotation may be

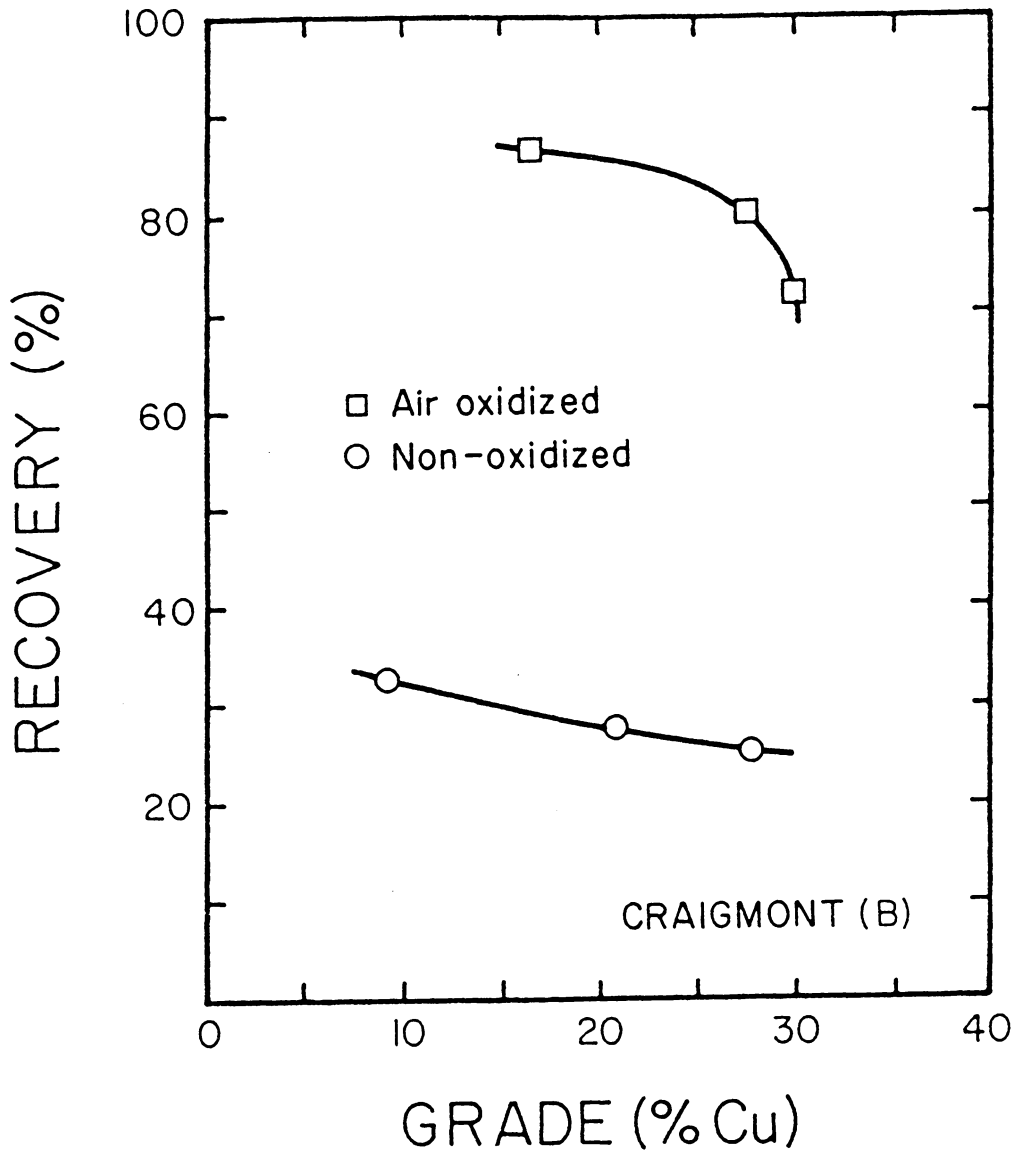

Figure 3.16 Recovery versus grade curves for the batch flotation of the air-oxidized and non-oxidized Craigmont copper ore samples using 3 lb/ton of Na_2S.

explained by the likelihood that the potential of the air-oxidized chalcopyrite was higher than that of the non-oxidized sample at the time of flotation. Presumably, the potential of the oxidized ore pulp was raised more rapidly since the S^{2-} ions were consumed in displacing hydrophilic surface species. Unfortunately, no potential measurements were made during these flotation experiments.

d. Effect of Conditioning Time: In view of the results shown in Figure 3.14, methods of improving flotation may be suggested. A longer conditioning time will allow the potential of the pulp to rise into a more positive region and, hence, give better results. Figure 3.17 shows this to be the case. After 30 minutes of conditioning time, the potential of the Ray Mines pulp reached +100 mV, and the rougher recovery was improved from 49% to 85%.

e. Effect of Sodium Sulfide Dosage: Another method of improving flotation may be to reduce the amount of sodium sulfide added to the pulp so that the potential may rise faster. Figure 3.18 shows the results of three flotation tests conducted by using 0.4, 1.8 and 3.0 lb/ton of sodium sulfide and 15 minutes of conditioning time for the Mission Unit sample. As shown, the best results were obtained when the least amount of sodium sulfide was used.

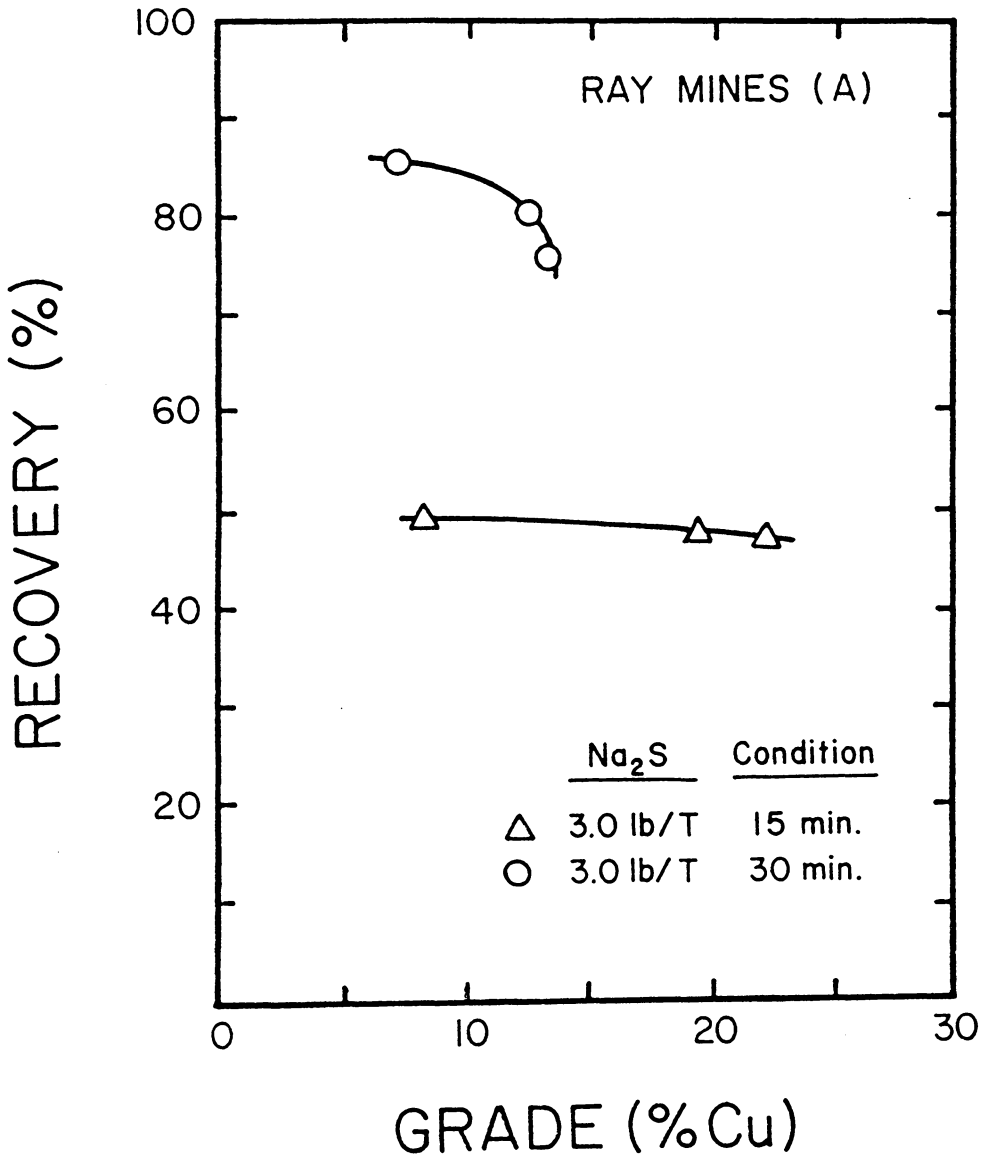

Figure 3.17 Recovery versus grade curves for the batch flotation of the Ray Mines copper ore samples using 3 lb/ton of sodium sulfide after 15 and 30 minutes of conditioning time.

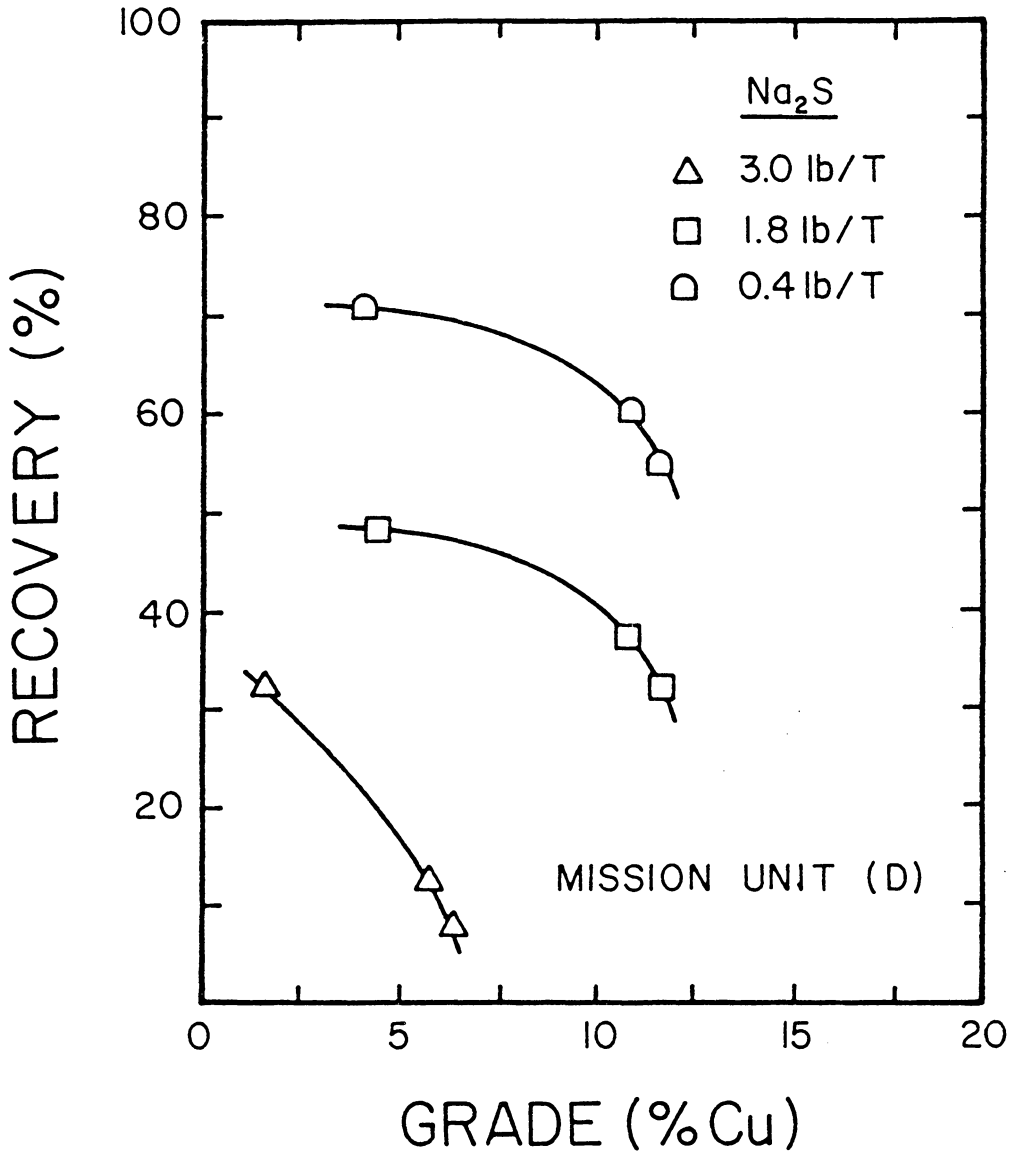

Figure 3.18 Recovery versus grade curves for the batch flotation of the Mission Unit ore using 0.4, 1.8 and 3.0 lb/ton of sodium sulfide.

f. Effect of Wet and Dry Grinding: Lepetic (1974) showed that some chalcopyrite ores floated well with frother alone after dry-autogenous grinding. A similar observation was made in the present work with the Mission Unit ore. As shown in Figure 3.19, the frother only flotation was much better after dry-grinding the ore sample than after wet-grinding. With the Falconbridge ore sample, however, the recovery was reduced slightly after dry-grinding.

3.2.2 Flotation of Sphalerite Ores

a. Effect of Sodium Sulfide and Cupric Sulfate: Figure 3.20 shows the results of flotation tests conducted on the Center Valley zinc ore, New Jersey Zinc Co., under various conditions. In each test, the ore was ground for 30 minutes, conditioned for 15 minutes, and floated at pH 11.0 using lime as a pH regulator. The first test was conducted with a frother (Dowfroth 250, 0.24 lb/ton) alone to see if this sphalerite was naturally floatable. Fuerstenau and Sabacky (1981) showed that clean, unactivated sphalerite floated approximately 50% without a collector in a micro-flotation cell under an oxygen-free atmosphere, while copper-activated sphalerite was 100% floatable.

The batch flotation tests conducted on the Center Valley zinc ore showed, however, that sphalerite was not floatable with frother alone (Figure 3.20). When activated with cupric sulfate (1.5 lb/ton as $CuSO_4 \cdot 5H_2O$), only a

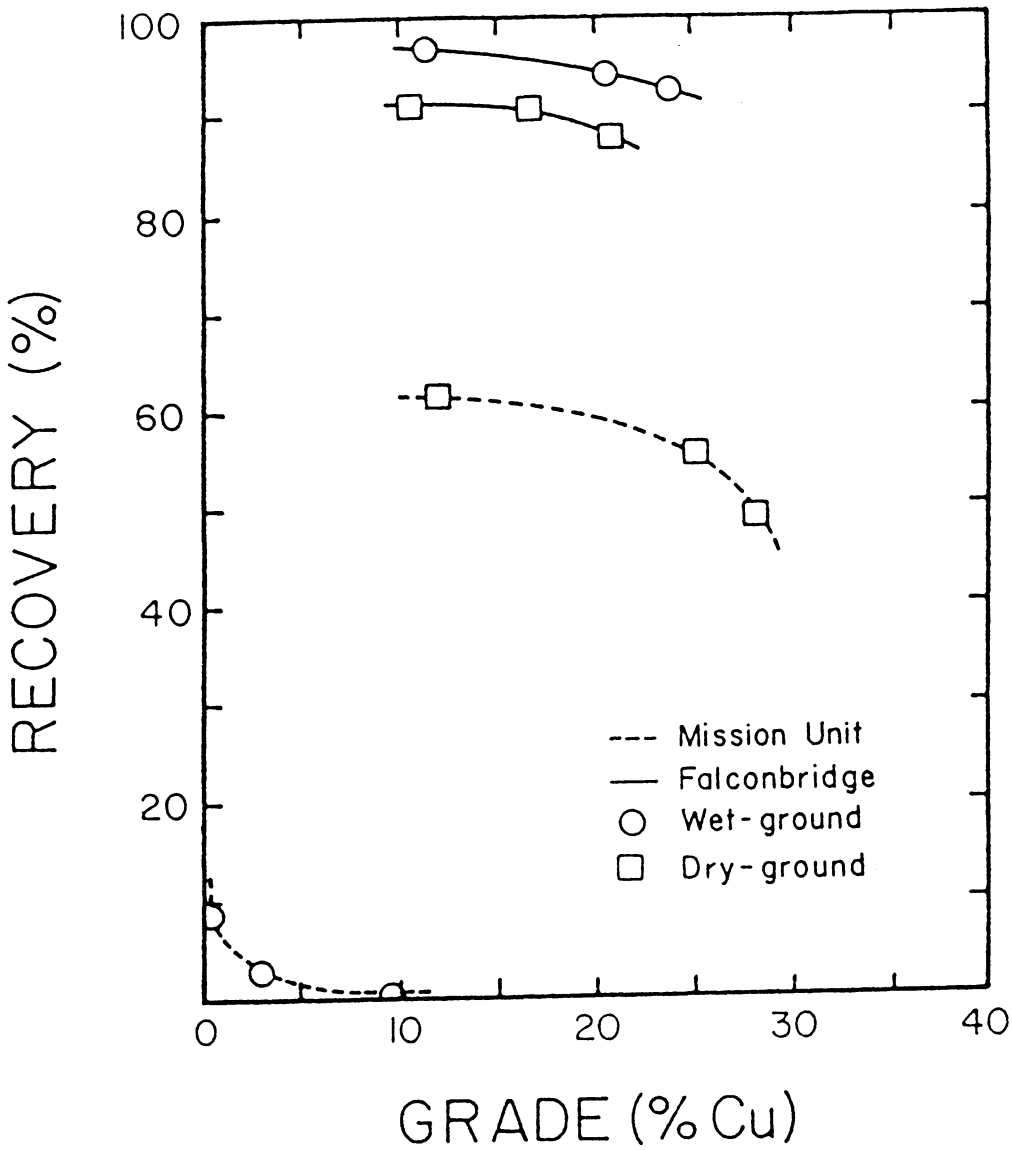

Figure 3.19 Recovery versus grade curves for the flotation of the Mission Unit and Falconbridge copper ores after wet- and dry-grinding. No reagent other than Dowfroth 250 was used.

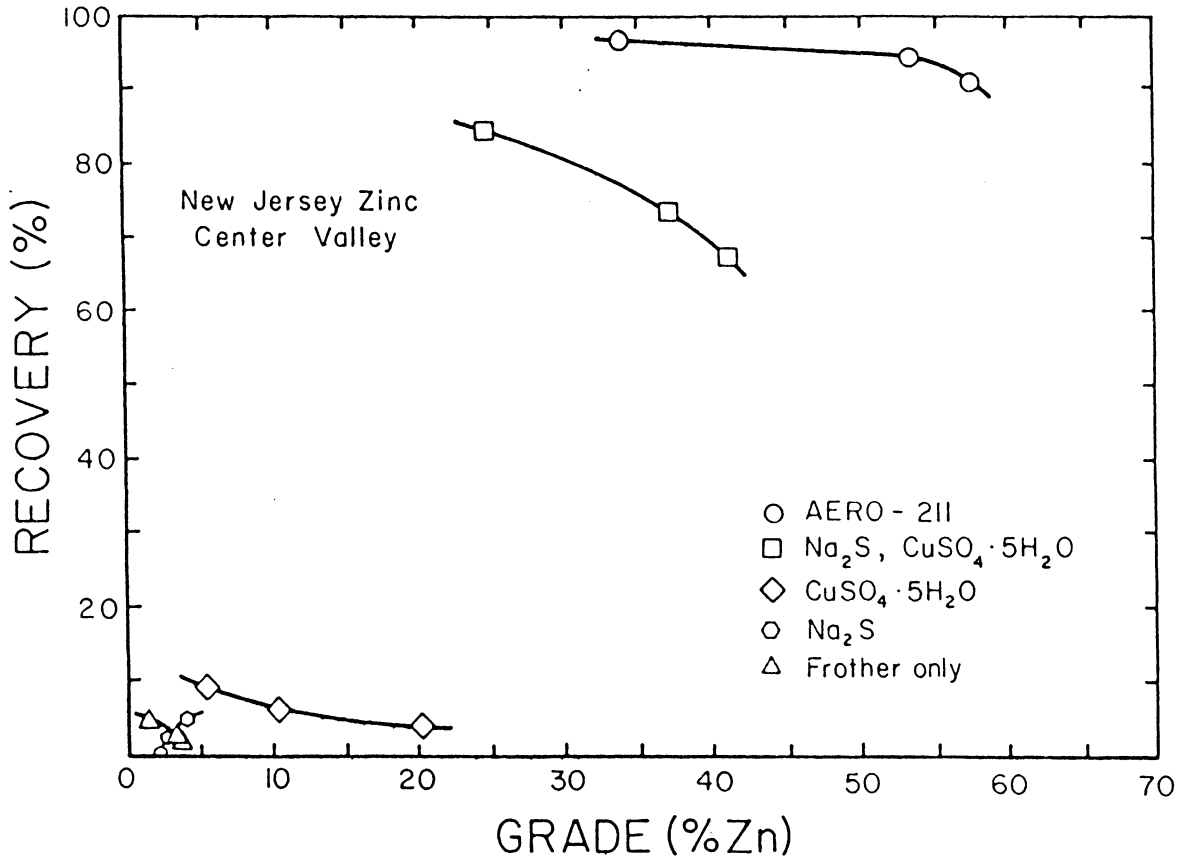

Figure 3.20 Recovery versus grade curves for the batch flotation of the Center Valley zinc ore.

minimal amount of sphalerite floated. Good flotation was obtained only when both cupric sulfate (1.5 lb/ton) and sodium sulfide (3.0 lb/ton) were added, although the results were still inferior to those obtained using AERO-211 (0.15 lb/ton) as a collector. No flotation was possible when only sodium sulfide (3.0 lb/ton) and a frother were employed.

Figure 3.21 presents the flotation recovery versus grade curves for the conventional and the collectorless flotation tests conducted on the Jefferson City zinc ore. In the conventional flotation tests, 0.075 lb/ton of AERO-211 and 0.25 lb/ton of Dowfroth 250 were used at pH 11. For collectorless flotation, 0.7 lb/ton of cupric sulfate and 1.2 lb/ton of sodium sulfide were used. The amount of Dowfroth 250 used for this test was the same as that used in conventional flotation. Results show that conventional flotation gave a considerably higher recovery than the collectorless flotation after two stages of cleaning (86.6 versus 68.0%), but with a significant loss in grade (25.3 versus 49.1% Zn).

b. Effect of Grinding Time: The effect of grinding time on the collectorless flotation of the Center Valley zinc ore using sodium sulfide (3.0 lb/ton) and cupric sulfate (1.5 lb/ton) is shown in Figure 3.22. These results show that optimum flotation recovery is obtained when the

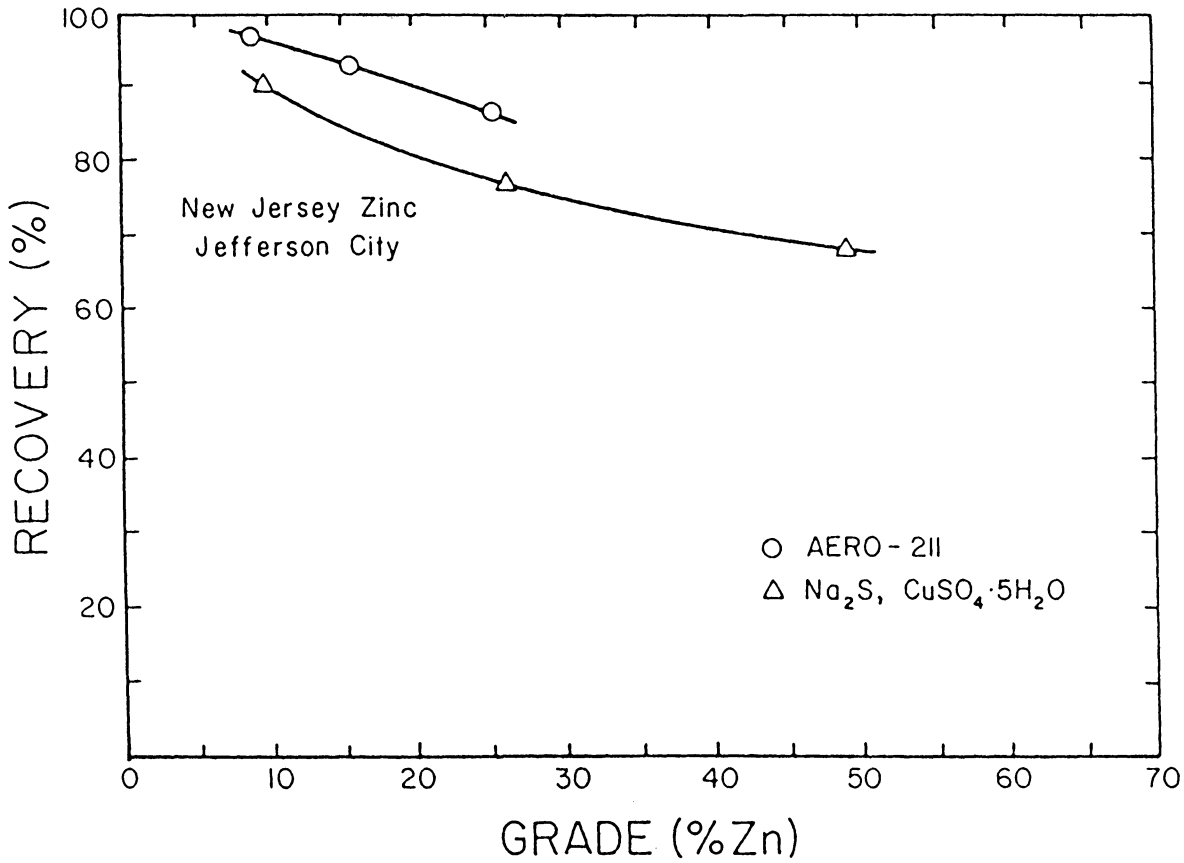

Figure 3.21 Recovery versus grade curves for the batch flotation of the Jefferson City zinc ore.

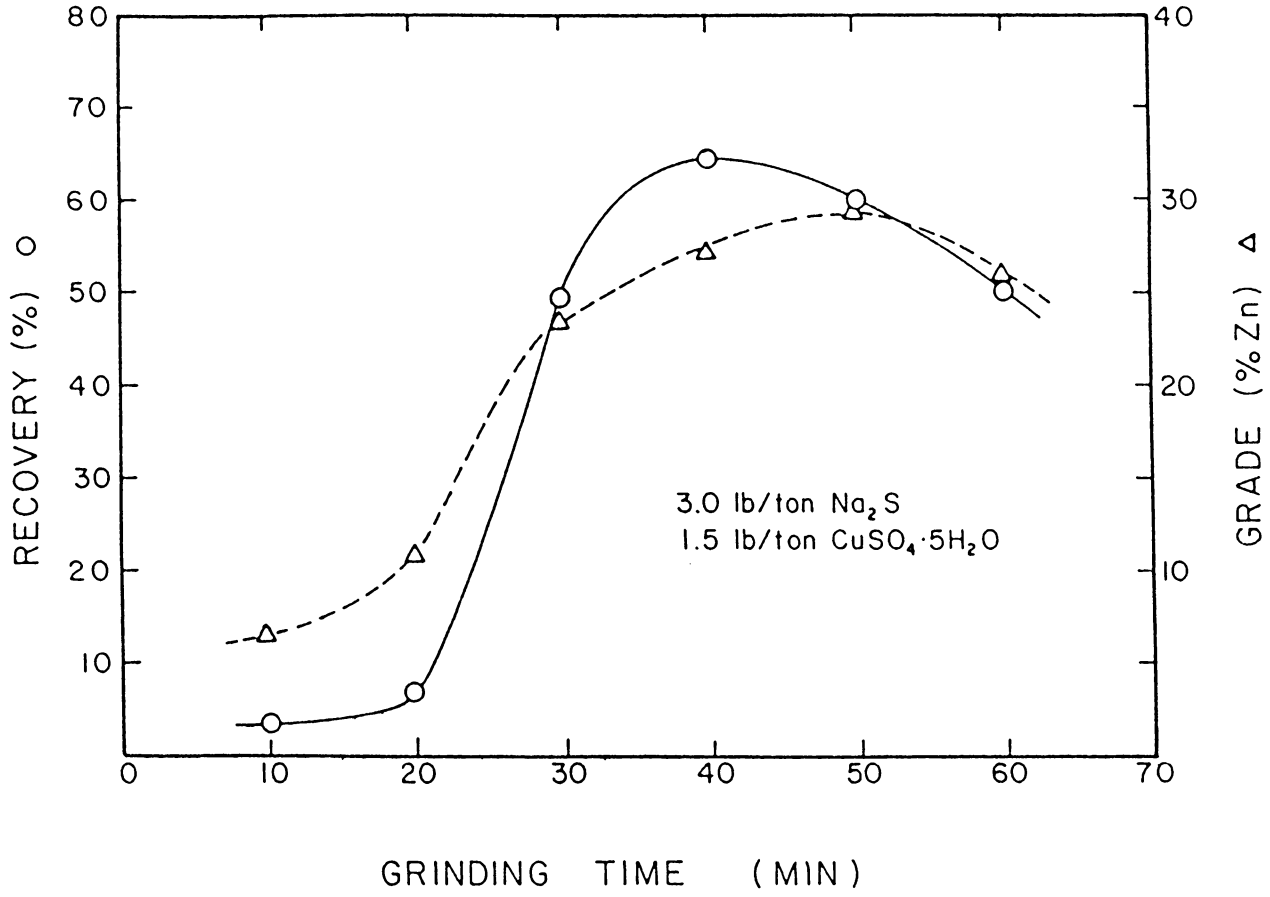

Figure 3.22 Effect of grinding time of the recovery and grade of zinc concentrates from the Center Valley zinc ore.

ore is ground for 40 minutes. It is likely that when the ore was ground less than 40 minutes, the liberation of the sphalerite was incomplete. Grinding beyond 40 minutes may have produced fines which are more difficult to float.

c. Effect of Conditioning Time: Figure 3.23 shows the recovery versus conditioning time for the flotation of the Center Valley zinc ore. In these experiments, the conditioning time plotted refers to the agitation time after the addition of sodium sulfide (1.8 lb/ton). Cupric sulfate (0.86 lb/ton) was always added 5 minutes prior to the flotation. As shown, flotation recovery increases with increasing conditioning time and passes through a maximum at approximately 15 minutes before decreasing again. The increase in floatability with increasing conditioning time has also been noted in the chalcopyrite flotation experiments (Figure 3.17), and was found to be related to the time required for the pulp potential to reach an oxidizing potential after the addition of sodium sulfide. Since the collectorless flotation of sphalerite is possible only under oxidizing conditions (private comm., Craynon, 1982), as has also been found to be the case with chalcopyrite, the potential of the sphalerite ore pulp must be returned to oxidizing conditions during the conditioning period. A 5-minute conditioning time was probably not sufficient to give an oxidizing environment. The poor results after 20 minutes

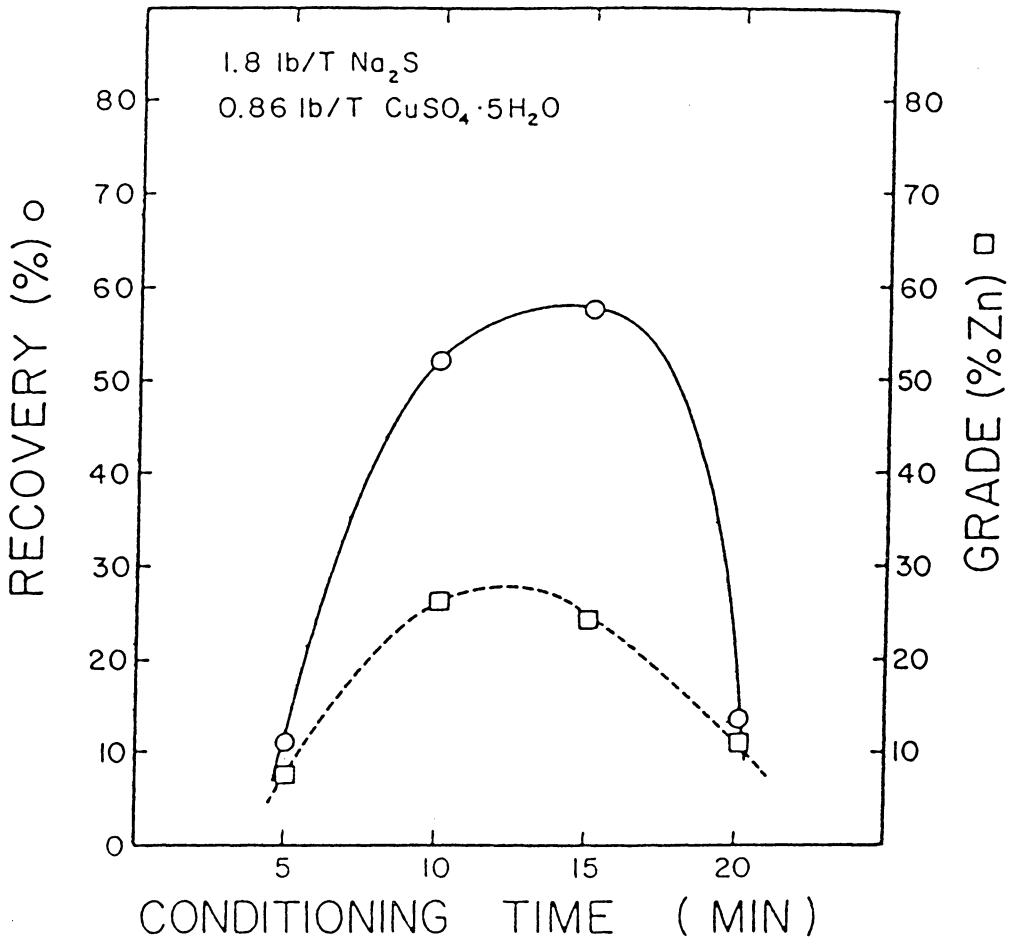

Figure 3.23 Effect of conditioning time on the recovery and grade of zinc concentrates from the Center Valley zinc ore.

of conditioning may be due to the presence of hydrophilic surface oxidation products formed after excessively long conditioning periods.

d. Effect of pH: Figure 3.24 shows the effect of pH on the collectorless flotation of the Center Valley zinc ore. The optimum pH for flotation was found to be between 6 and 7, but good flotation was obtained up to pH 10.5. The results show that the flotation recovery improves with decreasing pH, which may be attributed to the fact that elemental sulfur formation is thermodynamically more favorable at a lower pH. The poor recovery above pH 11 may be due to the formation of hydroxides on the mineral surface.

e. Effect of Cupric Sulfate Dosage: Figures 3.25, 3.26 and 3.27 show the flotation recovery as a function of cupric sulfate addition for the Center Valley zinc ore using 0.6, 1.8 and 3.0 lb/ton of sodium sulfide, respectively. As can be seen, good flotation occurs over a small range of cupric sulfate addition. Note that the flotation recovery drops sharply when the amount of cupric sulfate added exceeds the sodium sulfide dosage. This seems to support an earlier suggestion (Yoon, 1981) that there may be an optimum Cu^{2+}/S^{2-} atomic ratio for the collectorless flotation of sphalerite. In Figure 3.28, the recovery was plotted as a function of the Cu^{2+}/S^{2-} atomic ratio. The three curves

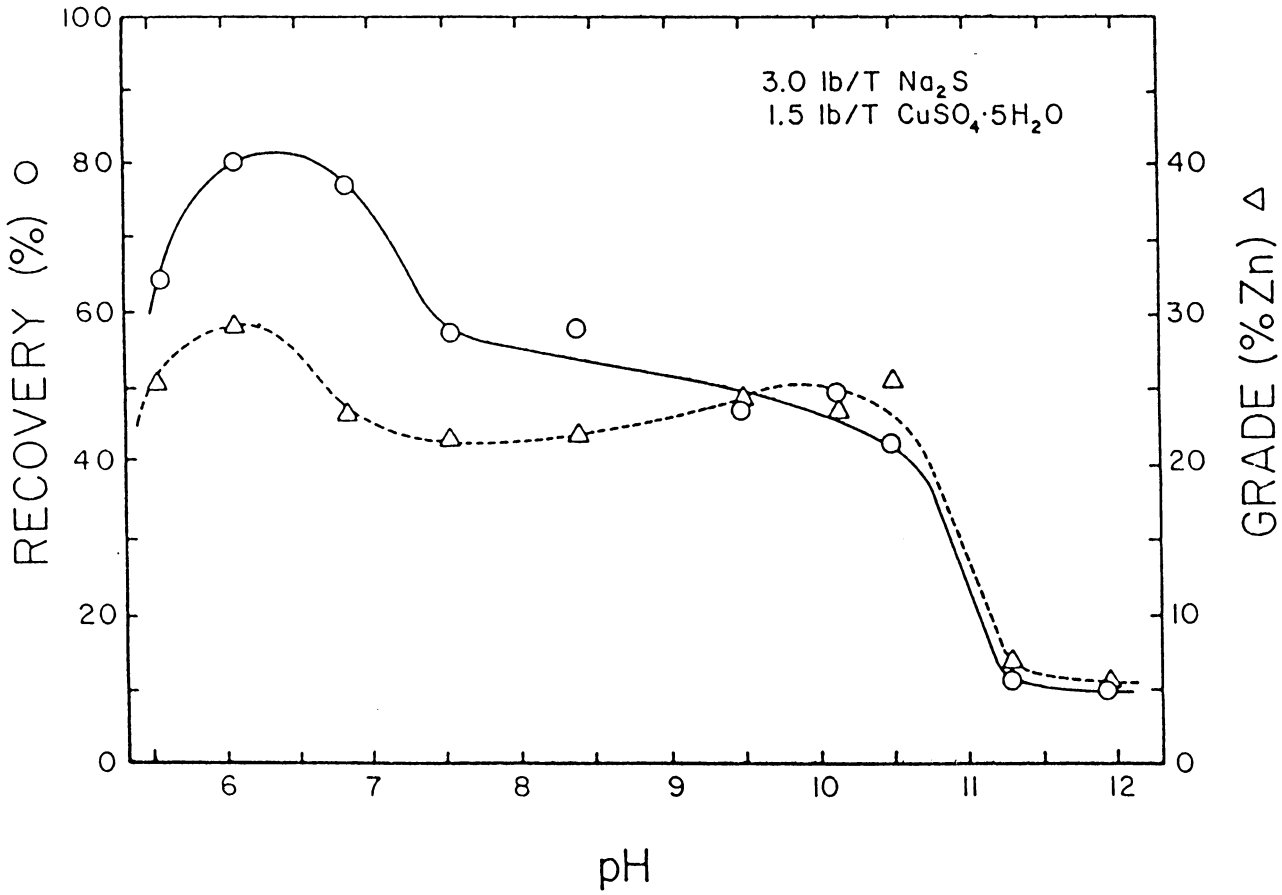

Figure 3.24 Effect of pH on the recovery and grade of zinc concentrates from the Center Valley zinc ore using 3 lb/ton sodium sulfide and 1.5 lb/ton copper sulfate.

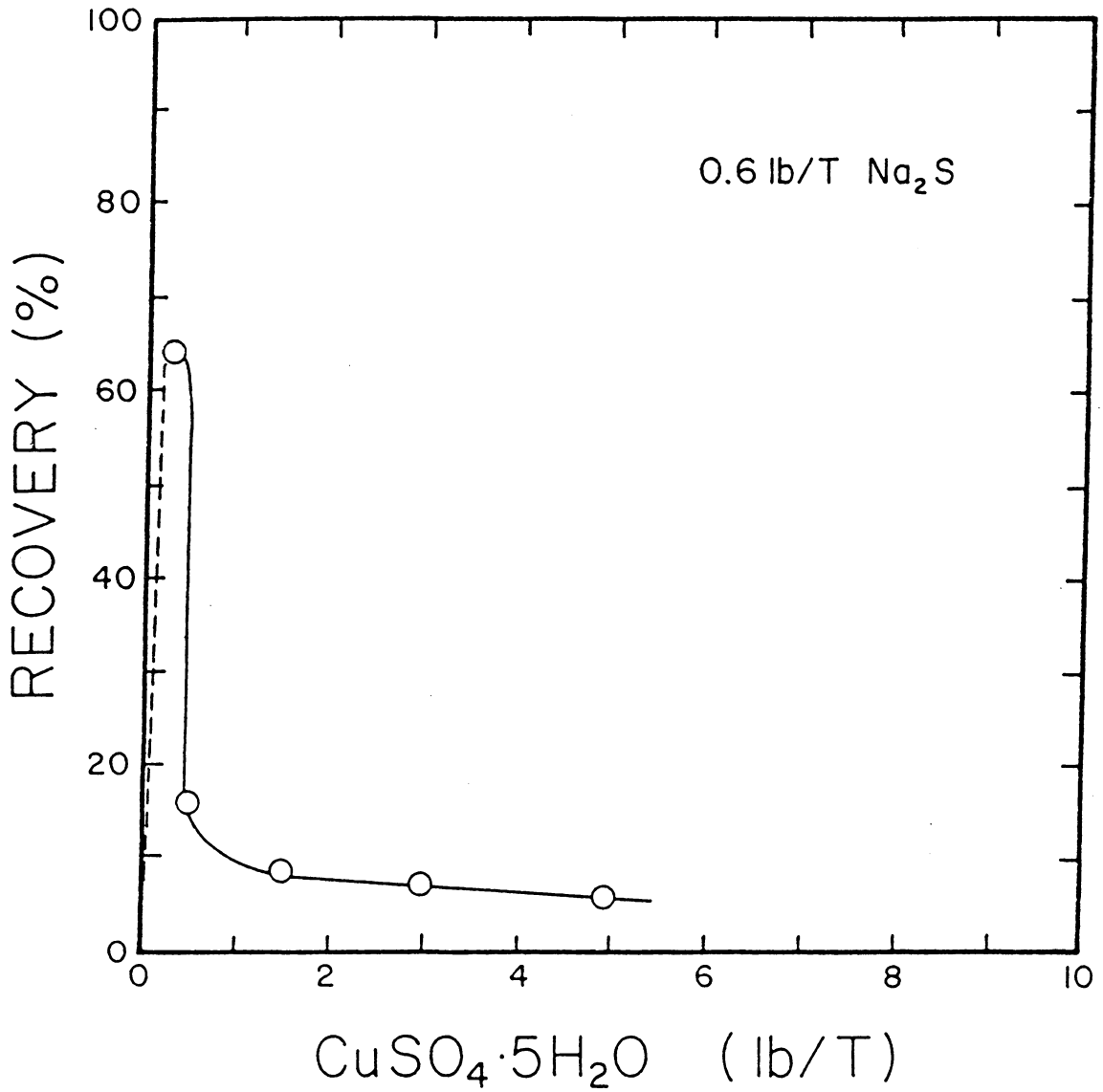

Figure 3.25 Effect of cupric sulfate dosage on the recovery of zinc from the Center Valley ore using 0.6 lb/ton of sodium sulfide.

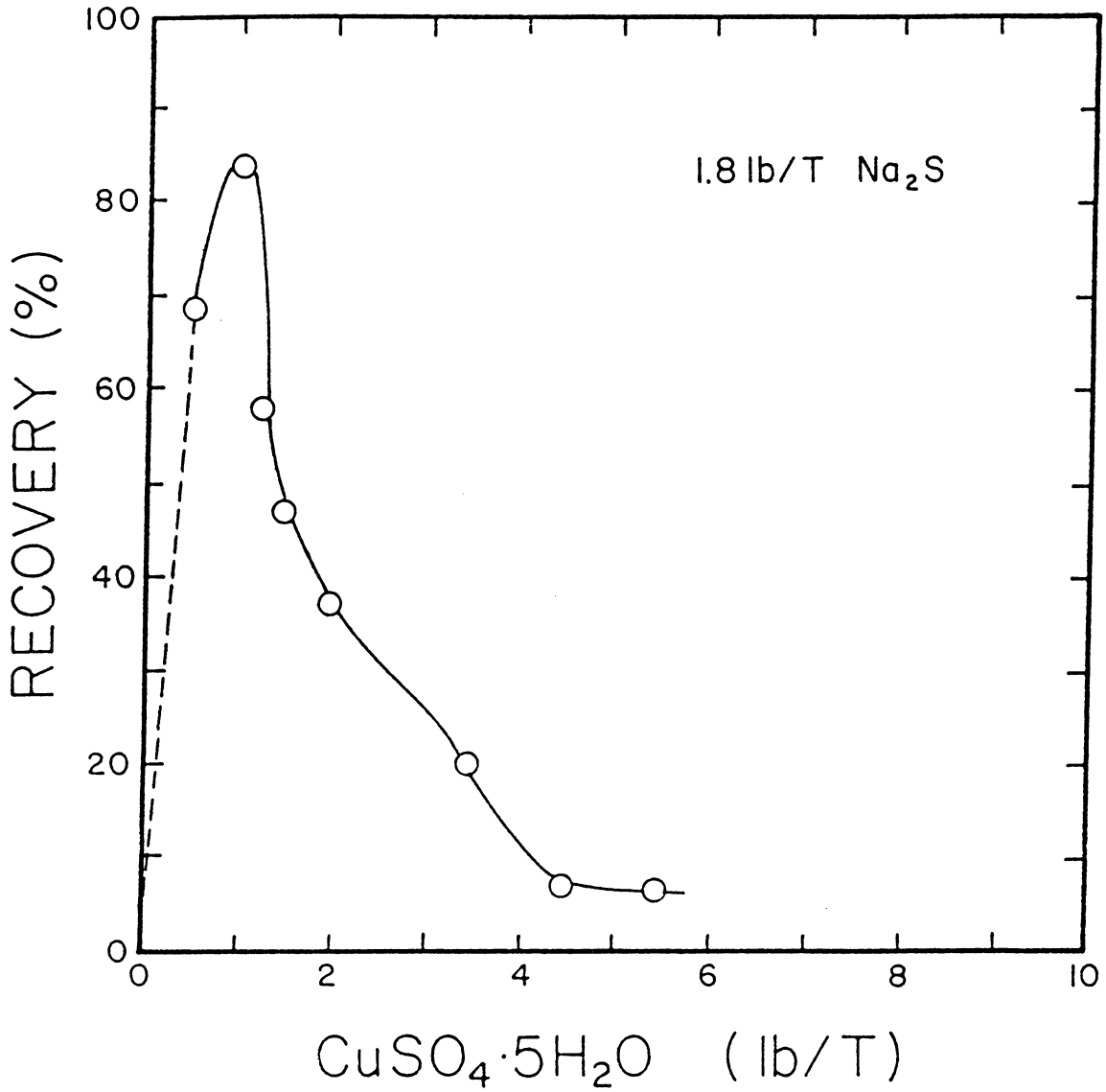

Figure 3.26 Effect of cupric sulfate dosage on the recovery of zinc from the Center Valley ore using 1.8 lb/ton of sodium sulfide.

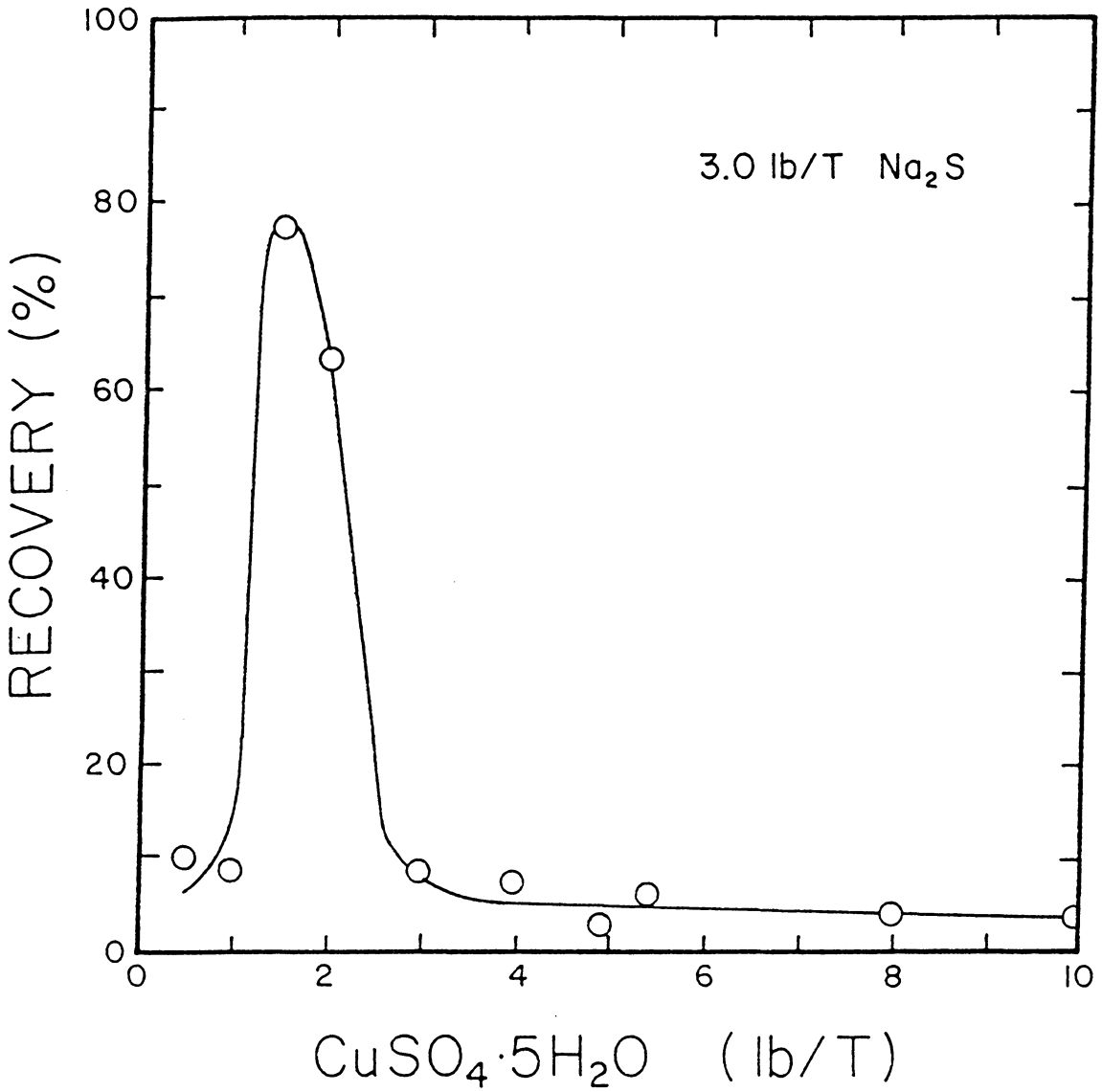

Figure 3.27 Effect of cupric sulfate dosage on the recovery of zinc from the Center Valley ore using 3.0 lb/ton of sodium sulfide.

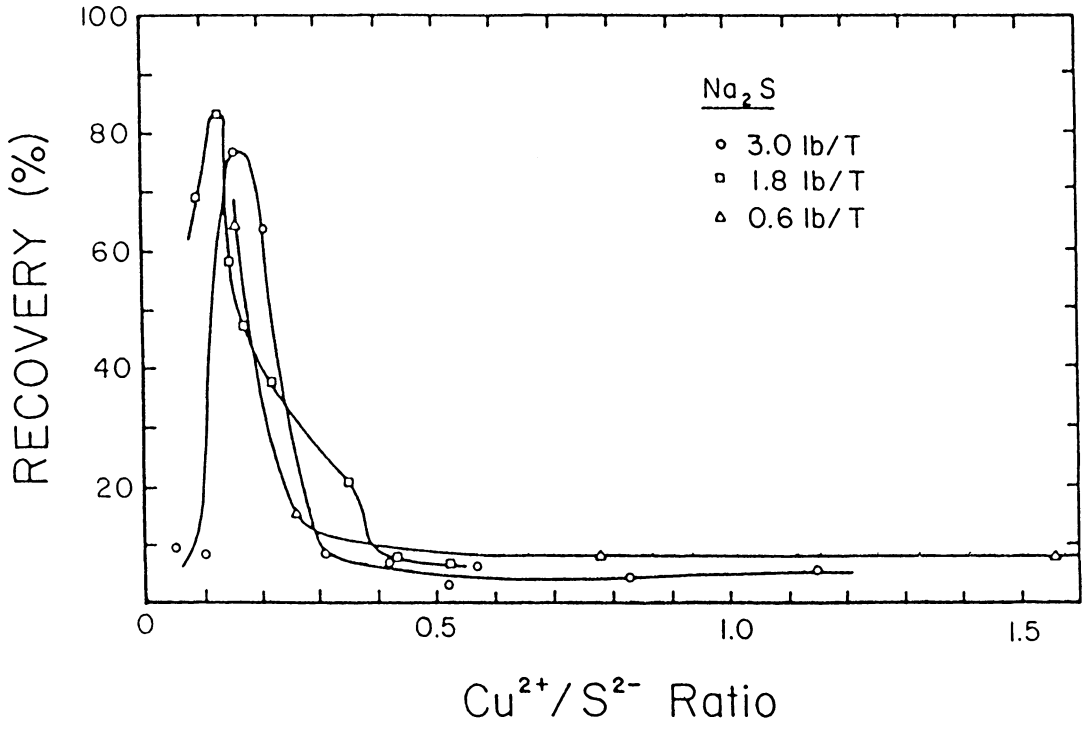

Figure 3.28 Effect of the Cu^{2+}/S^{2-} atomic ratio on the recovery of zinc from the Center Valley zinc ore at various sodium sulfide dosages.

representing different levels of sodium sulfide additions (i.e., 0.6, 1.8 and 3.0 lb/ton) have narrow peaks between 0.14 and 0.17 Cu^{2+}/S^{2-} atomic ratios. The curve for 0.6 lb/ton of sodium sulfide does not show a peak. However, there must be a peak even at this low sodium addition, because the recovery dropped to almost zero when no cupric sulfate was added ($Cu^{2+}/S^{2-} = 0$), as shown in Figure 3.20. Thus, there exists an optimum Cu^{2+}/S^{2-} atomic ratio for sphalerite flotation.

f. Effect of Sodium Sulfide Dosage: The results in the foregoing section suggest that good flotation can be achieved using small amounts of reagents if the optimum Cu^{2+}/S^{2-} atomic ratio is maintained. To demonstrate this, a series of collectorless flotation tests was carried out in which the reagent dosages were varied, but the Cu^{2+}/S^{2-} atomic ratio was held constant at 0.17. The results given in Figure 3.29 show that there are relatively small changes in recovery and grade over a ten-fold change in reagent addition.

Recall that the results of the collectorless flotation tests shown in Figure 3.20 were considerably inferior to those of the conventional flotation test. In view of the results given in Figures 3.28 and 3.29, improved results could have been obtained if the optimum Cu^{2+}/S^{2-} atomic ratio had been used.

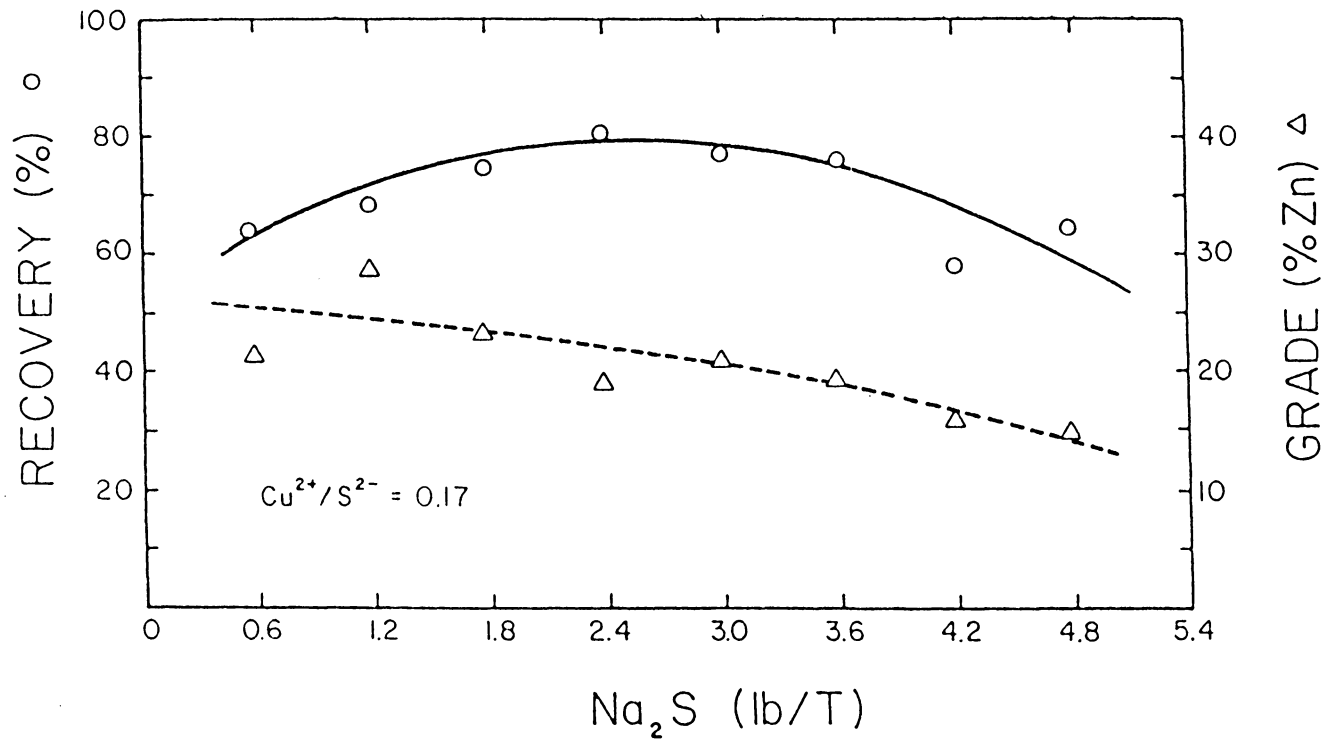

Figure 2.29 Effect of sodium sulfide dosage on the recovery and grade of zinc from the Center Valley ore. The ratio of Cu^{2+}/S^{2-} and pH were held constant at 0.17 and 6.5, respectively.

3.3 Mass Spectrometry

3.3.1 Elemental Sulfur Detection

Samples of finely pulverized chalcopyrite (surface area of 0.88 m^2/gram, see Appendix VI) were treated under various conditions and the amount of elemental sulfur was determined by means of mass spectrometry. The mass spectra obtained in the present study are included in Appendix VII.

a. Effect of pH: Figure 3.30 shows the relative peak intensity of elemental sulfur detected on chalcopyrite as a function of pH. In this set of tests, the instrument was not set to its full sensitivity in order to prevent damage to the electron multiplier by excessively high intensity signals. The zero peak intensities found above pH 10 indicate very small amounts of sulfur. This data agrees with the thermodynamic data of Garrels and Christ (1965) which indicates that elemental sulfur is not stable in alkaline pH solutions. A similar result has been observed for the stability of elemental sulfur on copper-activated sphalerite (Ralston, Alabaster and Healy, 1981).

In order to quantitatively determine the amount of elemental sulfur present in the alkaline pH regions, a second set of experiments was performed at the maximum sensitivity setting of the spectrometer. For calibration, standard samples of chalcopyrite were spiked with known

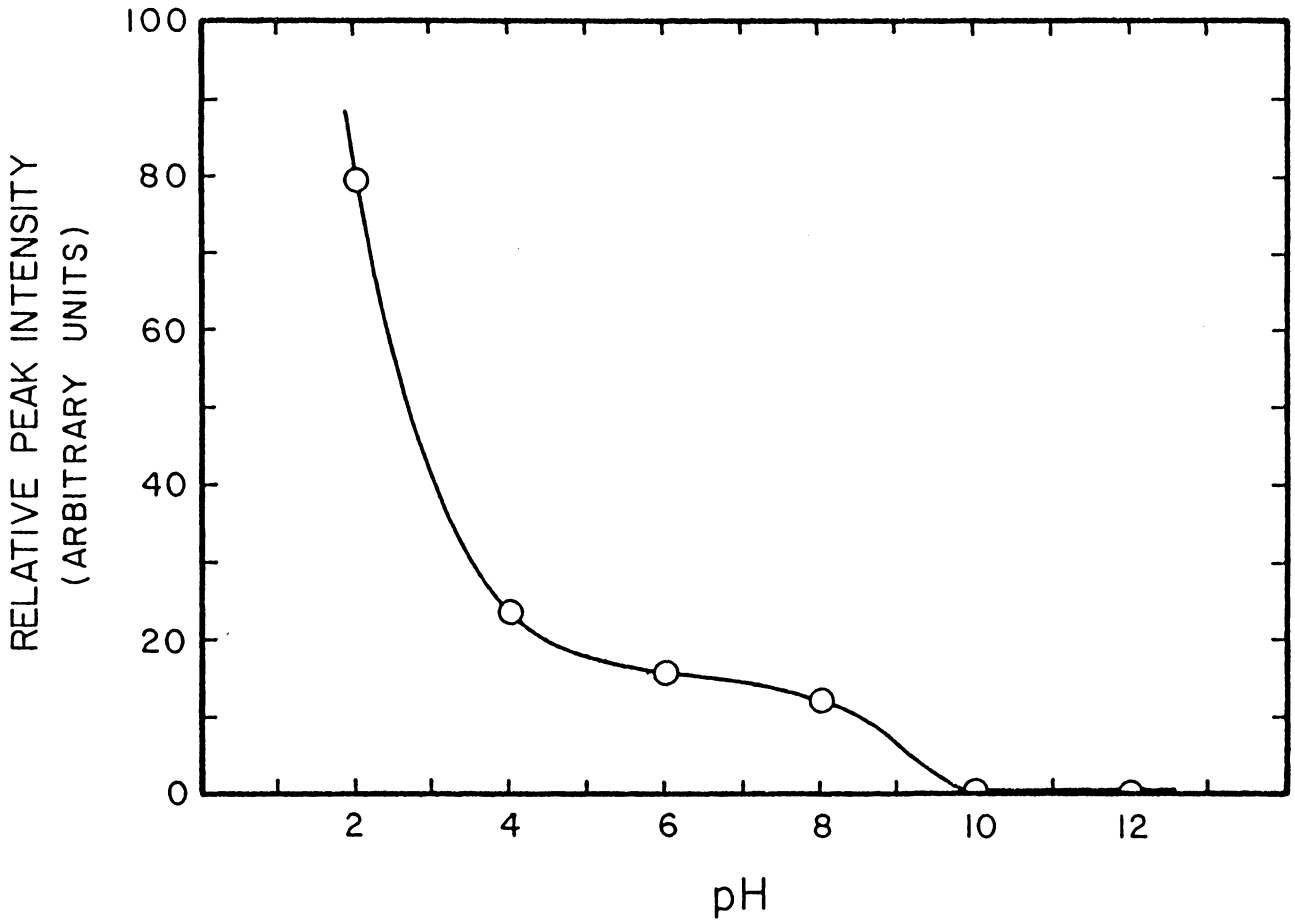

Figure 3.30 Relative peak intensity versus pH for the mass spectrometric determination of elemental sulfur (m/e = 64).

amounts of elemental sulfur prepared as described in Section 2.3.4. The samples were analyzed to establish a calibration curve, shown in Figure 3.31, in which the peak intensity was plotted against the weight percent of elemental sulfur spiked artificially on the chalcopyrite sample. Note that the blank samples showed some sulfur of unknown origin. Therefore, the calibration curve was corrected as shown in Figure 3.31. According to the corrected calibration curve, the blank chalcopyrite samples contained approximately 0.0013 percent sulfur by weight. The small amount of elemental sulfur found in the blank samples samples may have been due to the slight oxidation caused by exposure to air during sample preparation.

Mass spectra were also obtained for chalcopyrite samples conditioned at pH 10 and 12, and the weight percent of elemental sulfur was determined from the peak intensities using the calibration curve. The results are given in Table 3.2. In this table, the results obtained with the blank samples are also given. As shown, the percent elemental sulfur decreased upon conditioning in alkaline solutions. Note also that the percent sulfur decreased with increasing pH, which is in accordance with thermodynamic predictions.

From the weight percent sulfur, the monolayer coverages were calculated and are given in Table 3.2. For these calculations, three different values for the area occupied by elemental sulfur on the surface of chalcopyrite were

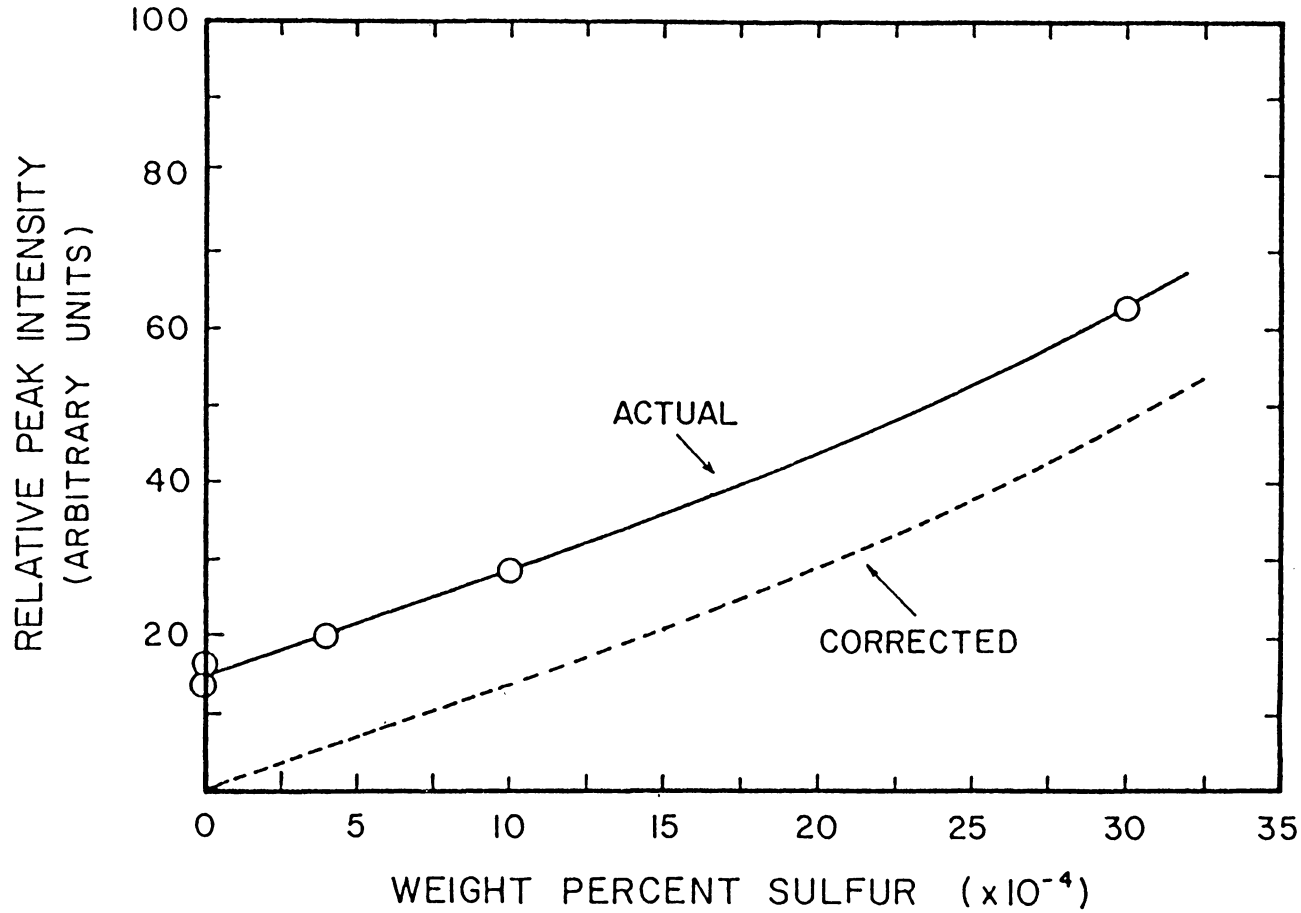

Figure 3.31 Relative peak intensity versus weight percent sulfur on chalcopyrite detected by mass spectrometry. The corrected curve was obtained by subtraction of the sulfur present in the blanks.

Table 3.2 Percent Monolayer Coverage of Elemental Sulfur on Chalcopyrite as Determined by Quantitative Mass Spectrometry

Sample Description	Peak Intensity	Wt% Sulfur*	Percent Monolayer $8.6A^2$/atom	$11.8A^2$/atom	$19.2A^2$/atom
blank #1	16.6	12.8	2.3	3.2	5.2
blank #2	13.5	10.3	1.9	2.6	4.2
pH 10.0	11.5	9.0	1.7	2.3	3.7
pH 12.0	6.6	5.2	0.95	1.3	2.1
pH 12.0	6.8	5.4	0.99	1.4	2.2

*Wt% x 10^{-4}

considered. The first value was obtained by assuming no specific disposition of elemental sulfur on chalcopyrite (i.e., the sulfur atoms were assumed to be close-packed). In this position, each sulfur atom (in orthorhombic form) would occupy 8.6 A^2 (Ralston, Alabaster and Healy, 1980). It should be pointed out that only orthorhombic sulfur is stable at standard temperature and pressure (Meyer, 1976). The other values for the area occupied by sulfur were obtained by assuming that elemental sulfur would occupy those crystallographic positions that would have been occupied by the lattice sulfide ions in an unoxidized chalcopyrite crystal. Although chalcopyrite has no distinct cleavage, single crystals are usually found to be tetrahedral with the {112} form dominant (Hurbut and Klein, 1977). Thus, the (112) plane shown in Figure 3.32 was used to calculate the area occupied by sulfur. As can be seen, only copper and iron are present in this particular plane. The projection of this plane showing the disposition of sulfur is given in Figure 3.33. In this arrangement, each sulfur occupies 11.8 A^2. The third value for the area occupied by elemental sulfur was determined on the (110) plane (Figure 3.34). This plane was chosen since it contained a minimum number of sulfur atoms per unit area of chalcopyrite and, hence, it would give the largest possible value (19.2 A^2) for the area occupied by elemental sulfur.

As shown in Table 3.2, the amount of elemental sulfur

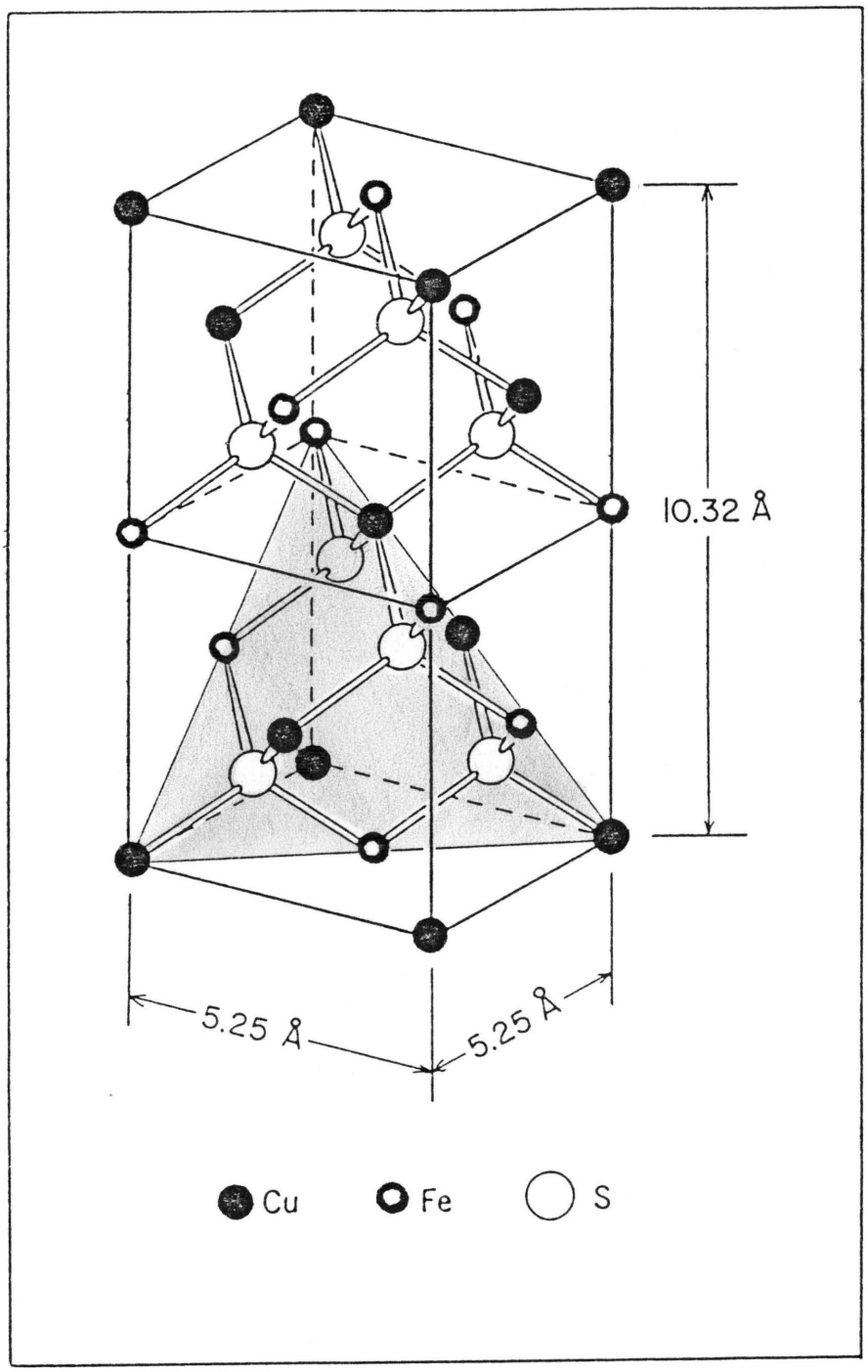

Figure 3.32 The unit cell of chalcopyrite with the (112) plane shaded (Herlbut and Klein, 1977).

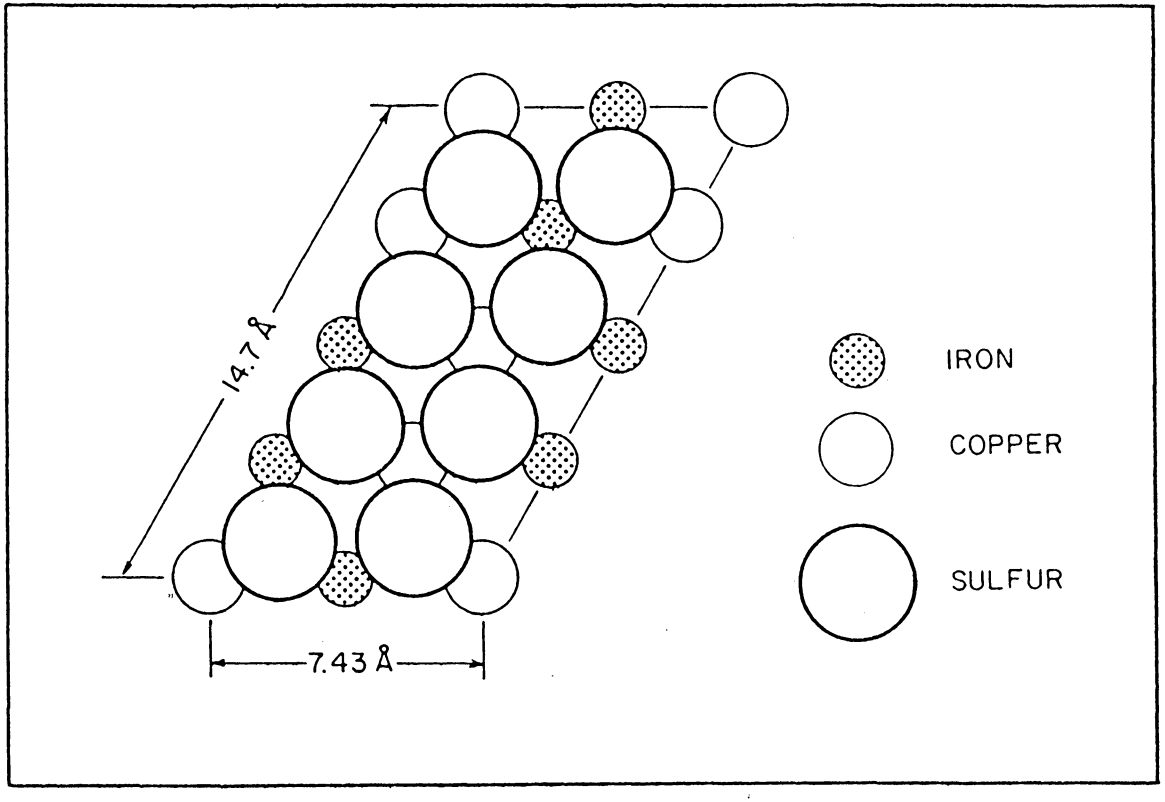

Figure 3.33 Atomic arrangement of the (112) plane of chalcopyrite.

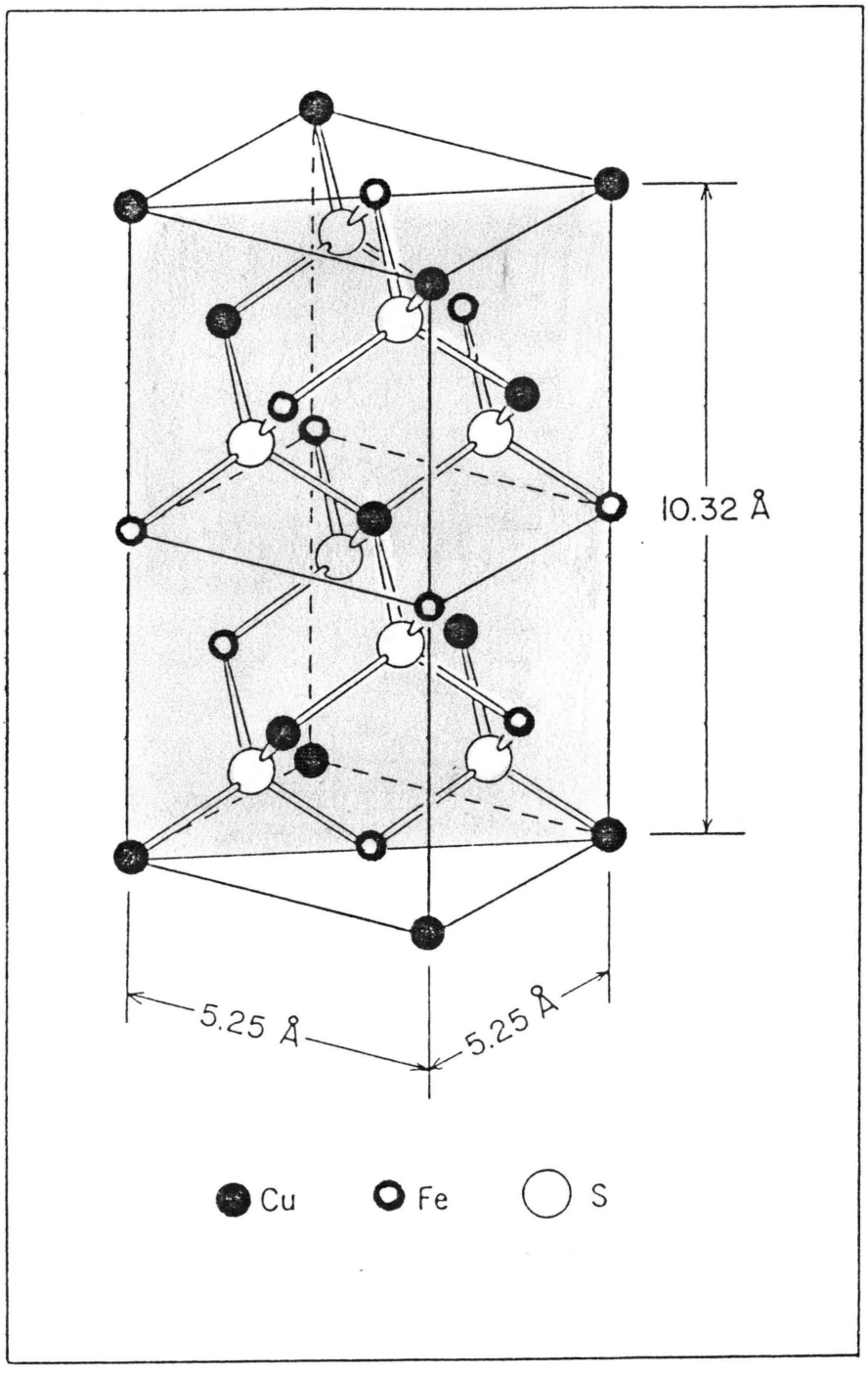

Figure 3.34 The unit cell of chalcopyrite with the (110) plane shaded (Herlbut and Klein, 1977).

determined by mass spectrometry was less than 3.7% of the monolayer capacity at pH values higher than 10. It seems unlikely that these small amounts of elemental sulfur could be responsible for the floatability of chalcopyrite observed in alkaline solutions. However, it is possible that the mass spectrometry may not be able to detect the elemental sulfur present in the first monolayer.

3.4 X-Ray Photoelectron Spectroscopy

3.4.1 Identification of Surface Species

a. Standards: XPS spectra of pure mineral samples of sulfur, covellite (CuS) and chalcopyrite ($CuFeS_2$) were obtained using a Dupont 650 Spectrometer. The binding energies and full peak widths measured at half peak intensities for the standard mineral samples are listed in Table 3.3. It should be noted that not all the spectra were curve-resolved to yield individual component peaks. Instead, the expected peak positions from the shapes of the envelopes were determined. For comparison, binding energies reported by Clifford, Purdy and Miller (1975) for chalcopyrite and covellite are also given in Table 3.3. The binding energies for the sulfur 2s and 2p peaks of elemental sulfur are given in Table 3.4, which includes those obtained in the present work and those reported in the literature. From Tables 3.3 and 3.4, one can see that the oxidation of sulfide (-2) to sulfur (0) accompanies a chemical shift of approximately 2 eV toward a higher binding energy.

b. Curve Resolved Sulfur Spectra: Gardner and Woods (1979) suggested that the oxidation of chalcopyrite yields both CuS and elemental sulfur as surface products. In order to test this hypothesis, a chalcopyrite sample was condi-

Table 3.3 Peak Locations and Widths Measured at Half Intensity for Sulfur, Covellite and Chalcopyrite

Sample Description	Peak	Binding Energy		Width
		Clifford, et. al. (1975)	Present Study	
Sulfur standard	S-2s		227.7	2.3
	S-2p		163.7	2.1
Covellite standard	S-2p		(168.3[1])	2.1
		164.5	163.7	2.1
		162.2	162.1	2.1
	$Cu\text{-}2p_{3/2}$		(935.3[2])	1.6
		934.6	933.5	1.6
		932.1	932.3	1.6
Chalcopyrite standard	S-2p	164.8	163.7	1.8
		162.6	162.1	1.8
		161.4	161.0	1.8
	$Cu\text{-}2p_{3/2}$		(933.6[3])	1.6
		932.2	932.0	1.6
	Fe-2p		unresolvable	

[1,2]Probably due to sulfate

[3]Probably due to copper oxide

Table 3.4 Comparison of Literature Values for the Binding Energy of Elemental Sulfur

	S2s	$S2p_{1/2}$	$S2p_{3/2}$
Present Study	227.7	163.7	
Seigbahn et al. (1967)	229	165	164
Jorgensen and Berthou (1972)	229	166	165
Clifford et al. (1975)	-	164.6	
Manocha and Park (1977)	-	164.6	
Zingg and Hercules (1978)	226.1	-	-
Pritzker, Yoon and Dwight (1980)	228.5	164.7	163.8

tioned in a 5% sodium sulfide solution for 30 minutes to remove preexisting oxidation products. The sample was then brought back into an oxidizing environment by rinsing the mineral several times with doubly distilled water adjusted to a pH value of 10.5 using sodium hydroxide. This procedure was immediately followed by vacuum-drying and XPS analysis. The sulfur 2p spectrum, thus obtained, was curve- resolved to identify the various sulfur species present. As shown in Figure 3.35, a best fit to the sulfur 2p envelope was obtained using the standard binding energies and peak widths given previously in Table 3.3 for elemental sulfur (163.7 eV), covellite (162.1 eV) and chalcopyrite (161.0 eV). This interpretation of the spectra appears to be consistent with the oxidation reaction of chalcopyrite (Equation 1.1) proposed by Gardner and Woods (1979).

c. Ion Sputtering: A comparison of the bulk and surface species for chalcopyrite was accomplished using the ion sputtering technique. The chalcopyrite concentrate (Texasgulf Type "A" ore) obtained after four stages of cleaner flotation was used in the analysis. Examination of the wide scans before and after sputtering to a depth of 40 A (Figures 3.36 and 3.37) showed an increased intensity of copper, sulfur and iron peaks, with that of oxygen being considerably diminished after sputtering. This indicates that some of the surface oxidation products were removed by

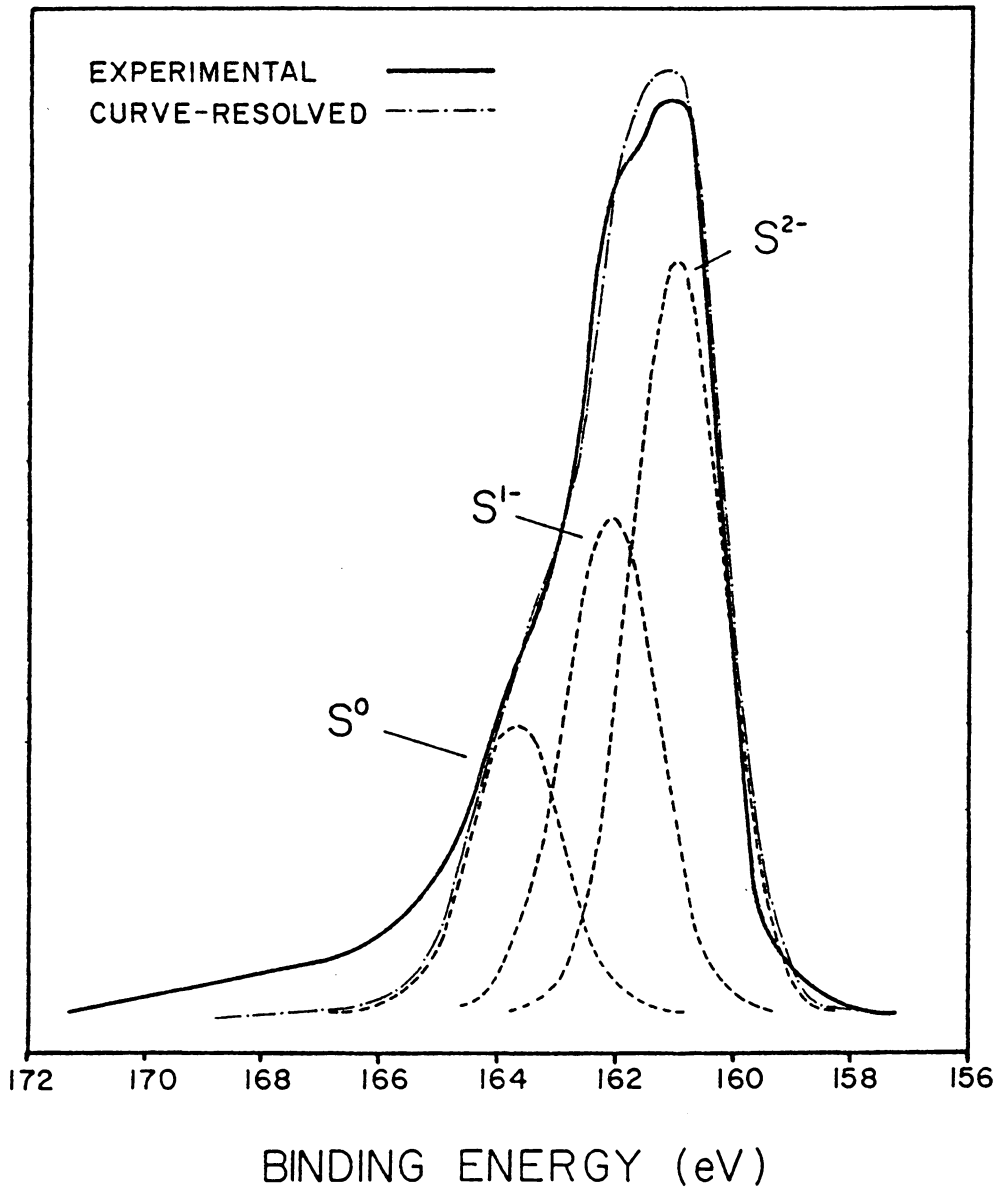

Figure 3.35 Curve-resolved sulfur 2p spectra of pure chalcopyrite (-65/+100 mesh). For the best fit, elemental sulfur, S^{1-} and S^{2-} are considered to have these characteristic peaks at 163.7, 162.1 and 161.0 eV, respectively.

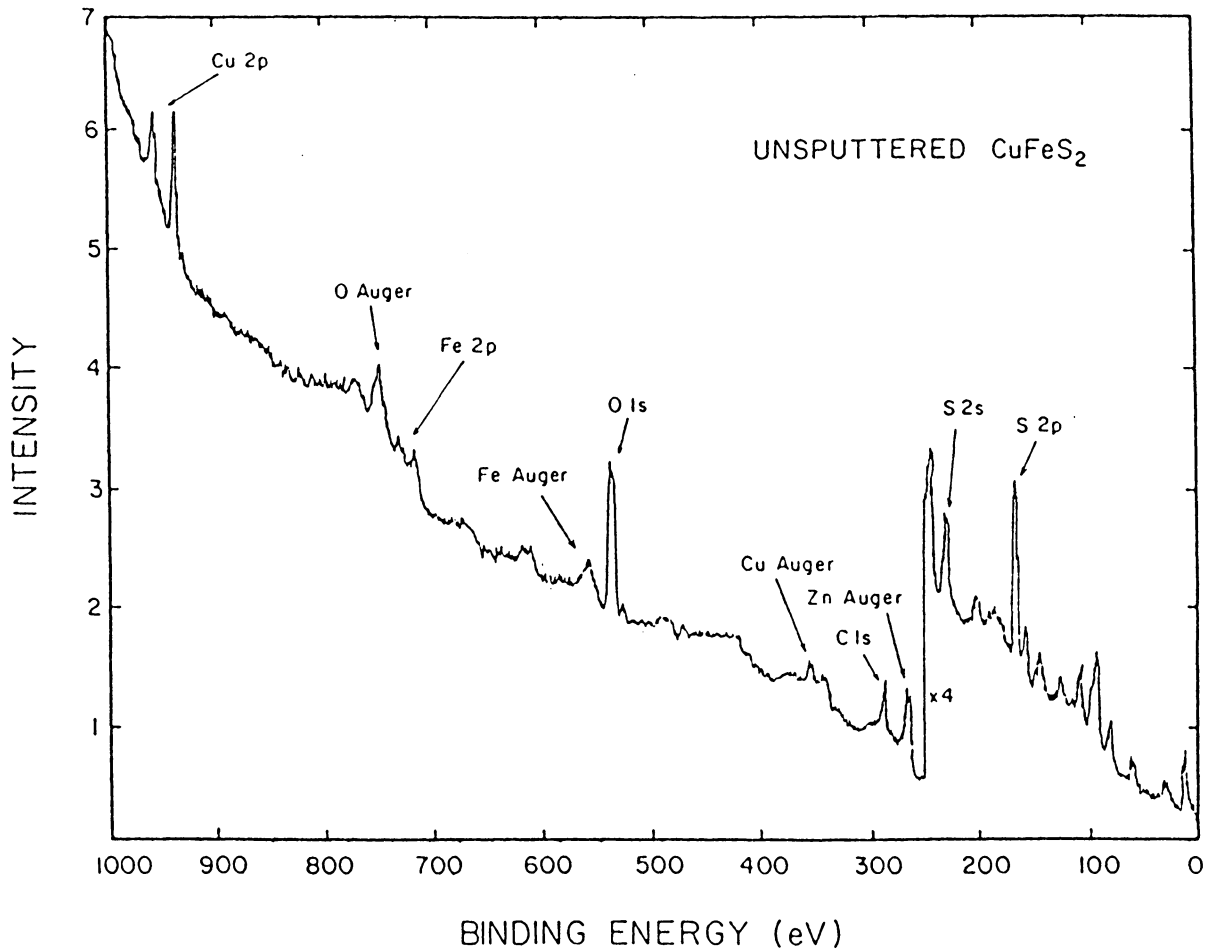

Figure 3.36 Wide scan XPS spectrum of a Texasgulf copper concentrate (floated at pH 6.5) prior to argon sputtering.

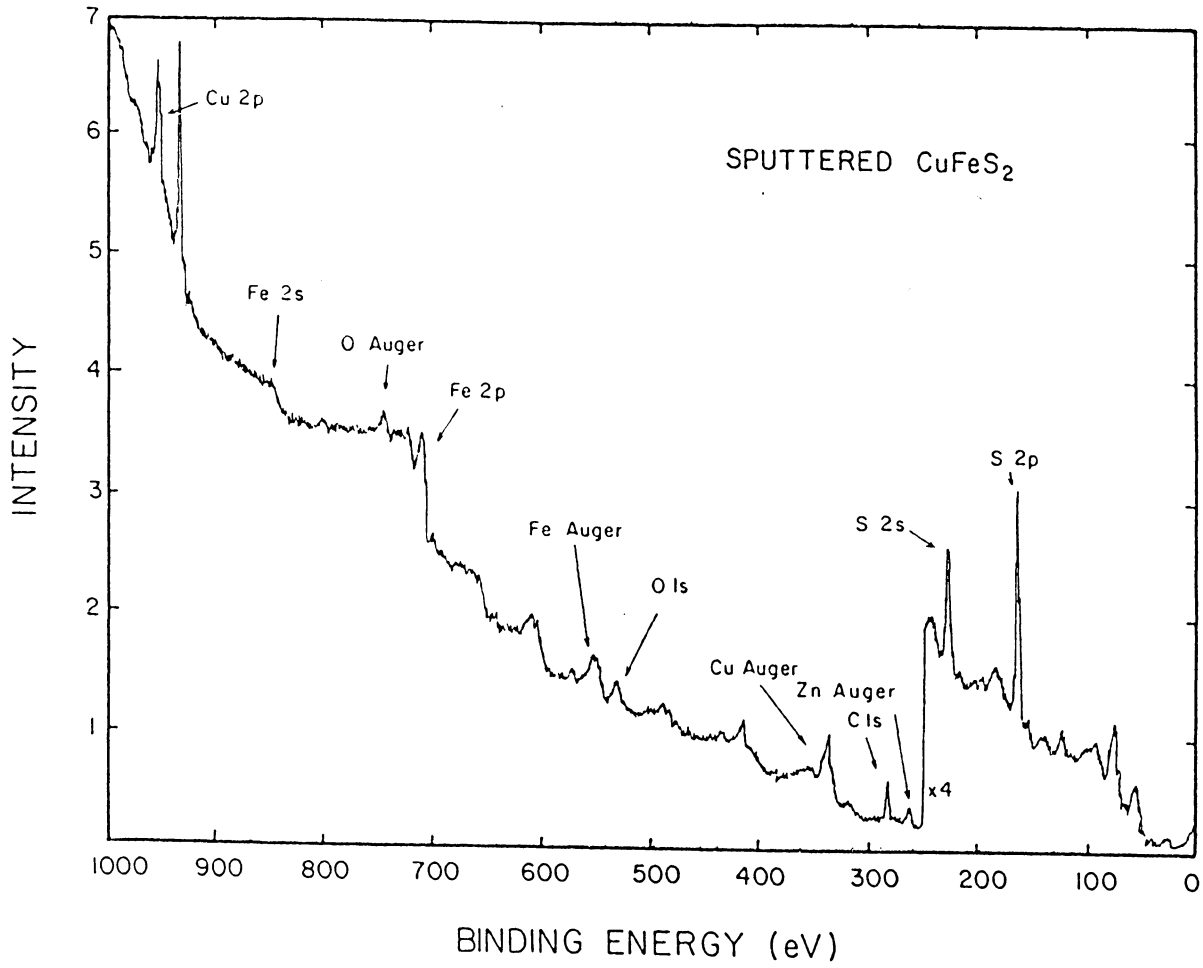

Figure 3.37 Wide scan XPS spectrum of a Texasgulf copper concentrate (floated at pH 6.5) after sputtering to a depth of approximately 40 A.

sputtering. The stoichiometric ratio of Cu:Fe:S was determined to be 1.5:1.0:6.3 before sputtering and 1.0:1.1:3.5 after sputtering. Thus, after sputtering, the stoichiometry approached that of bulk chalcopyrite, although the region was still very much richer in sulfur. The atomic ratios were calculated using the sensitivity factors tabulated by Wagner et al. (1979).

Figure 3.38 shows the sulfur 2p spectra for the chalcopyrite concentrate before and after sputtering. After sputtering, there was an increase in the intensity of the S^{2-} ion peak (161 eV) and a decrease in the $\overset{\circ}{S}$ peak (163.7 eV). The central peak (162.1 eV), which has been identified as S^{1-} in CuS (see Table 3.3), also displayed a decrease in intensity after sputtering. This finding shows that CuS and elemental sulfur peaks were indeed due to surface species formed by oxidation.

The copper $2p_{3/2}$ spectra for the chalcopyrite concentrate is shown in Figure 3.39. A slight shoulder near 934 eV in the spectrum of the unsputtered sample indicates the presence of cupric oxide. Its removal by sputtering confirms it as an oxidation product. The major peak (932 eV), corresponding to cuprous copper, can be assigned to both bulk chalcopyrite and surface product CuS since their copper $2p_{3/2}$ binding energies are nearly identical. Neither the copper nor sulfur spectra displayed peaks at binding energies characteristic of cupric sulfate.

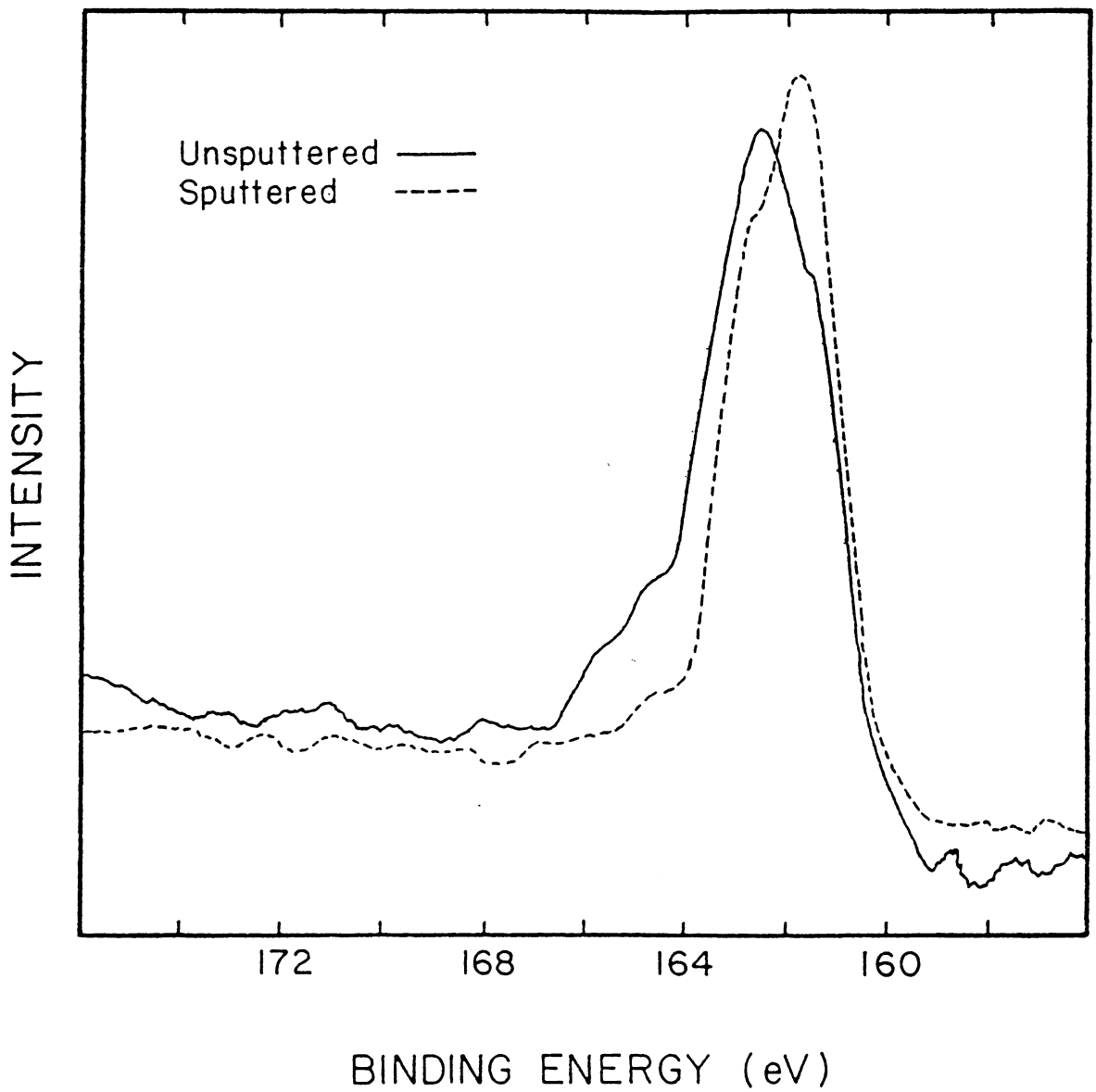

Figure 3.38 Sulfur 2p spectra of a Texasgulf copper concentrate (floated at pH 6.5) before and after sputtering.

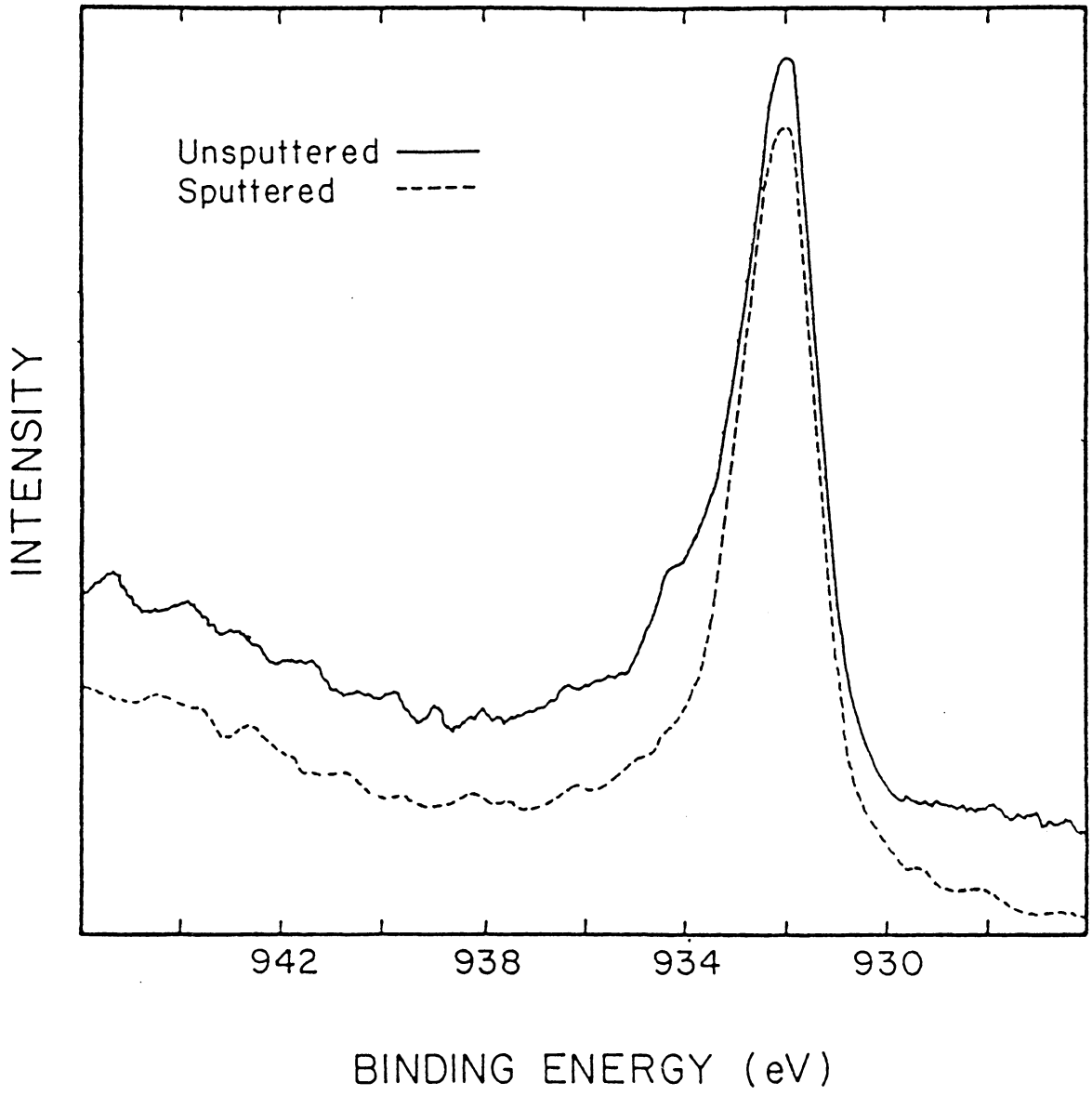

Figure 3.39 Copper $2p_{3/2}$ spectra of a Texasgulf copper concentrate (floated at pH 6.5) before and after sputtering.

Examination of the iron $2p_{3/2}$ spectra for this sample (Figure 3.40) revealed a considerable change in peak shape after sputtering. The spectra of the chalcopyrite prior to sputtering indicated the presence of an iron oxide which was responsible for the high binding energy peak. Upon sputtering, this peak was greatly diminished and replaced by a peak at a lower binding energy. The low binding energy peak was identified as iron in bulk chalcopyrite.

3.4.2 X-Ray Photoreduction

The application of the XPS technique to the analysis of copper-bearing minerals has been questioned since copper is known to be susceptible to photoreduction by x-rays (Clifford, Purdy and Miller, 1974; Ralston, Alabaster and Healy, 1981). Frost, Ishitani and McDowell (1972) found that soft x-rays could photoreduce cupric acetate to cuprous acetate within 30 minutes at room temperature. If the copper in copper sulfide is photoreduced, it might be possible that the sulfide ion could be oxidized to form elemental sulfur.

Thus, a series of spectra was collected from covellite (CuS) and chalcopyrite ($CuFeS_2$) samples over a period of approximately one hour to examine the photoreduction of the cuprous ion and the possible photo-oxidation of sulfide ion. Both the copper 2p and copper Auger spectra were collected to gather information necessary for the identification of

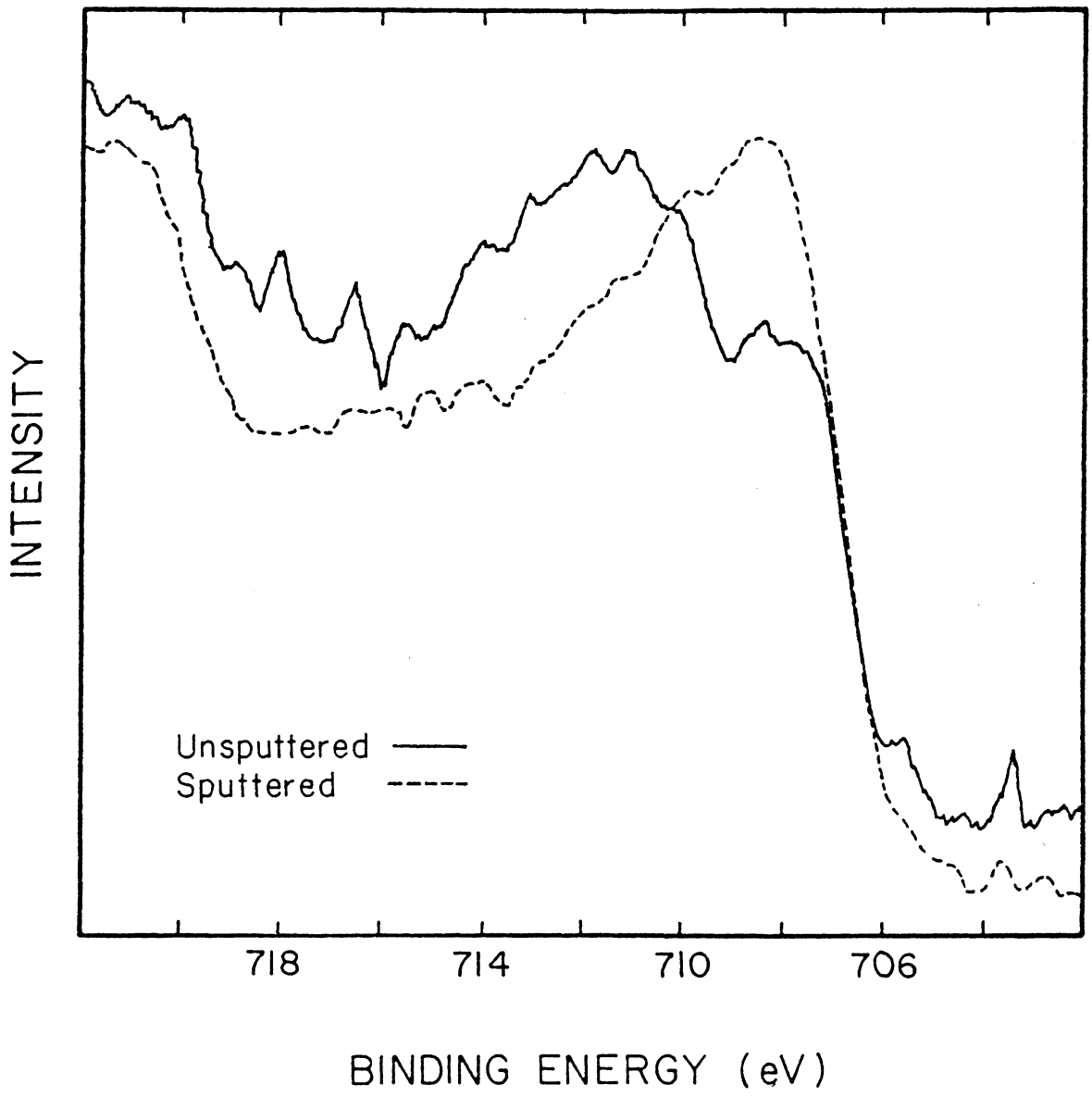

Figure 3.40 Iron $2p_{3/2}$ spectra of a Texasgulf copper concentrate (floated at pH 6.5) before and after sputtering.

species present on the mineral surface using the Auger parameters. The results of these experiments are shown in Figures 3.41 and 3.42 for covellite and chalcopyrite, respectively. As shown, copper was being reduced at the surface of both minerals to eventually produce copper metal after a long exposure time. Sulfur and copper spectra collected during the same period were curve-resolved, so that changes in the amounts of various species could be determined quantitatively. However, the amount of elemental sulfur detected on the mineral surfaces did not increase significantly while the copper was being photoreduced.

3.4.3 Effect of Potential:

The effect of potential on the natural floatability of chalcopyrite has been well established in the present work. However, the changing surface species at various potentials have not been well identified. Thus, micro-flotation tests were conducted on pure samples of chalcopyrite conditioned at various potentials in the alkaline pH region, and the flotation products were analyzed by XPS. The floatability of the mineral as a function of potential has already been shown in Figure 3.5. The sulfur 2p and copper 2p spectra of some of the flotation products are given in Figure 3.43. Samples conditioned at potentials of -236 mV and +215 mV showed a drastic difference in floatability (8% versus 77%). If the flotation is caused by

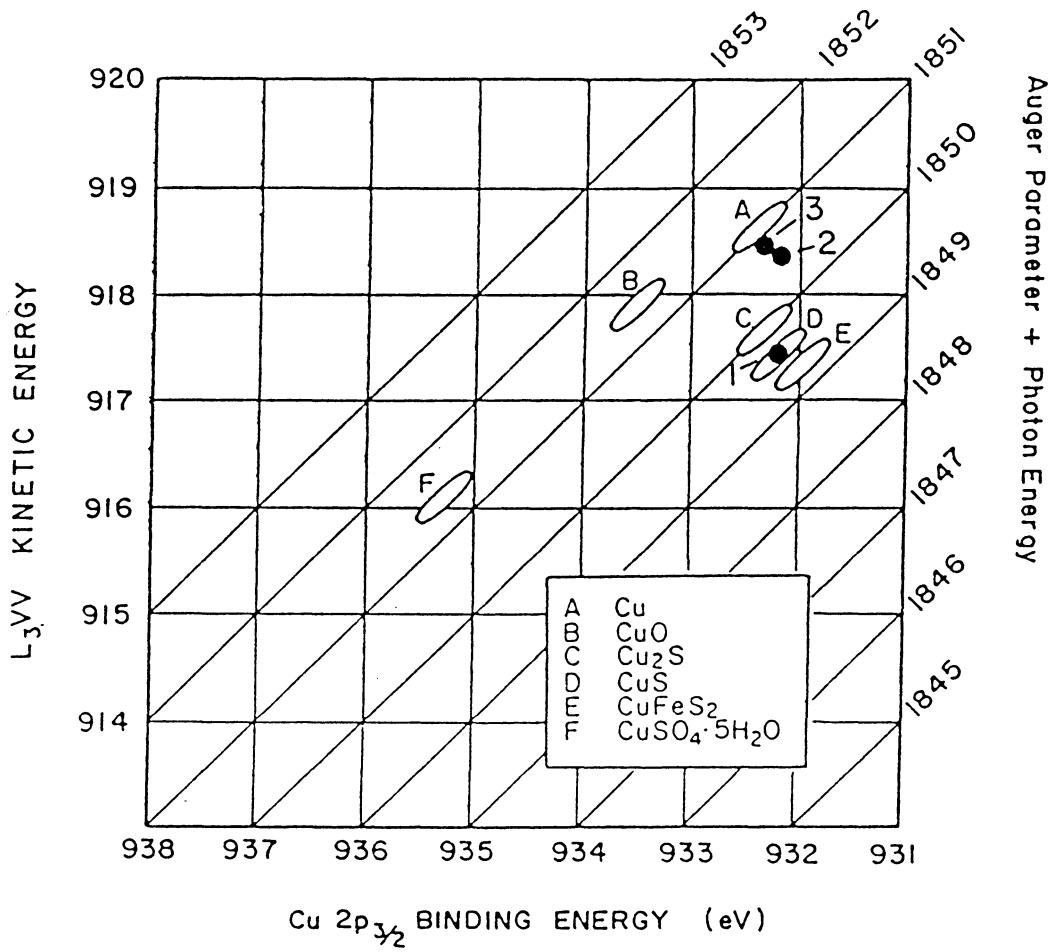

Figure 3.41 Auger parameter determination for covellite after x-ray exposure for varied lengths of time. 1 - 15 min., 2 - 30 min., 3 - 45 min. The data represented by A through F are from Wagner et al. (1979).

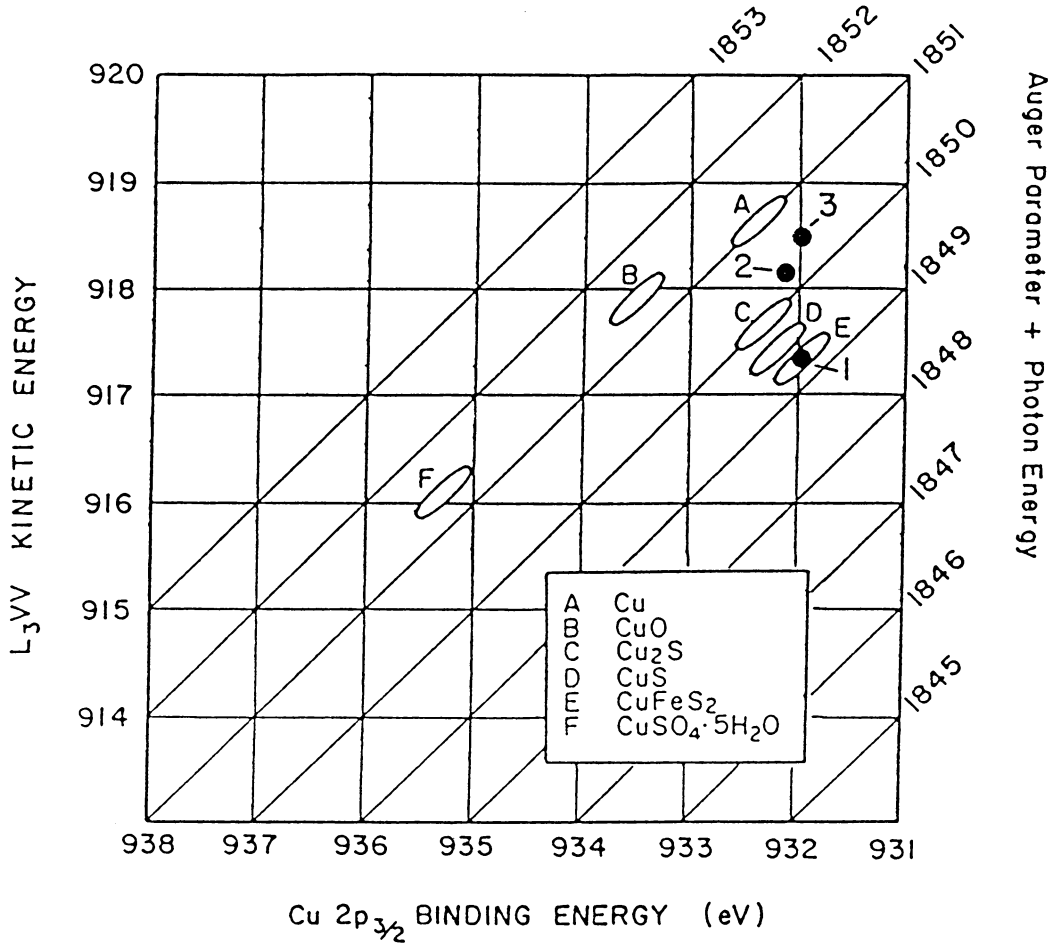

Figure 3.42 Auger parameter determination for $CuFeS_2$ after x-ray exposure for varied lengths of time. 1 - 15 min., 2 - 30 min., 3 - 45 min. The data represented by A through F are from Wagner et al. (1979).

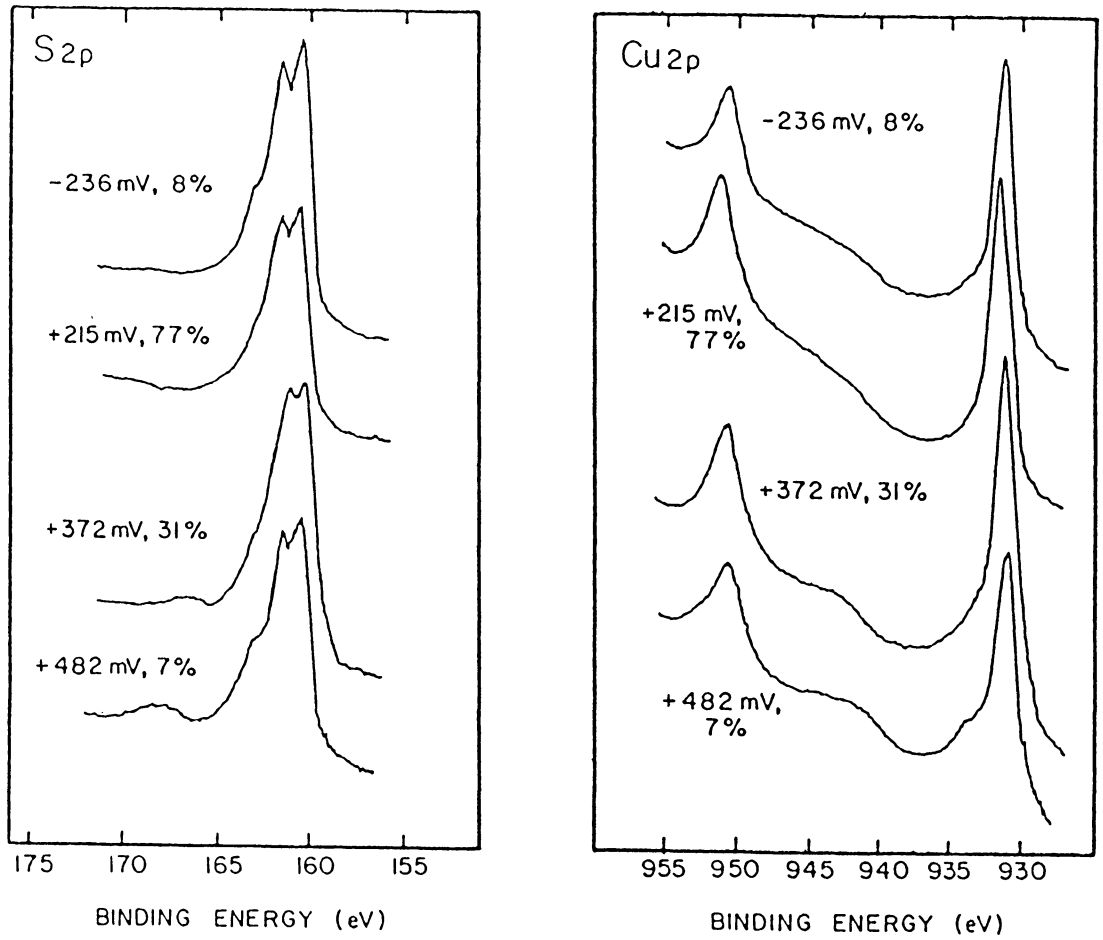

Figure 3.43 Sulfur and copper 2p spectra of chalcopyrite (Transvaal Deposit) concentrates from micro-flotation at various potentials. The potential at the time of flotation and floatability of the sample are given on each spectrum.

elemental sulfur, one should expect to see a larger amount of elemental sulfur on the chalcopyrite sample conditioned at +215 mV; however, the reverse appears to be the case. The peak at approximately 164 eV appears to be stronger at the reducing potential of -236 mV. A possible explanation might be that the sulfide ions added to reduce the potential may have been oxidized during the drying procedure to become elemental sulfur. The effect of drying will be considered further in Section 3.5.1.

As the potential was increased from +215 mV to +482 mV by the addition of small amounts of an oxidizing agent ($KMnO_4$), the intensity of the elemental sulfur peak increased considerably, as shown in Figure 3.43. Again, if elemental sulfur is responsible for flotation, the floatability should have increased with increasing amounts of elemental sulfur on the mineral surface. However, the floatability decreased with increasing potential. Two possible explanations may be given. First, at higher potentials, cupric sulfate is formed as indicated by the small shoulder near 168 eV in the sulfur 2p spectra and the peaks at 934 and 944 eV in the copper 2p spectra. This small shoulder at 934 eV and the broader satellite peak at 944 eV indicate copper II, presumably due to the presence of cupric sulfate. A second possibility for the lack of floatability is in the formation of manganese dioxide, as indicated by the manganese 2p spectrum shown in Figure 3.44.

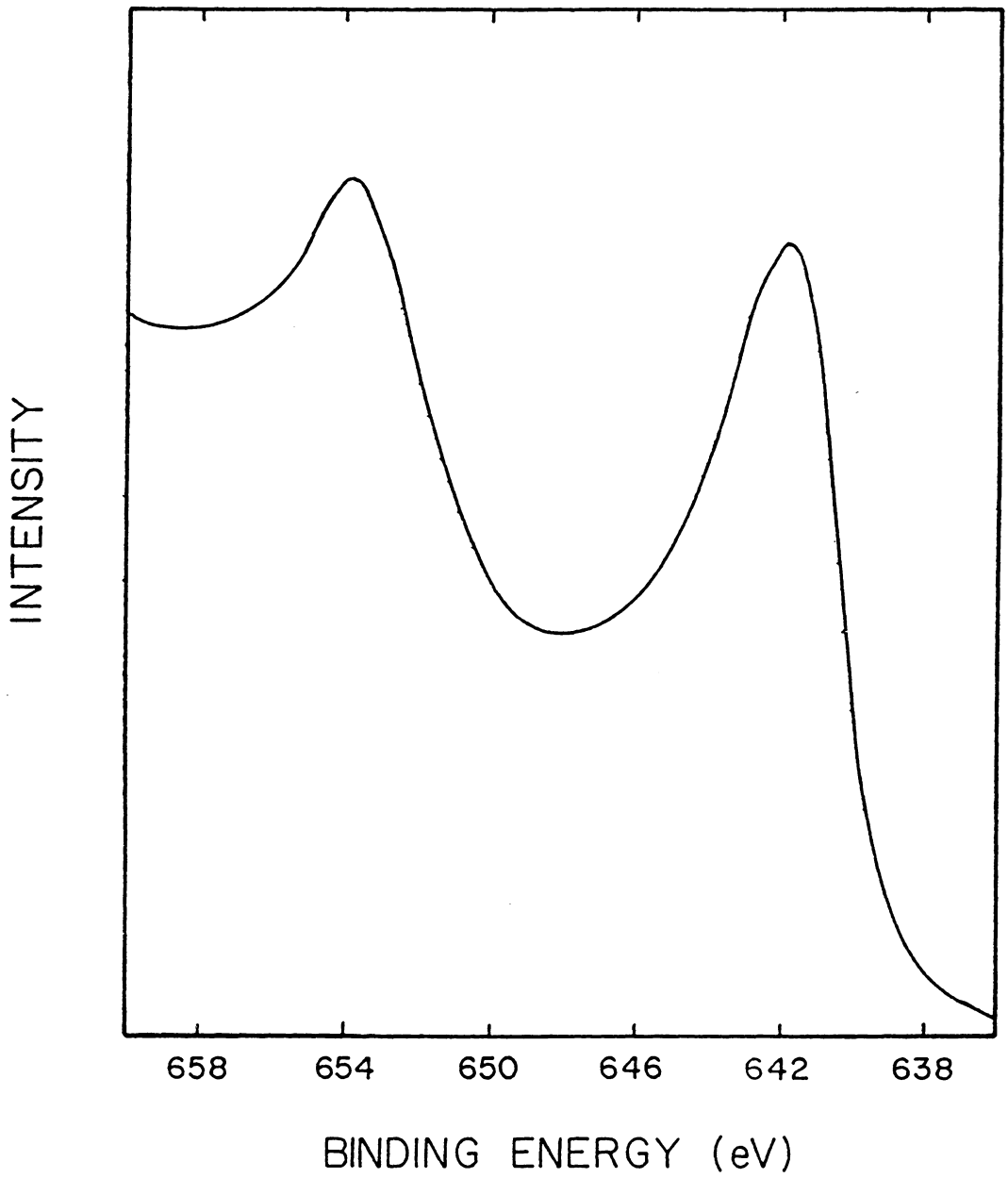

Figure 3.44 Manganese 2p spectra of nonfloating chalcopyrite obtained from micro-flotation using potassium permanganate to raise the potential to +482 mV.

This analysis verified the presence of large amounts of manganese on the mineral surface after potassium permanganate addition.

3.4.4 Analysis of Batch Flotation Concentrates

a. Effect of pH: In general, collectorless flotation is favored at a lower pH. For example, the flotation of the Mount Isa ore using 3 lb/ton of sodium sulfide gave 48% recovery with 26.4% Cu at pH 11.1 and 60% recovery with 28.8% Cu at pH 6.5. The flotation concentrates of these two tests were analyzed by XPS, and the total S/Cu ratios are given in Table 3.5. For comparison, the table also shows the XPS results obtained on the pure chalcopyrite samples separated from the same ore by gravity: one half of the sample was analyzed directly and the other half was analyzed after sodium sulfide treatment.

Note that the gravity-separated samples show an increase in the S/Cu ratio from 1.8 to 2.4 after the sodium sulfide treatment. One might suggest that excess sulfide ions, either adsorbed on the chalcopyrite surface or retained in the residual solution adhering to the filtered chalcopyrite, have been oxidized to elemental sulfur upon drying. However, the sulfur 2p spectrum of the sodium sulfide treated sample does not show a higher S or S^{1-} peak intensity relative to the S^{2-} peak. It appears that a considerable amount of the S^{2-} ion added may have

Table 3.5 Ratio of Total Sulfur to Total Copper as Determined by XPS for Concentrates from the Mount Isa Ore

Description	Ratio S/Cu
Gravity concentrated without sodium sulfide treatment	1.8
Gravity concentrated followed by sodium sulfide treatment	2.4
Concentrate after flotation at pH 10.0 with sodium sulfide	0.6
Concentrate after flotation at pH 6.5 with sodium sulfide	1.7

penetrated the surface region, making it sulfur-rich.

The flotation concentrate obtained at pH 6.5 shows a higher S/Cu ratio than the concentrate obtained at pH 10.0 (1.7 versus 0.6). Again, an examination of the sulfur 2p spectrum does not indicate that the higher S/Cu ratio is due to the increasing amount of elemental sulfur which is more stable at a lower pH. It is possible that at lower pH values, copper ions are more easily leached out, resulting in a higher ratio of S/Cu. Nevertheless, it is clear that regardless of the oxidation state of sulfur, a higher S/Cu ratio gives rise to better flotation.

b. Effect of Sodium Sulfide: Table 3.6 shows the total sulfur-to-total copper ratio (S/Cu) obtained by XPS for chalcopyrite concentrates from the Ray Mines ore that was exposed to various surface treatments. The chalcopyrite sample concentrated from the ore by a gravity technique shows a slight increase in the S/Cu ratio (from 1.3 to 1.5) after rinsing it several times with a 1% sodium sulfide solution. This result indicates that the surface becomes richer in sulfur after sodium sulfide treatment and vacuum drying. A similar finding was made with samples treated in the same manner and analyzed by mass spectrometry.

The flotation results obtained with the Ray Mines ore have been given in Figure 3.7. It is shown that the ore floated better when no sodium sulfide was added to the pulp.

Table 3.6 Ratio of Total Sulfur to Total Copper as Determined by XPS for Concentrates from the Ray Mines Ore

Description	Ratio S/Cu
Gravity concentrated without sodium sulfide treatment	1.3
Gravity concentrated followed by sodium sulfide treatment	1.5
Concentrate after flotation at pH 9.0 with a frother only	0.6
Concentrate after flotation at pH 10.0 with sodium sulfide	2.5

Surface analysis of the concentrates obtained after three cleaning stages with and without sodium sulfide yielded S/Cu ratios of 2.5 and 0.6, respectively. These results may suggest that a lower S/Cu ratio is more conducive to flotation. However, further investigation is necessary to obtain conclusive evidence.

Micro-flotation results obtained earlier showed that the pure chalcopyrite samples, which were treated with sodium sulfide and dried prior to flotation, gave 98% floatability, while those that were not dried floated only 80% (Table 3.1). Possibly, the drying procedure created an oxidizing condition, as has already been noted. Thus, the XPS technique of surface analysis requiring the samples to be dried may not give information pertinent to flotation.

3.4.5 Effect of Frother Adsorption:

Figure 3.45 shows the carbon 1s spectra of the chalcopyrite concentrate obtained at pH 6.0 using 1.5 lb/ton of sodium sulfide and 0.2 lb/ton of frother. The unsputtered sample shows the carbon peaks at 284.6 eV and 287.0 eV. The former is due to the standard carbon contamination, and the latter is probably due to the frother adsorption. Upon sputtering, the shoulder is removed, indicating that it is due to an adsorbed species. Such a shoulder was observed only on the concentrates of the Texasgulf Type "A" ore and the Mount Isa ore (Figure 3.46) treated at pH values of 6.0

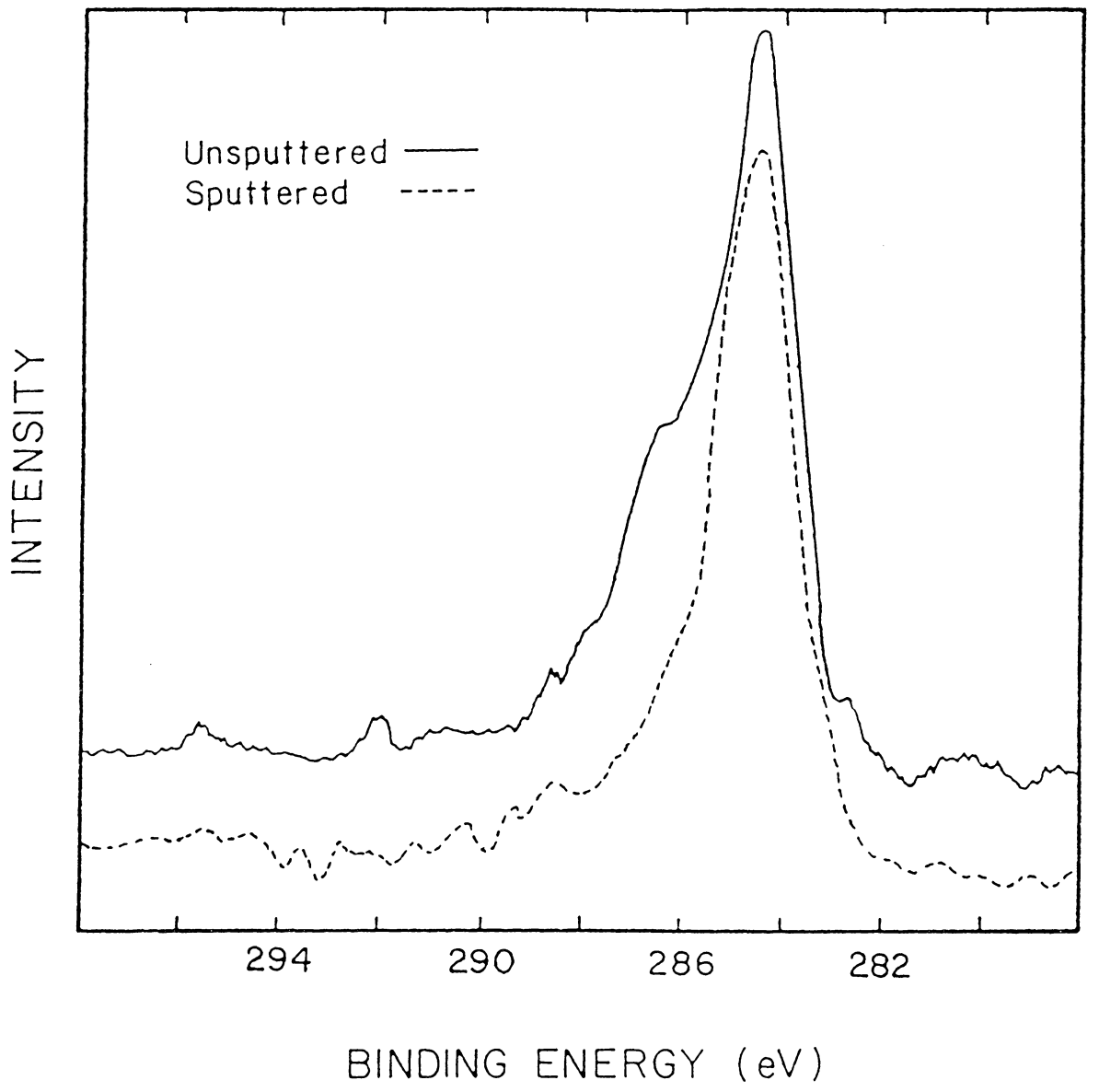

Figure 3.45 Carbon 1s spectra of a Texasgulf copper concentrate before and after sputtering.

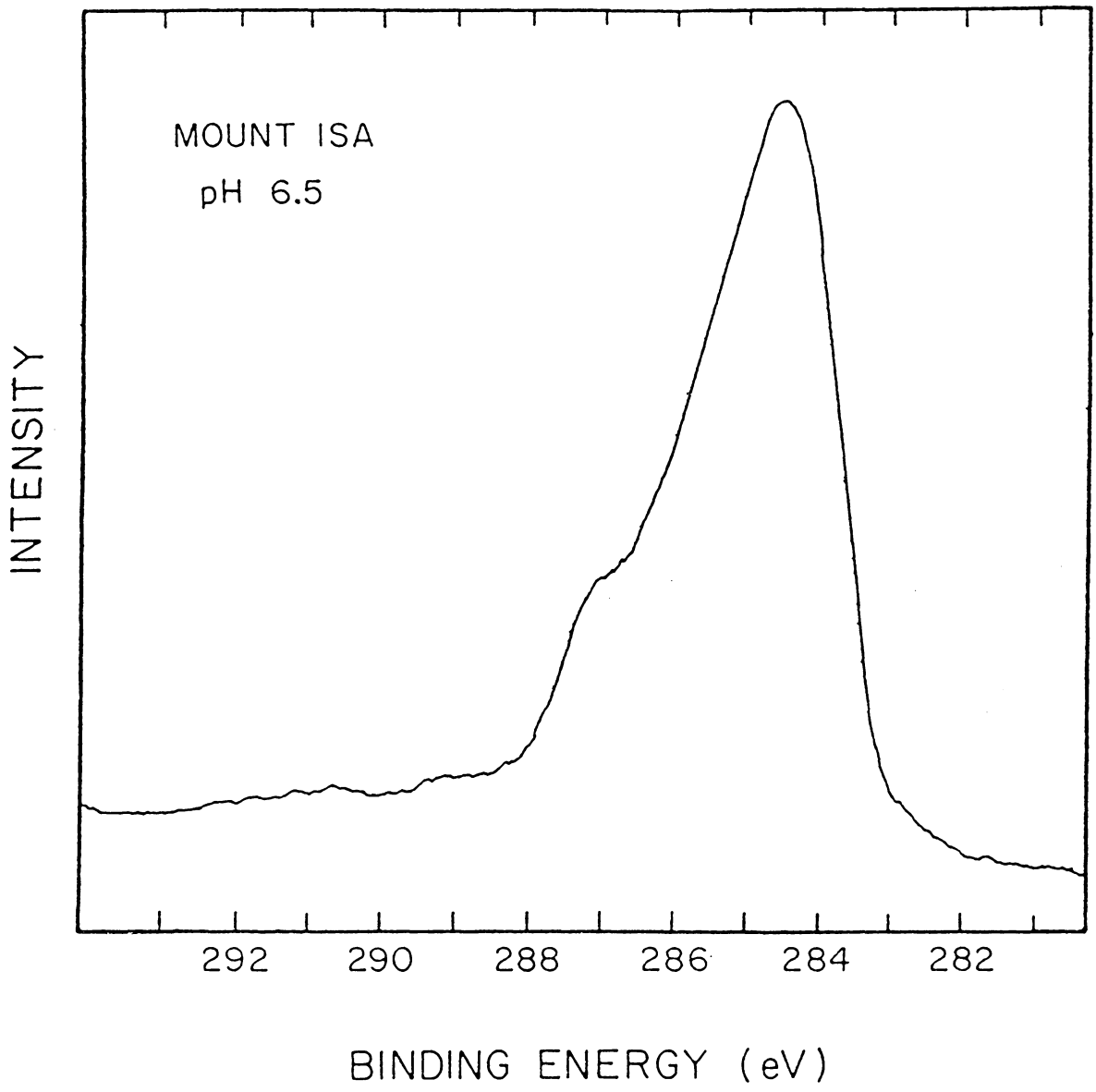

Figure 3.46 Carbon 1s spectrum of a Mount Isa copper concentrate floated at pH 6.5.

and 6.5, respectively. However, no such shoulder was observed on the concentrates obtained in the alkaline pH ranges. Since the adsorption of frother molecules, which is likely controlled by hydrophobic bonding, would be favored on hydrophobic surfaces, these results may suggest that chalcopyrite becomes more hydrophobic in slightly acidic solutions.

3.5 UV Spectrophotometry

3.5.1 Elemental Sulfur Detection

The UV absorption by elemental sulfur dissolved in organic liquids has long been known (Ford and LaMer, 1950; Freidman and Kerder, 1953; Bass, 1953). This property has been used by many investigators for the detection of elemental sulfur on mineral samples (Koren 1969; Rolia, 1977; Heyes and Trahar; 1977). In this method, sulfur is first extracted from the surface of the mineral by an organic solvent. The sulfur concentration in the extractant is then determined by measuring the absorbance at 260-280 nm. In the present work, ethanol was used as the solvent and the absorbance readings were taken at 275 nm. The solubility of sulfur in ethanol was reported to be 66 mg/liter (Trahar, 1982). The calibration curve used in this study is included in Appendix V.

The sulfur extraction procedure was applied to a finely pulverized chalcopyrite sample which had been allowed to oxidize in air for a period of approximately two months (surface area of 0.88 m^2/gram, see Appendix VI). The UV spectra of the ethanol extract is shown in Figure 3.47. From the absorbance reading at 275 nm, the sulfur concentration in the extract was determined using the calibration curve. The amount of sulfur, thus determined, corresponds to approximately 2.1 monolayer equivalents. Hence, it

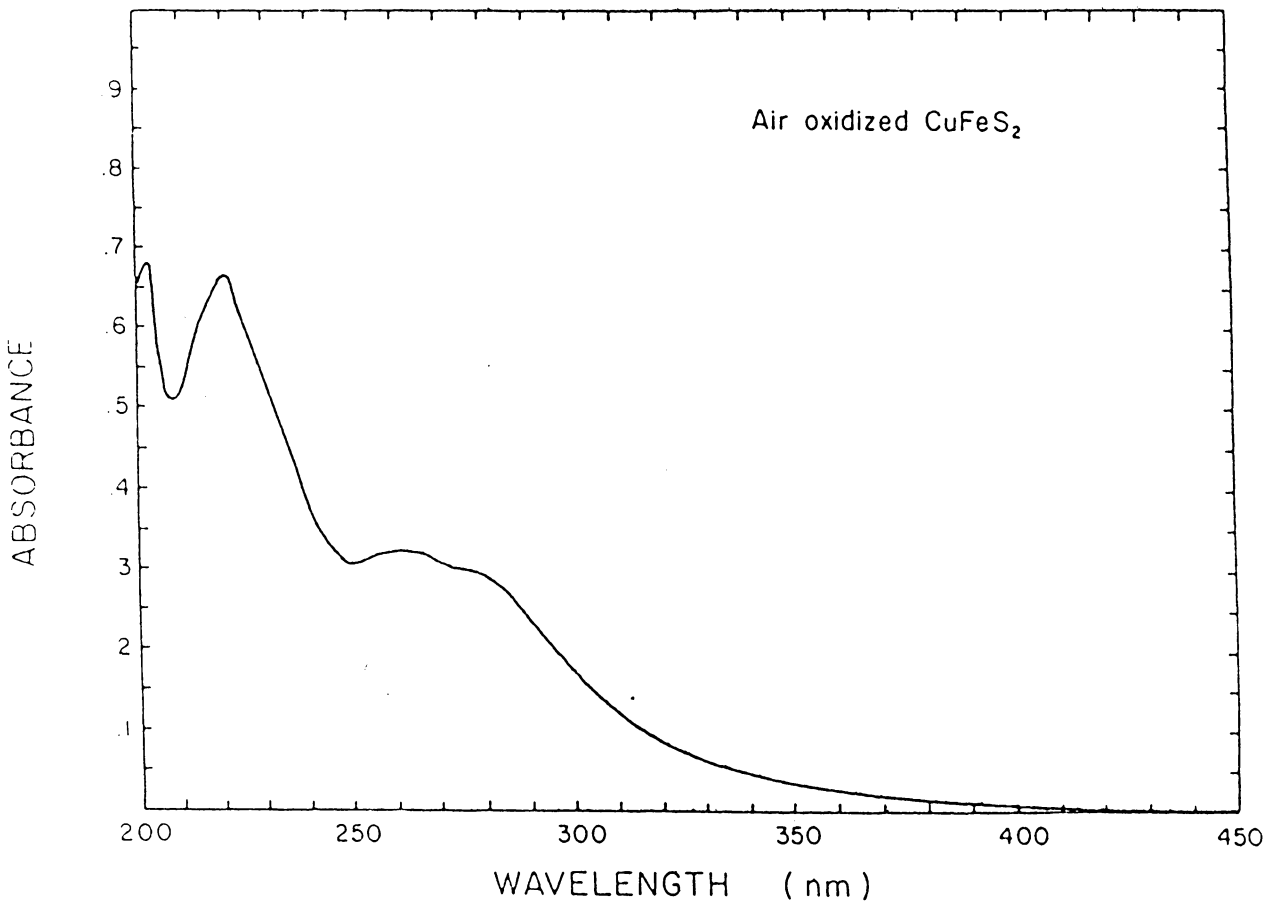

Figure 3.47 UV spectrum of ethanol contacted for 30 minutes with finely pulverized chalcopyrite. 0.01 gm $CuFeS_2$/ml ethanol was used.

appears that two months of air oxidation is adequate to form several monolayers of sulfur on the chalcopyrite surface.

The XPS results obtained earlier (Section 3.4.3) tend to suggest that drying a sample produces elemental sulfur. In order to test this possibility, a relatively clean chalcopyrite sample was analyzed for elemental sulfur by UV analysis with and without drying the sample. The oxidized chalcopyrite sample was washed three times with a 5% sodium sulfide solution to clean the surface. The sample was then rinsed several times with doubly distilled water until the potential of the final rinse water was measured to be +181 mV. Roughly one half of the chalcopyrite sample, thus prepared, was analyzed without drying the sample, and the other half was analyzed after vacuum-drying. The UV spectra of the ethanol extracts of these two samples are shown in Figure 3.48. Also shown in this figure is the spectrum of ethanol in which a small amount of sodium sulfide was dissolved. This spectrum was taken to ensure that sulfide ions did not interfere with the determination of elemental sulfur at 275 nm. From these spectra, it was calculated that approximately 2.8 monolayer equivalents of sulfur were extracted from the surface of the dried sample, while the wet-treated sample showed only 1.1 monolayers. This seems to confirm that vacuum-drying of chalcopyrite after sodium sulfide treatment enhances the formation of elemental sulfur.

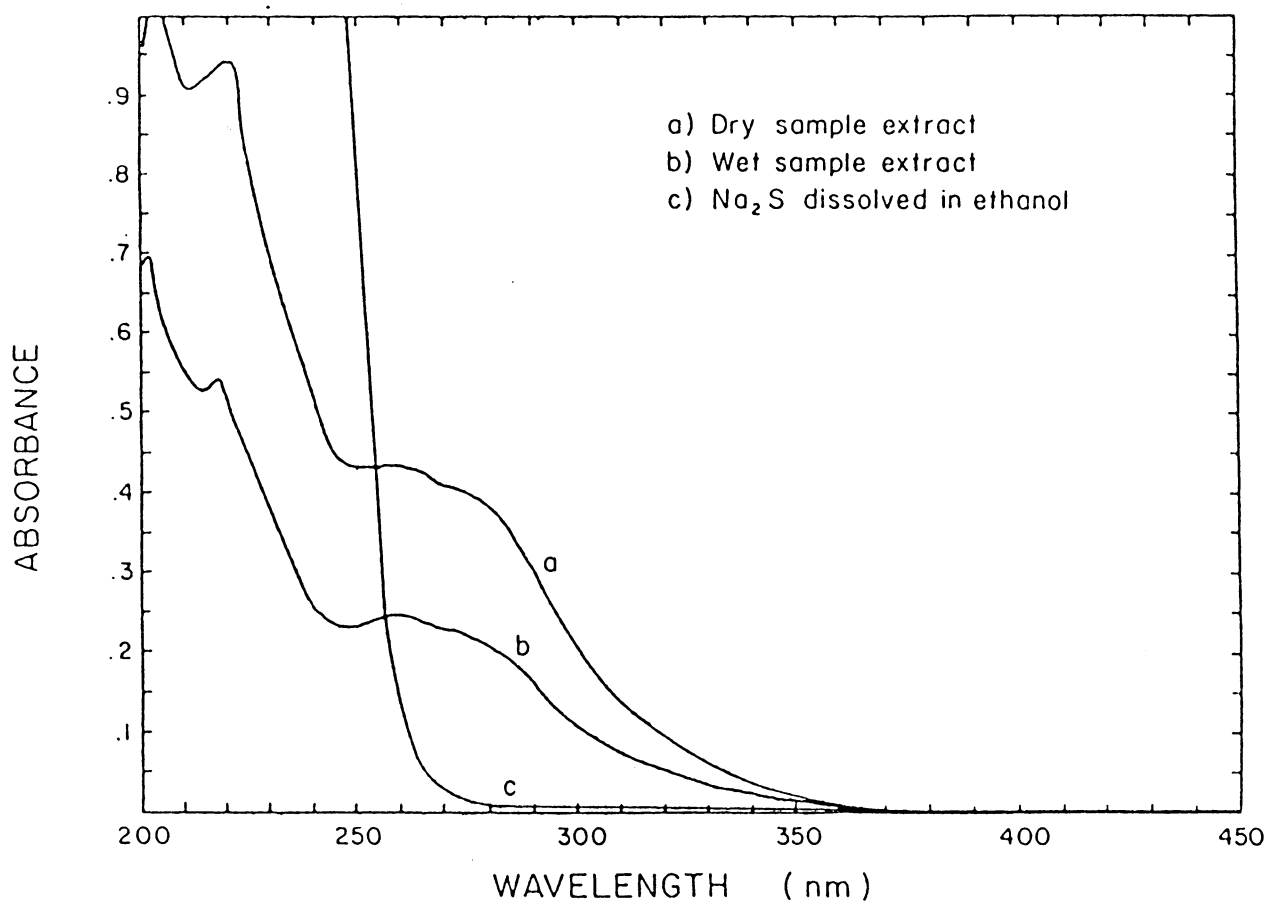

Figure 3.48 UV spectra of ethanol contacted for 30 minutes with finely pulverized chalcopyrite conditioned at +181 mV after sodium sulfide cleaning. a) 0.01 gm $CuFeS_2$/ml ethanol, b) 0.013 gm $CuFeS_2$/ml ethanol.

In another experiment, the oxidized chalcopyrite sample was cleaned three times with a 5% sodium sulfide solution and then left in the reducing solution (potential of -238 mV). As in the previous experiments, sulfur analysis was done on both wet and vacuum-dried samples. The samples were not rinsed with distilled water in an attempt to preserve the reducing conditions. The UV spectra of the ethanol extracts are given in Figure 3.49. The results of these tests indicate that 0.44 monolayer equivalents of sulfur were present on the wet-extracted sample and 3.1 monolayers of sulfur were detected on the vacuum-dried sample. Again, these results suggest that vacuum-drying induced additional sulfur formation, even with samples conditioned under reducing conditions.

The results of the UV analyses described above are summarized in Table 3.7. It clearly shows that the amount of sulfur determined for the vacuum-dried samples was approximately the same (2.95 ± .15 monolayers), regardless of the redox conditions in which the samples were conditioned. Assuming that the wet-analyzed results are more reliable, the amount of elemental sulfur was increased by about 150% (i.e., 0.4 to 1.1 monolayers) in going from reducing (-238 mV) to oxidizing (+264 mV) conditions. This might suggest that the elemental sulfur that forms under oxidizing conditions is responsible for collectorless flotation.

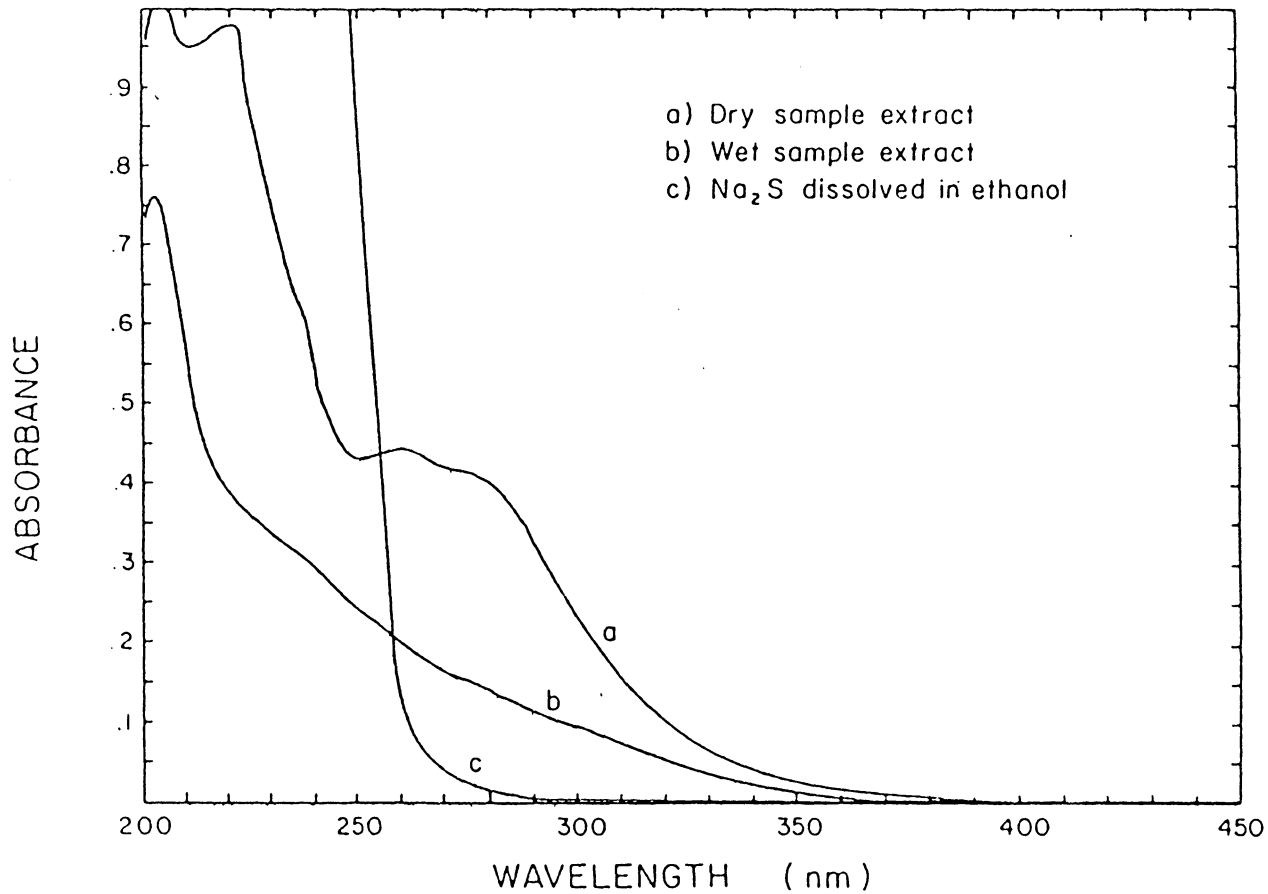

Figure 3.49 UV spectra of ethanol contacted for 30 minutes with finely pulverized chalcopyrite conditioned at -238 mV in a sodium sulfide solution. a) 0.01 gm $CuFeS_2$/ml ethanol, b) 0.022 gm $CuFeS_2$/ml ethanol.

Table 3.7 Quantitative Detection of Elemental Sulfur Extracted from a Finely Pulverized Chalcopyrite Sample Using UV Spectrophotometry

Sample Description	Monolayers of Sulfur	
	Wet Sample	Dry Sample
Air oxidized 2 months	---	2.1
Air oxidized 2 months, cleaned with Na_2S, rinsed with H_2O (+181 mV, pH 7.4)	1.1	2.8
Air oxidized 2 months, cleaned with Na_2S, no H_2O rinse (-238 mV, pH 10.8)	0.4	3.1
Air oxidized 2 months, cleaned with N_2H_4, no H_2O rinse (-236 mV, pH 10.4)	1.7	---

The lack of flotation under reducing conditions may be attributed to the absence of elemental sulfur on the chalcopyrite surface. However, a seemingly conflicting result was obtained when hydrazine, another reducing agent, was used in place of sodium sulfide in cleaning the sulfide mineral. The oxidized chalcopyrite sample was cleaned three times in a 5% hydrazine solution. The potential measured at the end of the third cleaning was -236 mV. The sulfur analysis by the UV technique conducted on this sample, without vacuum-drying, gave as much as 1.7 monolayer equivalents of elemental sulfur (Figure 3.50). Yet, the results shown previously in Figure 3.4 indicate that hydrazine suppresses chalcopyrite flotation at reducing potentials in the same manner as does sodium sulfide.

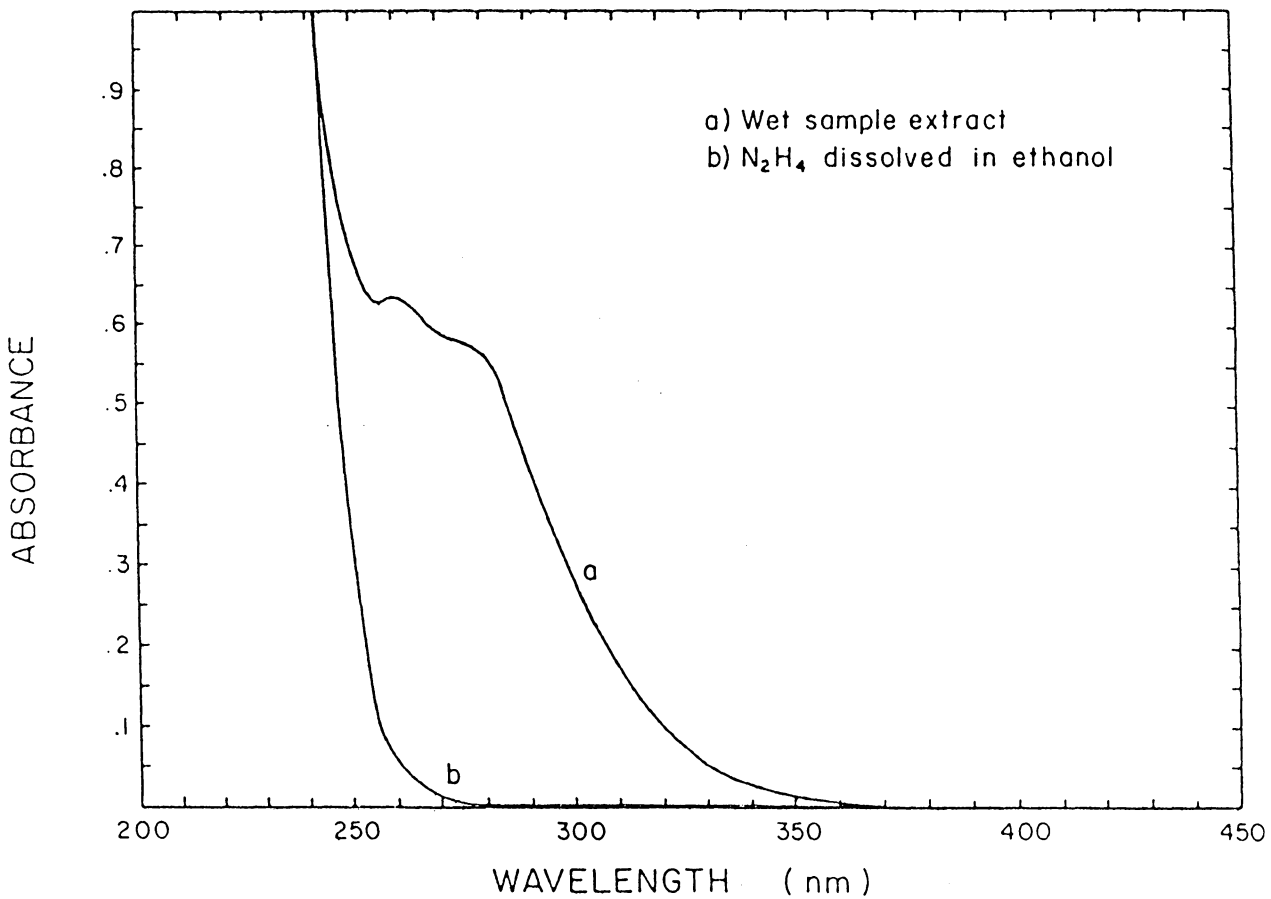

Figure 3.50 UV spectra of ethanol contacted for 30 minutes with finely pulverized chalcopyrite conditioned at -236 mV in a hydrazine solution. a) 0.024 gm $CuFeS_2$/ml ethanol.

IV. DISCUSSION

4.1 Flotation

4.1.1 Flotation of Chalcopyrite

a. Criteria for Collectorless Flotation: The results of the micro-flotation experiments presented in Section 3.1 clearly show that pure samples of chalcopyrite are floatable without a collector only in oxidizing conditions. This was first suggested by Heyes and Trahar (1977) and later confirmed by Gardner and Woods (1979). However, it appears that these authors failed to consider the effect of excessive oxidation on floatability. The results shown in Table 3.1 and Figure 3.2 indicate that an oxidizing environment is not the only requirement for flotation in the absence of a collector. A relatively fresh mineral surface, free of hydrophilic oxidation products, is also necessary for good flotation. Furthermore, the floatability in oxidizing conditions appears to depend on the degree to which the mineral surface has been oxidized.

There is experimental evidence pointing to the above generalization. Firstly, Heyes and Trahar (1977) reported that while the Mount Lyell chalcopyrite responded well to collectorless flotation, the chalcopyrite in the Mount Isa ore did not. The batch flotation data shown in Figure 3.11 indeed shows that the Mount Isa ore was not floatable with a frother alone. However, good flotation (48%

recovery with 26.4% grade) was obtained when the ore was treated with sodium sulfide. The role of sodium sulfide is one of a cleaning agent that removes hydrophilic oxidation products. All the other chalcopyrite samples tested in the present work are also floatable without collectors, requiring varying degrees of sulfidization. Note that some ores such as Ray Mines and Craigmont do not require sodium sulfide for flotation, presumably because the chalcopyrite in these ores was not severely oxidized.

Secondly, all the chalcopyrite ores tested in this investigation gave positive potentials after grinding for 30 minutes with steel balls in a porcelain mill (Figure 3.14). According to Heyes and Trahar (1977) and Gardner and Woods (1979), under these oxidizing conditions, all of these ores should float well with a frother alone. However, only three of these ores were floatable with a frother alone (Figures 3.7, 3.8 and 3.9). The other three ores became floatable only after treatment with sodium sulfide (Figures 3.10, 3.11 and 3.12) to remove excessive surface oxidation products. Finally, in the micro-flotation experiments, the oxidized chalcopyrite sample did not float (Table 3.1), regardless of potentials. Only after successive cleaning with sodium sulfide did the mineral become floatable under oxidizing conditions. Thus, the use of sodium sulfide is essential in the collectorless flotation of many sulfide ores.

An excessive addition of this reagent, however, leaves a large amount of sulfide ions in solution and creates reducing conditions for a prolonged period of time, thus preventing flotation. For example, the freshly ground Craigmont ore floated better with frother only than with 3 lb/ton of sodium sulfide and frother (Figure 3.8). The sodium sulfide added probably had not been consumed by the unoxidized ore during the 15 minutes of conditioning time, and the unconsumed sulfide ions created a reducing environment. However, when the ore was oxidized, good flotation was obtained with the same amount of sodium sulfide. This was most likely because the sulfide ions were consumed in displacing the oxidation products, thus allowing the potential to rise more quickly and the mineral to float. This finding suggests that ores which do not respond well to sodium sulfide treatment probably do not require it in the first place.

b. Effects of Wet- and Dry-Grinding: Figure 3.19 shows that the Mission Unit ore gave some flotation only after dry-grinding. Several possible explanations may be given to enucleate this result. Firstly, it has been suggested by Heyes and Trahar (1977) that wet-grinding in an iron mill creates a reducing environment and prevents flotation. This possibility seems unlikely, however, since the ore samples wet-ground using iron balls exhibited

oxidizing potentials (Figure 3.14). A second possibility, originally suggested by Plaksin (1949), is that the adsorption of molecular oxygen may occur when a sulfide mineral is ground in an oxygen environment. The presence of adsorbed oxygen would then promote the dehydration of the mineral, thus providing hydrophobicity. Finally, the oxidation behavior of an ore will most certainly be different under wet and dry conditions. Eadington (1977) has shown that the rate of wet-oxidation is approximately ten times greater than that of dry-oxidation. Thus, hydrophilic oxidation products may have been formed on the wet-ground sample but not on the dry-ground sample within the time frame of the flotation experiments employed in the present work. The reason for the slight drop in floatability of the Falconbridge ore after dry-grinding is, however, difficult to explain (Figure 3.19).

c. Effect of Potassium Permanganate Addition: Heyes and Trahar (1977) claimed that collectorless flotation of chalcopyrite could be enhanced by increasing the pulp potential through the addition of potassium permanganate, a strong oxidizing agent. The results of the micro-flotation tests conducted at pH 10.5 (Figure 3.5) seem to contradict this finding, however.

In alkaline solutions, the permanganate ions may react with sulfide ions as follows (Stewart, 1965):

$$8MnO_4^- + 3S^{2-} + 4H_2O \rightarrow 8MnO_2 + 3SO_4^{2-} + 8OH^- \qquad [4.1]$$

In view of this reaction mechanism, the sharp decrease in floatability by the addition of potassium permanganate may be explained by the formation of manganese dioxide and sulfate, both of which are hydrophilic. The XPS analyses of the flotation products indeed showed a large amount of manganese and some sulfate present (Figures 3.43 and 3.44).

4.1.2 Flotation of Sphalerite

Two important findings have been made concerning the collectorless flotation of sphalerite. Firstly, sodium sulfide must be added, presumably to remove surface oxidation products. Secondly, as in the case of conventional flotation, copper-activation, which may be represented by the following reaction (Sutherland and Wark, 1955, p. 155:)

$$ZnS(S) + Cu^{2+}(aq) \rightarrow CuS(S) + Zn^{2+}(aq), \qquad [4.2]$$

is necessary.

Although no potential measurements were made in the present study during the batch flotation of sphalerite, Craynon (1982) has recently found that sphalerite floats primarily at potentials above 0 mV. However, this critical

potential for flotation can be lowered with higher dosages of cupric sulfate. This observation may be useful in explaining the shape of the recovery versus pH curve shown in Figure 3.24. Below a pH value of approximately 8, the sphalerite flotation improves with decreasing pH. From the distribution diagram for sulfur-bearing species in solution (Figure 4.1), it can be seen that H_2S becomes dominant below pH 8. It is possible that the loss of H_2S gas to the atmosphere would more quickly bring the potential of the solution to the critical value for flotation. Furthermore, as the pH becomes increasingly acidic, the formation of elemental sulfur becomes more likely. Clifford, Purdy and Miller (1974) found that there was a direct relationship between elemental sulfur formed and the floatability of copper-activated sphalerite conditioned at pH 2.8 in an autoclave. They also demonstrated that an unoxidized sphalerite would not float without the addition of a collector.

The effect of the Cu^{2+}/S^{2-} atomic ratio on the floatability of sphalerite has previously been shown in Figure 3.28. The optimum ratio was found to be approximately 0.17 (or 1:6) and its physical significance may possibly be related to the crystal chemistry of the mineral. It is not known, however, whether this ratio remains constant for different ores, pH values, conditioning times or pulp densities. Nevertheless, it is important

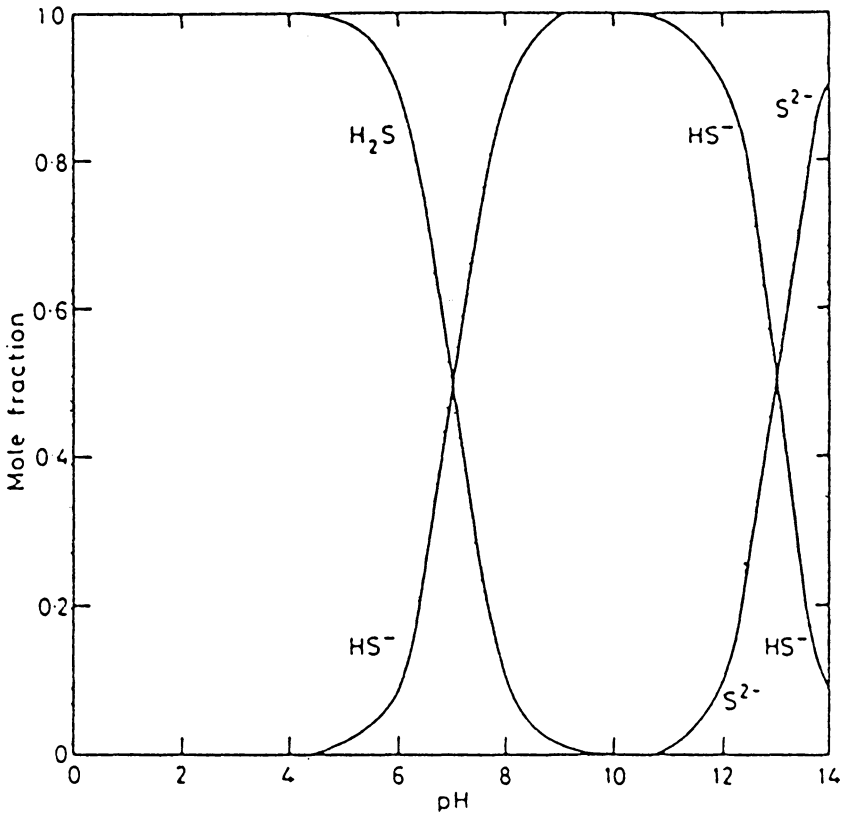

Figure 4.1 Proportion of total sulfide present as S^{2-}, HS^- and H_2S in aqueous solution as a function of pH (Jones and Woodcock, 1978).

to note that the floatability of sphalerite is not greatly affected by changes in reagent dosages when the Cu^{2+}/S^{2-} atomic ratio is maintained. As a result, good floatability may be possible with a minimum amount of reagents.

It is possible that a variation of the Cu^{2+}/S^{2-} atomic ratio is critical in determining the semi-conducting property of the mineral surface, which in turn may affect the floatability. Unactivated sphalerite has a relatively wide band gap (3.67 eV) and thus behaves essentially as an insulator (Teichmann, 1964), unable to take part in electrochemical reactions such as surface oxidation. Thus, copper-activation of the sphalerite may create a semi-conducting surface which can more readily be oxidized to form hydrophobic oxidation products such as elemental sulfur. This possibility has been discussed by Ralston, Alabaster and Healy (1980) who studied the activation mechanism of sphalerite in conjunction with the formation of elemental sulfur by surface oxidation.

4.1.3 Flotation of Pyrite

Like chalcopyrite and sphalerite, pyrite is also floatable in oxidizing conditions without a collector as shown in Figure 3.6. A comparison of this result to those obtained for the micro-flotation of chalcopyrite (Figure 3.2) would indicate that pyrite can float at a lower potential than chalcopyrite. Therefore, upon going from

reducing to oxidizing conditions, pyrite would float first while chalcopyrite remains in the pulp. This is, of course, contrary to what has been observed in the batch flotation experiments.

This discrepancy between the batch flotation and micro-flotation results was discussed by Yoon (1981). He suggested that if small amounts of sodium sulfide were added to a pulp containing several sulfide minerals, sulfidization, represented by Equation 1.4, would probably occur preferentially on those minerals which were least soluble. Using thermodynamic data, Yoon constructed a solubility diagram for various sulfide minerals as a function of pH in an oxygen-free atmosphere (Figure 4.2). As shown, both covellite and chalcopyrite are less soluble than pyrite, which suggests that they are more readily sulfidized than pyrite and become floatable first. Note in Figure 4.2 that the solubility of sphalerite is higher than that of pyrite. However, when the mineral is copper-activated, the surface would behave as copper sulfide, which is less soluble than pyrite and may explain the selectivity of copper-activated sphalerite over pyrite.

Another possible explanation may be given by considering the kinetics of oxidation of sulfide minerals, which are controlled by electrochemical mechanisms. Many investigators have shown that the oxidation of some sulfide minerals (e.g., galena, sphalerite, chalcopyrite and

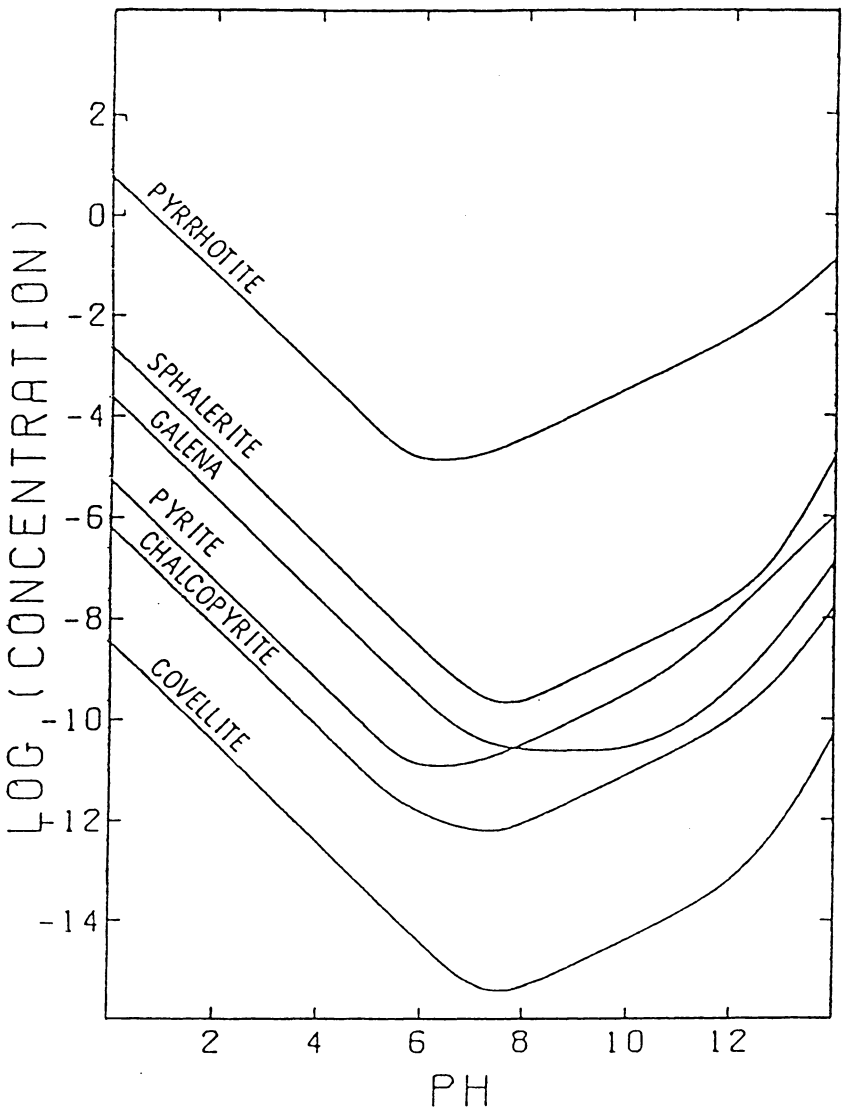

Figure 4.2 Total solubility of metal sulfides in the absence of oxygen as a function of pH (Yoon, 1981).

covellite) is enhanced by 8 to 20 times in the presence of pyrite (Gottschalk and Buehler, 1912; Weinig and Carpenter, 1934; Majima, 1970, 1971). Majima (1970, 1971) oxidized chalcopyrite, galena and sphalerite at pH 2 in the presence of pyrite and found that there was an increase in the amount of elemental sulfur formed over that which formed when the minerals were oxidized separately. This phenomenon may be explained by the fact that pyrite acts as a better catalyst for oxygen reduction than other sulfides (Peters and Majima, 1968; Majima, 1968). Therefore, a galvanic loop may be established between pyrite acting as a cathode and the other mineral acting as an anode. A hydrophobic species, such as elemental sulfur, may form on the chalcopyrite surface as an anodic oxidation product, but not on pyrite where oxygen reduction occurs.

4.2 Possible Mechanisms of Collectorless Flotation

4.2.1 Induced Hydrophobicity by Oxidation

a. Elemental Sulfur: It has long been known that metal sulfides are thermodynamically unstable in the presence of oxygen. Therefore, sulfide minerals are easily oxidized at ambient flotation conditions, at least on the mineral surface. Since most metal sulfides are semiconductors their oxidation is expected to proceed through coupled anodic and cathodic reactions much like the corrosion of metals.

Gardner and Woods (1979) proposed on the basis of their voltammetric studies that the oxidation of chalcopyrite proceeds via the anodic reaction:

$$CuFeS_2 \longrightarrow CuS + \overset{\circ}{S} + Fe^{2+} + 2e \qquad [1.2]$$

in acidic pH solutions, and

$$CuFeS_2 + 3H_2O \longrightarrow CuS + Fe(OH)_3 + \overset{\circ}{S} + 3H^+ + 3e \qquad [1.1]$$

in alkaline pH solutions. They further suggested that collectorless flotation is a result of the formation of elemental sulfur. They came to this conclusion since they had no evidence to indicate that CuS would display hydrophobic properties and the flotation of covellite can occur

when the mineral is oxidized.

However, a weakness of the elemental sulfur theory is that ferric hydroxide is also formed on the chalcopyrite surface as another oxidation product. It is well known that iron oxide minerals and hydrated iron oxide layers are quite hydrophilic. Unless elemental sulfur is formed during oxidation either at the outermost surface and the ferric hydroxide under it, or the elemental sulfur quickly forms patches of considerable size, it is difficult to explain the floatablity of the mineral by the presence of elemental sulfur alone.

It has been well documented that in acidic solutions the oxidation of many sulfide minerals does result in the formation of elemental sulfur (Vizsolyi, Veltman and Forward, 1963; Sato, 1966; Majima and Peters, 1966; Eadington and Prosser, 1969; Bjorling, 1973). However, the possibility that elemental sulfur is formed and remains stable in alkaline solutions is not thermodynamically favored. Examination of the E_h/pH diagram shown in Figure 4.3 (Garrels and Christ, 1965, p. 231) indicates that elemental sulfur is stable only up to a pH of approximately 7.5. Beyond this, sulfur would be further oxidized to either $S_2O_3^{2-}$ or SO_4^{2-} by the following reactions:

$$4S + 4OH^- \longrightarrow 2HS^- + S_2O_3^{2-} + H_2O \qquad K=10^{17.9} \qquad [4.3]$$

and

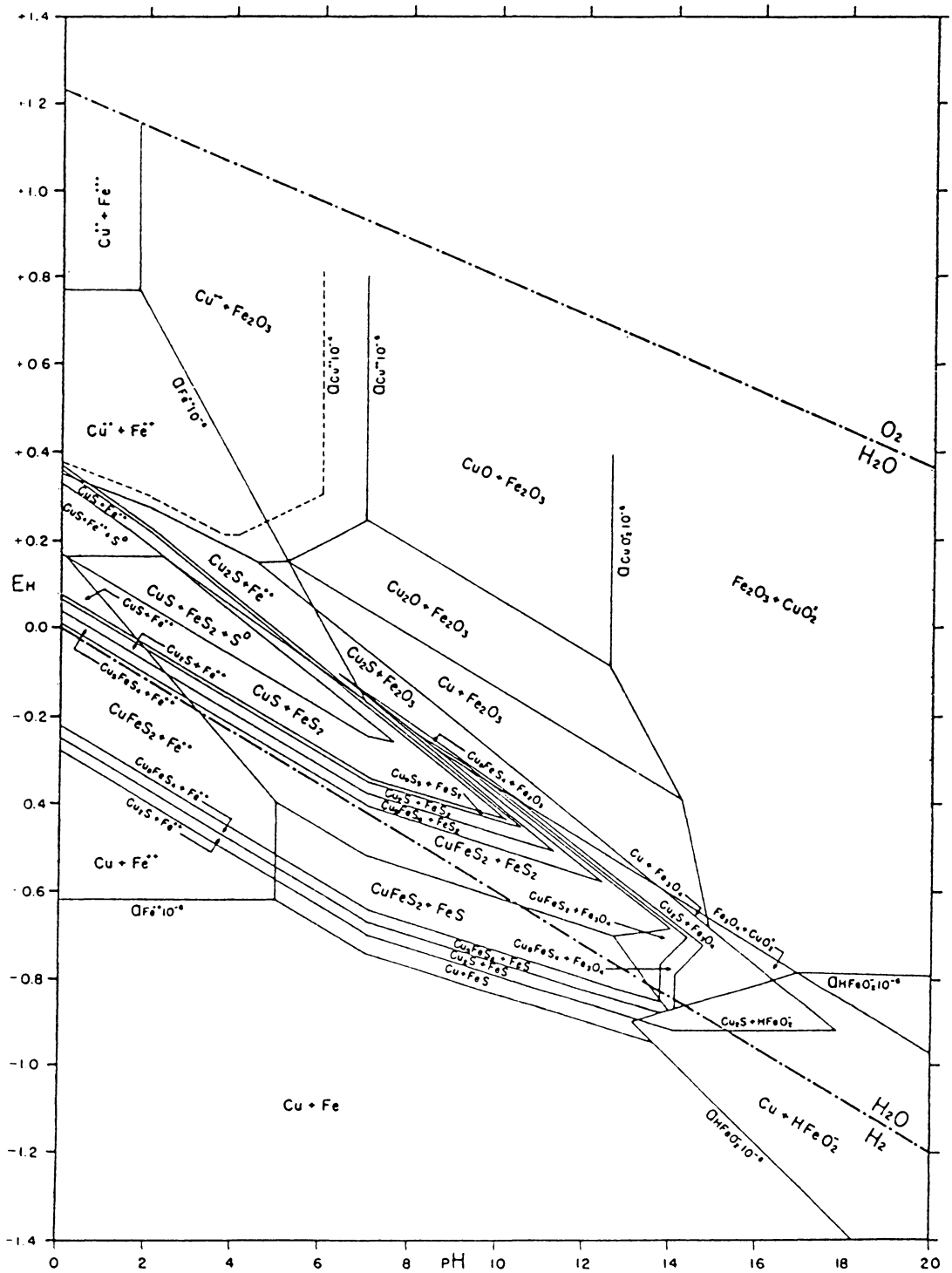

Figure 4.3 The system Cu-Fe-S-O-H (in part) at 25°C and 1 atm. total pressure. Total dissolved sulfur = 10^{-1}M (Garrels and Christ, 1965, p. 231).

$$4S + 5OH^- \longrightarrow 3HS^- + SO_4^{2-} + H_2O. \qquad K=10^{27.2} \qquad [4.4]$$

Care must be exercised, however, when conclusions are drawn from equilibrium calculations, since many reactions which are thermodynamically favored proceed at very slow rates. Sulfur species such as thiosulfate, polysulfides and polythionates appear in natural environments although they are considered to be thermodynamically unstable (Chen and Morris, 1972). Thus, it is possible that elemental sulfur present in alkaline solutions as a meta-stable species may play an important role during flotation. However, the mass spectrometric results obtained in the present work tend to suggest that this may not be the case. Figure 3.30 shows that at alkaline pH values, the relative intensity of sulfur dropped drastically, suggesting that elemental sulfur was not present on chalcopyrite in significant amounts after 15 minutes of conditioning in oxidizing conditions. For example, at pH 10, less than 4% of a monolayer equivalent of elemental sulfur was present (Table 3.2). It is difficult to believe that this small amount of elemental sulfur could be responsible for the observed floatability. Ralston, et al. (1980) also found very little elemental sulfur on copper-activated sphalerite at alkaline pH values using mass spectrometry.

In contrast to the results obtained by mass spectrometry, the XPS data presented in Figure 3.43 clearly shows

the presence of elemental sulfur on the surface of a chalcopyrite sample that floated at pH 10.5. There is also an indication that covellite is another oxidation product of chalcopyrite. These findings appear to support the reaction mechanism proposed by Gardner and Woods (Equation 1.1), and suggest that elemental sulfur is responsible for collectorless flotation even at an alkaline pH as high as 10.5. Recall that the results of extended periods of x-ray analysis showed no significant increase in the amount of elemental sulfur formed on chalcopyrite surfaces. It is, therefore, unlikely that the elemental sulfur detected is the result of photo-oxidation of sulfide ions coupled with the photoreduction of cuprous ions.

Some of the results obtained by the UV analyses appear to support the elemental sulfur theory. The results given in Table 3.7 show that by raising the potential from -238 mV to +181 mV, the amount of elemental sulfur found on the chalcopyrite surface was increased from 0.4 to 1.1 monolayer equivalents. The additional sulfur formed at the oxidizing potential may be considered responsible for flotation.

The UV analyses also presented evidence against the elemental sulfur theory. When the air-oxidized chalcopyrite sample was conditioned in hydrazine solution at -236 mV and was analyzed for elemental sulfur, as much as 1.7

monolayer equivalents of elemental sulfur was detected (Table 3.7). Apparently, hydrazine did not remove elemental sulfur, but it readily suppressed the flotation as shown in Figure 3.4. This finding suggests that the presence or absence of elemental sulfur may not be the only criterion for the collectorless flotation of chalcopyrite.

Note in Table 3.7 that much larger amounts of elemental sulfur were detected on dry samples than on wet samples by the UV analyses. Even the sample conditioned at a very reducing potential (-238 mV) showed a large amount (3.1 monolayer equivalents) of elemental sulfur upon drying. One possible explanation may be that the sulfide ions present in the film of sodium sulfide solution adhering to the mineral surface becomes rapidly oxidized to elemental sulfur during the drying process. Although the sample was dried in a vacuum dessicator, the small amount of oxygen remaining may be sufficient to form elemental sulfur. This possiblity raises a serious question on the validity of XPS analysis obtained in the present work, since all the samples had to be taken out of the solution and vacuum-dried prior to the analysis. It is not surprising that elemental sulfur was detected on virtually all of the samples analyzed and the peak intensity did not vary significantly from one sample to another. In fact, the elemental sulfur peak intensity was found to increase with

decreasing potential (Figure 3.43) simply because more sodium sulfide was added to reduce the potential. The mass spectrometric analysis probably has the same difficulty in determining the surface elemental sulfur. However, the results of the quantitative analysis shown in Figure 3.31 and Table 3.2 are more reliable since no extraneous sulfur (as sodium sulfide) was added to the system to control the potential.

b. Polysulfides: The mass spectrometric analysis given in Figure 3.30 shows that only insignificant amounts of elemental sulfur are present at alkaline pH values, which agrees well with the thermodynamic stability diagram (Figure 4.3). This result suggests either that no elemental sulfur is present at alkaline pH values, or that the elemental sulfur is held strongly to the surface so that it is not vaporizable at the temperature of the sample probe employed in the present work (90°C). Since it is difficult to imagine that elemental sulfur could be chemically bound to the surface, it might be suggested that polysulfide ions, instead of elemental sulfur, are present on the surface of chalcopyrite at alkaline pH values.

Polysulfides are known to form as a result of 1) the interaction of sulfur with an aqueous solution of sulfide (Chen and Morris, 1972) in which the general reaction may be expressed as:

$$HS^- + (x-1)S = S_x^{2-} + H^+, \qquad [4.5]$$

or 2) by the aging or oxidation of sulfides or hydrosulfides in solution (Karchmer, 1970, p. 347). Chen and Gupta (1973) have shown that when sulfur is formed in the presence of sulfide, polysulfides can be formed immediately. For instance, if sodium sulfide is dissolved in oxygen-free water, a clear solution is formed at any pH value. However, if the water contains dissolved oxygen and the pH value is between 6 and 9, a greenish-colored solution soon develops, indicating the formation of polysulfides (Chen and Morris, 1972). If acid is added to the colored solution, a suspension of colloidal sulfur rapidly forms.

The stability of polysulfides is critically dependent upon pH. It has been demonstrated (Chen and Morris, 1972; Chen and Gupta, 1973) that at pH 6.0, the concentration of polysulfides in solution is negligible compared to that of elemental sulfur. On the other hand, at pH 8.0, the concentration of polysulfides is dominant. According to Chen and Morris' mass balance calculations of the distribution of polysulfides, the concentration of polysulfides should increase as alkalinity is increased.

From the foregoing discussions, polysulfides may play a significant role in the oxidation and flotation of sulfide minerals. This may be particularly true in

alkaline solutions where polysulfides become increasingly dominant.

Allen and Hickling (1957) have demonstrated that a polysulfide ion, S_x^{2-}, can adsorb on a metal surface, M, through the following surface reaction:

$$S_x^{2-} + M \longrightarrow M---S_x^{2-} \qquad [4.6]$$

This concept is supported by the observation that the oxygenation of mildly alkaline sulfide solutions is increased up to 100-fold by the presence of transition metals (Chen and Morris, 1972). Sulfide minerals may play a similar role as transition minerals, and it is not difficult to imagine the adsorption of polysulfide ions on these minerals. Since the covalently bonded sulfur atoms in the polysulfide chain are much like those in elemental sulfur, polysulfide ions adsorbed on a mineral surface could make it hydrophobic. Note in Figure 3.24 that the pH of maximum floatability of copper-activated sphalerite closely corresponds to a pH of 7.0, which is the optimum pH for the formation of polysulfides from a sulfide solution (Chen and Morris, 1972).

Polysulfides may participate in electrochemical reactions involving sulfide mineral systems. Ho and Conway (1978) have suggested that sulfur may be adsorbed or deposited on a galena surface by the following oxidation

reaction:

$$S^{2-} + PbS \longrightarrow PbS + S_{ads} + 2e \qquad [4.7]$$

They also pointed out, however, that the oxidization of sulfide ions to polysulfides, produced in a step such as

$$2S^{2-} \longrightarrow S_2^{2-} \text{ (or higher species)} + 2e, \qquad [4.8]$$

could give rise to a similar electrochemical behavior. Thus, it is difficult to determine whether the adsorbed sulfur species is elemental sulfur or polysulfide by the electrochemical technique.

In order to better understand the stability of polysulfides, the distribution diagrams depicting the mole percents of various sulfur species as a function of E_h have been constructed from thermodynamic data listed by Latimer (1952). The thermodynamic data have been combined with the mass balance equations involving equilibrium between S^{2-}, H_2S, HS^-, S_2^{2-}, S_3^{2-}, S_4^{2-} and S_5^{2-} species. Oxidation was assumed to progress only up to the formation of polysulfides. Consequently, the formation of S°, $S_2O_3^{2-}$ and SO_4^{2-} species were not considered. The mass balance equations were solved by means of the computer program listed in Appendix VIII to determine the concentration and percent distributions of the various ions as a function of

E_h at constant pH. Figures 4.4, 4.5 and 4.6 display the percent distributions of various sulfur species at pH values of 8, 10 and 12, respectively. As shown in Figure 4.5, HS^- ions dominate at negative potentials and are converted primarily to S_5^{2-} at higher potentials. Comparison of these results with the results of micro-flotation experiments conducted as a function of potential indicates that both the polysulfide concentration and the floatability increase at roughly the same potential value at a given pH. Thus, the formation of polysulfides may account for the collectorless flotation observed at higher potentials.

The distribution diagrams also show that the percentage of polysulfides formed increased directly with the length of the polysulfide linkage (i.e., S_5^{2-} and S_4^{2-} are favored over S_3^{2-} and S_2^{2-}). Experimental evidence for this has been given by Schwarzenbach and Fischer (1960). In addition, the distribution diagrams show that the critical potential at which the polysulfide formation begins to occur is lowered with increasing pH: -0.17 V at pH 8, -0.25 V at pH 10 and -0.32 V at pH 12. These findings indicate that polysulfide formation is favored at higher pH values, as pointed out by Chen and Gupta (1973). It appears, therefore, that polysulfide formation may be responsible for collectorless flotation in alkaline solutions while in acidic solutions, elemental sulfur

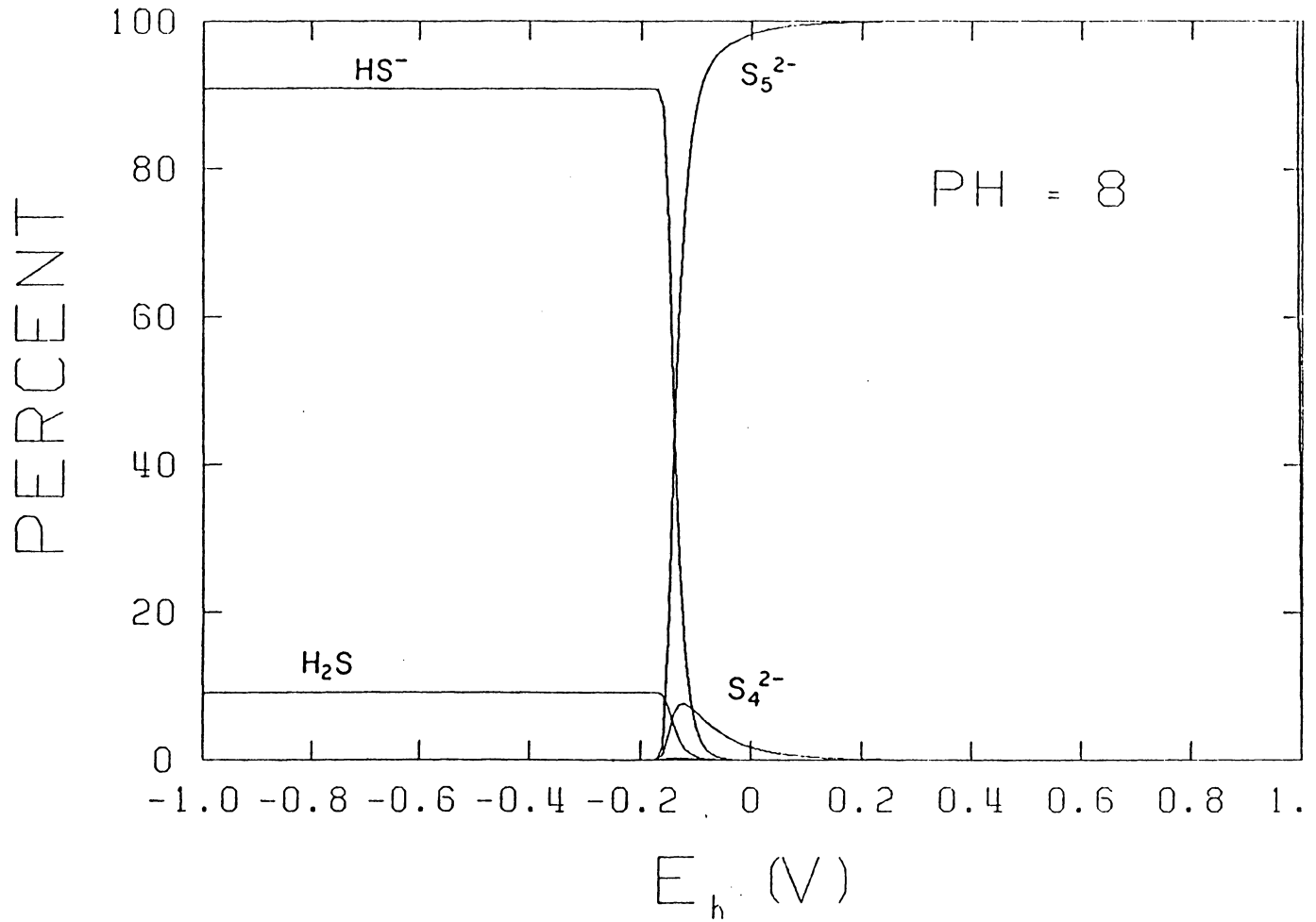

Figure 4.4 Distribution diagram of sulfur species as a function of E_h at pH 8 and 10^{-5} moles/l of total sulfur. The calculation has been made assuming that the oxidation does not proceed beyond polysulfide formation.

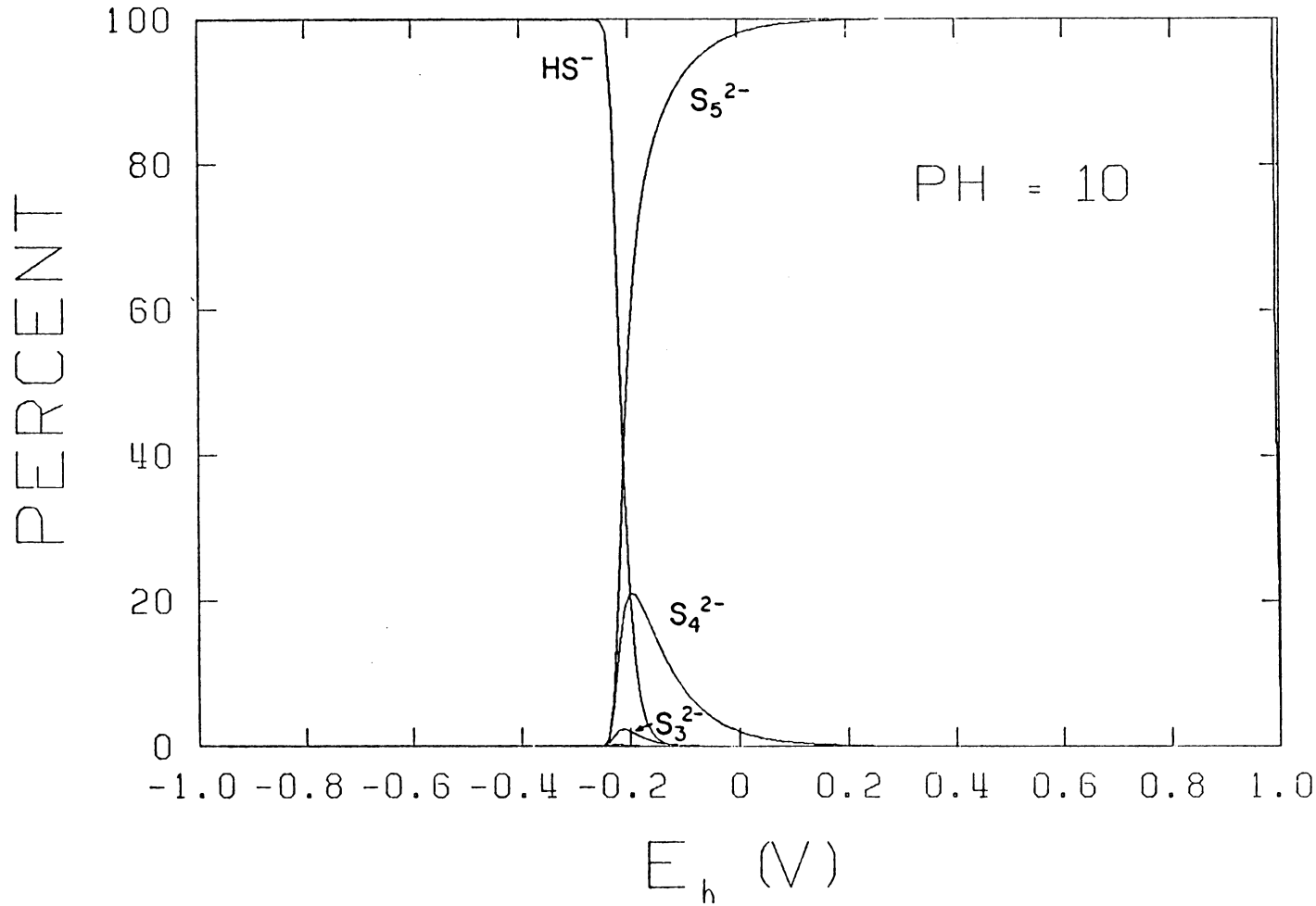

Figure 4.5 Distribution diagram of sulfur species as a function of E_h at pH 10 and 10^{-5} moles/l of total sulfur. The calculation has been made assuming that the oxidation does not proceed beyond polysulfide formation.

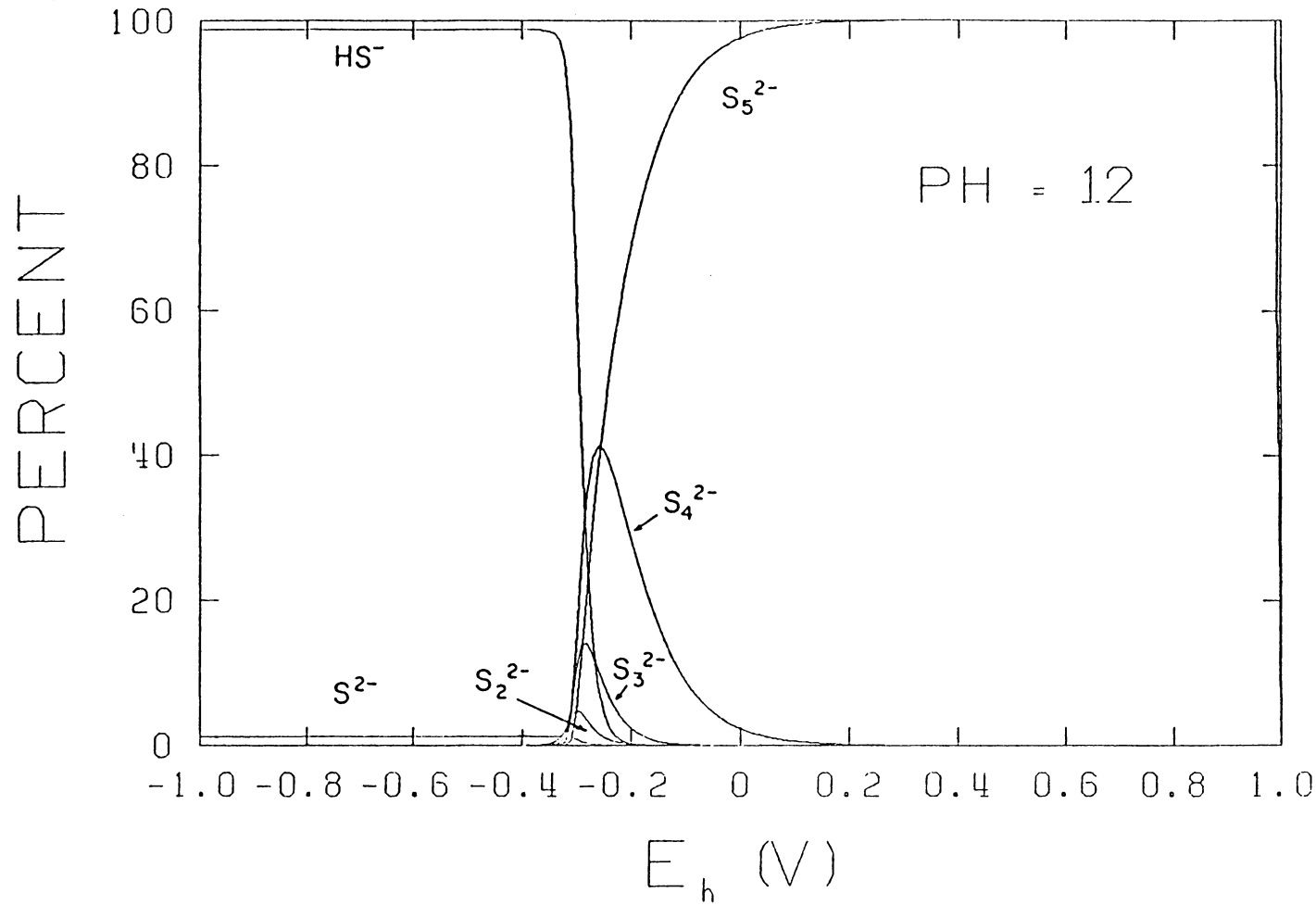

Figure 4.6 Distribution diagram of sulfur species as a function of E_h at pH 12 and 10^{-5} moles/l of total sulfur. The calculation has been made assuming that the oxidation does not proceed beyond polysulfide formation.

formation may account for it.

The UV analysis results given in Figure 3.7 suggest the presence of elemental sulfur. However, some of the elemental sulfur detected might in fact be polysulfides of various chain lengths. Unfortunately, it is difficult to distinguish elemental sulfur from polysulfides by UV analysis since their characteristic peaks appearing at 270-300 nm are very broad.

On the basis of their voltammetric studies, Gardner and Woods (1979) suggested that CuS and $\overset{\circ}{S}$ are the oxidation products of chalcopyrite in alkaline solutions. The XPS spectra obtained by Buckley and Woods (1981), and also in the present work, appear to show evidence for CuS, as indicated by the S^{1-} peak at approximately 162 eV. However, this peak might now be considered indicative of the presence of polysulfide ions on the surface which may form a surface compound by the following reaction:

$$2Cu^{+} + S_x^{2-} \longrightarrow Cu\text{-}S_x\text{-}Cu \qquad [4.9]$$

in which x represents the number of sulfur atoms in the polysulfide complex. Thus, the sulfur at both ends of the polysulfide chain may have an oxidation state close to -1 while those in the middle may have an oxidation state close to 0. This may account for the sulfur 2p peaks observed at approximately 164 and 162 eV, respectively.

4.2.2 Inherent Hydrophobicity

In the micro-flotation tests of chalcopyrite, various amounts of sodium sulfide were added to control the potential. Although the results indicate that floatability is reduced with decreasing potential, it essentially shows that chalcopyrite does not float in the presence of sodium sulfide. However, to better understand the role of sodium sulfide, one may consider the proportion of total sulfide present as S^{2-}, HS^-, or H_2S in aqueous solution as a function of pH. As shown in Figure 4.1, at pH values between approximately 7 and 13, the greatest proportion of sulfide in solution is present as HS^- ions (Jones and Woodcock, 1978). Also, recall from Figures 4.4, 4.5 and 4.6 that HS^- is the overwhelmingly dominant species at potentials below -150 mV to -50 mV. Thus, it might be considered that the HS^- ions are suppressing the natural floatability of chalcopyrite in reducing conditions.

The depressing action of HS^- ions in xanthate flotation has long been recognized and explained by the competition between HS^- ions and xanthate ions for the sulfide mineral surface (Gaudin, 1957, p. 288). In collectorless flotation, it has been claimed (Gardner and Woods, 1979; Trahar, 1982) that HS^- ions may prevent flotation by imposing a reducing environment which prohibits elemental sulfur formation. However, an alternative explanation might be that HS^- ions adsorbed at the mineral

surface may somehow render the mineral hydrophilic. It is known that an S-H group can be a proton donor and readily form hydrogen bonds (Vinogradov and Linnell, 1971, p. 12). It is possible, therefore, that the adsorbed HS^- ions can form hydrogen bonds with surrounding water molecules and render the mineral hydrophilic.

The above consideration may be used to explain the relationship between the potential measured with the platinum-calomel electrode pair during the batch flotation tests and the flotation recovery. Jones and Woodcock (1978) showed that the potential measured on a platinum-calomel electrode pair during flotation reflected changes in the S^{2-} (and hence HS^-) concentration. Likewise, the steady increase in potential during the conditioning period may be considered as indicating the decrease in the HS^- ion concentration due to oxidation rather than the redox conditions of the surface of the mineral. This view may be supported by the observation that the critical potential for flotation was found to remain the same irrespective of the type of chalcopyrite ore floated or regardless of how much sodium sulfide was added. Apparently, the controlling factor is that HS^- ions must be removed from the solution before flotation can be possible.

Therefore, elemental sulfur may not be necessary for collectorless flotation. This conjecture may also explain why many previous experiments failed to find a correlation

between elemental sulfur present on the mineral surface and the natural floatability (Finkelstein, 1975; Heyes and Trahar, 1977; Pritzker, Yoon and Dwight, 1980; Fuerstenau and Sabacky, 1981). The interpretation of some of the results obtained in the present work on the basis of the elemental sulfur theory has also met with difficulty (Section 3.5.1).

The XPS data shown in Figure 3.43 shows that elemental sulfur is present on practically all the samples of chalcopyrite examined, regardless of the potentials. Yet, the floatability of chalcopyrite varies critically with potential. Thus, the presence of elemental sulfur alone cannot explain their flotation behavior, although it is possible that the elemental sulfur detected by XPS on chalcopyrite samples conditioned under reducing conditions may be caused by the drying procedure.

In general, it has been demonstrated that collectorless flotation is improved in a slightly acidic pH. In light of the foregoing discussions, floatability may be enhanced in acidic solutions since excess HS^- ions would be removed from the system as H_2S gas. An alternative explanation may be, of course, that elemental sulfur is formed in acidic pH solutions and supplement the natural hydrophobicity of chalcopyrite. There has been overwhelming evidence gathered in the present work that elemental sulfur is indeed present on the mineral surface in acidic

pH values and enhances the natural floatability.

The idea that HS^- ions are rendering the chalcopyrite surface hydrophilic is based on the premise that clean sulfides are inherently hydrophobic. This concept is based on the fact that the sulfide ions are not capable of forming hydrogen bonds with surrounding water molecules (Finkelstein, et al., 1975; Fuerstenau and Sabacky, 1981). A weakness of this natural floatability theory is, of course, that sulfide minerals are extremely susceptible to oxidation. It has been pointed out by Gaudin (1972) that even at exceptionally low levels of dissolved oxygen (e.g., 10^{-10} moles/l), oxidation is likely to occur.

It has been shown in the present investigation that the underlying mechanism of collectorless flotation is undoubtedly related to the oxidation mechanisms of the sulfide minerals involved. Considering that the oxidation of sulfide proceeds in the following order,

$$S^{2-} \rightarrow S^{1-} \rightarrow S_x^{2-} \rightarrow \overset{\circ}{S} \rightarrow S_2O_3^{2-} \rightarrow SO_3^{2-} \rightarrow SO_4^{2-} \qquad [4.10]$$

the kinetics of oxidation must play a decisive role in determining the floatability of a sulfide mineral without a collector. In other words, the floatability of a mineral will most probably be directly influenced by the degree to which the oxidation of the mineral surface has proceeded when flotation is attempted.

V. SUMMARY AND CONCLUSIONS

The results of the present investigation may be summarized as follows:

1. Chalcopyrite ores used in the present work may be classified into two groups, one being floatable with a frother only, and the other requiring the use of xanthate and a frother. The latter group of ores, however, can be made floatable by treatment with sodium sulfide. The role of this reagent is regarded as one of a surface-cleaning agent which removes hydrophilic surface oxidation products from the mineral surface.

2. Micro-flotation experiments conducted on pure chalcopyrite and pyrite samples have shown that the floatability of these minerals was a direct function of potential and was not influenced by the chemical system used to obtain the potential. In general, it was shown that the floatability was improved in oxidizing potentials and suppressed in reducing potentials. The same characteristic was observed for the batch flotation of chalcopyrite.

3. The batch flotation experiments conducted on

sphalerite ores showed that both sodium sulfide and cupric sulfate activation were required to obtain adequate recovery of sphalerite in the absence of a collector. It was also demonstrated that good floatability could be achieved over a wide range of reagent additions if the Cu^{2+}/S^{2-} atomic ratio was maintained close to 0.17.

4. The selective flotation of sphalerite and chalcopyrite from pyrite has been explained by the possible preferential oxidation and sulfidization reactions occurring on the sulfide mineral surfaces.

5. Flotation of chalcopyrite and sphalerite was found to be improved in neutral to acidic pH solutions. This behavior was believed to be due either to an increase in the stability of elemental sulfur in acidic solutions or to the loss of HS^- by conversion to H_2S gas resulting from the protonation.

6. As was predicted thermodynamically, mass spectrometric results showed that elemental sulfur was not formed to a significant degree on chalcopyrite conditioned in alkaline solutions.

collectorless flotation of chalcopyrite at these pH values only by the presence of elemental sulfur. The flotation under these conditions may result from the adsorbed polysulfide ions, which may be bound to the surface metal ions to form a surface compound such as Cu_2S_x. These surface species may not be distinguishable from CuS and elemental sulfur by the XPS or UV analysis techniques employed in the present work.

7. Contrary to the view that the collectorless flotation of chalcopyrite results from the formation of a hydrophobic oxidation product, it may be possible that the mineral possesses an inherent hydrophobicity. This conjecture is based on the possibility that the HS^- ions prevailing in reducing environments adsorb on the mineral surface and make the surface hydrophilic. The adsorbed HS^- ions may represent hydrophilic sites because they could form hydrogen bonds with surrounding water molecules.

8. The mechanisms of collectorless flotation appear to be quite complex, and thus many possible explanations have been presented. However, the crux of the matter seems to lie in properly

understanding the kinetics of the surface oxidation of the minerals involved. The surface species responsible for collectorless flotation may be one or more of the species involved in the following oxidation step,

$$S^{2-} \rightarrow S^{1-} \rightarrow S_x^{2-} \rightarrow \overset{\circ}{S} \rightarrow S_2O_3^{2-} \rightarrow SO_3^{2-} \rightarrow SO_4^{2-}$$

depending on the redox conditions of flotation and the extent of surface oxidation. If sulfide minerals are inherently hydrophilic and thus require oxidation for collectorless flotation, the hydrophobic species are most likely those formed during the incipient oxidation process.

VI. INDUSTRIAL APPLICATIONS

The results of the present study have suggested several possible advantages of collectorless flotation over conventional flotation processes in upgrading sulfide ores. Certainly, the most obvious of these advantages is that the flotation can be achieved using only a frother, which may result in substantial savings in reagent costs depending on the ores to be treated. The reduction in xanthate used in a typical copper processing plant treating about 10,000 tons of ore per day could amount to a savings of over $100,000 per year. For those plants treating more complex ores, the savings would become more significant. In addition, the collectorless flotation process would eliminate the need for a pH regulating agent such as lime or soda ash, the cost of which can be staggering depending on the type of ore. According to a recent U. S. Bureau of Mines statistic (Minerals Yearbook, 1980), the average consumption of lime in flotation plants amounts to 3.2 lb/ton, larger than any other reagent used for flotation.

Some ores may require considerable amounts of sodium sulfide for collectorless flotation. However, sodium sulfide can be easily prepared on mine sites from sulfur, which is less than $0.10 per pound at present (Engineering and Mining Journal, November 1982). Further, if sodium sulfide is used in combination with conventional thiol-type

collectors, the reagent consumption may be significantly reduced.

Another important finding of the present work, and also of other investigators such as Heyes and Trahar (1977), is the realization that the monitoring of the E_h of a flotation pulp is vitally important in achieving good flotation. Thus, the use of E_h electrodes for process control may lead to improved flotation plant performance.

VII. RECOMMENDATIONS FOR FURTHER WORK

From the information gathered in the present work, further investigation in the following areas may be suggested.

1. By monitoring the potential of the flotation pulp and S^{2-} ion concentration during flotation, it is possible to minimize the sodium sulfide required for collectorless flotation of chalcopyrite. A further investigation with a specific purpose of reducing sodium sulfide consumption could lead to a practicable industrial process.

2. A series of batch flotation experiments should be conducted to see if the optimum Cu^{2+}/S^{2-} atomic ratio determined with the Center Valley zinc ore is found to be the same with other ores. The significance of this ratio should be investigated further with regard to crystal chemistry and the semi-conducting properties of copper-activated sphalerite.

3. Electrochemical flotation tests using a packed-mineral bed as an electrode would enable one to conduct flotation experiments as a function of

applied potential. At the same time, the solution chemistry can be monitored by circulating the electrolyte solution through a UV spectrophotometer. Similar work has been done (Walker, et al., 1982) on the chalcopyrite-xanthate flotation system.

4. Using a technique similar to that described by Eadington and Prosser (1969), a study of the relationship between the semi-conducting properties of chalcopyrite and flotation should prove fruitful.

5. The UV analysis technique employed in the present work for sulfur analysis has been proven useful in the present study. However, this technique requires samples of high specific surface, which are not suitable for micro-flotation experiments. One useful method of determining the hydrophobicity of a powdered sample would be calorimetric heat of immersion measurements. Hence, a correlation between heats of immersion and the elemental sulfur determined by the UV-analysis technique would prove useful.

REFERENCES

Allen, P. L. and Hickling, A., "Electrochemistry of Sulfur," Trans. Faraday Soc., 53 , 1626-1635 (1957).

Ballot, Sulman and Picard, British Patent No. 7803 and U. S. Patent No. 835120 (1905).

Bass, A. M., "The Optical Absorption of Sulfur," J. Chem. Physics, 21 (1), Jan., 80-82 (1953).

Bates, R. G., Determination of pH , Wiley, New York, N. Y., 458-483 (1964).

Berkowitz, J., "Molecular Composition of Sulfur Vapor," In: B. Meyer (Ed.), Elemental Sulfur, Interscience, London, Chpt. VII (1965).

Bjorling, G., "Leaching of Mineral Sulfides by Selective Oxidation at Normal Pressure," 2nd Int. Symp. Hydrometallurgy, Chpt. 26, 701-717 (1973).

Bradford, H., "Method of Saving Floating Materials in Ore Separation," U. S. Patent No. 345951 (1885).

Bradt, F. L. Mohler and Dibeler, V. H., "Mass Spectrum of Sulfur Vapor," J. Res. NBS, 57 (4), 223-225 (1956).

Boyce, J. R., Venter, W. J. and Adam, J., "Beneficiation Practice at the Tsumeb Concentrator," In: D. O. Raush and B. C. Mariacher (Editors), World Symp. on Min. and Met. of Lead and Zinc, AIME, New York, N. Y., 542-570 (1970).

Buckley, A. and Woods, R., "Investigation of the Surface Oxidation of Sulfide Minerals Via ESCA and Electrochemical Techniques," Engineering Foundation Conf. on Interfacial Phenomena in Mineral Processing, Aug. 2-7, Rindge, New Hampshire (1981).

Chander, S. and Fuerstenau, D. W., "On the Floatability of Sulfide Minerals with Thiol Collectors: The Chalcocite-Diethyldithiophosphate System," In: Proc. 11th Int. Min. Proc., Rome, 583-604 (1975).

Chen, K. Y. and Gupta, S. K., "Formation of Polysulfide in Aqueous Solution," Env. Letters, 4 , 187 (1973).

Chen, K. Y. and Morris, J. C., "Kinetics of Oxidation of Aqueous Sulfide by O ," Enviro. Sci. and Tech., 6 (6), 529-537 (1972).

Clifford, R. K., Purdy, K. L. and Miller, J. D., "Characterization of Sulfide Mineral Surfaces in Froth Flotation Systems Using Electron Spectroscopy for Chemical Analysis," AIChE Symp. Series, 150 , 138-147 (1974).

Craynon, J., Personal Consultation, October, 1982.

Dell, C. C. and Bunyard, M. J., "Development of an Automatic Flotation Cell for the Laboratory," Trans. IMM, 81 , C246-248 (1972).

Eadington, P., "Study of Oxidation Layers on Surfaces of Chalcopyrite by Use of Auger Electron Spectroscopy," Trans. IMM, Sect. C., 86 , C186-189 (1977).

Eadington, P. and Prosser, A. P., "Oxidation of Lead Sulfide in Aqueous Suspensions," Trans. IMM, June, C74-C82 (1969).

Engineering & Mining Journal, November (1982).

Everson, C. J., "Process of Concentrating Ores," U. S. Patent 348157 (1886).

Finkelstein, N. P., Allison, S. A., Lovell, V. M. and Stewart, B. V., "Natural and Induced Hydrophobicity in Sulfide Mineral Systems," In: P. Somasundaran and R. G. Grieves (Editors), Advances in Interfacial Applications to Flotation Research, Am. Inst. Chem. Engrg., Symp. Ser. No. 150, 71 , 165-175 (1975).

Ford, G. P. and La Mer, V. K., "Vapor Pressure of Supercooled Liquid Sulfur," J. Amer. Chem. Society, 72 , May, 1959-1964 (1950).

Friedman, H. L. and Kerker, M., "Ultraviolet Absorption of Aqueous Sulfur Solutions," J. Colloid Sci., 8 , 80-85 (1953).

Frost, D. C., Ishitani, A. and McDowell, C. A., Mol. Phys., 24 , 861 (1972).

Fuerstenau, M. C. and Sabacky, B. J., "On the Natural Floatability of Sulfides," Int. J. Miner. Process., 8 , 79-84 (1981).

Gardner, J. R. and Woods, R., "An Electrochemical Investigation of the Natural Floatability of Chalcopyrite," Int. J. Mineral Processing, 6 , 1-16 (1979).

Garrels, R. M. and Christ, C. L., Solutions, Minerals and Equilibria , Harper and Row, New York, N. Y. (1965).

Gaudin, A. M., Flotation , McGraw-Hill Book Co., New York, N. Y., 2nd ed. 1957 (1932).

Gaudin, A. M., Miaw, H. L. and Spedden, H. R., "Native Floatability and Crystal Structure," Proc. 2nd Annual Congress of Surface Activity, Butterworth Sci., London, 3 (1957).

Gaudin, A. M., "The Role of Oxygen in Flotation," Jour. Coll. Interface Sci., 47 , 309-314 (1972).

Glembotskii, V. A., Klassen, V. I. and Plaksin, I. N., Flotation, Primary Sources, New York (1963).

Gottschalk, V. H. and Buehler, H. A., Econ. Geol., 7 , 15 (1912).

Hagihara, H., J. Phys. Chem., 56 , 610-616 (1952).

Harris, C. C. and Raja, A., "A Modified Laboratory Flotation Cell," Trans. AIME, 325 , 150-156 (1966).

Haynes, W., British Patent No. 488, Feb. 23 (1980).

Herd, H. H. and Ure, W., J. Phys. Chem., 45 , 93 (1941).

Heyes, G. W. and Trahar, W. J., "The Natural Floatability of Chalcopyrite," Int. J. Mineral Processing, 4 , 317-344 (1977).

Ho, F. C. and Conway, B. E., "Electrochemical Behavior of the Surface of Lead Sulfide Crystals as Revealed by Potentiodynamic, Reflectance, and Rotating-Electrode Studies," Jour. Coll. and Interface Sci., 65 (1), 19-35 (1978).

Hurlbut, C. S. and Klein, C., Manual of Mineralogy , 19th Ed., John Wiley & Sons Pub., New York (1977).

Jones, M. H. and Woodcock, J. T., "Evaluation of Ion-Selective Electrode for Control of Sodium Sulfide Additions During Laboratory Flotation of Oxidized Ores," Trans. IMM, C99-C105 (1978).

Kamienski, B., "So-Called Flotation," Przem. Chem., 15 , 201-202 (1931).

Kamienski, B. and Pomianowski, A., "The Influence of Hydrogen Ion on the Potential of a Mineral Electrode During the Process of Flotation," Bull. Acad. Polon. Sci., Cl III, 2 , 85-89 (1954).

Karchmer, J. H., The Analytical Chemistry of Sulfur and Its Compounds , Wiley-Interscience, New York, N. Y. (1970).

Knoll, A. F. and Baker, D. B., AIME Tech. Pub. 1313, Mining Technology, May (1941).

Koren, J. G., Applied Spectroscopy, 23 (3), 275 (1969).

Latimer, W. M., Oxidation Potentials , Prentice-Hall, New York, N. Y., 2nd Ed., 409 (1952).

Leja, J., Surface Chemistry of Froth Flotation , Plenum Press, New York, N. Y. (1982).

Leja, J., Little, L. H. and Poling, G. W.,"Xanthate Adsorption Studies Using Infrared Spectroscopy," Trans. IMM, 72 ,407-423 (1963).

Lepetic, V. M., "Flotation of Chalcopyrite Without Collector After Dry Autogenous Grinding," C.I.M. Bulletin, June, 71-77 (1974).

Majima, H. and Peters, E., "Oxidation Rates of Sulfide Minerals by Aqueous Oxidation at Elevated Temperatures," Trans. AIME, 236 , 1409-1413 (1966).

Majima, H. and Takeda, M., "Electrochemical Studies of the Xanthate-Dixanthogen System on Pyrite," Trans. Soc. Mining Engrg., AIME, 241 , 431-436 (1968).

Majima, H., "The Effect of Oxidation on Selective Flotation of Complex Sulfide Ores," Presentation Conf. of Metall., University British Columbia, Vancouver, B. C., August 25-28 (1968).

Majima, H., "How Oxidation Affects Selective Flotation of Complex Sulfide Ores," Can. Met. Quarterly, 8 , 269-273 (1970).

Majima, H., "Electrochemistry of Pyrite and its Significance in Sulfide Flotation," Presentation Annual Meeting AIME, N. Y. (1971).

Meyer, B., "Elemental Sulfur," Chem. Rev., 76 , 367-388 (1976).

Mineral Facts and Problems 1980 , U. S. Government Printing Office, Washington, D.C., 1 (1981).

Minerals Yearbook ,"Froth Flotation," U.S. Dept. of the Interior, Bureau of Mines (1980).

Natarajan, K. A. and Iwasaki, I., "Practical Implications of Eh Measurements in Sulfide Flotation Circuits," Trans AIME, 254 , Dec., 323-328 (1973).

Partridge, A. C. and Smith, G. W., "Small-Sample Flotation Testing: A New Cell," Trans. IMM, Sect. C., 80 , C199-200 (1971).

Peters, E. and Majima, H., Presentation Annual Meeting AIME, N. Y. (1968).

Plaksin, I. N., "Causes of the Natural Hydrophobicity of Sulfide Minerals in Flotation, Doklady Akad. Nauk SSSR, 66 (1), 91-93 (1949).

Plaksin, I. N., "Interaction of Minerals with Gases and Reagents in Flotation," Mining Engrg., March (1959).

Plaksin, I. N. and Bessonov, S. V., "Role of Gases in Flotation Reactions," 2nd Int. Cong. of Surf. Activity, London, Butterworth, 361-367 (1957).

Pridmore, D. F. and Shuey, R. T., "The Electrical Resistivity of Galena, Pyrite and Chalcopyrite," Amer. Mineralogist, 61 , 248-259 (1976).

Pritzker, M. D., Yoon, R. H. and Dwight, D. W., "An ESCA Study of the Chalcopyrite Concentrate Produced by Collectorless Flotation," 54th Colloid And Surface Sci., Lehigh Univ., June (1980).

Ralston, J., Alabaster, P. and Healy, T. W., "Activation of Zinc Sulfide with Cu^{2+}, Cd^{2+} and Pb^{2+}: III. The Mass Spectrometric Determination of Elemental Sulfur," Int. J. Mineral Process., 7 , 279-310 (1981).

Ravitz, S. F., AIME Tech. Pub. 1147, Mining Technology, Jan. (1940).

Ravitz, S. F. and Porter, R. R., "Oxygen Free Flotation," AIME Tech. Publ. No. 513 (1933).

Rolia, E., "Methods of Analyses for Sulfate, for Industrial Thiosalts, and for Elemental Sulfur Produced During the Oxidation of Sulfide Ores," CANMET, Metall. Chem. Sect., Phys. Sci. Laboratory., Report MRP/MSL 77-21 (TR), (1977).

Salamy, S. G. and Nixon, J. C., "The Application of Electrochemical Methods to Flotation Research," In: Recent Developments in Mineral Dressing, IMM, London, 503-516 (1953).

Sato, M., "Oxidation of Sulfide Ore Bodies, II. Oxidation Mechanisms of Sulfide Minerals at 25°C," Econ. Geol., 55 , 1202-1231 (1966).

Schroeder, H. J., "Copper" , Mineral Commodity Profiles, U. S. Bureau of Mines (1979).

Schwarzenbach, G. and Fisher, A., "Die Aciditat der Sulfane und die Zusammensetzung wasseriger Polysulfidlosungen" , Helv. Chem Acta, 169 , 1365-1390 (1960).

Stewart, R., "Oxidation by Permanganate," Oxidation in Organic Chemistry , Part A., (Kenneth B. Wiberg, Ed.), Academic Press, New York, N. Y. (1965).

Sulman, H. L., "A Contribution to the Study of Flotation," IMM Bulletin No. 311 (1930).

Sutherland, K. L. and Wark, I. W., Principles of Flotation , Australasian Inst. of Mining and Metallurgy, Melbourne (1955).

Taggart, A. F., del Giuduce, G. R. M. and Ziehl, O. A., "The Case for the Chemical Theory of Flotation," Trans. AIMME, 112 , 348-381 (1934).

Teichmann, H., Semiconductors , transl. L. F. Secretan, Butterworths, London (1964).

Tolun, R. and Kitchener, J. A., "Electrochemical Study of the Galena-Xanthate-Oxygen Flotation System," Trans. IMM, 73 , 312-322 (1964).

Toperi, D. and Tolun R., "Electrochemical Study and Thermodynamic Equilibria of the Galena-Oxygen-Xanthate Flotation System," Trans. IMM, 78 , 191-197 (1969).

Trahar, W. J., "A Laboratory Study of the Influence of Sodium Sulfide and Oxygen on the Collectorless Flotation of Chalcopyrite," 56th Colloid and Surface Sci., Symp., Virginia Tech, June 13-16, 1982.

Vinogradov, S. N. and Linnell, R. H., Hydrogen Bonding , Van Nostrand Reinhold Company, New York, N. Y., (1971).

Vizsolyi, A., Veltman, H., and Forward, F. A., Trans. Met. Soc. AIME, 227 , 215 (1963).

Wagner, C. D., Riggs, W. M., Davis, L. E., Moulder, J. F. and Muilenberg, G. E., Handbook of X-Ray Photoelectron Spectroscopy , Published by Perkin-Elmer Corporation, Minnesota (1979).

Walker, G. W., Stout III, J. V. and Richardson, P. E., "Electrochemical Flotation of Sulfides: Reactions of Chalcocite in Aqueous Solution," 56th Colloid and Surface Sci. Symp., Virginia Tech, June 13-16, 1982.

Wark, I. W., Principles of Flotation , 1st Ed., Australasian Inst. of Mining and Metallurgy, Melbourne (1955).

Weinig, A. P. and Carpenter, C. B., Quarterly Colo. School Mines, 32 (4), 16 (1934).

Willard, H. H., Merritt, L. L. and Dean, J. A., Instrumental Methods of Analysis , 4th Ed., Nostrand Reinhold Publ., New York, N. Y. (1965).

Yoon, R. H., CANMET Report MRP/MSL, CF 77-35 (1977).

Yoon, R. H., "Collectorless Flotation of Chalcopyrite and Sphalerite Ores by Using Sodium Sulfide," Int. J. Miner. Process., 8, 31-48 (1981).

APPENDIX I

AUTOMATED FLOTATION MACHINE

AUTOMATION OF A LABORATORY FLOTATION MACHINE FOR IMPROVED PERFORMANCE

by

G. H. Luttrell and R. H. Yoon

Department of Mining and Minerals Engineering
Virginia Polytechnic Institute and State University
Blacksburg, Virginia 24061

INTRODUCTION

Improvements in flotation testing have been made through automation of a Denver laboratory flotation machine. The major advantages of this automation include improved reproducibility of test results, minimized operator bias, ease of operation, and interchangeability of cells. Although modifications have been made on a Denver Model D-12 laboratory flotation machine in the present work, most other commercial devices may also be easily adapted.

There are four important variables essential to the control of batch flotation experiments, i.e., impeller speed, froth removal rate, air-flow rate, and pulp level (Dell and Bunyard, 1972; Harris and Raja, 1966; Klassen and Mokrousov, 1963). The present design allows for control of these variables independently from one another.

DESCRIPTION

Cell Design and Froth Removal Mechanism

Figure 1 shows the two-paddle design of the flotation cell which is similar to the one that has been used at the U. S. Department of Energy (Miller, 1980). The D.O.E. cell was constructed from stainless steel and was used for coal flotation. In the present work, however, the cell has been made from Plexiglass, so that events occurring during flotation can be observed through the cell walls.

The basic cell design incorporates features much like those in a full-scale industrial cell. Two mechanical scrapers, one on each side, rotate about a fixed horizontal axis at a fixed depth. The scraper paddles rotate in teflon sleeves since conventional bearings are susceptible to corrosion and contaminate the pulp by leaking grease. The paddle rotation speed can be adjusted between 0 and 60 rpm by means of a constant torque speed controller and a gear motor drive. The paddles are relatively large as compared to the cell volume in order to cover as much of the froth surface as possible. Since the top of the cell is open, the paddles and the sides of the cell can be easily cleaned by spraying water during operation (see Figures 2 and 3).

The present unit has been designed to accommodate interchangeable cells of two different capacities. The 4-liter cell (see Figure 3) is used for rougher flotation, and the 2-liter cell (not shown) for cleaner flotation. After each experiment, the cell can be removed from the unit, emptied, and cleaned for the next experiment. This is easily done by raising the impeller and sliding the cell from its slotted aluminum baseplate and gear motor drive shaft.

Air Flow Control

Air can be introduced into the cell in two different ways. One way is simply to open the standard air inlet valve on the impeller tube which allows air to be drawn in by suction. In this case, the air volume input would be controlled by the impeller speed. Air may also enter the cell from the opposite side of the impeller tube from an air pump. (An extra threaded hole is already provided in the impeller tube of the Denver machine for use as an air inlet.) A short-stroke diaphragm pump has been chosen for this purpose rather than other mechanical pumps to avoid contamination of the air by oil and to provide a steady air flow rate. The pump is connected to a 3-way valve and flowmeter assembly to allow for close control of air flow rate. Compressed gases, for example, nitrogen, may be used in place of air. The air pump and scraper paddles are

activated simultaneously by means of a timer.

Pulp Level Control

The most notable feature of the automated flotation unit is the method by which make-up water is added to the cell. Although several methods were suggested in the literature for pulp level control (Harris and Raja, 1966; Dell and Bunyard, 1972; Lynch, Johnson, Manlapig and Thorne, 1981), in general, they are bulky, not very sensitive to small changes in pulp level, have slow response times, and allow contact between the make-up water in storage and the pulp in the flotation cell. With this in mind, a probe-type electronic level controller has been developed. The operation of the controller relies on the fact that the electrical resistance of the pulp and froth are different. Its circuit diagram is given in Figure 4.

The two-pronged probe, shown in Figure 5, is clamped to the impeller tube and can easily be moved up or down. Prior to flotation, the probe tip is set to a desired pulp level. Initially, the tip of the probe is just in contact with the pulp. This holds the water pump in the "off" position. As flotation progresses, the pulp level drops and the probe tip becomes exposed to the froth layer. The increased resistivity sensed by the probe will signal the controller to actuate the water pump to deliver make-up

water into the cell.

The pulp level controller incorporates a potentiometer, as shown in its electrical circuit diagram (Figure 4). This potentiometer is adjusted prior to the test to a threshold setting so that the water pump is switched off when the probe tips are in contact with the pulp. A potentiometer setting too low would cause the device not to respond to the pulp, while a setting too high would cause the device to become sensitive to the froth and thus stop the addition of make-up water prematurely. Since only a small a-c current flows between the two prongs exposed at the tip of the probe, no electroplating occurs. The prongs of the probe can be made from any corrosion-resistant metal wire. In the present work, nickel-chromium wire is used.

Instead of adding tap water as the make-up water during flotation, one could use a reagent solution to keep the reagent, such as a pH modifier or a frother, at a constant level. Also, if a tailings-removal system is installed, it would be possible to perform tests continuously by pumping slurry instead of make-up water into the cell. The electronic pulp level controller is easy to adjust, sensitive, and can be used equally well with either a modified or a standard cell.

EXPERIMENTAL

Comparative Flotation Tests

Two series of flotation kinetic tests were performed - one using the automated machine, and one using a standard Denver machine. In each series, three identical flotation tests were made to determine reproducibility. Details of the experiments are as follows:

Sample Preparation: In each series, a 1.5 kg copper ore (-20 mesh) from the Kidd Creek Mine, Ontario, Canada, was well-mixed and carefully split with a Jones riffler into three identical 500 gram lots. Each 500 g sample was wet-ground for thirty minutes at 90 rev/min in a porcelain laboratory ball mill (18 X 14 cm) with 300 ml of tap water and 4 kg of steel balls.

Flotation Tests: The ore from the Kidd Creek Mine is a copper-zinc ore assaying 1.8% Cu and 5.8% Zn. The flotation kinetic experiments were conducted only for chalcopyrite, however. The ground ore samples were conditioned as follows:

Impeller speed = 1200 rev/min

Collector = 2 ml of 1% w/v potassium amyl xanthate (0.04 kg/ton)

Frother = 3 ml of 1% v/v Dowfroth 250 (0.06 kg/ton)

pH = adjusted to 9.0 with lime

Conditioning time = 3 minutes

Froth products were collected at predetermined intervals of ¼, ½, 1, 2, 3, 5, and 8 minutes in separate trays. The flotation conditions are given below:

	Denver	Automated
Impeller speed	1200 rpm	1200 rpm
Air flow rate	---	5 liters/min
Paddle speed	---	10 rpm
Pulp height	1 cm below lip	1 cm below lip
Cell volume	2.5 liters	2 liters

Each timed-cut sample was assayed for copper using a Spectrospan IV plasma emission spectrometer. Results of these tests are plotted in Figures 6 and 7. Note that the results from the automated machine show a higher initial flotation rate than the standard Denver machine. This was due to the fact that the paddle speed was set to remove the froth faster than the manual technique.

CONCLUSIONS

The results presented in this note demonstrate that the automated flotation machine produced more reproducible data than the standard Denver flotation machine. One

notable feature of our automated flotation machine is that it incorporates minimal changes to the basic design of standard flotation machines. Thus, many of the convenient features of the manual flotation machines have not been lost. For example, the ease of cleaning the system and the fact that two different size cells can be used interchangeably are convenient features of the present unit.

The automated flotation machine has been in use in our laboratory for the past year with much satisfaction. Several hundred flotation tests have been conducted by both experienced and inexperienced operators, yet the results are reproducible with minimum operator bias. Further details of the equipment construction are available upon request.

ACKNOWLEDGEMENTS

The authors are thankful to Mr. Ken Miller of the U. S. Department of Energy for providing the blue prints for the two-paddle stainless steel flotation cell. They also appreciate Mr. Wayne Slusser for his mechanical services and Mr. Michael Luttrell for his electrical services in the construction of the automated flotation unit. The present work is a result of projects funded by the National Science Foundation (Grant No. CPE - 8011456)

and the U. S. Department of Energy (Grant No. DE - FG22 - 80PC30234).

REFERENCES

Dell, C. C. and Bunyard, M. J., 1972. Development of an automatic flotation cell for the laboratory. Trans. I. M. M., 81: C246-C248.

Harris, C. C. and Raja, A., 1966. A modified laboratory flotation cell. Trans. A. I. M. E., 235: 150-156.

Klassen, V. I. and Mokrousov, V. A., 1963. An Introduction to the Theory of Flotation. Butterworth and Co., London.

Lynch, A. J., Johnson, N. W., Manlapig, E. V., Thorne, C. G., 1981. Mineral and Coal Flotation Circuits. Vol. 3. Elsevier Scientific Publishing Company, Amsterdam.

Miller, K. J., 1980. Evaluation of collector addition in the flotation of various U. S. coals. Report of Investigations, U. S. Dept. of Energy, PMTC - 7 (80).

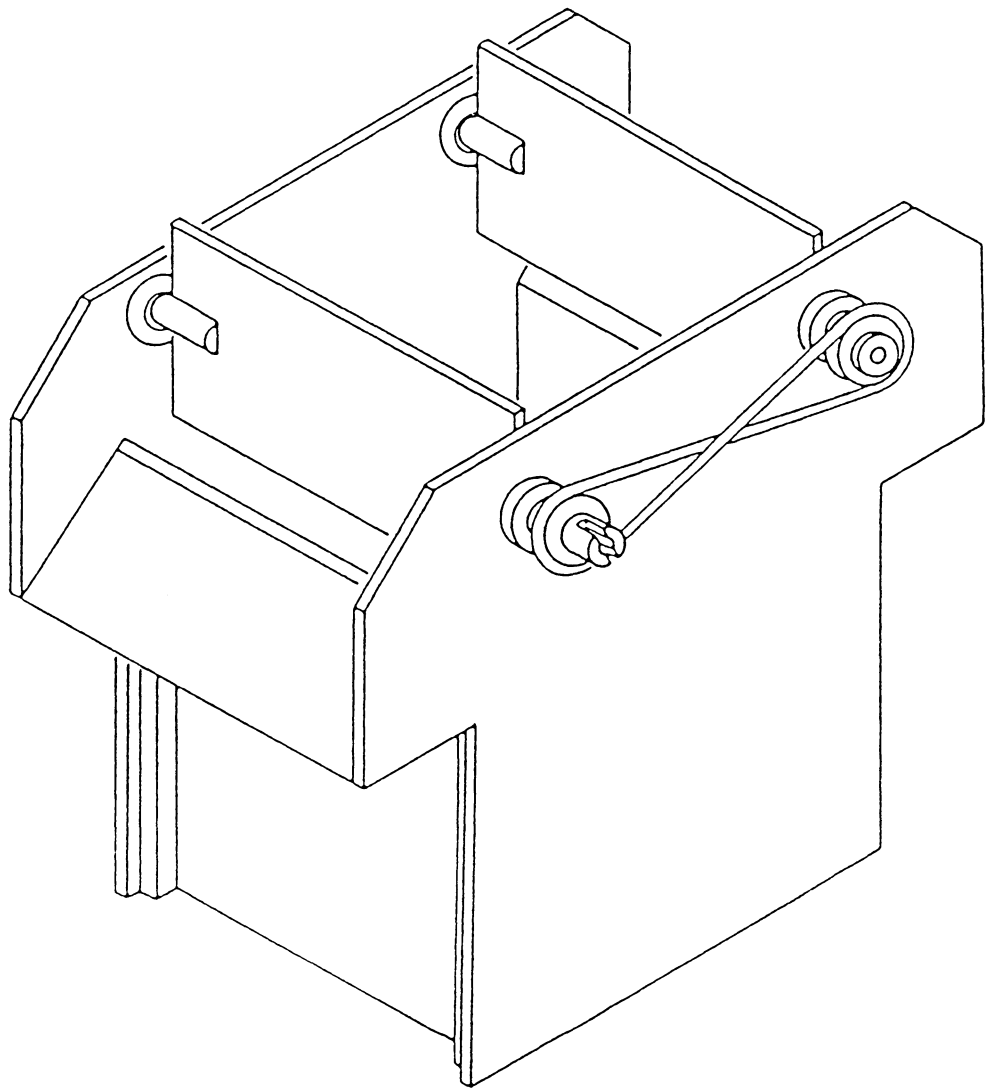

Figure 1. Two-paddle design of the plexi-glas flotation cell.

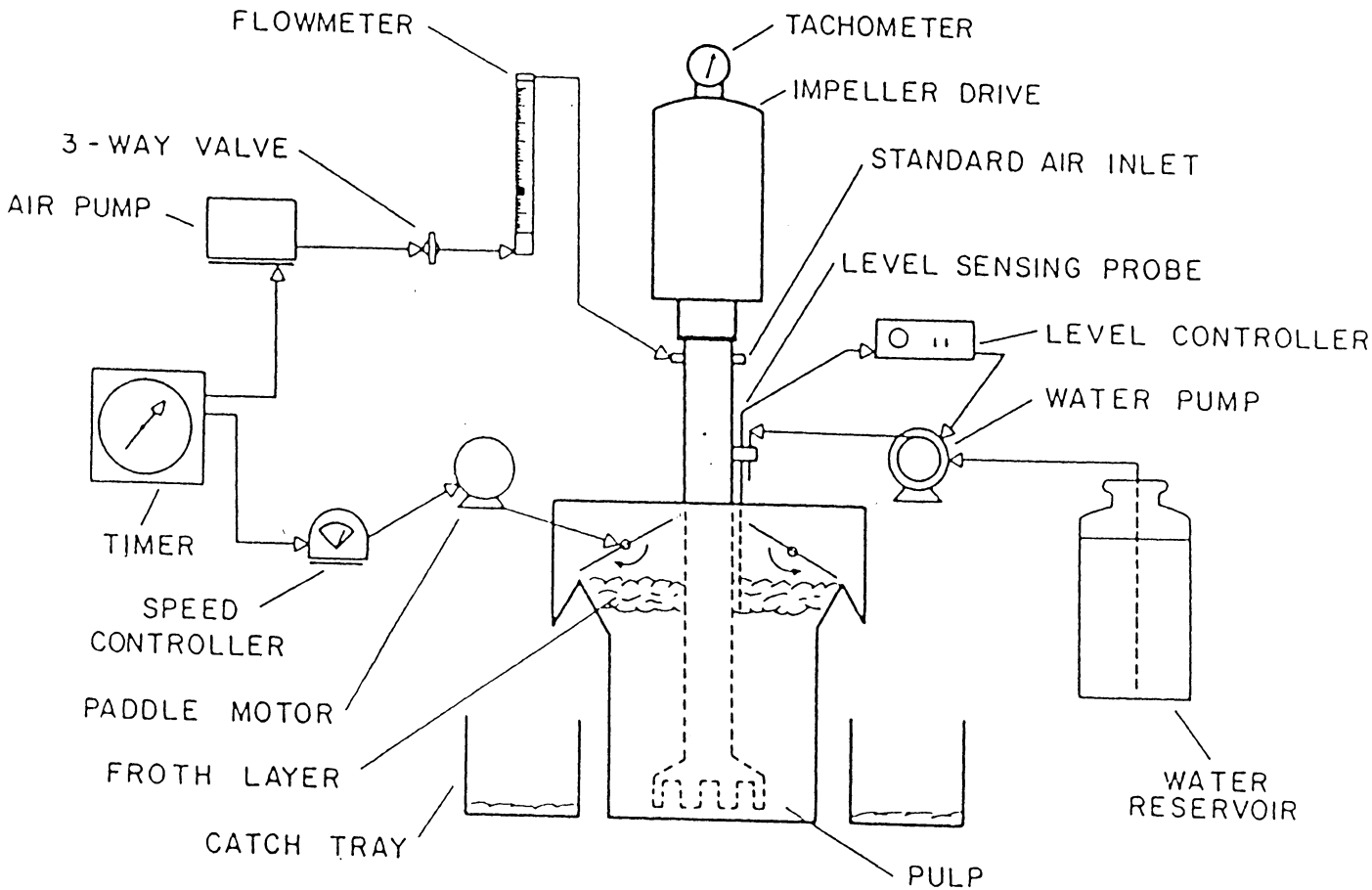

Figure 2. Schematic diagram of the automated batch flotation apparatus.

Figure 3. Photograph of the automated laboratory flotation apparatus.

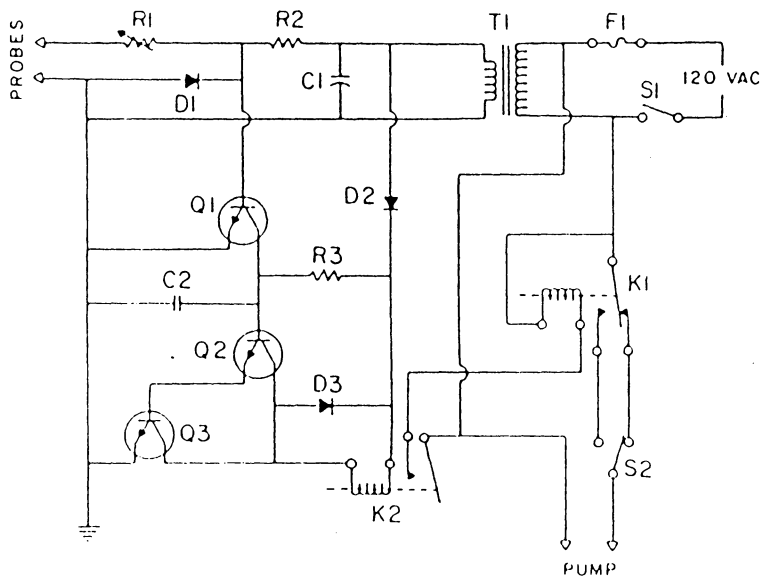

LEVEL CONTROLLER - PARTS LIST

R1 - 50,000 ohm Potentiometer
R2 - 300,000 ohm, 0.5 watt, 5% Resistor
R3 - 470,000 ohm, 0.5 watt, 5% Resistor
T1 - 120 VAC to 6.3 VAC @ 300 mA Power Transformer
F1 - 8 amp Fuse
S1 - SPST Switch
S2 - SPDT Switch
Q1,Q2,Q3 - 2N3904 NPN Transistor
K1 - 110 VAC, SPST Relay (Coil rated at 250 to 500 ohms)
D1,D2,D3 - 1N4002 Diode
C1 - 500 uF, 25 VDC, Electrolytic Capacitor
C2 - 0.5 uF, 25 VDC, Mylar Capacitor

Figure 4. Electrical circuit diagram of the pulp level controller.

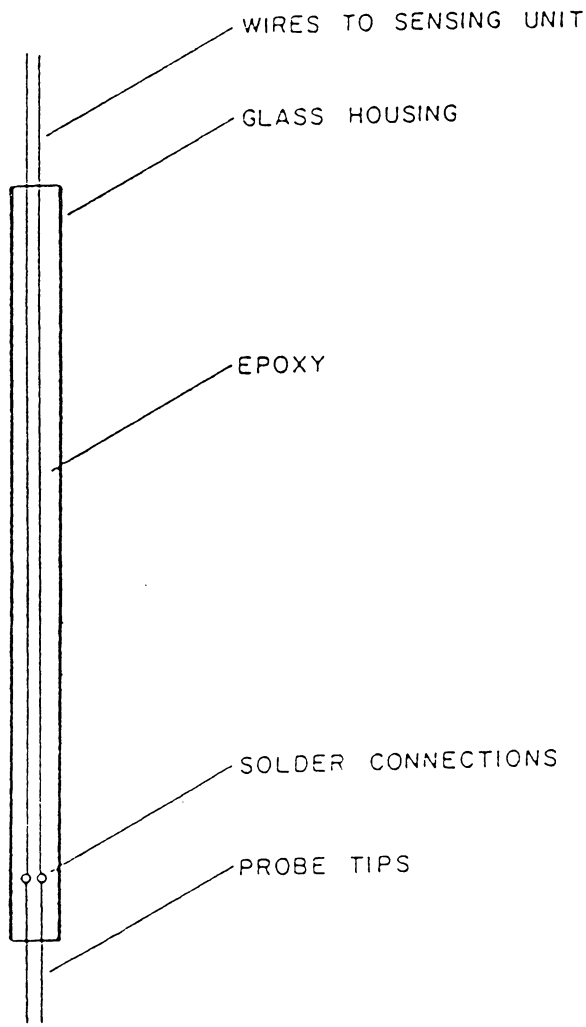

Figure 5. Pulp level controller probe.

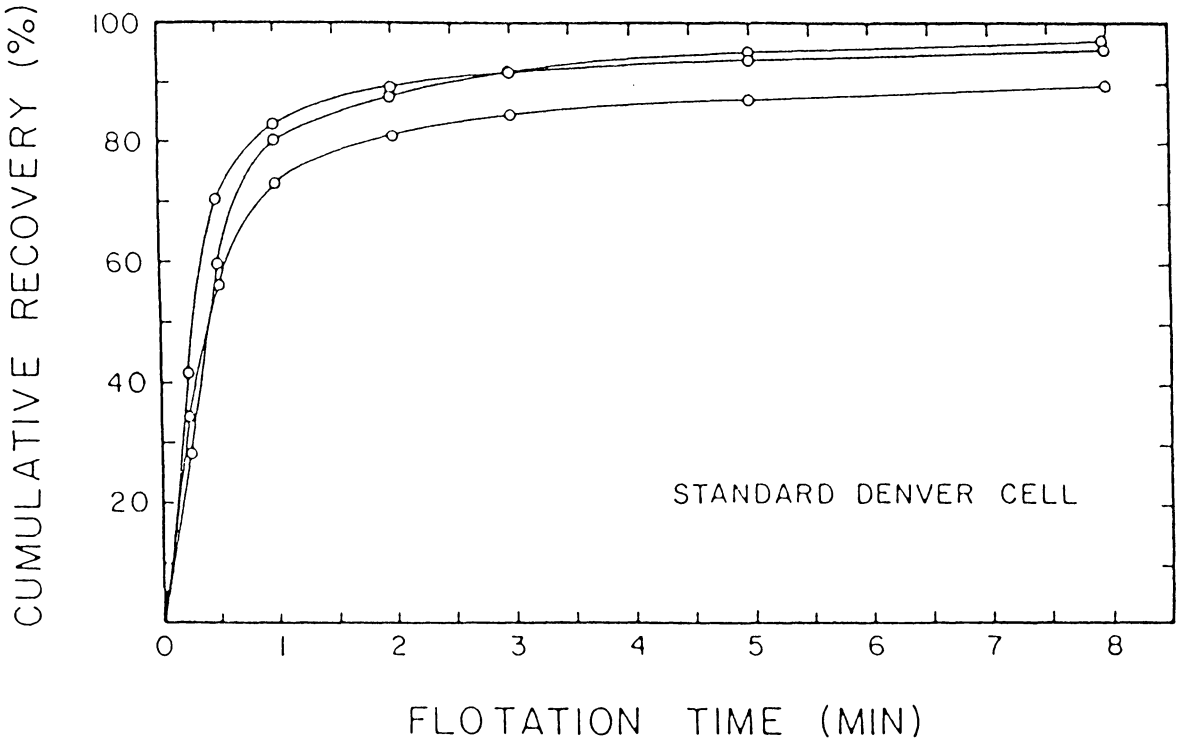

Figure 6. Results of the flotation kinetic tests conducted using the Denver laboratory flotation machine, Model D-12.

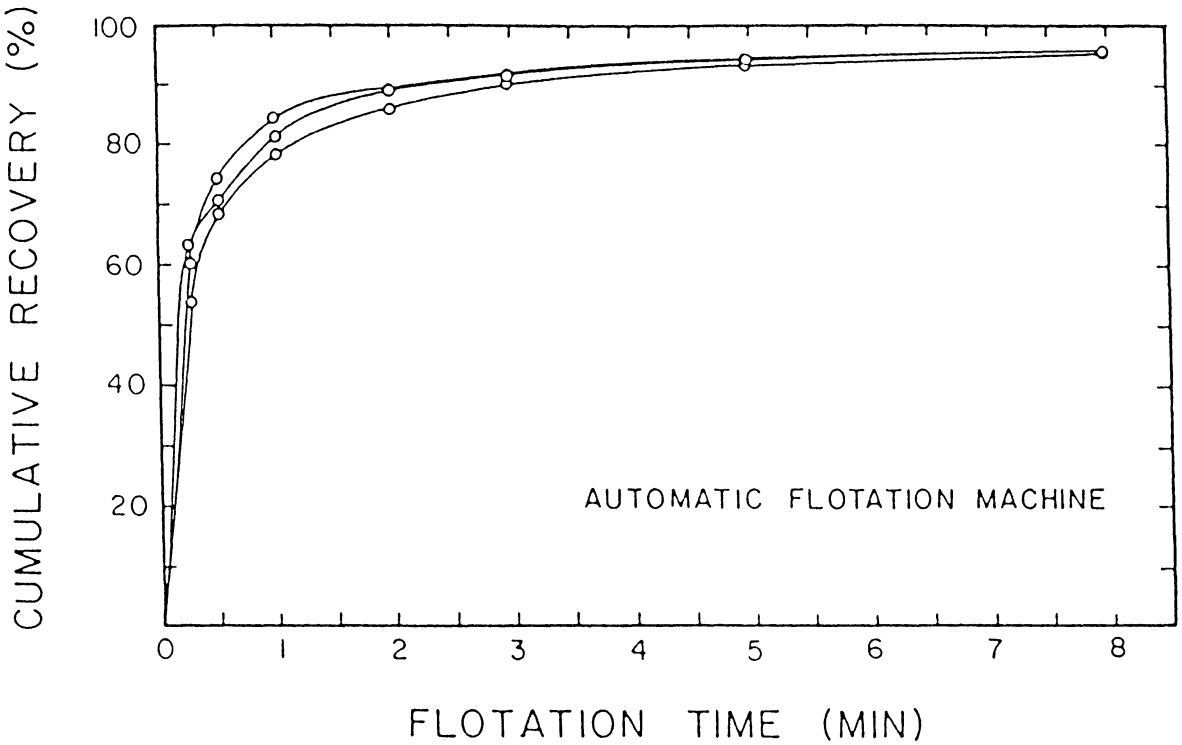

Figure 7. Results of the flotation kinetic tests conducted using the automated laboratory flotation machine.

APPENDIX II

XPS CURVE FITTING PROGRAM

```
1000 REM ************************************************************
1010 REM **                                                          **
1020 REM **          ESCA CURVE RESOLVING PROGRAM                    **
1030 REM **                                                          **
1040 REM **                                                          **
1050 REM **  Northstar Basic - Release 5.1                           **
1060 REM **  Numonics Model 1224 Electronic Digitizer                **
1070 REM **                                                          **
1080 REM **  Written by - Gerald H. Luttrell                         **
1090 REM **  Date - May 1982                                         **
1100 REM **                                                          **
1110 REM ** Department of Mining and Minerals Engineering           **
1120 REM ** Virginia Tech                                           **
1130 REM **                                                          **
1140 REM ************************************************************
1150 REM
1160 REM
1170 DIM X(50),Y(50),C(50),V1(50),V2(50),V3(50),G(50)
1180 DIM V4(50),V5(50),V6(50),G1(50),N$(50),A$(20)
1190 N1=0
1200 U=9999999
1210 PRINT CHR$(27),CHR$(69)
1220 INPUT "SAMPLE I.D.?  ",N$
1230 PRINT
1240 PRINT "**** INPUT COORDINATES FROM THE DIGITIZER ****"
1250 PRINT
1260 INPUT #1,A$
1270 Y$=A$(1,8)
1280 X$=A$(9,16)
1290 IF VAL(Y$)<0 THEN 1370
1300 N1=N1+1
```

```
1300 N1=N1+1
1310 Y(N1)=VAL(Y$)
1320 X(N1)=VAL(X$)
1330 PRINT
1340 PRINT " * ",%6I,N1,"     ",%8F4,X(N1),%8F4,Y(N1)
1350 GOTO 1260
1360 PRINT
1370 M=(Y(N1)-Y(1))/(X(N1)-X(1))
1380 B=(X(N1)*Y(1)-X(1)*Y(N1))/(X(N1)-X(1))
1390 FOR I=1 TO N1
1400 C(I)=Y(I)-(M*X(I)+B)
1410 NEXT I
1420 PRINT
1430 INPUT "NUMBER OF PEAKS IN THE ENVELOPE?  ",N2
1440 PRINT
1450 FOR I=1 TO N2
1460 PRINT "PEAK #",(4-I)," STANDARD B.E. AND WIDTH?  ",
1470 INPUT "",L(4-I),W(4-I)
1480 NEXT I
1490 PRINT
1500 FOR I=1 TO N2
1510 PRINT "PEAK #",(4-I)," HIGH AND LOW VALUES?  ",
1520 INPUT "",Z1(4-I),Z2(4-I)
1530 NEXT I
1540 IF N2=2 THEN Z1(1)=0
1550 IF N2=1 THEN Z1(1)=0
1560 IF N2=1 THEN Z1(2)=0
1570 READ J
1580 FOR S1=Z2(1) TO Z1(1) STEP J
1590 H(1)=S1
1600 K=1
```

```
1600 K=1
1610 GOSUB 2340
1620 IF A(K)=0 THEN 1670
1630 FOR I=1 TO N1
1640 T=((L(K)-X(I))/A(K))^2
1650 V1(I)=H(K)*EXP(-T)
1660 NEXT I
1670 FOR S2=Z2(2) TO Z1(2) STEP J
1680 H(2)=S2
1690 K=2
1700 GOSUB 2340
1710 IF A(K)=0 THEN 1760
1720 FOR I=1 TO N1
1730 T=((L(K)-X(I))/A(K))^2
1740 V2(I)=H(K)*EXP(-T)
1750 NEXT I
1760 FOR S3=Z2(3) TO Z1(3) STEP J
1770 H(3)=S3
1780 K=3
1790 GOSUB 2340
1800 FOR I=1 TO N1
1810 IF A(K)=0 THEN 1840
1820 T=((L(K)-X(I))/A(K))^2
1830 V3(I)=H(K)*EXP(-T)
1840 NEXT I
1850 GOSUB 2360
1860 NEXT S3
1870 FOR I=1 TO 60
1880 PRINT "-",
1890 NEXT I
1900 NEXT S2
```

```
1900 NEXT S2
1910 NEXT S1
1920 IF J=0.1 THEN 2050
1930 IF N2=1 THEN 2010
1940 IF N2=2 THEN 1980
1950 Z2(1)=Q1-J/2
1960 Z1(2)=Q1+J/2
1970 IF Z2(1)<0 THEN Z2(1)=0
1980 Z2(2)=Q2-J/2
1990 Z1(2)=Q2+J/2
2000 IF Z2(2)<0 THEN Z2(2)=0
2010 Z2(3)=Q3-J/2
2020 Z1(3)=Q3+J/2
2030 IF Z2(3)<0 THEN Z2(3)=0
2040 GOTO 1570
2050 X$=CHR$(7)
2060 FOR I=1 TO 2000
2070 PRINT X$,
2080 NEXT I
2090 PRINT N$
2100 PRINTPRINT
2110 PRINT "                EST       EST       STD        STD"
2120 PRINT "      PEAK     HEIGHT    AREA      B.E.      WIDTH"
2130 PRINT "    -------- -------- -------- -------- --------"
2140 PRINT
2150 PRINT "     #1   ",%9F2,Q1,%9F2,(Q1*W(1)),%9F2,L(1),%9F2,W(1)
2160 PRINT "     #2   ",%9F2,Q2,%9F2,(Q2*W(2)),%9F2,L(2),%9F2,W(2)
2170 PRINT "     #3   ",%9F2,Q3,%9F2,(Q3*W(3)),%9F2,L(3),%9F2,W(3)
2180 PRINT
2190 PRINT "FIT ERROR:  ",%7F3,U
2200 PRINTPRINT
```

```
2200 PRINTPRINT
2210 INPUT "",Q$
2220 PRINT"  B.E.     RAW      CORR     EST       #1       #2       #3   "
2230 PRINT"------- ------- ------- ------- ------- ------- -------"
2240 PRINT
2250 FOR I=1 TO N1
2260 PRINT %6F2,X(I),%8F2,Y(I),%8F2,C(I),%8F2,G1(I),
2270 PRINT %8F2,V4(I),%8F2,V5(I),%8F2,V6(I),%8F2
2280 NEXT I
2290 PRINTPRINT
2300 INPUT "",Q$
2310 GOTO 2090
2320 END
2330 DATA 6,2,1,0.5,0.2,0.1
2340 A(K)=SQRT(-(W(K)∧2)/(4*LOG(0.5)))
2350 RETURN
2360 U1=0
2370 FOR I=1 TO N1
2380 G(I)=V1(I)+V2(I)+V3(I)
2390 U1=((C(I)-G(I))∧2)+U1
2400 NEXT I
2410 U2=U1/(N1+1)
2420 PRINT " ",%6F1,S1,%6F1,S2,%6F1,S3,
2430 PRINT "        ",%15F4,U2,%15F4,U
2440 IF U2>U THEN RETURN
2450 U=U2
2460 Q1=S1Q2=S2Q3=S3
2470 FOR P=1 TO N1
2480 V4(P)=V1(P)
2490 V5(P)=V2(P)
2500 V6(P)=V3(P)
```

```
2500 V6(P)=V3(P)
2510 G1(P)=G(P)
2520 NEXT P
2530 RETURN
```

APPENDIX III

METALLURGICAL BALANCE SHEETS FOR FLOTATION TESTS

Batch Flotation of Chalcopyrite

Test No.	Reagent Additions, lb/ton			pH	Comments
	AERO-350	Na_2S	DF-250		
A001	0.03	-	0.14	9.0	
A002	-	-	0.14	9.0	
A003	-	3.0	0.14	10.1	
A004	-	3.0	0.14	Natural	Condition 30"
B001	0.12	-	0.26	9.5	
B002	-	-	0.26	9.5	
B003	-	3.0	0.26	10.2	
B004	-	-	0.26	Natural	Dry Ground
C001	0.05	-	0.20	9.0	
C002	-	-	0.20	9.0	
C003	-	3.0	0.20	10.4	
C004	-	3.0	0.20	10.3	Air Oxidized

Batch Flotation of Chalcopyrite (Cont.)

Test No.	Reagent Additions, lb/ton			pH	Comments
	AERO-350	Na_2S	DF-250		
D001	0.06	-	0.12	9.0	
D002	-	-	0.12	9.0	
D003	-	3.0	0.12	10.4	
D004	-	1.8	0.12	9.7	
D005	-	0.4	0.12	Natural	
D006	-	3.0	0.12	6.5	
D007	-	-	0.12	Natural	Dry Ground
E001	0.15	-	0.12	9.0	
E002	-	-	0.12	9.0	
E003	-	3.0	0.12	11.1	
E004	-	3.0	0.12	6.5	
F001	0.03	-	0.12	9.0	
F002	-	-	0.12	9.6	
F003	-	3.0	0.12	9.8	

A001

PRODUCT	WEIGHT PERCENTS Ind	Cum	ASSAY, %Cu Ind	Cum	DISTRIBUTION Ind	Cum
Concentrate	2.5	2.5	12.36	12.36	71.5	71.5
2nd CLR Tail	.6	3.1	4.33	10.81	6.0	77.6
1st CLR Tail	6.7	9.8	.64	3.86	9.9	87.5
Tail	90.2	100.0	.06	.43	12.5	100.0
Feed	100.0		.43		100.0	

A002

PRODUCT	WEIGHT PERCENTS Ind	Cum	ASSAY, %Cu Ind	Cum	DISTRIBUTION Ind	Cum
Concentrate	1.5	1.5	20.58	20.58	59.6	59.6
2nd CLR Tail	.6	2.1	7.31	16.79	8.5	68.1
1st CLR Tail	3.8	5.9	1.87	7.18	13.7	81.8
Tail	94.1	100.0	.10	.52	18.2	100.0
Feed	100.0		.52		100.0	

A003

PRODUCT	WEIGHT PERCENTS Ind	Cum	ASSAY, %Cu Ind	Cum	DISTRIBUTION Ind	Cum
Concentrate	2.0	2.0	22.43	22.43	47.8	47.8
2nd CLR Tail	.3	2.3	1.79	19.74	.6	48.4
1st CLR Tail	3.2	5.5	.35	8.46	1.2	49.6
Tail	94.5	100.0	.50	.53	50.4	100.0
Feed	100.0		.53		100.0	

A004

PRODUCT	WEIGHT PERCENTS Ind	Cum	ASSAY, %Cu Ind	Cum	DISTRIBUTION Ind	Cum
Concentrate	2.8	2.8	13.43	13.43	75.0	75.0
2nd CLR Tail	.3	3.1	8.12	12.92	4.9	79.9
1st CLR Tail	2.4	5.5	1.06	7.74	5.1	84.9
Tail	94.5	100.0	.08	.50	15.1	100.0
Feed	100.0		.50		100.0	

B001

PRODUCT	WEIGHT PERCENTS Ind	Cum	ASSAY, %Cu Ind	Cum	DISTRIBUTION Ind	Cum
Concentrate	9.3	9.3	22.09	22.09	89.1	89.1
2nd CLR Tail	1.4	10.7	5.75	19.95	3.5	92.6
1st CLR Tail	5.7	16.4	1.83	13.65	4.5	97.1
Tail	83.6	100.0	.08	2.31	2.9	100.0
Feed	100.0		2.31		100.0	

B002

PRODUCT	WEIGHT PERCENTS Ind	Cum	ASSAY, %Cu Ind	Cum	DISTRIBUTION Ind	Cum
Concentrate	9.0	9.0	23.84	23.84	91.5	91.5
2nd CLR Tail	1.8	10.8	3.46	20.44	2.7	94.1
1st CLR Tail	9.1	19.9	.63	11.38	2.4	96.6
Tail	80.1	100.0	.10	2.35	3.4	100.0
Feed	100.0		2.35		100.0	

B003

PRODUCT	WEIGHT PERCENTS Ind	Cum	ASSAY, %Cu Ind	Cum	DISTRIBUTION Ind	Cum
Concentrate	11.0	11.0	20.93	20.93	89.1	89.1
2nd CLR Tail	1.7	12.7	5.09	18.81	3.4	92.5
1st CLR Tail	8.5	21.2	1.26	11.77	4.1	96.6
Tail	78.8	100.0	.11	2.58	3.4	100.0
Feed	100.0		2.58		100.0	

B004

PRODUCT	WEIGHT PERCENTS Ind	Cum	ASSAY, %Cu Ind	Cum	DISTRIBUTION Ind	Cum
Concentrate	10.0	10.0	20.99	20.99	87.8	87.8
2nd CLR Tail	2.3	12.3	2.19	17.47	2.1	89.9
1st CLR Tail	8.2	20.5	.71	10.77	2.4	92.4
Tail	79.5	100.0	.23	2.39	7.6	100.0
Feed	100.0		2.39		100.0	

C001

PRODUCT	WEIGHT PERCENTS Ind	Cum	ASSAY, %Cu Ind	Cum	DISTRIBUTION Ind	Cum
Concentrate	4.3	4.3	32.39	32.39	83.3	83.3
2nd CLR Tail	1.8	6.1	6.84	24.85	7.4	90.6
1st CLR Tail	11.5	17.6	.79	9.13	5.4	96.1
Tail	82.4	100.0	.08	1.67	3.9	100.0
Feed	100.0		1.67		100.0	

COO2

PRODUCT	WEIGHT PERCENTS Ind	Cum	ASSAY, %Cu Ind	Cum	DISTRIBUTION Ind	Cum
Concentrate	3.6	3.6	33.55	33.55	76.0	76.0
2nd CLR Tail	1.9	5.5	3.16	23.05	3.8	79.8
1st CLR Tail	8.9	14.4	1.97	10.02	11.0	90.8
Tail	85.6	100.0	.17	1.59	9.2	100.0
Feed	100.0		1.59		100.0	

COO3

PRODUCT	WEIGHT PERCENTS Ind	Cum	ASSAY, %Cu Ind	Cum	DISTRIBUTION Ind	Cum
Concentrate	1.6	1.6	27.63	27.63	26.3	26.3
2nd CLR Tail	.7	2.3	4.68	20.65	1.9	28.2
1st CLR Tail	4.0	6.3	2.08	8.86	4.9	33.2
Tail	93.7	100.0	1.20	1.68	66.8	100.0
Feed	100.0		1.68		100.0	

COO4

PRODUCT	WEIGHT PERCENTS Ind	Cum	ASSAY, %Cu Ind	Cum	DISTRIBUTION Ind	Cum
Concentrate	3.6	3.6	29.60	29.60	71.7	71.7
2nd CLR Tail	.7	4.3	16.49	27.47	7.8	79.5
1st CLR Tail	3.5	7.8	2.64	16.33	6.2	85.7
Tail	92.2	100.0	.23	1.48	14.3	100.0
Feed	100.0		1.48		100.0	

DOO1

PRODUCT	WEIGHT PERCENTS Ind	Cum	ASSAY, %Cu Ind	Cum	DISTRIBUTION Ind	Cum
Concentrate	1.2	1.2	15.73	15.73	42.0	42.0
2nd CLR Tail	.7	1.9	10.67	13.87	16.6	58.6
1st CLR Tail	9.0	10.9	.98	3.23	19.6	78.2
Tail	89.1	100.0	.11	.45	21.8	100.0
Feed	100.0		.45		100.0	

DOO2

PRODUCT	WEIGHT PERCENTS Ind	Cum	ASSAY, %Cu Ind	Cum	DISTRIBUTION Ind	Cum
Concentrate	.0	.0	9.74	9.74	.5	.5
2nd CLR Tail	.2	.3	2.30	3.19	.9	1.5
1st CLR Tail	5.7	5.9	.64	.75	6.7	8.2
Tail	94.1	100.0	.53	.54	91.8	100.0
Feed	100.0		.54		100.0	

DOO3

PRODUCT	WEIGHT PERCENTS Ind	Cum	ASSAY, %Cu Ind	Cum	DISTRIBUTION Ind	Cum
Concentrate	.6	.6	6.74	6.74	7.7	7.7
2nd CLR Tail	.5	1.1	5.55	6.20	5.3	12.9
1st CLR Tail	7.9	9.0	1.32	1.92	19.8	32.7
Tail	91.0	100.0	.39	.53	67.3	100.0
Feed	100.0		.53		100.0	

DOO4

PRODUCT	WEIGHT PERCENTS Ind	Cum	ASSAY, %Cu Ind	Cum	DISTRIBUTION Ind	Cum
Concentrate	1.7	1.7	11.72	11.72	31.2	31.2
2nd CLR Tail	.4	2.1	8.31	11.07	5.2	36.4
1st CLR Tail	4.6	6.7	1.52	4.51	11.0	47.4
Tail	93.3	100.0	.36	.64	52.6	100.0
Feed	100.0		.64		100.0	

DOO5

PRODUCT	WEIGHT PERCENTS Ind	Cum	ASSAY, %Cu Ind	Cum	DISTRIBUTION Ind	Cum
Concentrate	2.0	2.0	12.55	12.55	54.4	54.4
2nd CLR Tail	.4	2.4	7.01	11.63	6.1	60.5
1st CLR Tail	4.0	6.4	1.28	5.16	11.1	71.6
Tail	93.6	100.0	.14	.46	28.4	100.0
Feed	100.0		.46		100.0	

DOO6

PRODUCT	WEIGHT PERCENTS Ind	Cum	ASSAY, %Cu Ind	Cum	DISTRIBUTION Ind	Cum
Concentrate	1.3	1.3	13.18	13.18	34.7	34.7
2nd CLR Tail	.6	1.9	10.08	12.20	12.2	46.9
1st CLR Tail	3.2	5.1	2.26	5.96	14.6	61.6
Tail	94.9	100.0	.20	.49	38.4	100.0
Feed	100.0		.49		100.0	

D007

PRODUCT	WEIGHT PERCENTS Ind	Cum	ASSAY, %Cu Ind	Cum	DISTRIBUTION Ind	Cum
Concentrate	.9	.9	28.04	28.04	50.0	50.0
2nd CLR Tail	.2	1.1	13.06	25.32	5.2	55.1
1st CLR Tail	1.5	2.6	2.12	11.93	6.3	61.4
Tail	97.4	100.0	.20	.51	38.6	100.0
Feed	100.0		.51		100.0	

E001

PRODUCT	WEIGHT PERCENTS Ind	Cum	ASSAY, %Cu Ind	Cum	DISTRIBUTION Ind	Cum
Concentrate	16.0	16.0	30.75	30.75	55.2	55.2
2nd CLR Tail	12.2	28.2	13.81	23.42	18.9	74.1
1st CLR Tail	11.3	39.5	12.29	20.24	15.6	89.7
Tail	60.5	100.0	1.52	8.91	10.3	100.0
Feed	100.0		8.91		100.0	

E002

PRODUCT	WEIGHT PERCENTS Ind	Cum	ASSAY, %Cu Ind	Cum	DISTRIBUTION Ind	Cum
Concentrate	3.9	3.9	24.28	24.28	10.5	10.5
2nd CLR Tail	2.1	6.0	8.55	18.77	2.0	12.4
1st CLR Tail	7.1	13.1	3.43	10.46	2.7	15.1
Tail	86.9	100.0	8.85	9.06	84.9	100.0
Feed	100.0		9.06		100.0	

EOO3

PRODUCT	WEIGHT PERCENTS Ind	Cum	ASSAY, %Cu Ind	Cum	DISTRIBUTION Ind	Cum
Concentrate	17.7	17.7	26.40	26.40	47.8	47.8
2nd CLR Tail	5.4	23.1	12.65	23.19	7.0	54.8
1st CLR Tail	8.7	31.8	6.74	18.69	6.0	60.7
Tail	68.2	100.0	5.63	9.78	39.3	100.0
Feed	100.0		9.78		100.0	

EOO4

PRODUCT	WEIGHT PERCENTS Ind	Cum	ASSAY, %Cu Ind	Cum	DISTRIBUTION Ind	Cum
Concentrate	20.6	20.6	28.82	28.82	60.4	60.4
2nd CLR Tail	5.2	25.8	19.36	26.91	10.2	70.7
1st CLR Tail	9.6	35.4	11.16	22.64	10.9	81.6
Tail	64.6	100.0	2.81	9.84	18.4	100.0
Feed	100.0		9.84		100.0	

FOO1

PRODUCT	WEIGHT PERCENTS Ind	Cum	ASSAY, %Cu Ind	Cum	DISTRIBUTION Ind	Cum
Concentrate	3.2	3.2	17.52	17.52	71.2	71.2
2nd CLR Tail	1.2	4.4	3.59	13.72	5.5	76.7
1st CLR Tail	8.5	12.9	.83	5.23	9.0	85.6
Tail	87.1	100.0	.13	.79	14.4	100.0
Feed	100.0		.79		100.0	

FOO2

PRODUCT	WEIGHT PERCENTS Ind	Cum	ASSAY, %Cu Ind	Cum	DISTRIBUTION Ind	Cum
Concentrate	3.2	3.2	17.52	17.52	71.2	71.2
2nd CLR Tail	1.2	4.4	3.59	13.72	5.5	76.7
1st CLR Tail	8.5	12.9	.83	5.23	9.0	85.6
Tail	87.1	100.0	.13	.79	14.4	100.0
Feed	100.0		.79		100.0	

FOO3

PRODUCT	WEIGHT PERCENTS Ind	Cum	ASSAY, %Cu Ind	Cum	DISTRIBUTION Ind	Cum
Concentrate	.9	.9	29.86	29.86	36.0	36.0
2nd CLR Tail	.6	1.5	10.37	22.06	8.3	44.4
1st CLR Tail	4.7	6.3	1.71	6.63	10.8	55.1
Tail	93.8	100.0	.36	.75	44.9	100.0
Feed	100.0		.75		100.0	

Batch Flotation of Sphalerite

Test No.	Reagent Additions, lb/ton				pH	Comments
	AERO-211	Na_2S	$CuSO_4$	DF-250		
H000	0.15	-	1.5	0.50	10.0	
H001	-	-	1.5	0.50	10.0	
HOO2	-	-	-	0.50	10.0	
HOO3	-	3.0	1.5	0.50	10.3	
H004	-	3.0	-	0.50	10.0	
H005	-	3.0	1.5	0.16	10.5	10" Grind
H006	-	3.0	1.5	0.16	10.5	20" Grind
H007	-	3.0	1.5	0.16	10.4	30" Grind
H008	-	3.0	1.5	0.16	10.3	40" Grind
H009	-	3.0	1.5	0.16	10.1	50" Grind
H010	-	3.0	1.5	0.16	10.1	60" Grind
H011	-	3.0	1.5	0.16	5.6	
H012	-	3.0	1.5	0.16	6.1	
H013	-	3.0	1.5	0.16	6.9	
H014	-	3.0	1.5	0.16	7.6	
H015	-	3.0	1.5	0.16	8.4	
H016	-	3.0	1.5	0.16	9.5	
H017	-	3.0	1.5	0.16	10.2	
H018	-	3.0	1.5	0.16	10.5	
H019	-	3.0	1.5	0.16	11.3	
H020	-	3.0	1.5	0.16	12.0	

Batch Flotation of Sphalerite (Cont.)

Test No.	Reagent Additions, lb/ton				pH	Comments
	AERO-211	Na_2S	$CuSO_4$	DF-250		
H021	-	1.8	0.9	0.16	6.8	Condit. 5"
H022	-	1.8	0.9	0.16	6.8	Condit. 10"
H023	-	1.8	0.9	0.16	6.8	Condit. 15"
H024	-	1.8	0.9	0.16	6.8	Condit. 20"
H025	-	3.0	0.5	0.16	6.8	
H026	-	3.0	1.0	0.16	6.8	
H027	-	3.0	1.5	0.16	6.8	
H028	-	3.0	2.0	0.16	6.8	
H029	-	3.0	3.0	0.16	6.8	
H030	-	3.0	4.0	0.16	6.8	
H031	-	3.0	5.0	0.16	6.8	
H032	-	3.0	5.5	0.16	6.8	
H033	-	3.0	8.0	0.16	6.8	
H034	-	3.0	11.0	0.16	6.8	
H035	-	1.8	0.5	0.16	6.8	
H036	-	1.8	1.0	0.16	6.8	
H037	-	1.8	1.3	0.16	6.8	
H038	-	1.8	1.5	0.16	6.8	
H039	-	1.8	2.0	0.16	6.8	
H040	-	1.8	3.5	0.16	6.8	
H041	-	1.8	4.5	0.16	6.8	

Batch Flotation of Sphalerite (Cont.)

Test No.	Reagent Additions, lb/ton				pH	Comments
	AERO-211	Na_2S	$CuSO_4$	DF-250		
H042	-	1.8	5.5	0.16	6.8	
H043	-	0.6	0.3	0.16	6.8	
H044	-	0.6	0.5	0.16	6.8	
H045	-	0.6	1.5	0.16	6.8	
H046	-	0.6	3.0	0.16	6.8	
H047	-	0.6	5.0	0.16	6.8	
H048	-	1.0	0.3	0.16	6.8	
H049	-	2.0	0.6	0.16	6.8	
H050	-	3.0	1.0	0.16	6.8	
H051	-	4.0	1.3	0.16	6.8	
H052	-	5.0	1.6	0.16	6.8	
H053	-	6.0	1.9	0.16	6.8	
H054	-	7.0	2.2	0.16	6.8	
H055	-	8.0	2.6	0.16	6.8	
I001	0.15	-	1.5	0.06	11.0	
I002	-	2.0	0.7	0.06	6.5	

H000

PRODUCT	WEIGHT PERCENTS Ind	Cum	ASSAY, %Cu Ind	Cum	DISTRIBUTION Ind	Cum
Concentrate	9.5	9.5	57.83	57.83	90.3	90.3
2nd CLR Tail	1.2	10.7	17.84	53.36	3.5	93.8
1st CLR Tail	6.6	17.3	2.22	33.77	2.4	96.2
Tail	82.7	100.0	.28	6.07	3.8	100.0
Feed	100.0		6.07		100.0	

H001

PRODUCT	WEIGHT PERCENTS Ind	Cum	ASSAY, %Cu Ind	Cum	DISTRIBUTION Ind	Cum
Concentrate	.5	.5	20.34	20.34	1.5	1.5
2nd CLR Tail	1.2	1.7	6.29	10.42	1.1	2.7
1st CLR Tail	8.2	9.9	4.34	5.37	5.4	8.1
Tail	90.1	100.0	6.69	6.56	91.9	100.0
Feed	100.0		6.56		100.0	

H002

PRODUCT	WEIGHT PERCENTS Ind	Cum	ASSAY, %Cu Ind	Cum	DISTRIBUTION Ind	Cum
Concentrate	.3	.3	3.70	3.70	.2	.2
2nd CLR Tail	1.0	1.4	3.46	3.52	.6	.8
1st CLR Tail	5.9	7.3	1.03	1.50	1.0	1.7
Tail	92.7	100.0	6.67	6.29	98.3	100.0
Feed	100.0		6.29		100.0	

H003

PRODUCT	WEIGHT PERCENTS Ind	Cum	ASSAY, %Cu Ind	Cum	DISTRIBUTION Ind	Cum
Concentrate	9.8	9.8	41.00	41.00	66.8	66.8
2nd CLR Tail	2.1	11.8	17.88	36.95	6.2	73.0
1st CLR Tail	8.7	20.5	7.43	24.45	10.8	83.8
Tail	79.5	100.0	1.22	5.98	16.2	100.0
Feed	100.0		5.98		100.0	

H004

PRODUCT	WEIGHT PERCENTS Ind	Cum	ASSAY, %Cu Ind	Cum	DISTRIBUTION Ind	Cum
Concentrate	.7	.7	2.41	2.41	.3	.3
2nd CLR Tail	1.3	2.1	3.54	3.15	.7	1.0
1st CLR Tail	6.9	9.0	4.33	4.06	4.4	5.4
Tail	91.0	100.0	7.09	6.82	94.6	100.0
Feed	100.0		6.82		100.0	

H005

PRODUCT	WT%	ASSAY	UNITS	DIST
Concentrate	3.38	6.78	22.92	3.40
Tailing	96.62	6.73	650.25	96.60
Feed	100.00	6.73	673.17	100.00

H006

PRODUCT	WT%	ASSAY	UNITS	DIST
Concentrate	4.31	10.77	46.44	6.88
Tailing	95.69	6.57	628.67	93.12
Feed	100.00	6.75	675.11	100.00

H007

PRODUCT	WT%	ASSAY	UNITS	DIST
Concentrate	13.81	30.36	419.15	69.05
Tailing	86.19	2.18	187.90	30.95
Feed	100.00	6.07	607.05	100.00

H008

PRODUCT	WT%	ASSAY	UNITS	DIST
Concentrate	13.83	26.97	373.04	64.72
Tailing	86.17	2.36	203.36	35.28
Feed	100.00	5.76	576.40	100.00

H009

PRODUCT	WT%	ASSAY	UNITS	DIST
Concentrate	12.83	29.11	373.59	60.15
Tailing	87.17	2.84	247.55	39.85
Feed	100.00	6.21	621.14	100.00

H010

PRODUCT	WT%	ASSAY	UNITS	DIST
Concentrate	12.07	25.55	308.47	50.49
Tailing	87.93	3.44	302.47	49.51
Feed	100.00	6.11	610.93	100.00

H011

PRODUCT	WT%	ASSAY	UNITS	DIST
Concentrate	15.89	25.35	402.69	64.63
Tailing	84.11	2.62	220.38	35.37
Feed	100.00	6.23	623.07	100.00

H012

PRODUCT	WT%	ASSAY	UNITS	DIST
Concentrate	17.27	29.14	503.18	80.11
Tailing	82.73	1.51	124.93	19.89
Feed	100.00	6.28	628.10	100.00

H013

PRODUCT	WT%	ASSAY	UNITS	DIST
Concentrate	20.34	23.48	477.54	77.10
Tailing	79.66	1.78	141.80	22.90
Feed	100.00	6.19	619.34	100.00

H014

PRODUCT	WT%	ASSAY	UNITS	DIST
Concentrate	16.19	21.90	354.52	57.39
Tailing	83.81	3.14	263.17	42.61
Feed	100.00	6.18	617.69	100.00

H015

PRODUCT	WT%	ASSAY	UNITS	DIST
Concentrate	16.68	22.13	369.02	59.22
Tailing	83.32	3.05	254.14	40.78
Feed	100.00	6.23	623.16	100.00

H016

PRODUCT	WT%	ASSAY	UNITS	DIST
Concentrate	10.57	24.54	259.43	47.32
Tailing	89.43	3.23	288.85	52.68
Feed	100.00	5.48	548.28	100.00

H017

PRODUCT	WT%	ASSAY	UNITS	DIST
Concentrate	14.66	23.74	348.01	49.68
Tailing	85.34	4.13	352.46	50.32
Feed	100.00	7.00	700.47	100.00

H018

PRODUCT	WT%	ASSAY	UNITS	DIST
Concentrate	9.61	25.84	248.27	42.94
Tailing	90.39	3.65	329.93	57.06
Feed	100.00	5.78	578.20	100.00

H019

PRODUCT	WT%	ASSAY	UNITS	DIST
Concentrate	11.07	7.07	78.28	11.75
Tailing	88.93	6.61	587.81	88.25
Feed	100.00	6.66	666.09	100.00

H020

PRODUCT	WT%	ASSAY	UNITS	DIST
Concentrate	12.61	5.58	70.35	11.03
Tailing	87.39	6.49	567.18	88.97
Feed	100.00	6.38	637.53	100.00

H021

PRODUCT	WT%	ASSAY	UNITS	DIST
Concentrate	9.27	7.88	73.06	11.11
Tailing	90.73	6.44	584.29	88.89
Feed	100.00	6.57	657.35	100.00

H022

PRODUCT	WT%	ASSAY	UNITS	DIST
Concentrate	12.50	26.32	328.99	52.22
Tailing	87.50	3.44	301.00	47.78
Feed	100.00	6.30	629.99	100.00

H023

PRODUCT	WT%	ASSAY	UNITS	DIST
Concentrate	15.05	24.16	363.58	57.92
Tailing	84.95	3.11	264.20	42.08
Feed	100.00	6.28	627.78	100.00

H024

PRODUCT	WT%	ASSAY	UNITS	DIST
Concentrate	7.84	11.12	87.20	13.41
Tailing	92.16	6.11	563.09	86.59
Feed	100.00	6.50	650.29	100.00

H025

PRODUCT	WT%	ASSAY	UNITS	DIST
Concentrate	9.37	5.32	49.83	9.72
Tailing	90.63	5.11	463.13	90.28
Feed	100.00	5.13	512.97	100.00

H026

PRODUCT	WT%	ASSAY	UNITS	DIST
Concentrate	7.10	7.56	53.66	8.25
Tailing	92.90	6.42	596.43	91.75
Feed	100.00	6.50	650.09	100.00

H027

PRODUCT	WT%	ASSAY	UNITS	DIST
Concentrate	20.34	23.48	477.54	77.10
Tailing	79.66	1.78	141.80	22.90
Feed	100.00	6.19	619.34	100.00

H028

PRODUCT	WT%	ASSAY	UNITS	DIST
Concentrate	16.27	24.16	393.02	63.65
Tailing	83.73	2.68	224.40	36.35
Feed	100.00	6.17	617.42	100.00

H029

PRODUCT	WT%	ASSAY	UNITS	DIST
Concentrate	8.68	6.13	53.18	8.42
Tailing	91.32	6.33	578.09	91.58
Feed	100.00	6.31	631.26	100.00

H030

PRODUCT	WT%	ASSAY	UNITS	DIST
Concentrate	4.87	9.71	47.24	7.01
Tailing	95.13	6.59	626.94	92.99
Feed	100.00	6.74	674.18	100.00

H031

PRODUCT	WT%	ASSAY	UNITS	DIST
Concentrate	3.84	5.05	19.37	3.06
Tailing	96.16	6.39	614.49	96.94
Feed	100.00	6.34	633.86	100.00

H032

PRODUCT	WT%	ASSAY	UNITS	DIST
Concentrate	8.58	4.76	40.85	6.33
Tailing	91.42	6.61	604.28	93.67
Feed	100.00	6.45	645.12	100.00

H033

PRODUCT	WT%	ASSAY	UNITS	DIST
Concentrate	6.28	4.58	28.75	4.42
Tailing	93.72	6.63	621.38	95.58
Feed	100.00	6.50	650.13	100.00

H034

PRODUCT	WT%	ASSAY	UNITS	DIST
Concentrate	8.25	4.40	36.32	5.65
Tailing	91.75	6.61	606.44	94.35
Feed	100.00	6.43	642.76	100.00

H035

PRODUCT	WT%	ASSAY	UNITS	DIST
Concentrate	20.34	21.29	433.07	69.11
Tailing	79.66	2.43	193.57	30.89
Feed	100.00	6.27	626.64	100.00

H036

PRODUCT	WT%	ASSAY	UNITS	DIST
Concentrate	23.13	23.07	533.52	83.72
Tailing	76.87	1.35	103.78	16.28
Feed	100.00	6.37	637.30	100.00

H037

PRODUCT	WT%	ASSAY	UNITS	DIST
Concentrate	16.19	21.90	354.52	57.39
Tailing	83.81	3.14	263.17	42.61
Feed	100.00	6.18	617.69	100.00

H038

PRODUCT	WT%	ASSAY	UNITS	DIST
Concentrate	17.11	17.03	291.34	47.21
Tailing	82.89	3.93	325.77	52.79
Feed	100.00	6.17	617.10	100.00

H039

PRODUCT	WT%	ASSAY	UNITS	DIST
Concentrate	80.73	2.86	230.89	37.39
Tailing	19.27	20.07	386.70	62.61
Feed	100.00	6.18	617.60	100.00

H040

PRODUCT	WT%	ASSAY	UNITS	DIST
Concentrate	25.68	5.18	133.04	20.84
Tailing	74.32	6.80	505.36	79.16
Feed	100.00	6.38	638.39	100.00

H041

PRODUCT	WT%	ASSAY	UNITS	DIST
Concentrate	10.45	4.60	48.08	7.37
Tailing	89.55	6.75	604.45	92.63
Feed	100.00	6.53	652.53	100.00

H042

PRODUCT	WT%	ASSAY	UNITS	DIST
Concentrate	10.02	4.44	44.49	6.90
Tailing	89.98	6.67	600.16	93.10
Feed	100.00	6.45	644.65	100.00

H043

PRODUCT	WT%	ASSAY	UNITS	DIST
Concentrate	18.98	21.34	405.05	64.10
Tailing	81.02	2.80	226.85	35.90
Feed	100.00	6.32	631.91	100.00

H044

PRODUCT	WT%	ASSAY	UNITS	DIST
Concentrate	12.98	7.64	99.19	15.22
Tailing	87.02	6.35	552.56	84.78
Feed	100.00	6.52	651.75	100.00

H045

PRODUCT	WT%	ASSAY	UNITS	DIST
Concentrate	10.69	5.36	57.29	8.81
Tailing	89.31	6.64	593.03	91.19
Feed	100.00	6.50	650.32	100.00

H046

PRODUCT	WT%	ASSAY	UNITS	DIST
Concentrate	10.81	5.11	55.24	8.02
Tailing	89.19	7.10	633.25	91.98
Feed	100.00	6.88	688.49	100.00

H047

PRODUCT	WT%	ASSAY	UNITS	DIST
Concentrate	9.19	5.16	47.45	6.78
Tailing	90.81	7.18	651.98	93.22
Feed	100.00	6.99	699.43	100.00

H048

PRODUCT	WT%	ASSAY	UNITS	DIST
Concentrate	18.98	21.34	405.05	64.10
Tailing	81.02	2.80	226.85	35.90
Feed	100.00	6.32	631.91	100.00

H049

PRODUCT	WT%	ASSAY	UNITS	DIST
Concentrate	14.91	28.22	420.84	69.12
Tailing	85.09	2.21	188.04	30.88
Feed	100.00	6.09	608.88	100.00

H050

PRODUCT	WT%	ASSAY	UNITS	DIST
Concentrate	19.00	23.50	446.59	74.88
Tailing	81.00	1.85	149.84	25.12
Feed	100.00	5.96	596.43	100.00

H051

PRODUCT	WT%	ASSAY	UNITS	DIST
Concentrate	26.55	19.05	505.86	80.86
Tailing	73.45	1.63	119.72	19.14
Feed	100.00	6.26	625.58	100.00

H052

PRODUCT	WT%	ASSAY	UNITS	DIST
Concentrate	23.81	20.14	479.52	77.00
Tailing	76.19	1.88	143.24	23.00
Feed	100.00	6.23	622.75	100.00

H053

PRODUCT	WT%	ASSAY	UNITS	DIST
Concentrate	24.20	19.09	461.98	75.67
Tailing	75.80	1.96	148.57	24.33
Feed	100.00	6.11	610.55	100.00

H054

PRODUCT	WT%	ASSAY	UNITS	DIST
Concentrate	22.07	15.68	346.09	58.66
Tailing	77.93	3.13	243.91	41.34
Feed	100.00	5.90	590.00	100.00

H055

PRODUCT	WT%	ASSAY	UNITS	DIST
Concentrate	25.41	15.04	382.14	64.99
Tailing	74.59	2.76	205.87	35.01
Feed	100.00	5.88	588.01	100.00

I001

PRODUCT	WEIGHT PERCENTS Ind	Cum	ASSAY, %Cu Ind	Cum	DISTRIBUTION Ind	Cum
Concentrate	7.9	7.9	25.26	25.26	86.6	86.6
2nd CLR Tail	5.8	13.7	2.53	15.70	6.3	92.8
1st CLR Tail	11.5	25.2	.82	8.93	4.1	96.9
Tail	74.8	100.0	.10	2.32	3.1	100.0
Feed	100.0		2.32		100.0	

I002

PRODUCT	WEIGHT PERCENTS Ind	Cum	ASSAY, %Cu Ind	Cum	DISTRIBUTION Ind	Cum
Concentrate	3.2	3.2	49.12	49.12	68.0	68.0
2nd CLR Tail	3.6	6.8	5.90	26.30	9.1	77.1
1st CLR Tail	14.8	21.6	2.04	9.66	13.1	90.2
Tail	78.4	100.0	.29	2.31	9.8	100.0
Feed	100.0		2.31		100.0	

APPENDIX IV

ASSAY PROCEDURE

Assay Procedure: One-half to two grams of each flotation product, depending on the expected metal content, was riffled out and accurately weighed in separate 150 ml beakers. Ten ml each of concentrated HCl and HNO_3 were added to each beaker and placed on a hotplate. A watchglass was placed on each beaker to reflux the evaporated solution and to continually wash down the sides of the beaker. Sufficient heat was applied to maintain a slight boiling condition and the samples were evaporated almost to dryness. The sides of each beaker were rinsed with warm doubly distilled water to prevent precipitation of metal ions and to maximize the extraction of soluble metal into solution.

The samples were then allowed to cool and filtered through Whatman number 2 filter paper into appropriated volumetric flasks. The remaining volumes were filled with doubly distilled water. Samples were further diluted according to their respective metal concentrations to fit within the range of calibration standards.

The metal content of each sample was determined with a Spectraspan IV Plasma Emission Spectrometer. The wavelengths used for each metal were as follow:

Cu	3247.54 Angstroms
Zn	2025.52 Angstroms

All glassware used throughout sample assaying

procedures was cleaned in Micro cleaning solution, thoroughly rinsed with tap water, and finally rinsed with distilled water.

APPENDIX V

UV-VIS SPECTROPHOTOMETRIC CALIBRATION PROCEDURE

Calibration Procedure: A calibration curve was constructed as follows. A 50 mg sample of vacuum-dried sulfur was weighed using an analytical balance. The sulfur was completely transferred to a 1-liter volumetric flask and made up to volume using ethanol. The solution was allowed to mix until all the sulfur had dissolved. Aliquotes of up to 10 ml of this solution (50 micrograms of sulfur/ml of ethanol) were transferred to 50 ml volumetric flasks and made up to volume with ethanol. Each solution, thus prepared, was pipetted into a 1-cm fused silica cuvette. The absorbance was scanned over the range of wavelengths from 200 nm to 450 nm against pure ethanol. Instrument parameters were set as follows:

slit width = 1.0 nm

scan rate = 100 nm/min

X-Y chart expansion = 10 nm/cm

The absorbance measured at 275 nm was assigned as the absorbance peak for sulfur (Rolia, 1979).

All glassware used was cleaned once with acetone and then rinsed several times with hot distilled water. The glassware was then dried at approximately 120°C in an oven.

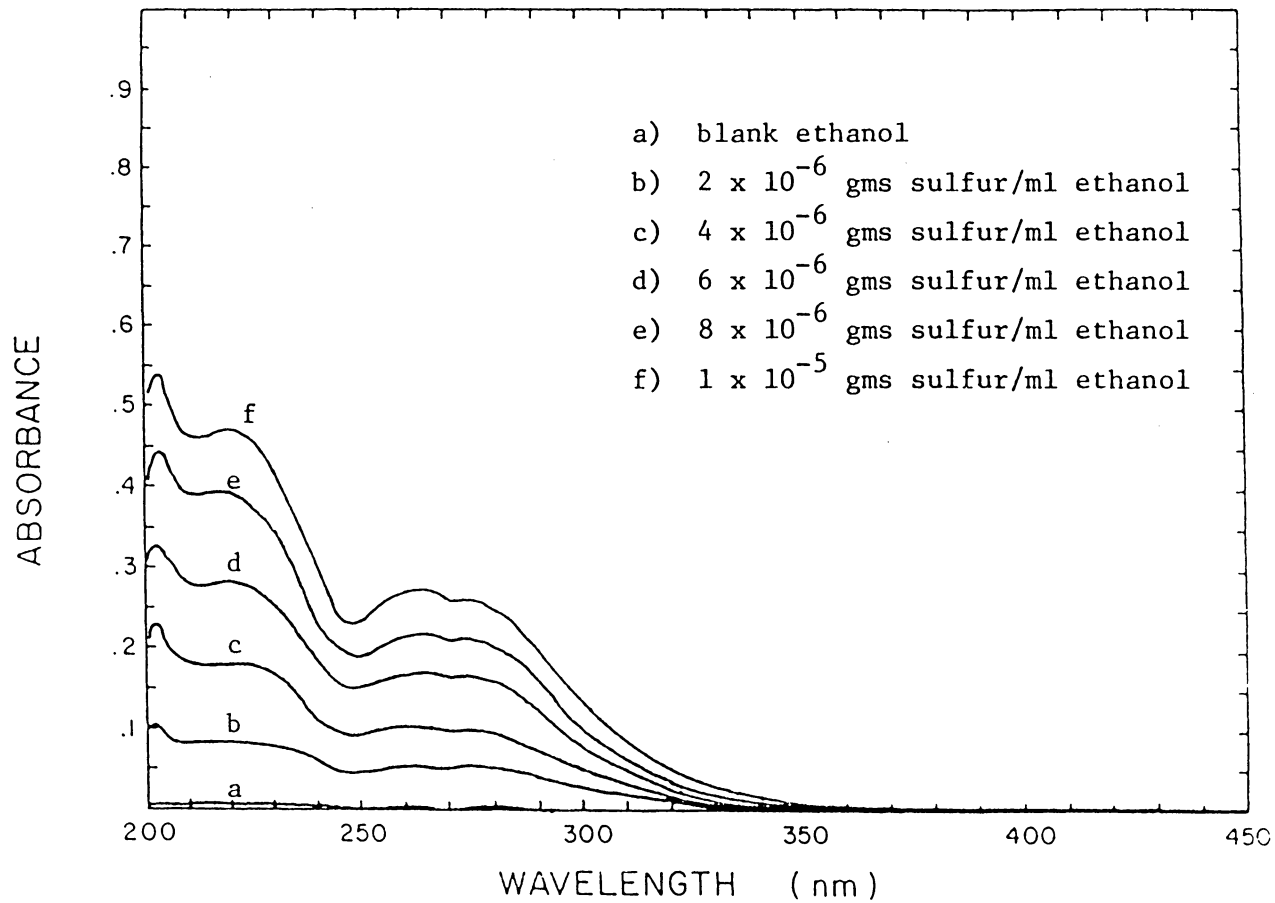

Figure 1 Absorbance spectra for sulfur dissolved in ethanol.

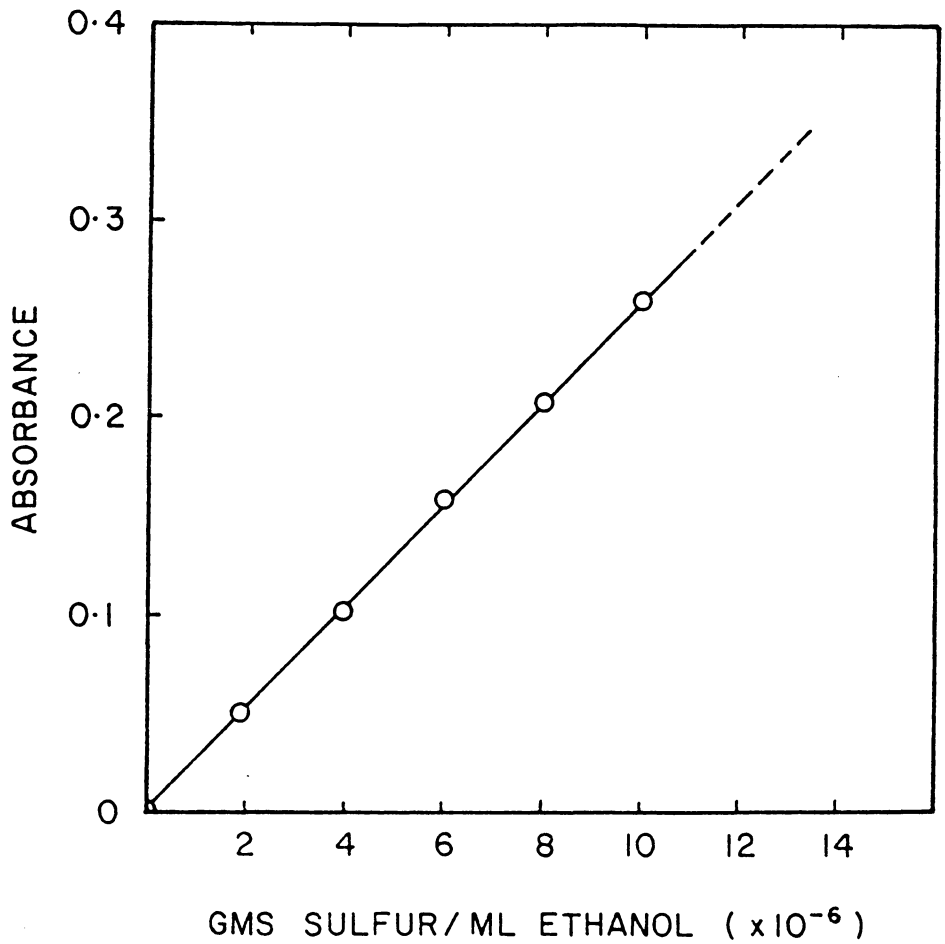

Figure 2 Calibration curve for determining the concentration of elemental sulfur in ethanol from absorbance at 275 nm.

APPENDIX VI

SURFACE AREA

micromeritics
Liquid Chromatography Instruments/Particle Technology Instruments

July 9, 1982

Va. Polytechnic Inst.
Mining & Minerals Engr.
213 Holden Hall
Blacksburg, VA 24061-2899

Reference: Your Purchase Order No. LV157648
Micromeritics' File No. 100798-072-PSP

Dear Sirs:

The Materials Analysis Laboratory has analyzed your samples on our AccuSorb Physical Adsorption Analyzer. The specific surface area was determined by a multi-point B.E.T. calculation using krypton adsorption.

Summary of the results:

Sample Identification	Specific Surface Area (m^2/g)
$CuFeS_2$	0.88

If you have any questions, or if we can better serve you, please contact us.

Sincerely,

Pat McCann
Materials Analysis Laboratory

PM/ds

Represented by: Micromeritics' District Office
3411 Saluda Road
Baltimore, MD 21236
Mr. Bill Travers
301/661-7866

********** M I C R O M E R I T I C S **********

M A T E R I A L S A N A L Y S I S L A B O R A T O R Y

MODEL 2100D
SURFACE AREA DATA AND COMPUTATION

DATE RUN 04-29-82

SAMPLE IDENTIFICATION: VIRGINIA TECH CU F252

MANIFOLD VOLUME: 30.030 ML (STP) EXTRA VOLUME: 131.900 ML (STP)

ADSORBATE: KRYPTON

STATION 4 FLASK NO. 29 OUTGAS TEMP 50 (C) OUTGAS TIME 961 MIN

W1	20.1540 G	H1	550.080 MM HG	PS	2.4085 MM HG
W2	18.5510 G	H2	151.630 MM HG	ALPHA	0.000030 $(MM\ HG)^{-1}$
WS	1.6030 G	TS	77.210 (K)	S	21.0000 A^2
VS	18.3671 ML				

	EV	P1 (MM HG)	P2 (MM HG)	V (ML/STP)	X (P2/PS)	Y $(ML/STP)^{-1}$	% Y ERROR
INPUT POINT 1	Y	0.3006	0.0052	0.0346	**********	**********	*******
INPUT POINT 2	Y	0.7000	0.0683	0.1055	**********	**********	*******
INPUT POINT 3	Y	0.4008	0.1407	0.1321	0.0584	0.469690	0.0225
INPUT POINT 4	Y	0.3508	0.2049	0.1456	0.0851	0.638518	0.0926
INPUT POINT 5	Y	0.4005	0.2730	0.1568	0.1133	0.815506	-0.1213
INPUT POINT 6	Y	0.4500	0.3406	0.1658	0.1414	0.993494	-0.0263
INPUT POINT 7	Y	0.5001	0.4034	0.1736	0.1675	1.158980	0.0475

SLOPE = 6.3154 INTERCEPT = 0.1006

SURFACE AREA = 0.8795 M^2/G

STANDARD ERROR OF LEAST SQUARES LINE = 0.000585 % ERROR = 0.0718

********** = DATA OUT OF LINEAR REGION OF ISOTHERM,
NOT USED FOR LEAST SQUARES CALCULATION

APPENDIX VII

MASS SPECTROMETRY SPECTRA

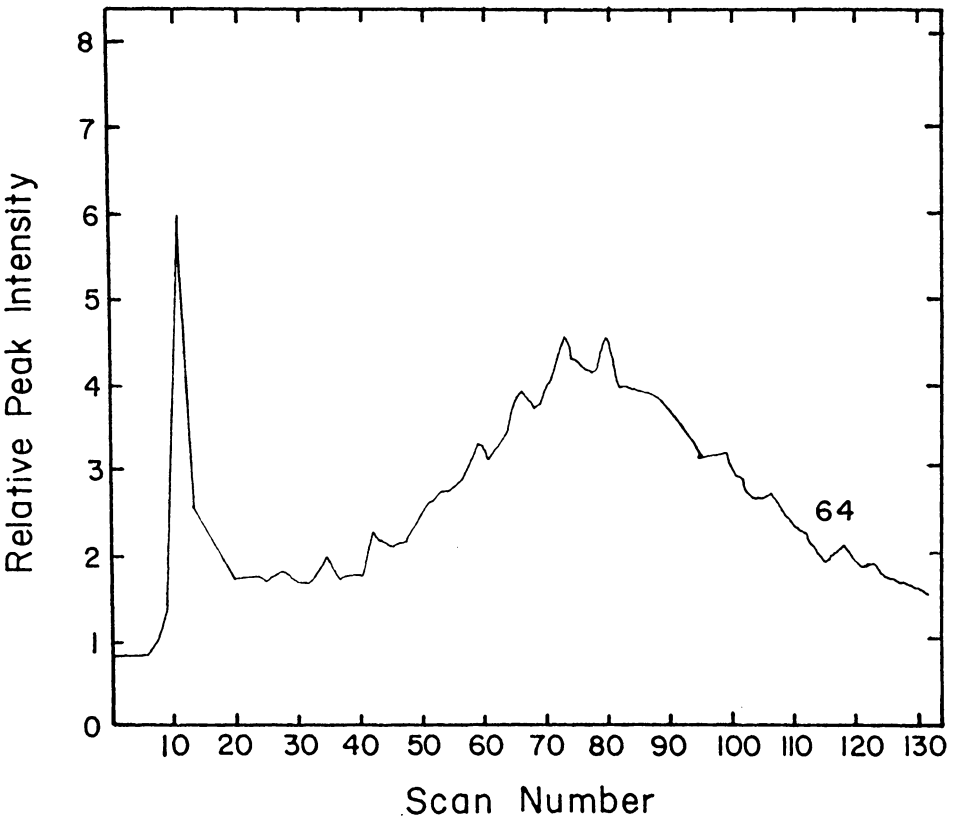

Figure 1. Mass spectrum scan of chalcopyrite condition at pH 2.0.

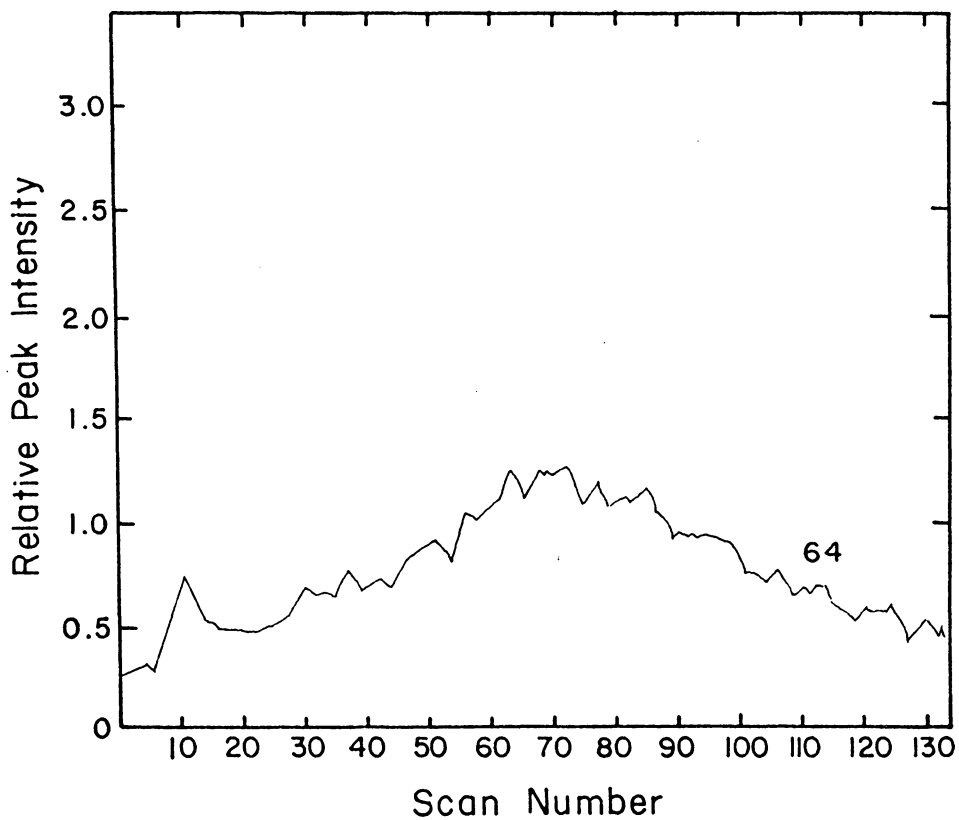

Figure 2. Mass spectrum scan of chalcopyrite conditioned at pH 4.0.

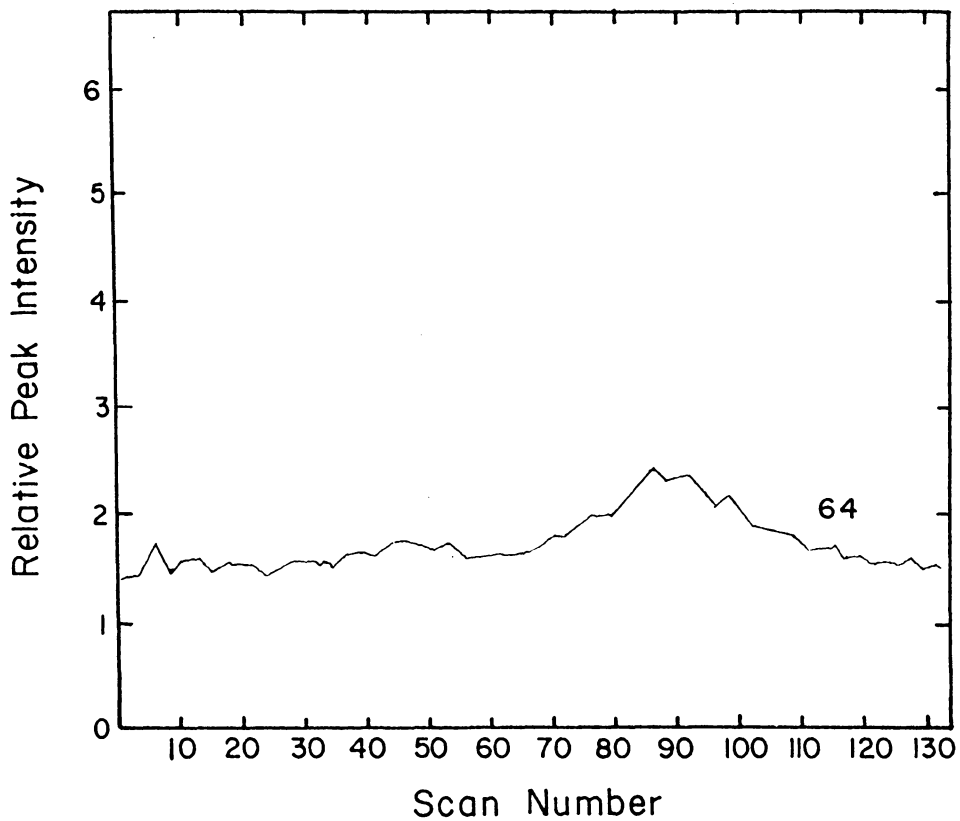

Figure 3. Mass spectrum scan of chalcopyrite conditioned at pH 6.0.

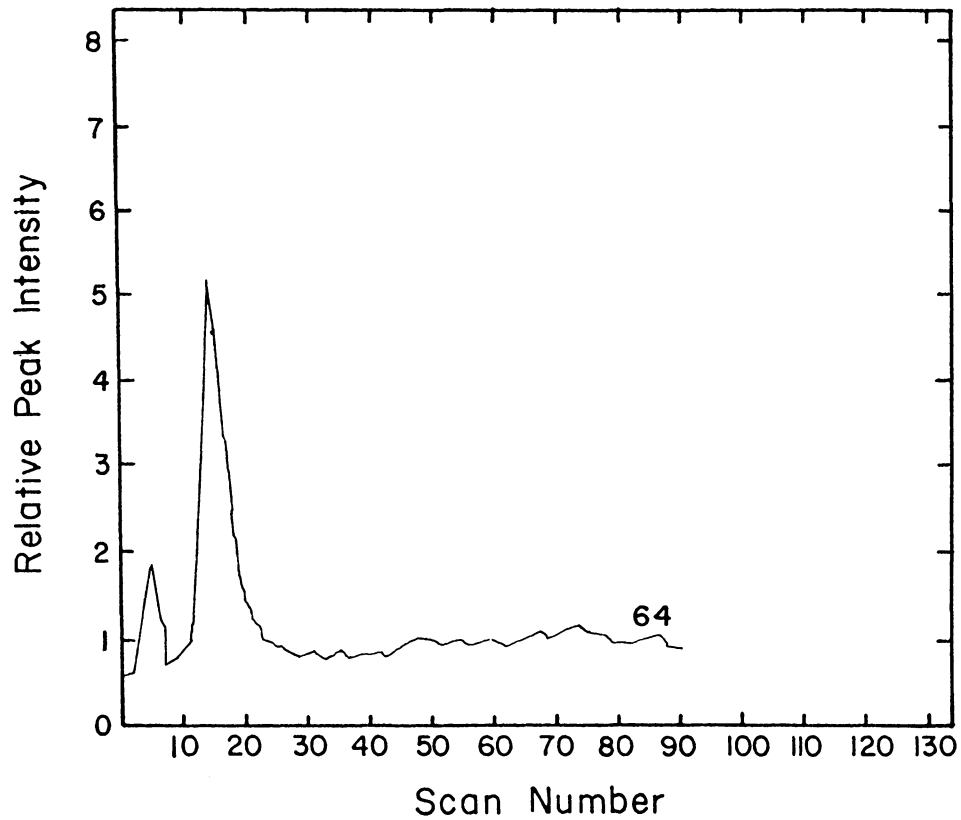

Figure 4. Mass spectrum scan of chalcopyrite conditioned at pH 8.0.

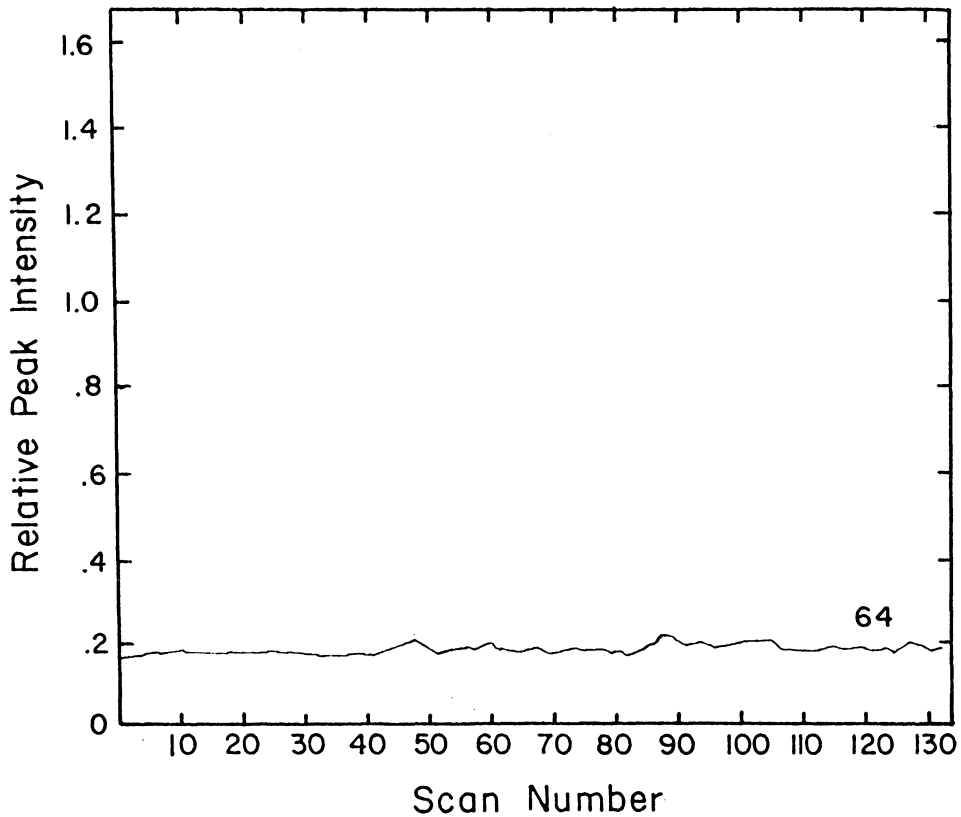

Figure 5. Mass spectrum scan of chalcopyrite conditioned at pH 10.0.

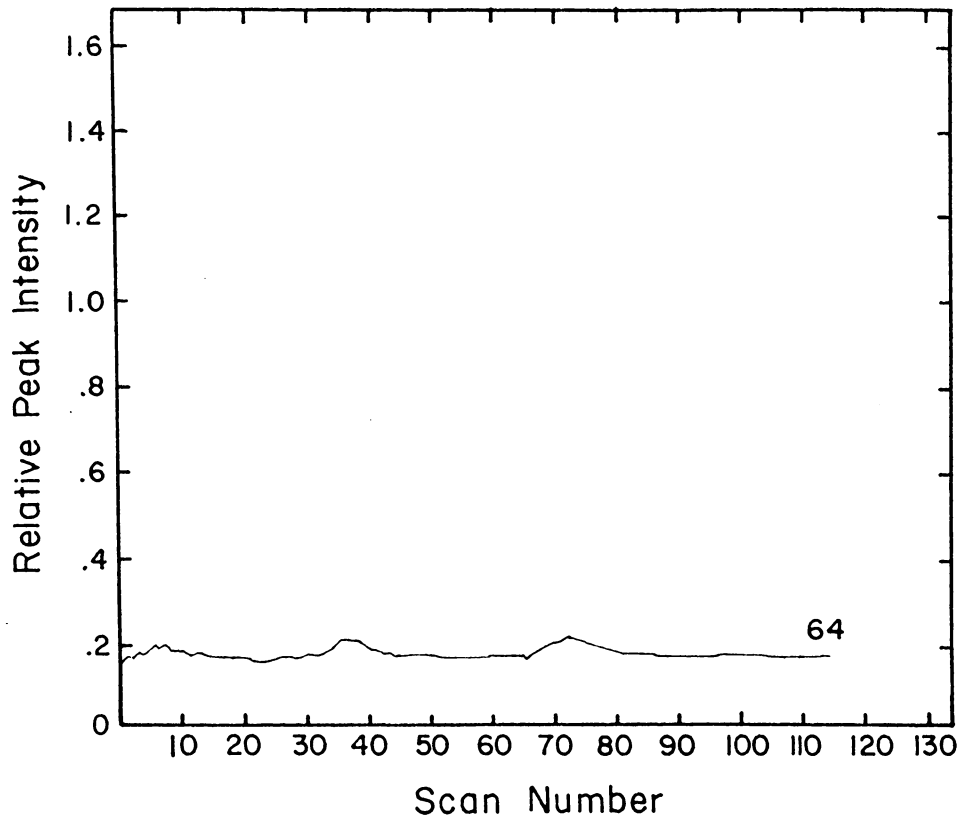

Figure 6. Mass spectrum scan of chalcopyrite conditioned at pH 12.0.

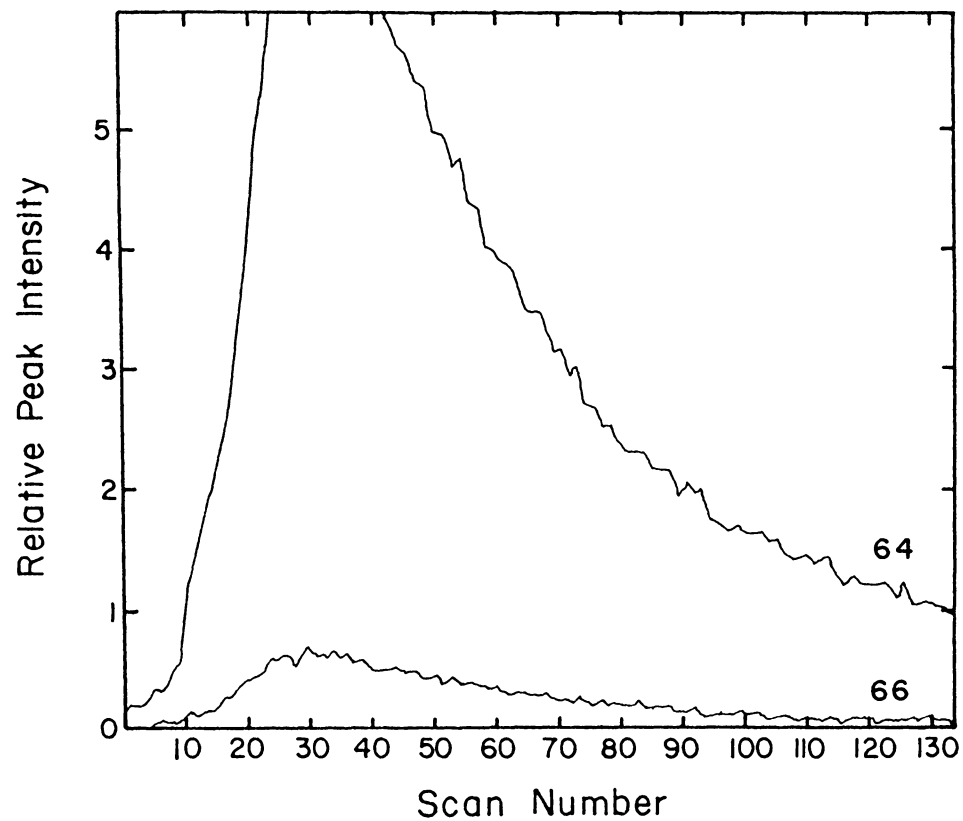

Figure 7. Mass spectrum scan of chalcopyrite blank.

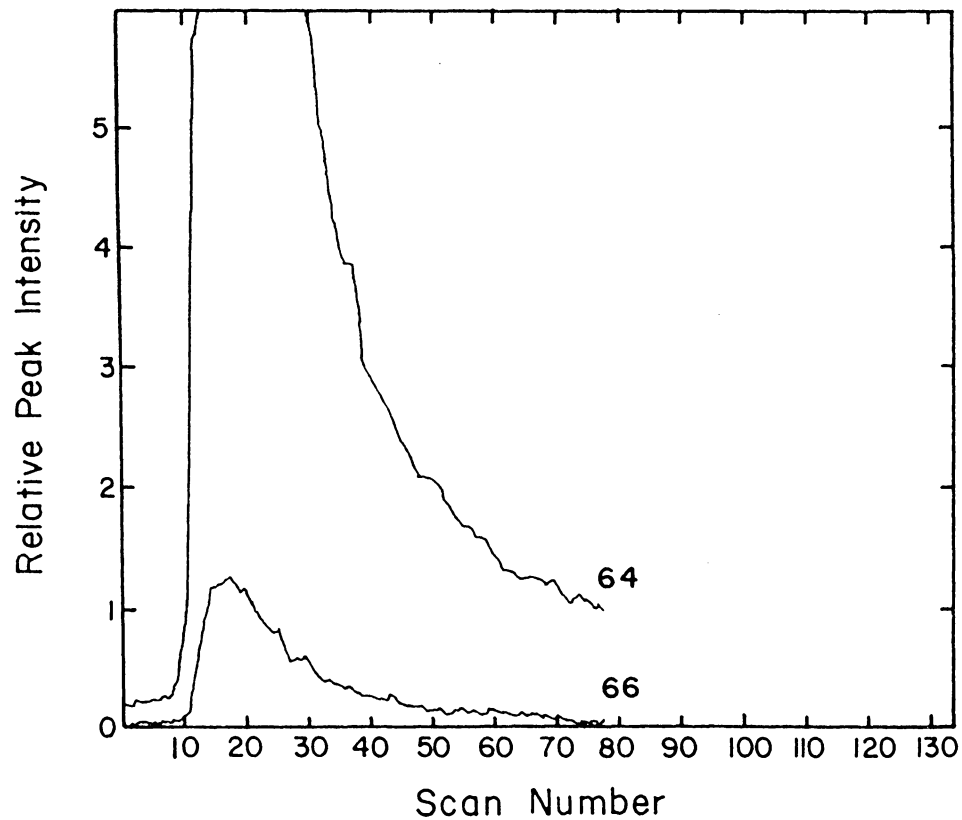

Figure 8. Mass spectrum scan of chalcopyrite blank.

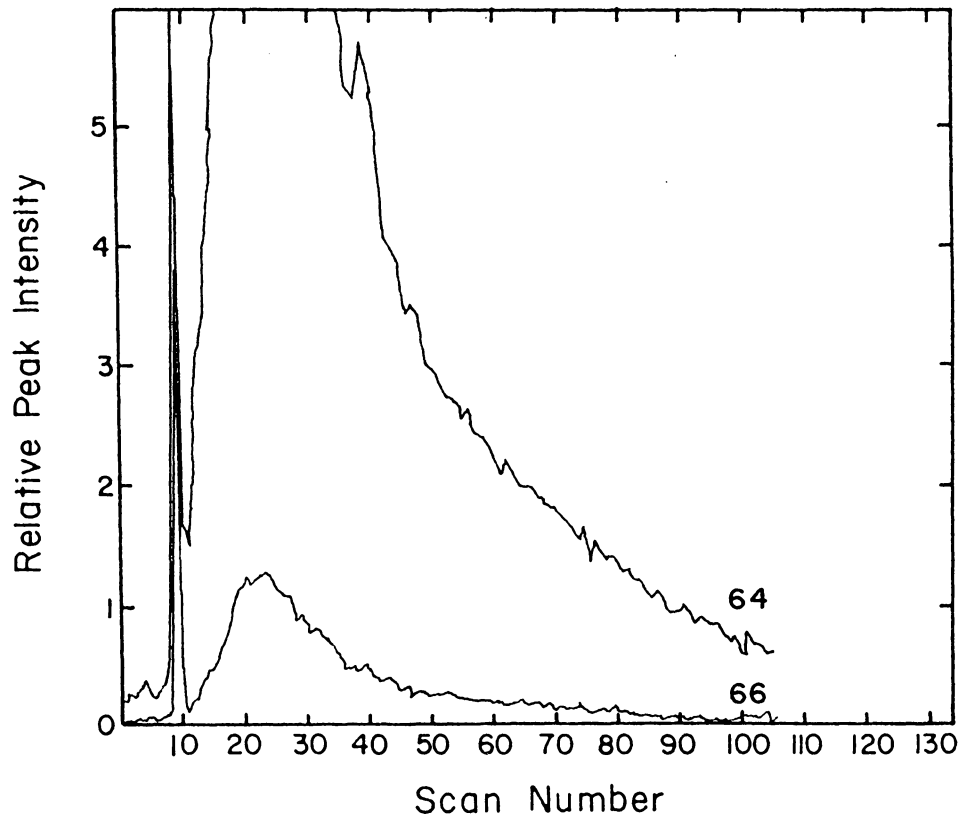

Figure 9. Mass spectrum scan of chalcopyrite spiked with 4 ng of sulfur.

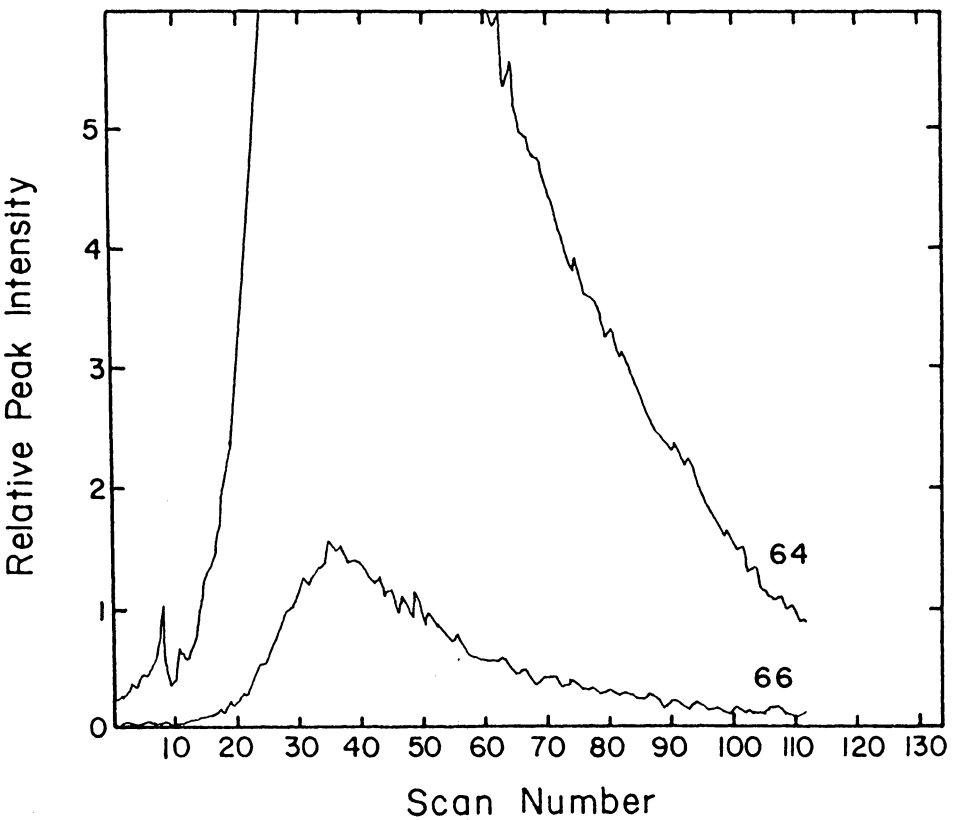

Figure 10. Mass spectrum scan of chalcopyrite spiked with 20 ng of sulfur.

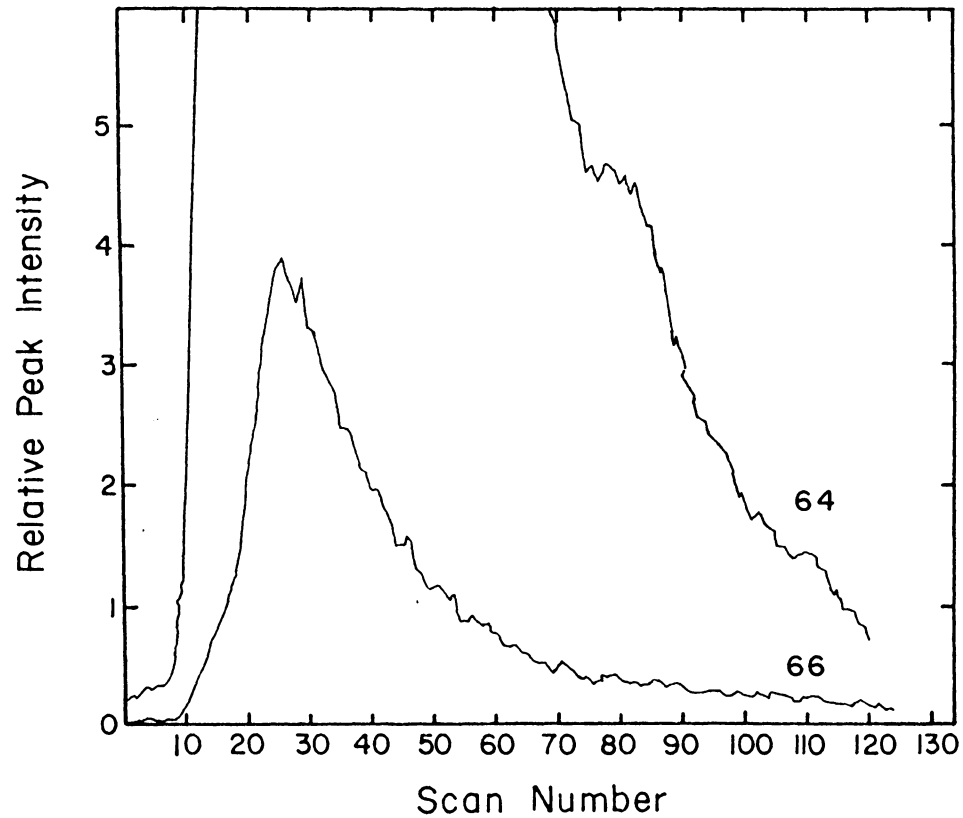

Figure 11. Mass spectrum scan of chalcopyrite spiked with 60 ng of sulfur.

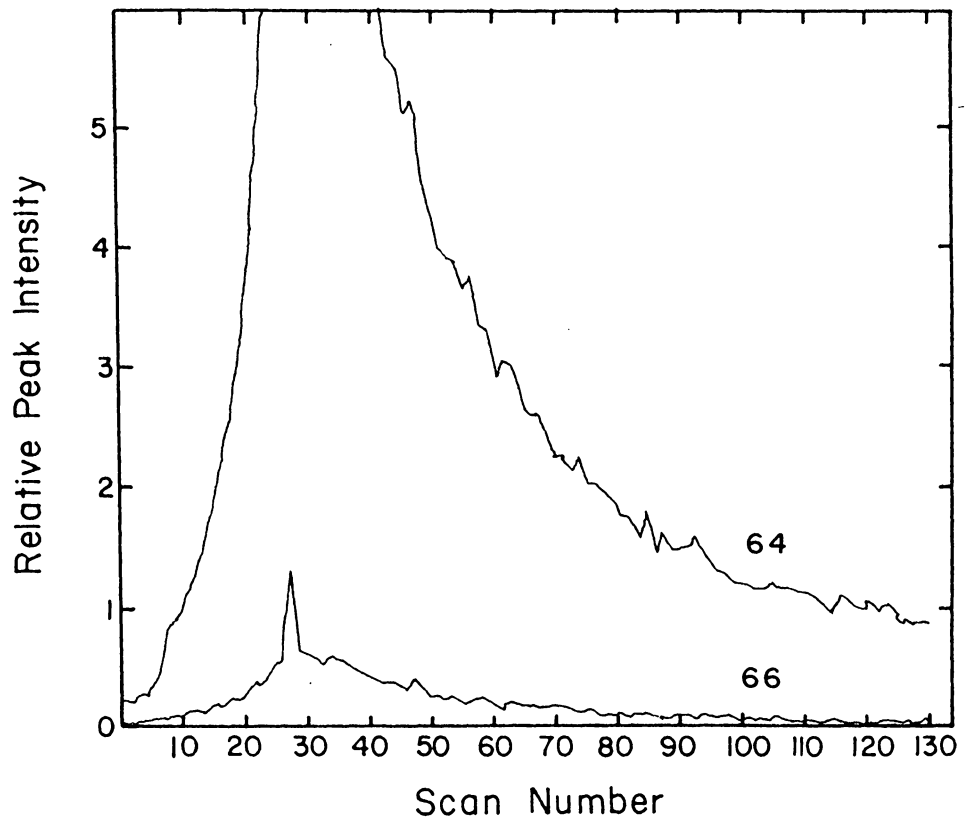

Figure 12. Quantitative mass spectrum scan of chalcopyrite conditioned at pH 10.0.

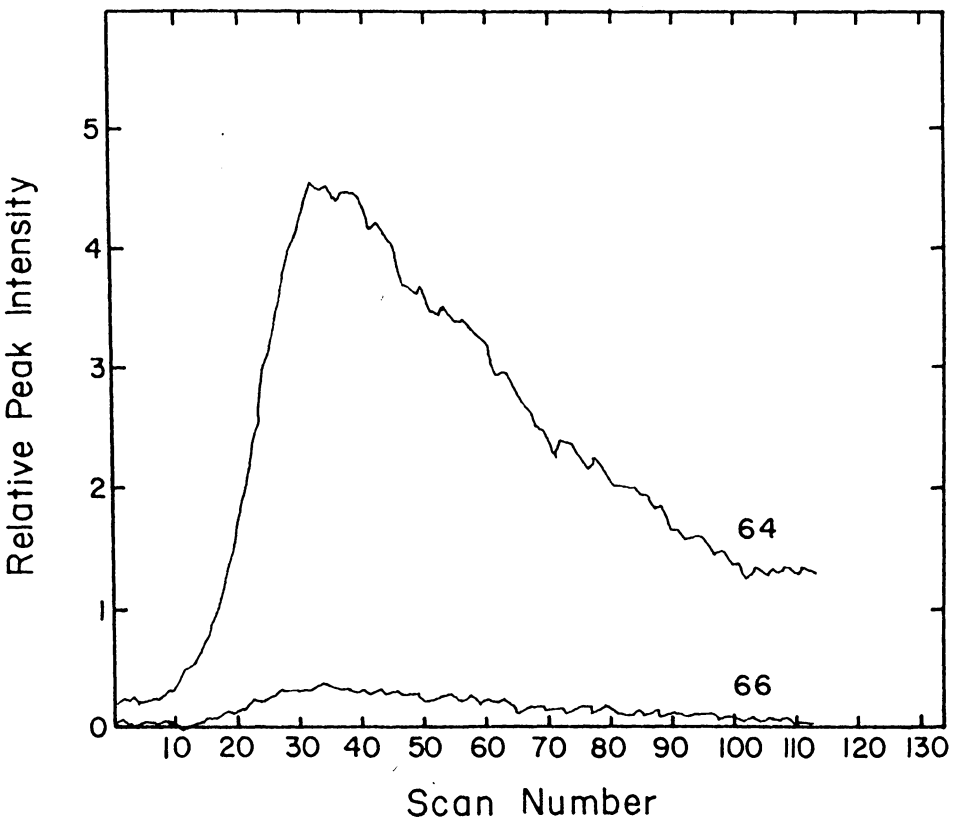

Figure 13. Quantitative mass spectrum scan of chalcopyrite conditioned at pH 12.0.

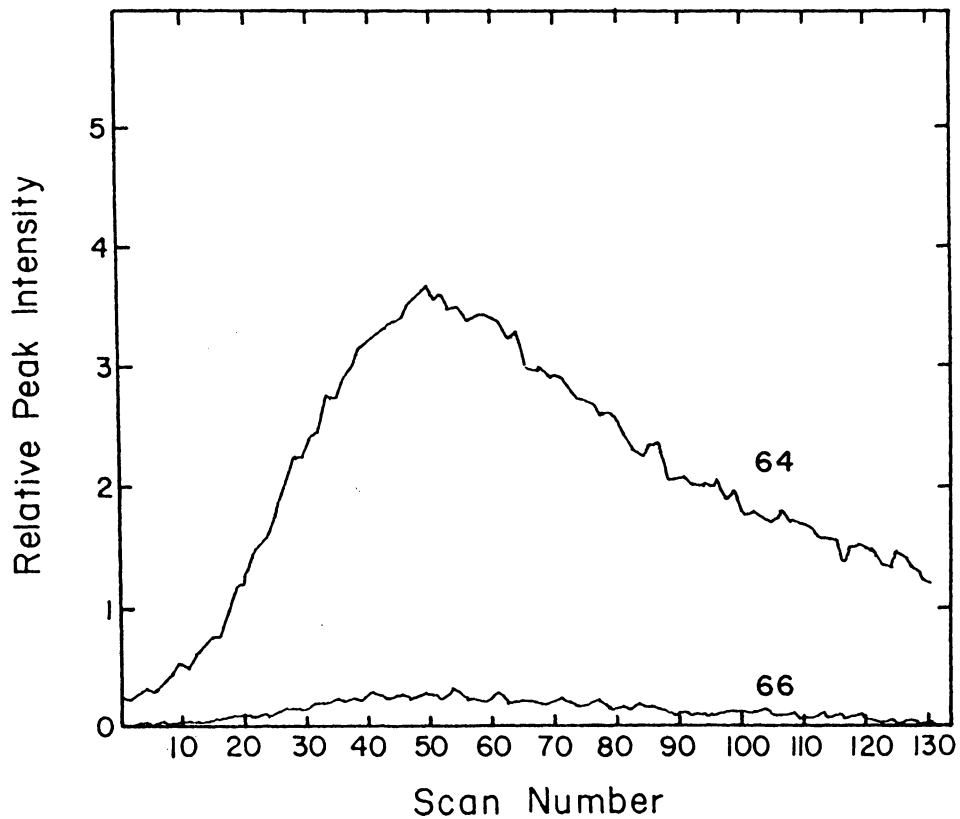

Figure 14. Quantitative mass spectrum scan of chalcopyrite conditioned at pH 12.0.

APPENDIX VIII

POLYSULFIDE CALCULATIONS

```
C
C
C        THIS PROGRAM DETERMINES THE EQUILIBRIUM IONIC CONCENTRATIONS
C        OF SOLUBLE SULFUR-BEARING SPECIES AT A CONSTANT PH OVER A RANGE
C        OF ELECTRODE POTENTIALS.
C        THE TOTAL CONCENTRATION OF SULFUR SPECIES IS FIXED AND MASS
C        BALANCE EQUATION CAN BE SET UP. THE USER SPECIFIES THE TOTAL
C        IONIC CONCENTRATION, THE PH AND THE POTENTIAL RANGE. THE
C        POTENTIALS ARE BASED ON THE HYDROGEN SCALE.
C        THE SULFUR SPECIES CONSIDERED ARE S**--, HS-, H2S, S2**--,
C        S3**--, S4**-- AND S5**--.
C        THE PROGRAM HAS BEEN WRITTEN IN TERMS OF DOUBLE PRECISION
C        VARIABLES.
C
C
      IMPLICIT REAL*8(A-H,O-Z)
      DIMENSION E(250)
      DIMENSION HS(250),H2SULF(250),SULF(250),S2(250),S3(250)
     *,S4(250),S5(250),ST(250)
      DIMENSION PERSU(250),PERHS(250),PERH2S(250),PERS2(250),
     *PERS3(250),PERS4(250),PERS5(250)
      DIMENSION CAP(20)
      DIMENSION DISK(10,250)
C
C        THE TITLE FOR THE OUTPUT IS READ AS AN ALPHANUMERIC ARRAY FROM
C        UNIT 31, WHICH IS DEFINED AT THE BOTTOM OF THE PROGRAM.
C
      READ(31,80) (CAP(I),I=1,18)
 80   FORMAT(18A4)
C
C        THE TITLE HEADING IS PRINTED OUT AT THE TOP OF THE FIRST PAGE
C        OF OUTPUT. THE TITLE GIVES THE INPUT DATA TO THE PROGRAM.
C
      WRITE(6,85) (CAP(I),I=1,18)
 85   FORMAT(///2X,18A4)
C
C        THE INPUT DATA IS READ FROM UNIT 31. THE VARIABLES HAVE THE
C        FOLLOWING DEFINITIONS:    PH = PH
C                                  XS = TOTAL MOLAR SULFUR CONCENTRATION
C                                  E(1) = MOST NEGATIVE POTENTIAL
C                                  EFINAL = MOST POSITIVE POTENTIAL
C
      READ(31,100) PH,XS,E(1),EFINAL
 100  FORMAT(4D10.4)
C        SOLVING THE MASS BALANCE EQUATION ENTAILS SOLVING A FIFTH ORDER
C        POLYNOMIAL EQUATION IN ONE UNKNOWN. THE MASS BALANCE HAS BEEN
C        SET UP SO THAT THE UNKNOWN IS THE EQUILIBRIUM CONCENTRATION OF
C        THE HS  ION. THIS EQUATION WILL BE SOLVED USING THE SECANT
C        METHOD. XS WILL BE THE INITIAL GUESS AT THE ROOT OF THE
C        EQUATION, WHICH IS REQUIRED TO BEGIN THE ALGORITHM.
```

```
C        I IS THE INDEX FOR THE ARRAYS STORING THE POTENTIALS AND IONIC
C        CONCENTRATIONS. HERE IT IS BEING INITIALIZED.
C
      X2=XS
      I=1
C
C        SOLVE IS A SUBROUTINE IN WHICH THE SECANT METHOD ALGORITHM IS
C        PERFORMED. THE OUTPUT FROM SOLVE IS THE VARIABLE HS, WHICH IS
C        THE LOGARITHM OF THE ROOT OF THE EQUATION (LOGARITHM OF THE HS
C        ION CONCENTRATION).
C        SOLVE CALLS A FUNCTION SUBPROGRAM CALC WHICH EVALUATES THE
C        POLYNOMIAL FOR THE VALUES OF X GENERATED BY THE ALGORITHM.
C
 5    CALL SOLVE(I,X2,E,PH,XS,HS)
C
C        SCALC IS A SUBROUTINE WHICH CALCULATES THE LOGARITHMS OF THE
C        IONIC CONCENTRATIONS ONCE THE POLYNOMIAL EQUATION HAS BEEN
C        SOLVED.
C        THESE ARE DEFINED AS THE FOLLOWING ARRAYS:
C                  HS = LOGARITHM OF HS  CONCENTRATION
C                  SULF = LOGARITHM OF S  CONCENTRATION
C                  H2SULF = LOGARITHM OF H2S CONCENTRATION
C                  S2 = LOGARITHM OF S  CONCENTRATION
C                  S3 = LOGARITHM OF S  CONCENTRATION
C                  S4 = LOGARITHM OF S  CONCENTRATION
C                  S5 = LOGARITHM OF S  CONCENTRATION
C                  ST = LOGARITHM OF TOTAL SULFUR CONCENTRATION
C
      CALL SCALC(I,LL,E,PH,HS,SULF,H2SULF,S2,S3,S4,S5,ST,XS)
C
C        THE INDEX I AND THE POTENTIAL E ARE INCREMENTED. THE POTENTIAL
C        IS INCREASED AT INTERVALS OF 0.01 VOLTS. ONCE A NEW VALUE OF
C        E IS CALCULATED, IT IS CHECKED TO SEE IF IT EXCEEDS THE UPPER
C        LIMIT OF THE POTENTIAL RANGE. IF IT DOES, THE PROGRAM JUMPS
C        TO THE OUTPUT SECTION. IF IT DOES NOT, THE PROGRAM RETURNS TO
C        THE TOP OF THE LOOP.
C
      I=I+1
      E(I)=E(I-1)+0.01D0
      IF(E(I).GT.EFINAL) GO TO 20
      GO TO 5
C
C        THIS IS THE BEGINNING OF THE OUTPUT SECTION OF THE PROGRAM. IN
C        THE FIRST PART, THE FRACTIONAL DISTRIBUTION OF THE VARIOUS
C        IONS IS DETERMINED. THIS THE RATIO OF THE CONCENTRATION OF AN
C        ION TO THE TOTAL SULFUR CONCENTRATION EXPRESSED AS A PERCENTAGE.
C        THE ARRAYS BELOW CORRESPOND TO THE DISTRIBUTIONS OF THE FOLLOW-
C        ING SPECIES:
C                        PERSU = S2-
C                        PERHS = HS-
```

```
C                          PERH2S = H2S
C                          PERS2 = S2 2-
C                          PERS3 = S3 2-
C                          PERS4 = S4 2-
C                          PERS5 = S5 2-
C
 20    J=I-1
       DO 30 K=1,J
       PERSU(K)=10.D0**SULF(K)/XS*100.D0
       PERHS(K)=10.D0**HS(K)/XS*100.D0
       PERH2S(K)=10.D0**H2SULF(K)/XS*100.D0
       PERS2(K)=2.D0*10.D0**S2(K)/XS*100.D0
       PERS3(K)=3.D0*10.D0**S3(K)/XS*100.D0
       IF(S4(K).LT.-74.D0) PERS4(K)=0.00D0
       IF(S4(K).GE.-74.D0) PERS4(K)=4.D0*10.D0**S4(K)/XS*100.D0
       IF(S5(K).LT.-74.D0) PERS5(K)=0.00D0
       IF(S5(K).GE.-74.D0) PERS5(K)=5.D0*10.D0**S5(K)/XS*100.D0
C
C         THE FRACTIONAL DISTRIBUTIONS ARE BEING STORED ON A DISK SO THAT
C         THEY CAN BE USED LATER PLOTTED LATER IN A SEPARATE PROGRAM.
C         THEREFORE, THEY ARE TRANSFERRED TO A TWO-DIMENSIONAL ARRAY DISK
C         WHICH WILL BE READ ONTO A DISK DESIGNATED AS UNIT 9WRITTEN ON.
C
       DISK(1,K)=PERSU(K)
       DISK(2,K)=PERHS(K)
       DISK(3,K)=PERH2S(K)
       DISK(4,K)=PERS2(K)
       DISK(5,K)=PERS3(K)
       DISK(6,K)=PERS4(K)
 30    DISK(7,K)=PERS5(K)
C
C         THE ARRAY IS NOW WRITTEN ONTO THE DISK
C
       DO 800 KK=1,7
 800   WRITE(9,850) (DISK(KK,K),K=1,J)
 850   FORMAT(201F14.5)
C
C         IN THIS SECTION, THE LOGARITHMS OF THE IONIC CONCENTRATIONS
C         AND THE FRACTIONAL DISTRIBUTIONS ARE PRINTED OUT ON PAPER.
C
       WRITE(6,150)
 150   FORMAT(T1,'1',////3X,'E(V)',8X,'S--',10X,'HS-',11X,'H2S',
     *11X,'S2',11X,'S3',11X,'S4',11X,'S5')
       DO 200 K=1,J
 200   WRITE(6,205) E(K),SULF(K),HS(K),H2SULF(K),S2(K),S3(K),
     *S4(K),S5(K)
 205   FORMAT(//1X,F5.2,7F14.5)
       WRITE(6,160)
 160   FORMAT(T1,////3X,'E(V)',8X,'STOT',9X,'% S--',9X,'% HS-',
     *8X,'% H2S',9X,'% S2',9X,'% S3',9X,'% S4')
```

```
      DO 240 K=1,J
  240 WRITE(6,250) E(K),ST(K),PERSU(K),PERHS(K),PERH2S(K),PERS2
     *(K),PERS3(K),PERS4(K)
  250 FORMAT(//1X,F5.2,7F14.5)
      WRITE(6,170)
  170 FORMAT(T1,////3X,'E(V)',8X,'% S5')
      DO 260 K=1,J
  260 WRITE(6,270) E(K),PERS5(K)
  270 FORMAT(//1X,F5.2,F14.5)
  340 STOP
      END
C
C        THIS IS SUBROUTINE SOLVE IN WHICH THE SECANT METHOD IS USED TO
C        DETERMINE THE ROOT TO THE POLYNOMIAL EQUATION.
C        THE POLYNOMIAL IS EVALUATED AT TWO VALUES OF X (THE INDEPENDENT
C        VARIABLE IN THE POLYNOMIAL). THESE VALUES OF X ARE CALLED X1
C        AND X2 AND THE CORRESPONDING VALUES OF THE POLYNOMIAL ARE F1
C        AND F2. USING THESE, THE ALGORITHM DETERMINES NEW VALUES OF X
C        AND THE POLYNOMIAL: XN AND FN.  X2,XN,F2 AND FN ARE THEN USED
C        TO GENERATE A NEW XN AND FN. THIS IS REPEATED UNTIL THE MAGNI-
C        TUDE OF FN IS SMALL ENOUGH.
C        CALC IS THE FUNCTION SUBPROGRAM IN WHICH THE POLYNOMIALS ARE
C        EVALUATED.
C
      SUBROUTINE SOLVE(I,X2,E,PH,XS,HS)
      IMPLICIT REAL*8(A-H,O-Z)
     .DIMENSION E(250),HS(250)
      X1=X2/2.D0
      F1=CALC(X1,I,E,PH,XS)
      F2=CALC(X2,I,E,PH,XS)
    5 XN=(X1*F2-X2*F1)/(F2-F1)
      FN=CALC(XN,I,E,PH,XS)
      PERDIF=FN/XS
      IF(DABS(PERDIF).LT.1.D-05) GO TO 4
      X1=X2
      X2=XN
      F1=F2
      F2=FN
      GO TO 5
    4 HS(I)=DLOG10(XN)
      RETURN
      END
      FUNCTION CALC(X,I,E,PH,XS)
      IMPLICIT REAL*8(A-H,O-Z)
      DIMENSION E(250)
      DX=DLOG10(X)
      DA=5.D0*DX+(E(I)-0.003D0+0.0369D0*PH)/0.0074D0
      IF(DA.LT.-74.D0) A=0.D0
      IF(DA.GE.-74.D0) A=10.D0**DA
      DB=4.D0*DX+(E(I)-0.033D0+0.0394D0*PH)/0.0098D0
```

```
      IF(DB.LT.-74.D0) B=0.D0
      IF(DB.GE.-74.D0) B=10.D0**DB
      DC=3.D0*DX+(E(I)-0.097D0+0.0443D0*PH)/0.0148D0
      IF(DC.LT.-74.D0) C=0.D0
      IF(DC.GE.-74.D0) C=10.D0**DC
      DD=2.D0*DX+(E(I)-0.298D0+0.0591D0*PH)/0.0296D0
      IF(DD.LT.-74.D0) D=0.D0
      IF(DD.GE.-74.D0) D=10.D0**DD
      F=(1.D0+10.D0**(PH-13.9D0)+10.D0**(-PH+7.D0))*X
      CALC=5.D0*A+4.D0*B+3.D0*C+2.D0*D+F-XS
      RETURN
      END
C
C        SCALC IS A SUBROUTINE WHICH DETERMINES THE LOGARITHMS OF THE
C        CONCENTRATIONS OF THE IONIC DISSOLVED SPECIES.
C
      SUBROUTINE SCALC(I,LL,E,PH,HS,SULF,H2SULF,S2,S3,S4,S5,ST,XS)
      IMPLICIT REAL*8(A-H,O-Z)
      DIMENSION E(250),HS(250),SULF(250),H2SULF(250),S2(100 ),
     *S3(250),S4(250),S5(250),ST(250)
      SULF(I)=HS(I)+PH-13.9D0
      H2SULF(I)=HS(I)-PH+7.D0
      S2(I)=2.D0*HS(I)+(E(I)-0.298D0+0.0591D0*PH)/0.0296D0
      S3(I)=3.D0*HS(I)+(E(I)-0.097D0+0.0443D0*PH)/0.0148D0
      S4(I)=4.D0*HS(I)+(E(I)-0.033D0+0.0394D0*PH)/0.0098D0
      IF(S4(I).LT.-74.D0) SD=0.D0
      IF(S4(I).GE.-74.D0) SD=10.D0**S4(I)
      S5(I)=5.D0*HS(I)+(E(I)-0.003D0+0.0369D0*PH)/.0074D0
      IF(S5(I).LT.-74.D0) SP=0.D0
      IF(S5(I).GE.-74.D0) SP=10.D0**S5(I)
      STOTAL=10.D0**HS(I)+10.D0**H2SULF(I)+10.D0**SULF
     *(I)+2.D0*10.D0**S2(I)+3.D0*10.D0**S3(I)+4.D0*SD+5.D0*SP
      ST(I)=DLOG10(STOTAL)
      RETURN
      END
/*
//GO.FT09F001  DD UNIT=SYSDA,
//             DSN=A11AA1.JERRY3,DISP=(NEW,CATLG),VOL=SER=USERPK,
//             DCB=(RECFM=FB,LRECL=2814,BLKSIZE=11256),
//             SPACE=(TRK,(2,1))
//GO.FT31F001  DD *
 INPUT DATA  PH= 8.D0  SULF=1.D-05  INITIAL EH= -1.0 V  FINAL EH = 1.0 V
    8.D0    0.00001D0      -1.D0      1.D0
/*
//
```

```
C
C         THIS PROGRAM PRODUCES A PLOT OF THE FRACTIONAL DISTRIBUTIONS
C         OF THE VARIOUS SULFUR SPECIES AS A FUNCTION OF ELECTRODE
C         POTENTIAL (E ) AT A GIVEN PH.
C
      REAL DISK(10,250), X1 (250), YY (250), XX (250)
      DIMENSION LABX ( 8 ), LABY ( 20 )
C
C         THE ARRAY X1 STORES THE COORDINATES (POTENTIALS) TO BE PLOTTED
C         AS ABSCISSAE IN THE PLOT. X1(1) IS THE LOWER LIMIT OF THE POT-
C         ENTIAL RANGE. THE POTENTIALS ARE INCREMENTED AT INTERVALS OF
C         0.01 VOLTS.
C
C
C         THE FIRST PORTION OF THE PROGRAM READS IN THE DATA NEEDED TO DO
C         THE PLOTTING.
C
      X1 (1) =-1.0
      DO 112 II = 2, 201
  112 X1 ( II ) = X1 (II-1) +.01
C
C         THE DATA SAMPLING FREQUENCY IS READ IN.
C
      READ ( 5, * ) ISF
C
C         THE NUMBER OF PLOTS TO BE MADE IS READ IN.
C
      READ ( 5, * ) NPLOTS
C
C         THE LENGTHS OF THE X AND Y AXES FOR THE PLOT ARE NOW SPECIFIED.
C
      READ ( 5, * ) XLEN, YLEN
C
C         NOW THE RANGES OF THE X AND Y AXES AS WELL AS THE DISTANCE
C         BETWEEN THE TICK MARKS ON EACH AXIS ARE GIVEN.
C
      READ ( 5, * ) XORG, XMAX, YORG, YMAX, XDIV, YDIV
C
C         NODDX AND NODDY ARE INTEGER CODES THAT ARE USED IN THE SUBROU-
C         TINE NUMBER WHICH PLOTS NUMBERS ALONG EACH AXIS. THEY SPECIFY
C         WHETHER THE NUMBER IS TO BE WRITTEN AS AN INTEGER OR AS A REAL
C         VARIABLE. IF THE NUMBERS ARE TO BE REAL, THEN THE CODE ALSO
C         GIVES THE NUMBER OF DIGITS TO THE RIGHT OF THE DECIMAL POINT.
C
      READ ( 5, * ) NODDX, NODDY
C
C         NCHARX SPECIFIES THE NUMBER OF CHARACTERS APPEARING IN THE
C         LABEL ALONG THE X AXIS.
C
      READ ( 5, * ) NCHARX
```

```
C
C         THE LABEL ALONG THE X AXIS IS READ IN FROM THE DATA AS AN
C         ALPHANUMERIC VARIABLE.
C
      READ ( 5, 28 ) LABX
C
C         THE NUMBER OF CHARACTERS IN THE LABEL FOR THE Y AXIS AND THE
C         LABEL ITSELF ARE ENTERED.
C
      READ ( 5, * ) NCHARY
      READ ( 5, 29 ) LABY
C
C         XINC AND YINC ARE THE INCREMENTS OF X AND Y FOR THE TICK MARKS.
C
      XINC = ( XMAX - XORG ) * XDIV / XLEN
      YINC = ( YMAX - YORG ) * YDIV / YLEN
C
C         PLOTS IS A SUBROUTINE THAT MUST BE CALLED IN ORDER TO INITIATE
C         THE PLOTTING ROUTINES.
C
      CALL PLOTS ( 0, 0, 50 )
C
C         THE LOOP FOR EACH PLOT IS SET UP. III IS THE INDEX FOR THE NUM-
C         BER OF PLOTS TO BE MADE.
C
      DO 100 III = 1, NPLOTS
C
C         THE RECTANGULAR BOUNDARY FOR THE PLOT IS DRAWN. IN ADDITION,
C         THE ORIGINS FOR EACH DRAWING ARE SET.
C
      NODDX= 1
      IF (III.EQ.1) CALL PLOT ( 5.0, 3.0, -3)
      IF (III.EQ.2.OR.III.EQ.3) CALL PLOT (10.0, 0.0, -3)
      CALL PLOT ( 0.0, YLEN, 2 )
      CALL PLOT ( XLEN, YLEN, 2 )
      CALL PLOT ( XLEN, 0.0, 2 )
      CALL PLOT ( 0.0, 0.0, 2 )
      I = IFIX ( XLEN / XDIV + 0.001 ) - 1
C
C         THE TICK MARKS ALONG THE BOTTOM SCALE ARE PUT IN. I IS THE NUM-
C         BER OF TICK MARKS.
C
      DO 1 J = 1, I
      X = J * XDIV
      CALL PLOT ( X, 0.0, 3 )
      CALL PLOT ( X, 0.1, 2 )
    1 CONTINUE
      X = XLEN - .1
C
C         THE SCALE ALONG THE RIGHT BOUNDARY IS DRAWN.
```

```
C
      I = IFIX ( YLEN / YDIV + 0.001 ) - 1
      DO 2 J = 1, I
      Y = J * YDIV
      CALL PLOT ( XLEN, Y, 3 )
      CALL PLOT ( X, Y, 2 )
    2 CONTINUE
C
C        THE TOP SCALE IS NOW DRAWN.
C
      I = IFIX ( XLEN / XDIV + 0.001 ) - 1
      Y = YLEN - 0.1
      DO 3 J = 1, I
      X = J * XDIV
      CALL PLOT ( X, YLEN, 3 )
      CALL PLOT ( X, Y, 2 )
    3 CONTINUE
C
C        FINALLY, THE TICK MARKS ON THE LEFT SIDE ARE PUT IN.
C
      I = IFIX ( YLEN / YDIV + 0.001 ) - 1
      DO 4 J = 1, 4
      X = 0.1
      Y = J * YDIV
      CALL PLOT ( 0.0, Y, 3 )
      CALL PLOT ( X, Y, 2 )
    4 CONTINUE
C
C        THE NUMBERS ALONG THE AXIS ARE NOW DRAWN IN. J GIVES THE NUMBER
C        OF THESE. XP ARE THE NUMBERS TO BE WRITTEN AND XPOS AND YPOS
C        ARE THE COORDINATES WITH RESPECT TO THE ORIGIN AT WHICH THEY
C        ARE LOCATED. NODDX SPECIFIES WHETHER THE NUMBERS ARE WRITTEN AS
C        INTEGERS OR REAL VARIABLES.
C
      J = IFIX ( ( XMAX - XORG ) / XINC + 0.001 ) + 1
      DO 5 I = 1, J
      XP = XORG + ( I - 1 ) * XINC
      IF (I.EQ.6) XP= 0.0
      IF (I.EQ.6) NODDX = -1
      IF (I.GT.6) NODDX = 1
      XPOS = (I-1) *XDIV - 0.28
      IF (I.EQ.6) XPOS= 2.96
      IF (I.GT.6) XPOS=  (I-1)*XDIV - 0.17
      YPOS = -0.28
      CALL NUMBER ( XPOS, YPOS, 0.13, XP, 0.0, NODDX )
    5 CONTINUE
C
C        THE LABEL ALONG THE X AXIS IS NOW MADE. XI AND YI GIVE THE POS-
C        ITION OF THE FIRST CHARACTER IN THE STRING. CHEI IS THE SIZE OF
C        EACH CHARACTER.
```

```
C
      CHEI = 0.25
      XI = ( XLEN - NCHARX * CHEI ) / 2. + 0.50
      YI = -0.78
      CALL VPISYM ( XI, YI, CHEI, LABX, 0.0,  8)
C
C        THE TITLE FOR EACH PLOT IS WRITTEN. IN THE CASE SHOWN, THREE
C        PLOTS ARE BEING DONE.
C
      IF (III.EQ.1) CALL VPISYM (4.0, 3.0, 0.19, 7HPH = 12, 0.0, 7)
      IF (III.EQ.2) CALL VPISYM (4.0, 3.0, 0.19, 7HPH = 10, 0.0, 7)
      IF (III.EQ.3) CALL VPISYM (4.0, 3.0, 0.19, 6HPH = 8, 0.0, 7)
C
C        NOW THE NUMBERS ARE PLOTTED ALONG THE SCALE FOR THE Y AXIS.
C        YP ARE THE NUMBERS WRITTEN AND NODDY IS THE CODE TO DECIDE
C        WHETHER THE NUMBERS ARE INTEGERS OR REAL VARIABLES. XPOS AND
C        YPOS ARE THE COORDINATES OF THE NUMBERS.
C
      J = IFIX (( YMAX - YORG) / YINC + 0.001 ) + 1
      DO 10 I=1,J
      YP = (I-1)*20.
      XPOS = -0.37
      IF(YP.EQ.0.) XPOS = -0.25
      IF(YP.EQ.100.) XPOS = -0.50
      YPOS = YDIV*(I-1) - 0.065
      CALL NUMBER ( XPOS, YPOS,+0.13,YP, 0.0, NODDY )
   10 CONTINUE
C
C        THE LABEL FOR THE Y AXIS IS THEN WRITTEN.
C
      CHEI= 0.25
      YI = ( YLEN - NCHARY * CHEI ) / 2
      CALL VPISYM (-0.75, YI, CHEI, LABY, 90.0, 7 )
C
C        THIS SECTION NOW DRAWS THE ACTUAL CURVES FOR EACH PLOT. THE
C        FACTORS FOR THE X AND Y VALUES ARE CALCULATED.
C
      XSCALE = ( XMAX - XORG ) / XLEN
      YSCALE = ( YMAX - YORG ) /  YLEN
C
C        NP IS THE NUMBER OF POINTS TO BE PLOTTED.
C
      NP = 201
C
C        THE DATA TO BE PLOTTED (IN THIS CASE, FRACTIONAL DISTRIBUTIONS)
C        IS READ FROM A DISK.
C
      DO 1012 KK=1,7
      IF (III.EQ.1) READ(25,201) (DISK(KK,JJ),JJ=1,NP)
      IF (III.EQ.2) READ(26,201) (DISK(KK,JJ),JJ=1,NP)
```

```
 1012 IF (III.EQ.3) READ(27,201) (DISK(KK,JJ),JJ=1,NP)
 201  FORMAT(201D14.5)
      CALL PLOT (0.0, 0.0, -3)
C
C        THIS LOOP PLOTS THE CURVES. XX AND YY ARE THE ARRAYS WHICH CON-
C        TAIN THE COORDINATES TO BE PLOTTED. THE MINIMUM VALUES OF X AND
C        Y (XORG AND YORG) AND THE SCALE FACTORS (XSCALE AND YLE) ARE
C        ADDED TO THE END OF THE XX AND YY ARRAYS. THIS IS REQUIRED BY
C        THE SUBROUTINE LINE WHICH DRAWS THE CURVES.
C
      DO 199 KK= 1,7
      DO 15 J = 1, NP
      JJ = ( J - 1 ) * ISF + 1
      XX ( J ) = X1 ( JJ )
      YY ( J ) = DISK(KK,J)
      IF ( YY ( J ) .LT. YORG ) YY ( J ) = YORG
   15 IF ( YY ( J ) .GT. YMAX ) YY ( J ) = YMAX
      XX ( NP + 1 ) = XORG
      XX ( NP + 2 ) = XSCALE
      YY ( NP + 1 ) = YORG
      YY ( NP + 2 ) = YSCALE
      CALL LINE ( XX, YY, NP, 1, 0, 1 )
  199 CONTINUE
  100 CONTINUE
   28 FORMAT ( 8A4 )
   29 FORMAT ( 20A4 )
C
C        PLOT IS CALLED A FINAL TIME TO INDICATE THAT NO MORE PLOTS WILL
C        BE MADE.
C
      CALL PLOT (20., 0., 999 )
      STOP
      END
/*
//GO.SYSIN     DD  *
1
3
6.0 4.0
-1.0  1.0  0.0 100. 0.6 0.8
+1 -1
8
ES&H (V)
7
PERCENT
//GO.FT25F001  DD  DSN=A11AA1.JERRY1,DISP=SHR
//GO.FT26F001  DD  DSN=A11AA1.JERRY2,DISP=SHR
//GO.FT27F001  DD  DSN=A11AA1.JERRY3,DISP=SHR
//GO.SYSIN     DD  *
/*
//
```

The vita has been removed from the scanned document

COLLECTORLESS FLOTATION OF CHALCOPYRITE AND SPHALERITE ORES

by

Gerald H. Luttrell

(ABSTRACT)

The flotation of chalcopyrite and sphalerite has been accomplished without the use of collectors. Of the six chalcopyrite ores tested in the present work, some floated well using only a frother, while others required the addition of sodium sulfide, presumably to remove the hydrophilic surface oxidation products. On the other hand, the flotation of sphalerite ores was found to require both sodium sulfide treatment and copper-activation. The ratio of these two reagents was most critical, the optimum Cu^{2+}/S^{2-} atomic ratio being approximately 0.17 over a wide range of reagent dosages.

Potential measurements taken during both batch and micro-flotation experiments demonstrated that the collectorless flotation of chalcopyrite was possible only in oxidizing conditions, which confirms an earlier finding by Heyes and Trahar (1977). In relation to this phenomenon, three possible mechanisms have been discussed: i) elemental sulfur formed under oxidizing conditions is responsible for the collectorless flotation, ii) polysulfide ions formed during the incipient surface oxidation process render the

mineral hydrophobic, and iii) HS^- ions, which may render the mineral hydrophilic upon adsorption, are removed from the system under oxidizing conditions. The first mechanism may operate primarily in acidic solutions, while the second mechanism operates in alkaline solutions where elemental sulfur is thermodynamically unstable. The third mechanism is based on the assumption that a clean, unoxidized surface is inherently hydrophobic. Spectroscopic evidence has been presented to support these proposed mechanisms.